

Boronic Acid Functionalized Polymers and Hydrogels for Biomedical Applications

Martin Piest

BORONIC ACID FUNCTIONALIZED POLYMERS AND HYDROGELS FOR BIOMEDICAL APPLICATIONS

PROEFSCHRIFT

Ter verkrijging van
de graad van doctor aan de Universiteit Twente,
op gezag van de rector magnificus,
prof. dr. H. Brinksma,
volgens besluit van het College voor Promoties
in het openbaar te verdedigen
op vrijdag 30 september 2011 om 14:45 uur

door

Martin Piest

Geboren op 24 juli 1981
te Steenwijk

Dit proefschrift is goedgekeurd door:

prof. dr. J.F.J. Engbersen (promotor)

Dit werk is auteursrechtelijk beschermd

M. Piest

2011

ISBN: 978-90-365-3249-5

Committee

Chairman:	prof. dr. G. van der Steenhoven	University of Twente
Promotor:	prof. dr. J.F.J. Engbersen	University of Twente
Members:	prof. dr. Ir. J. Huskens	University of Twente
	prof. dr. J. Feijen	University of Twente
	prof. dr. G. Storm	Utrecht University
	prof. dr P.J. Dijkstra	University Soochow (China)
	prof. dr. B.J. Ravoo,	University Münster (Germany)

The research in this thesis was carried out from 2006 until 2010 in the research group Biomedical Chemistry of the MIRA institute for Biomedical Technology and Technical Medicine, University of Twente, Enschede, The Netherlands.

UNIVERSITY OF TWENTE.

The research described in this thesis was financially supported by the Dutch Organization for Scientific Research (NWO) with a grant for Excellent Chemical Research (ECHO grant).



The printing of this thesis was sponsored by InGell Labs BV and PolyVation BV.



And by the Dutch Society for Biomaterials and Tissue engineering (NBTE)



Nederlandse vereniging voor Biomaterialen en Tissue Engineering
Netherlands society for Biomaterials and Tissue Engineering

Boronic acid functionalized polymers and hydrogels for biomedical applications.

PhD Thesis with references; with summary in English and Dutch.

University of Twente, Enschede, The Netherlands

ISBN: 978-90-365-3249-5

<http://dx.doi.org/10.3990/1.9789036532495>

Copyright © 2011 by M. Piest. All rights reserved.

Cover: An artistic expression of fluorescent therapeutic nanoparticles, and DNA and siRNA polyplexes within a macromolecular network. The artwork was done by PEACED-design.



Printed by Wöhrmann Print Service, Zutphen, Nederland

Voorwoord en dankwoord

Ongeveer een jaar na afloop van het promotieonderzoek ligt er dan toch een proefschrift! Ik wil toch enige woorden besteden aan de totstandkoming van dit proefschrift, voordat ik over ga tot het bedanken van mensen. Toen ik in 2005 gefascineerd raakte door het onderwerp van gentherapie met kationische polymeren, heb ik me vastgebeten in een afstudeeropdracht bij de werkgroep Biomedische Chemie van Johan Engbersen. Na deze opdracht succesvol te hebben afgerond dacht ik, na een korte verlenging om nog wat losse eindjes af te maken voor publicatie van dit werk, met een vliegende start aan een promotietraject bij dezelfde werkgroep te kunnen beginnen. Er lag een afstudeerverslag van Rong Jin, die in dezelfde periode haar Master thesis onderzoek deed bij Johan Engbersen. Dit onderzoek heb ik van dichtbij kunnen volgen en vond ik altijd erg boeiend. Ik was dan ook erg blij met de kans om een promotietraject in het verlengde van dit onderzoek te mogen doen.

Aanvankelijk begon ik met het reproduceren van deze polymeren en de bijbehorende transfectie data. Ondertussen kon ik mijn afstudeerverslag, na wat aanvullende experimenten en vele revisies, in 2008 vertalen naar een publicatie in *Journal of Controlled Release* volume 130. Met het boorzuur onderzoek verliep het iets grilliger, vaak was er een positief effect van de aanwezigheid van boorzuren op de transfectie eigenschappen van de poly(amido amine)s en soms ook niet. Vele syntheses en transfectie experimenten later bleek dat de substitutiegraad (dat wil zeggen de hoeveelheid boorzurgroepen die aan het polymeer gezet worden) en daarmee de hoeveelheid aan overgebleven vrije amino groepen bepalend waren voor de uitkomst van de transfectie experimenten en dan in het bijzonder voor de toxiciteit van deze materialen. Er is besloten om dit eens systematisch uit te zoeken en dit leverde weer een mooie publicatie op in 2010 in *Journal of Controlled Release* volume 148 over de effecten van acetylering en benzoylering van disulfide houdende poly(amido amine)s met aminobutyl zijketens.

Het boorzuuronderzoek was inmiddels erg versnipperd geraakt. De oorzaak hiervan was dat de mogelijkheden met de boorzuren eindeloos leken en overal waar verkennende experimenten werden gedaan, werden ook bemoedigende resultaten gevonden. Om dit allemaal uit te zoeken was dan ook te veel werk voor een enkele promovendus en al snel werden er bachelor en master studenten geworven om delen van het onderzoek uit te voeren. Dit resulteerde er in dat er vaak meerdere studenten tegelijk aan dit project werkten. Vaak hield de ene student zich bezig met synthese van monomeren, terwijl een tweede werkte aan de synthese van polymeren of hydrogelen en een derde celkweek en transfectie experimenten uitvoerde. Vanwege de diversiteit aan onderwerpen en versnippering van resultaten bleek het bijzonder lastig om een

rode draad voor dit proefschrift op papier te krijgen. Zo bleek het mogelijk om een proefschrift te vullen over poly(amido amine)s voor gentherapie en drug delivery (hoofdstukken 3 t/m 6) met eventueel de beide artikelen in Journal of Controlled Release. Alternatief bleek het mogelijk om een proefschrift samen te stellen over de boorzuurhoudende hydrogelen (hoofdstukken 7 t/m 10). Tot mijn vreugd, is het uiteindelijk toch gelukt om beide onderwerpen te verenigen in dit proefschrift, waarin de hoofdstukken elkaar logisch opvolgen met als gemeenschappelijk onderwerp de boorzuren voor biomedische toepassingen.

Vanwege de inventiviteit van dit onderzoek was het noodzakelijk om eerst een aantal zaken te patenteren alvorens de resultaten publiekelijk gemaakt konden worden. Dit traject heeft enige tijd in beslag genomen en er helaas in geresulteerd dat het niet mogelijk was gedurende het promotietraject om resultaten te presenteren op congressen of manuscripten in te sturen naar tijdschriften. Het goede nieuws is echter wel dat de resultaten gepresenteerd in dit proefschrift volledig nieuw zijn. Inspanningen om de behaalde resultaten alsnog publiekelijk te maken zijn nog in volle gang op het moment van schrijven.

Tot zover de tot stand koming van dit proefschrift. Rest mij nog om een aantal mensen te bedanken voor hun bijdrage aan dit proefschrift en hun ondersteuning tijdens dit promotie traject. Allereerst mijn promotor Johan Engbersen. Bedankt voor de goede coaching, alle input in het onderzoek en de veelvuldige correcties tijdens de supervisie van dit promotie traject. Jouw deur stond altijd open voor adviezen of een discussie, vaak over een chemisch onderwerp en soms over meer wereldse zaken. Met als vertrekpunt de organische chemie zijn we toch een heel eind gekomen in de ontwikkeling van nanoparticles en hydrogelen en zelfs het opzetten en interpreteren van cel-experimenten, waar ik met veel trots op terugkijk.

Mijn dank gaat uit naar de studenten die hebben bijgedragen aan dit onderzoek. Allereerst Peter van Es, jij hebt in het begin meegeholpen met de synthese en karakterisering van boorzuurhoudende poly(amido amine)s. Claudi van de Vegt, jij hebt veel van de resultaten uitgebreid en waar nodig herhaald. De inzichten die jullie werk heeft opgeleverd hebben geleid tot de resultaten die in hoofdstuk 3 staan beschreven.

Kristian Göeken, jij hebt vooral bijgedragen aan de dynamic light scattering metingen en transfecties van deze polymeren. Deze resultaten zijn deels herhaald en deels opgenomen in de hoofdstukken 4, 5, en 6. Remco Oskam en Benjamin Wohl, jullie hebben gewerkt aan de synthese van salicylhydroxamzuur-gefunctionaliseerde PEG-verbindingen. Ondanks jullie goede inspanningen is dit helaas uiteindelijk niet gelukt. Tijs Beuving, jij hebt ook nog een aantal aanvullende pogingen gedaan om SHA-PEG te maken en nog een aantal resultaten van Peter en Claudi herhaald en

uitgebreid met een mooie serie gePEGyleerde boorzuurhoudende poly(amido amine)s. Deze uitkomsten zijn uiteindelijk niet in dit proefschrift opgenomen, maar de inzichten uit deze experimenten hebben wel bijgedragen aan het opzetten en interpreteren van latere experimenten. Jeffrey Trinidad, jij was de eerste Master student in dit rijtje en je hebt de aftrap gegeven voor het hydrogel onderzoek zoals beschreven in hoofdstuk 7 en 8. Ook je uitgebreide literatuurverslag was erg behulpzaam bij het schrijven van hoofdstuk 2 van dit proefschrift. Sry Dewi Hujaya, you continued the research from Jeffrey with an equal impressive literature report. In addition, you have contributed the data presented in Chapter 9 on this thesis and contributed significantly to chapter 8 and 10. Xiaolin Zhang, you finalized the work from Sry Dewi and Jeffrey in chapter 8 and completed it with release data presented in chapter 10. Ik wil jullie dan ook graag allemaal bedanken voor jullie enthousiaste bijdrage aan het onderzoek en de plezierige samenwerking gedurende jullie afstudeertrajecten.

Verder hebben er een aantal collega's bijgedragen aan dit proefschrift. Allereerst wil ik Anika Embrechts bedanken voor alle AFM metingen in dit proefschrift, waaronder die in de hoofdstukken 3, 6 en 10, evenals voor de metingen waarvan de resultaten niet zijn opgenomen. Hartelijk dank voor de prettige samenwerking en voor alle discussies die tot een beter begrip van de materie hebben geleid. En natuurlijk bedankt voor het klaagurtje over de ontberingen van de PhD-student.

Het uitvoeren van celkweek experimenten en transfectiestudies in Enschede was geen vanzelfsprekendheid. Dankzij de hulp en informatie van Wim Hennink en Martin Lok (Universiteit Utrecht) konden aanvankelijk Miguel Mateos Timoneda en ik hiermee een begin maken in Twente. Miguel bedankt voor alles! Later heb ik veel hulp gehad van alle andere bewoners van het celkweeklab en in het bijzonder van Marloes Kamphuis, Andries van de Meer, Tom Groothuis, Mark Poels, Hemant Unadkat en Anouk Mentink. Jullie hebben mij niet alleen geholpen met celkweek en transfectiestudies, maar ook bij het uitvoeren van diverse analyses, waaronder FACS metingen, confocale microscopie en geautomatiseerde fluorescentie microscopie en de mooiste resultaten van deze metingen zijn in dit proefschrift opgenomen. Bedankt!

Marc Ankoné, vanwege onze gedeelde passies voor motorrijden, goede muziek en bovenal de krijgskunsten hadden we altijd iets om over te praten. Dit heeft dan ook geleid tot een hechte vriendschap, die ik nog altijd koester. Naast alle gesprekken over onze hobbies konden we ook nog wat experimenten samen doen. De resultaten hiervan zijn de elektronenmicroscopieplaatjes, zoals gepresenteerd in hoofdstuk 6 en 10. Bedankt!

Hans van der Aa, onze wegen lopen al heel lang parallel. Vanaf de eerste dag op de UT in 1999, waar we "doegroep-broertjes" waren, tot het afstuderen op de labs van PBM in 2005-2006. Nog later volgden we in dezelfde periode een promotietraject op een vergelijkbaar onderwerp bij de vakgroep BMC, waar we gedurende 4 jaar

niet alleen hetzelfde laboratorium, maar ook hetzelfde kantoor hebben gedeeld. We waren lange tijd samen verantwoordelijk voor de veiligheid en organisatie van de synthesruimte ZH282 en we hadden de wind er altijd goed onder! Ik kan terugkijken op een heel plezierige samenwerking waarin we soms elkaars experimenten waarnamen of materialen en gegevens deelden. Een deel van de data over p(ABOL) is van jouw hand en is meegenomen ter vergelijking in de hoofdstukken 4, 5 en 6. Naast alle prettige inhoudelijke discussies waren er onder meer de roadtrips naar Århus (Denemarken), Cardiff (Wales) en later de tripjes naar onze vriendinnen in Groningen. Heel hartelijk bedankt voor alles!

Ik wil graag Kevin Braeckmans en Dries Vercauteren bedanken voor de plezierige samenwerking. Niet alleen heeft dit geresulteerd in een gezamenlijke publicatie in *Biomaterials*, maar ook hebben onze discussies tijdens conferenties en andere ontmoetingen er mede toe bijgedragen aan het kunnen opzetten en interpreteren van de FACS experimenten zoals in hoofdstukken 4 en 6 zijn beschreven. Federico Martello, thanks for the pleasant cooperation and trips to the Vestingbar on Tuesday evenings. Hopefully, we will be able to finalize our joint publication soon!

Mijn dank gaat ook uit naar alle overige collega's en stafleden van PBM en BMC voor de goede infrastructuur en inspirerende omgeving die de randvoorwaarden hebben geschapen voor het ontstaan van dit proefschrift. Daarbij niet te vergeten alle studenten, die kwamen en gingen. Ik wil niet iedereen opsommen, met de kans dat ik iemand vergeet, maar allemaal ontzettend bedankt voor de gezelligheid tijdens kantooruren, maar ook daarbuiten tijdens borrels, promoties, afstudeerfeestjes, werkweken, congressen en alle andere activiteiten! Zlata en Karin bedankt voor alle ondersteuning.

Tijdens het promoveren was er gelukkig altijd de uitlaatklep bij de vechtsportvereniging V.A.S. Arashi. Ik wil dan ook alle trainers en mijn trainingsmaatjes bedanken voor de mogelijkheid om met jullie te kunnen sporten. Ook gaat mijn dank uit naar de hele Campus Ninja III-crew, en dan in het bijzonder naar Bas Mesman en Emile van Wijk die voor een leuke onderbreking van het promoveren hebben gezorgd. Ook wil ik graag mijn examen-partner Tom Huijgen bedanken, evenals Bas van Wel voor de gang naar alle jiu-jitsu stages en activiteiten. Ook bijzondere dank aan Bart Rossy en Wouter van de Berg met wie ik een gooi naar zwarte band judo heb gedaan. Mark van Oudheusden, bedankt voor je support en begeleiding naar de 1^e en 2^e dan jiu-jitsu en je rol als stagebegeleider in het behalen van mijn diploma als assistent leraar jiu-jitsu!

Dit promotietraject heeft er soms toe geleid dat mijn omgeving mij minder heeft gezien en dat ik wel eens af heb moeten zeggen of er in het weekend uitgeblust bij zat. Ik wil al mijn vrienden dan ook bedanken voor hun begrip en ondersteuning en in het

bijzonder Jurjen, Anouk, Tijs, Yvonne, Roy, Kristian, Marleen, Mathijs, Tanja, Johan, Niek, Merle, Gerben, Ingrid, Lennert, Jacoba, Paul en Laura.

Mijn ouders Harry en Karin en mijn broer Wilco, bedankt voor jullie support! Jullie waren altijd geïnteresseerd in de vorderingen van het onderzoek en hebben altijd geprobeerd om te begrijpen waar ik mee bezig was (in ieder geval in grote lijnen). Wilco bedankt voor het grafisch ontwerpen van verschillende filmpjes voor presentaties en voor de voorkant van dit proefschrift.

Mijn vriendin Jessica, ik denk dat jij de enige bent die werkelijk een idee heeft gekregen van de frustratie en stress die mij de laatste anderhalf jaar hebben achtervolgd. Vooral wanneer ik verbolgen was als het proefschrift te langzaam vorderde. Dit heeft zeker in het begin onze afstandsrelatie flink onder druk gezet. Het heeft er echter ook toe geleid dat we snel wisten wat we aan elkaar hebben en het gezegde “In nood leer je je ware vrienden kennen” lijkt me hier redelijk op zijn plaats. We hebben onze relatie bezegeld met de geboorte van de allermooiste dochter Robyn en nu dit promotietraject achter ons ligt, kunnen we ons helemaal richten op onze gezamenlijke toekomst als gezin. Jessica, bedankt dat jij mijn maatje wilt zijn!

Martin

Contents

Chapter 1	General introduction	3
Chapter 2	Boronic acid chemistry and the potential application in biomedical materials	9
Chapter 3	Role of boronic acid moieties in poly(amido amine)s for non-viral gene delivery	33
Chapter 4	Boronic acid functionalized poly(amido amine) with improved polyplex stability for pDNA and siRNA delivery in vitro	63
Chapter 5	A boronic acid functionalized poly(amido amine) for drug delivery and combined drug and gene delivery	91
Chapter 6	The presence of dextran improves the transfection efficiency of a boronic acid functionalized poly(amido amine)	111
Chapter 7	Boronic acid functionalized poly(amido amine)s form bioresponsive, restructuring hydrogels with poly(vinyl alcohol) by reversible covalent crosslinking	133
Chapter 8	Dynamically restructuring hydrogels from the reversible covalent crosslinking of poly(vinyl alcohol) by ortho- or para-aminomethylphenylboronic acid functionalized PPO-PEO-PPO spacers (Jeffamines®)	163
Chapter 9	Effects of arm length and number of arms of phenylboronic acid functionalized poly(ethylene glycol)s on the viscoelastic properties of reversible covalent crosslinked poly(vinyl alcohol) hydrogels	175
Chapter 10	Glucose-induced drug delivery from reversible covalent crosslinked poly(vinyl alcohol) by boronated multi-arm PEGs	195
Chapter 11	Final conclusions	217
Appendix A.	Unfinished Work	221
Appendix B.	Summary	227
	Samenvatting	231
	Curriculum Vitae	236

General introduction

Outline of the thesis

1.1 General introduction

Traditionally, diseases are treated by administration of herbs and more recently by the administration of natural or synthetic drugs. These therapeutic molecules are typically delivered orally as pills, via injection, or via inhalation. These routes of administration frequently result in limited bioavailability of the therapeutic due to rapid renal clearance, poor solubility or poor stability. To solve this problem in many cases a higher dose is administered, which in turn may lead to the onset of unwanted side effects. Consequently, over the last decades various controlled drug delivery systems have been developed to prolong the bioavailability of therapeutics. These systems are typically composed of biodegradable polymers, and examples include microspheres, liposomes, cationic gene complexes, but also implantable drug depots such as hydrogels, drug eluting stents, or polymer coated prostheses. With increasing knowledge of the metabolic pathways that are influenced by the therapeutic molecules, materials capable of more accurate dosing of the therapeutics are needed, both time-wise (predictable release kinetics) and spatially (local/targeted delivery versus systematic delivery). The new generation of biomaterials is also bioresponsive, meaning that the materials respond to an environmental stimulus and adjust the release of therapeutic content to the specific demand of the patient at a given time, for example using pH-responsive hydrogels.

1.2 Boronic acids

With the search for new biomaterials for the development of increasingly sophisticated drug delivery systems new chemistries are considered. In this respect, boron chemistry is only rarely applied in the field of controlled drug delivery and even less frequently in the field of gene therapy.

The unique properties of boron are extensively discussed in Chapter 2 of this thesis. Briefly, boron has the possibility to form reversible covalent bonds with nitrogen and oxygen. Consequently, boronic acids form reversible boronic esters with alcohols and polyols. [1] The boronic acid/boronic ester equilibrium is sensitive towards pH, temperature, and competing hydroxyl compounds and is also influenced by the proximity of amino groups (see Scheme 1.1). Thus, boronic acid containing materials are intrinsically bioresponsive. [2]

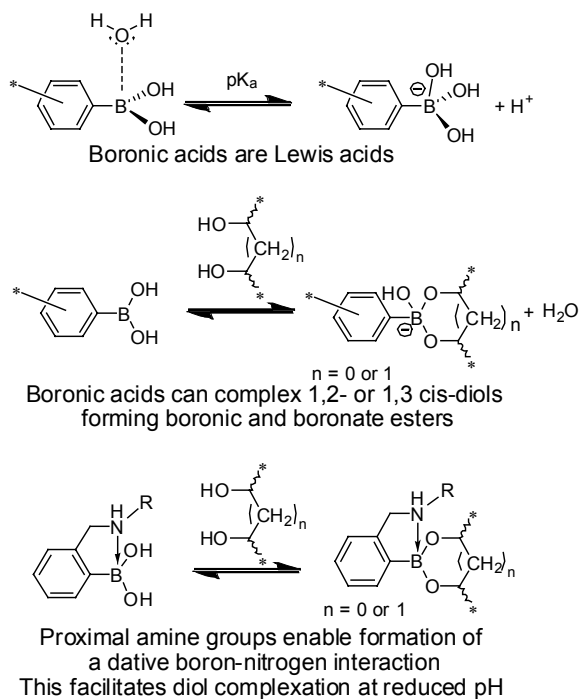
1.3 Prior art

In 2005 during her Master thesis work, Rong Jin explored the possibility to include boronic acids in poly(amido amine)s and she briefly studied the effect on the gene delivery properties. Gene therapy is a promising technique to cure various metabolic diseases by administration of a therapeutic “healthy” gene to compensate for a malfunctioning gene in the body. [3] Compared to viral vectors, cationic polymeric vectors are considered to be safer [4], but generally show much lower efficiency. Our research group led by Johan Engbersen focuses on the very interesting class of materials being poly(amido amine)s (PAAs).

These polymers are typically well soluble in water and their structure can be tuned to form stable nanoparticles that can be used for delivery of a great variety of therapeutic molecules including peptides, plasmid DNA, and siRNA. We have demonstrated that synthesis of PAAs by poly Michael addition of primary or bis(secondary) amines to bis(acrylamides) allows for large structural variation of the main chain and side chains of the polymer. Introduction of repetitive disulfide bonds in the polymer main chain facilitated the DNA release in the reductive environment of the cytosol through disulfide bond reduction, causing fast degradation of the polymer [5-9].

In the first approach by Rong Jin, boronic acids were grafted on aminobutyl side chains of poly(cystamine bisacrylamide/diaminobutane) (abbreviated as p(DAB)). At the start of this PhD thesis, this work was repeated more systematically and it was found that the charge density of the polymer can be relatively tuned by partially acylation of the aminobutyl side chains, having major effects on the gene delivery properties. The interested reader is reverted to Journal of Controlled Release volume 148 issue 1 [10]. This work is not included in this thesis as it does not deal with boronic acid functionalized materials, though it provides additional information on the

Chemical principles



Scheme 1.1. Chemical principles that serve as arguments to include boronic acids in biomaterials.

degree of grafting of acetyl or benzoyl groups on the p(DAB) system described in Chapter 3 of this thesis.

1.4 Outline of the thesis

The concept of introducing phenylboronic acids in the side chains of SS-PAA for gene delivery provokes many new ideas for potential applications. This led to the following hypotheses:

1. Introduction of phenylboronic acids allows for additional binding of polyplexes of SS-PAA with the glycoproteins of the cell membrane (boronic ester formation), resulting in increased particle uptake and ultimately in higher transfection efficiencies [11, 12]. This hypothesis is addressed in Chapter 3.
2. Introduction of phenylboronic acids in SS-PAA containing hydroxybutyl side chains could result in polyplexes formed with nucleic acids with increasing stability due to crosslinking of the polymer chains in the polyplex upon boronic ester formation. This increased particle stability may prove especially beneficial for siRNA polyplexes, as the 3' ribose end group is also capable of additional boronic ester formation [13-16]. These hypotheses are addressed in Chapter 4.
3. The presence of boronic acid moieties on the periphery of SS-PAA nanoparticles and polyplexes could allow for decoration of these particles with:
4. Saccharides [17-22] for targeting specific cells in order to enhance transfection or gene silencing efficiency. This hypothesis is also addressed in Chapter 4.
5. Therapeutic diols (such as dopamine or L-dopa) [23] for intracellular drug delivery and combined intracellular drug and gene delivery. This hypothesis is addressed in Chapter 5.
6. Polysaccharides such as dextran to reduce the zeta potential and provide stealth properties to the cationic polyplexes and may provide a possible alternative for PEGylation. This hypothesis is addressed in Chapter 6.
7. The presence of phenylboronic acids in PAA allows for crosslinking with polyvinylalcohol (PVA) resulting in a dynamically restructuring and bioresponsive hydrogel. This hypothesis is addressed in Chapter 7.
8. The presence of phenylboronic acids in PAA may allow for easy incorporation of polyplexes in other phenylboronic acid functionalized polymer based gels. In Chapter 8-10 work was expanded to other phenylboronic acid functionalized polymers with good water-solubility and biocompatibility to form hydrogels:
9. Jeffamine spacers (PPO-PEO-PPO) for PVA crosslinking. (Chapter 8)
10. Multi-arm PEG spacers for PVA crosslinking. (Chapter 9 and 10)

All these concepts are summarized in a schematic overview of this thesis:

Nanoparticles and polyplexes

Gene delivery vector for siRNA and pDNA

Boronated SS-PAA abbreviated as p(ABOL/2AMPBA)

+

Therapeutic oligonucleotide

↓

cationic polyplex

Chemical principles: Particle stabilization

Chapter 3 +4

Particle stability through boronate ester formation and stabilization through interaction with proximal amines

Boronic ester formation with vicinal diols at 3' end of RNA

Combined drug and gene therapy

+

alizarin red S (ARS)

↓

fluorescent boronic acid-ARS complex

Chapter 5

Chemical principles: Improved cell adhesion

Boronic acid can complex with carbohydrates resulting in a carbohydrate decorated particle

Polyplex

Carbohydrate decorated particle can bind with specific receptor

Binding with glycosylated phospholipids of cells (glycocalix)

Target cell

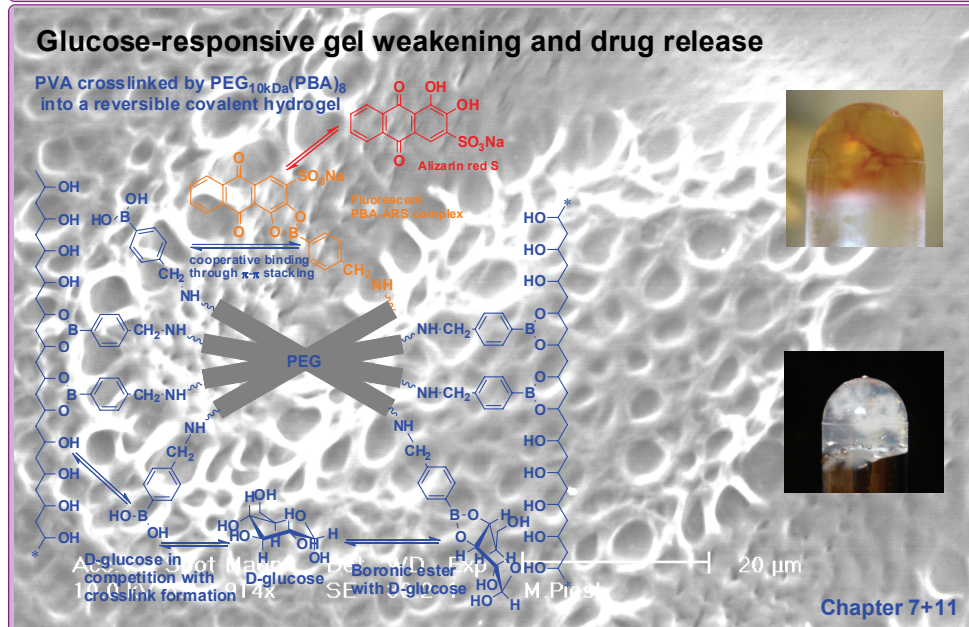
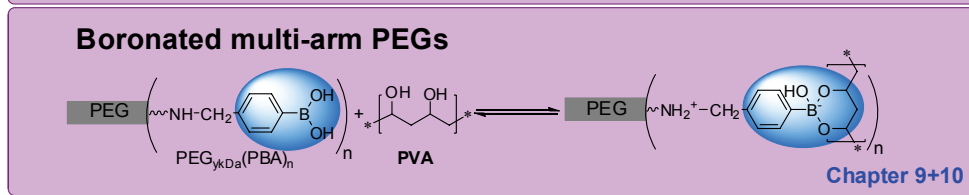
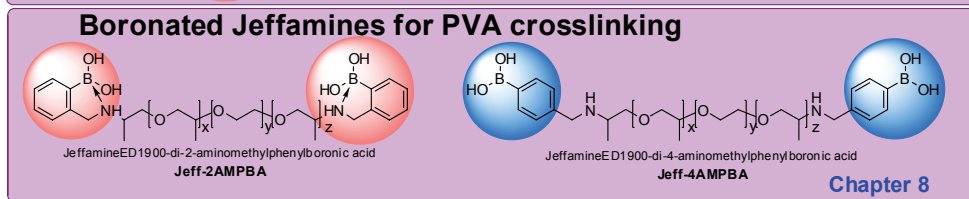
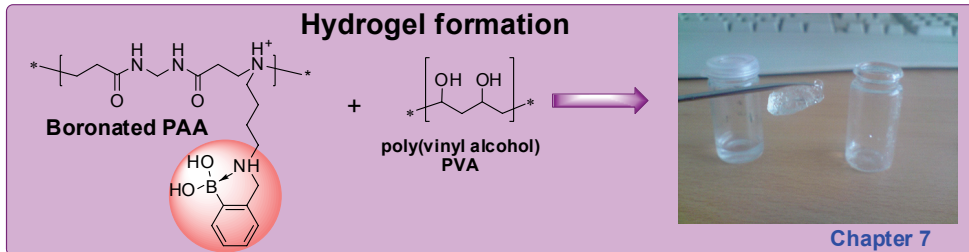
Chapter 4

Addition of dextran to coat a polyplex

Chapter 6

Uptake of polyplexes with (FITC-)dextran

Hydrogels



1.6 References

- [1] D.G. Hall, *Boronic Acids - Preparation and applications in organic synthesis and medicine*, John Wiley & Sons, 2005.
- [2] W.Q. Yang, X.M. Gao, B.H. Wang, Boronic acid compounds as potential pharmaceutical agents, *Med. Res. Rev.*, 23 (2003) 346-368.
- [3] E. Wagner, J. Kloeckner, Gene delivery using polymer therapeutics, *Adv. Polym. Sci.*, 192 (2006) 135-173.
- [4] I.M. Verma, N. Somia, Gene therapy - promises, problems and prospects, *Nature*, 389 (1997) 239-242.
- [5] C. Lin, Z.Y. Zhong, M.C. Lok, X.L. Jiang, W.E. Hennink, J. Feijen, J.F.J. Engbersen, Linear poly(amido amine)s with secondary and tertiary amino groups and variable amounts of disulfide linkages: Synthesis and in vitro gene transfer properties, *J. Control. Release*, 116 (2006) 130-137.
- [6] C. Lin, Z.Y. Zhong, M.C. Lok, X.L. Jiang, W.E. Hennink, J. Feijen, J.F.J. Engbersen, Novel bioreducible poly(amido amine)s for highly efficient gene delivery, *Bioconjugate Chem.*, 18 (2007) 138-145.
- [7] M. Piest, C. Lin, M.A. Mateos-Timoneda, M.C. Lok, W.E. Hennink, J. Feijen, J.F.J. Engbersen, Novel poly(amido amine)s with bioreducible disulfide linkages in their diamino-units: Structure effects and in vitro gene transfer properties, *J. Control. Release*, 130 (2008) 38-45.
- [8] C. Lin, C.J. Blaauboer, M.M. Timoneda, M.C. Lok, M. van Steenberg, W.E. Hennink, Z.Y. Zhong, J. Feijen, J.F.J. Engbersen, Bioreducible poly(amido amine)s with oligoamine side chains: Synthesis, characterization, and structural effects on gene delivery, *J. Control. Release*, 126 (2008) 166-174.
- [9] M.A. Mateos-Timoneda, M.C. Lok, W.E. Hennink, J. Feijen, J.F.J. Engbersen, Poly(amido amine)s as gene delivery vectors: Effects of quaternary nicotinamide moieties in the side chains, *Chemmedchem*, 3 (2008) 478-486.
- [10] M. Piest, J.F.J. Engbersen, Effects of charge density and hydrophobicity of poly(amido amine)s for non-viral gene delivery, *J. Control. Release*, 148 (2010) 83-90.
- [11] H. Kitano, M. Kuwayama, N. Kanayama, K. Ohno, Interfacial recognition of sugars by novel boronic acid-carrying amphiphiles prepared with a lipophilic radical initiator, *Langmuir*, 14 (1998) 165-170.
- [12] A.E. Ivanov, I.Y. Galaev, B. Mattiasson, Interaction of sugars, polysaccharides and cells with boronate-containing copolymers: from solution to polymer brushes, *J. Mol. Recognit.*, 19 (2006) 322-331.
- [13] A.E. Ivanov, I.Y. Galaev, B. Mattiasson, Binding of adenosine to pendant phenylboronate groups of thermoresponsive copolymer: a quantitative study, *Macromol Biosci.*, 5 (2005) 795-800.
- [14] A. Ozdemir, A. Tuncel, Boronic acid-functionalized HEMA-based gels for nucleotide adsorption, *J. Appl. Polym. Sci.*, 78 (2000) 268-277.
- [15] H. Cicek, Nucleotide isolation by boronic acid functionalized hydrogel beads, *J. Bioact. Compat. Pol.*, 20 (2005) 245-257.
- [16] B. Elmas, M.A. Onur, S. Senel, A. Tuncel, Temperature controlled RNA isolation by Nisopropylacrylamide-vinylphenyl boronic acid copolymer latex, *Colloid Polym. Sci.*, 280 (2002) 1137-1146.
- [17] M. Monsigny, P. Midoux, R. Mayer, A.C. Roche, Glycotargeting: Influence of the sugar moiety on both the uptake and the intracellular trafficking of nucleic acid carried by glycosylated polymers, *Bioscience Rep.*, 19 (1999) 125-132.
- [18] H.B. Yan, K. Tram, Glycotargeting to improve cellular delivery efficiency of nucleic acids, *Glycoconjugate J.*, 24 (2007) 107-123.
- [19] I.Y. Park, I.Y. Kim, M.K. Yoo, Y.J. Choi, M.H. Cho, C.S. Cho, Mannosylated polyethylenimine coupled mesoporous silica nanoparticles for receptor-mediated gene delivery, *Int. J. Pharm.*, 359 (2008) 280-287.
- [20] J.S. Remy, A. Kichler, V. Mordvinov, F. Schubert, J.P. Behr, Targeted gene-transfer into hepatomacells with lipopolyamine-condensed DNA particles presenting galactose ligands - a stage toward artificial viruses, *P. Natl. Acad. Sci. USA*, 92 (1995) 1744-1748.
- [21] J. Han, Y.I. Yeom, Specific gene transfer mediated by galactosylated poly-L-lysine into hepatoma cells, *Int. J. Pharm.*, 202 (2000) 151-160.
- [22] M. Hashida, S. Takemura, M. Nishikawa, Y. Takakura, Targeted delivery of plasmid DNA complexed with galactosylated poly(L-lysine), *J. Control. Release*, 53 (1998) 301-310.
- [23] A. Coskun, E.U. Akkaya, Three-point recognition and selective fluorescence sensing of L-DOPA, *Org. Lett.*, 6 (2004) 3107-3109.

Boronic acid chemistry and the potential application in biomedical materials

Abstract

Boron chemistry is not frequently applied in the biomedical field and this review provides an overview of bor(on)ic acid chemistry and the possibilities to develop new biomaterials using boronic acid functionalized polymers. Boronic acids are Lewis acids that interact with Lewis bases and their unique feature to form reversible covalent boronic esters with diols has been explored extensively as sensor devices for the detection of sugars. Additionally, boronic acid functionalized materials have been deployed as enzyme inhibitors, as membrane transporter molecules, in boron neutron capture therapy, and in affinity column separation chromatography. Most importantly, boronic acids can also be key elements in drug delivery systems. For example boronic acid functionalized materials have been successfully used for the preparation of dynamically restructuring hydrogels that are bioresponsive and chemoresponsive. These boronic acid gel systems are described here in detail, providing an overview of the recent progress that has been made in this field.

2.1. Introduction to boronic acid chemistry

In order to take maximal advantage of the unique properties of boronic acids for the development of new biomaterials and therapies it is necessary to have a profound understanding of boronic acid chemistry. However, the average organic chemistry book does not discuss boron chemistry in great detail and generally the information is limited to the reduction reactions with sodium borohydride [1]. Boronic acids are belonging to the larger class of organoboranes also known as boric acids, which are treated in specific chemistry textbooks, such as “The organic chemistry of boron”[2] “Organoboron chemistry”[3-4], and “Boranes in organic chemistry” [5]. More recent information is provided by Hall in a review of “Boronic acids-Preparation and applications in organic synthesis and medicine” [6]. Also in the field of fluorescent sensors, James has written several review articles on the application of boronic acids, thereby providing a profound overview of boronic acid chemistry [7-8].

1.1. The element boron

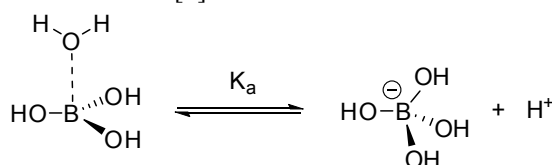
The element boron is found in rocks, soil and water typically with < 20 ppm concentrations [9]. Boron is mined as different borate minerals in parts of the western United States (Death Valley) and in other sites stretching from the Mediterranean to Turkey and Kazakhstan. Typically, these sites all have a history of volcanic or hydrothermal activity. Borate minerals and their refined products are used in glass and related vitreous applications, in laundry bleaches, fire retardants, as micronutrients in fertilizers, and as emulsifiers in the paper and oil industry [10].



Figure 2.1. From left to right: borax mineral, advertisement for borax, ulexite mineral.

Already 4000 years ago the Babylonians have been credited for importing borax as a flux for working gold, which was also used by European goldsmiths dating back to the 12th century [9]. From the 1950's several patents emerged using boric and boronic acids as additives in fuels and/or for stabilization of polymeric materials. In the 1960's patents by distilleries emerged for the purification of saccharides using boronic acids, and it took until the early 1990's until the first patents for biomedical applications emerged, predominantly for glucose-triggered insulin devices, or as boron containing enzyme inhibitors (e.g. Bortezomib).

The unique and versatile properties of boron containing materials are due to the rapid interconversion from the trivalent, planar sp^2 hybridized (neutral) to the tetravalent, tetrahedral sp^3 hybridized (anionic) boron. This is due to the unique electron configuration of the element boron with atom number five, as the electron configuration $1s^2 2s^2 2p^1$ allows for the formation of three covalent bonds in a sp^2 geometry. In the sp^2 hybridized conformation boron only has 6 valence electrons and can accept an electron-pair, hence it is a Lewis acid. As a result boron has an “electron hole” that can interact with a Lewis base, thereby forming a covalent bond with tetrahedral sp^3 geometry. For example, trigonal boric acid can coordinate with water and form a tetrahedral borate anion, thereby releasing a proton (Scheme 2.1) [7]. Herein the pK_a value is used as the definition when 50 percent of the trigonal planar structure is coordinated to form the tetrahedral anionic structure and the pK_a of boric acid in water is reported to be 9.2 [6].



Scheme 2.1. Boric acid–water conjugate in equilibrium with the borate anion.

2.1.2. Nomenclature of boron compounds

A boronic acid is an alkyl or aryl substituted boric acid containing a carbon to boron chemical bond, see Figure 2.2. The type of carbon group (R) directly bonded to boron determines the reactivity and properties of the boronic acids that are classified conveniently in subtypes such as alkyl-, alkenyl-, alkynyl-, and aryl- boronic acids [6]. Similarly, a disubstituted boric acid is referred to as a borinic acid and a trisubstituted boric acid as a borane. The prefix borono is employed to name the boronyl group and the prefix boro is also used for small cyclic derivatives such as boronic esters. The anion is given the suffix “ate” and for example the anion of boronic acid is referred to as boronate (Figure 2.2).

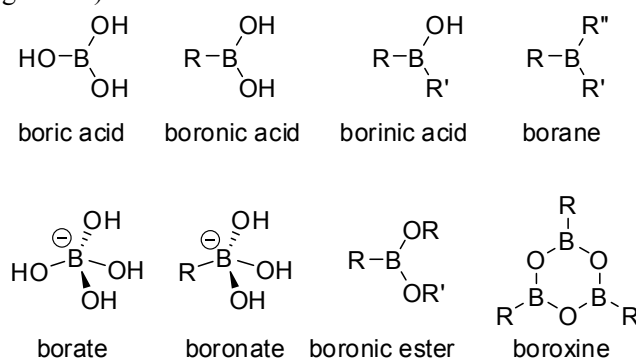


Figure 2.2. Different boron species, where R, R', and R'' can be alkyl, alkenyl, alkynyl, or aryl.

2.1.3. Reactivity of boron centers

Boron can be introduced in a wide variety of organic compounds through the formation of covalent bonds with carbon, oxygen, nitrogen, sulfur and phosphorus. Due to the fact that boronic acids are not found in natural compounds containing a carbon–boron covalent bond, synthetic organoborane chemistry is emerging only since the 1960's. Most boronic compounds are present as boronic esters, as the boron–oxygen bond is 30–40 kcal/mol (125–165 kJ/mol) stronger than the boron–carbon bond [11]. Boronic acid containing compounds can be synthesized from Grignard or lithium reagents in which trialkyl borates are reacted as electrophile with a nucleophilic alkyl- or aryl magnesium halide. Alternatively, hydroboration of a borane and an unsaturated carbon–carbon (C=C) bond can be used to introduce boron in organic compounds [11-12]. As the boron–carbon bond is fairly weak it can be used to form more stable C–N or C–O bonds and hence boronic acids are used to form esters, amides or substituted amines [13-18]. Boronic acids can be used in the Petasis reaction (also referred to as the borono-Mannich reaction) in which a boronic acid, an aldehyde and an amine react to form the product and boric acid [13-14]. More importantly, boronic acids can be used to establish the formation of carbon–carbon covalent bonds (C–C) in the Suzuki-Miyaura reaction (also referred to as Suzuki coupling) [15]. Since the discovery of the Suzuki coupling reaction there is an ever increasing interest for boronic acid compounds [16]. Consequently, many boronic acids are currently commercially available and they are used extensively in synthetic organic chemistry as chemical building blocks and intermediates [17]. In many cases boronic esters are used in which the ester serves as protecting group to reduce the reactivity of the boron centre or to improve the handling of the boronic compounds, e.g. to improve the solubility or to facilitate crystallization [7].

2.1.4. Lewis acidity of boronic acids

Similar to carboxylic acids or nitro compounds, the reactivity of the boron centre is highly dependent upon their single variable substituent, being the carbon group R directly bonded to the boron atom as depicted in Figure 2.3.

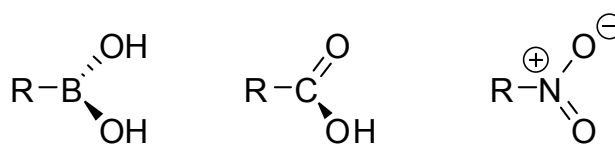


Figure 2.3: Boronic acid, carboxylic acid and a nitro compound. R can be alkyl, alkenyl, alkynyl, or aryl.

Boronic acids as well as carboxylic acids and nitro compounds are flat, because they are sp^2 hybridized. However in boronic acids, boron has only 6 electrons,

whereas carbon and nitrogen have 8 valence electrons in their analogous carboxylic and nitrous structures. Owing to the deficiency of two electrons, according to the octet rule, boronic acids possess a vacant p-orbital and thus can be defined as Lewis acids that can coordinate with base. The Lewis acidity of boronic acids results in a complexation equilibrium in water similar as previously described for boric acid (Scheme 2.1). Hence the transition to the anionic sp^3 hybridized boronate occurs at reduced pH [18]. This acidity has been known for quite a while, however the structure of the boronate ion was found to be tetrahedral by Lorand and Edwards only in 1959 [19]. Similar to carboxylic acids, strong electron-withdrawing substituents decrease the electro-negativity of the boron centre, thereby increasing its electrophilicity and its Lewis acidity.

For example, phenylboronic acid (PBA) can react with water to form the anionic phenylboronate, thereby filling its “electron gap” and releasing a proton that reduces the pH of the surrounding medium. The pK_a for the transition from the trigonal planar structure of phenylboronic acid to its tetrahedral phenylboronate structure is 8.7–8.9 [6-7, 18]. Generally, boronic acids with alkyl substituents have a higher pK_a value than those with aromatic substituents. The influence of different substitution groups and substitution sites of PBA are listed in Table 2.1 [6, 18, 20]. Electron-donating groups, (e.g. 2-methoxy PBA) increase of the pK_a value of PBA to 9, whereas electron-withdrawing groups can decrease the pK_a value of PBA to as low as 6. The pyridium boronic acids have the lowest pK_a values of *ca.* 4, although they are also susceptible to hydrolytic deboration, indicating that in these compounds the carbon–boron bond is fairly weak [14-15, 17, 27].

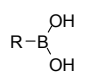
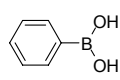
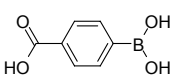
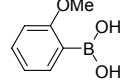
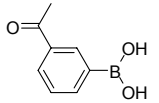
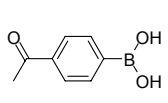
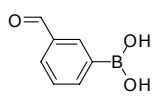
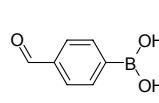
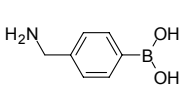
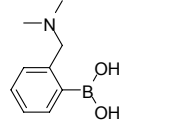
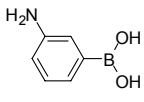
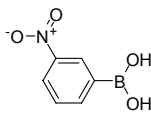
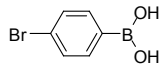
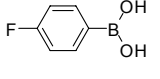
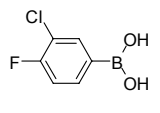
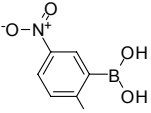
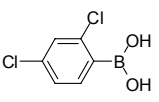
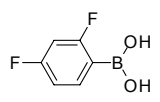
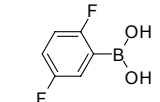
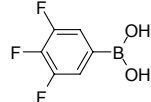
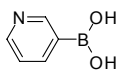
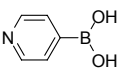
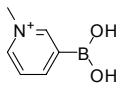
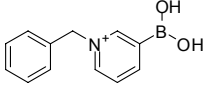
2.1.5. The boron–nitrogen interaction

Because of their mild organic Lewis acidic character, boronic acids can coordinate with (organic) bases. From Table 2.1, for 2-dimethylaminomethylphenylboronic acid a relatively low pK_a of 6.7 can be observed. This reduced pK_a is due to the so-called boron–nitrogen (B–N or N→B) interaction in which an adjacent amine donates its free electron pair to the boron centre, thereby forming a dative bond. The amine group functions as an internal Lewis base and thus interact with the boronic acid, which acts as a Lewis acid as is given in Scheme 2.2 [20-23]. Other neighboring groups such as acetamido, pyridine, thiourea and acetamidine have also been found to be effective in this capacity [24].

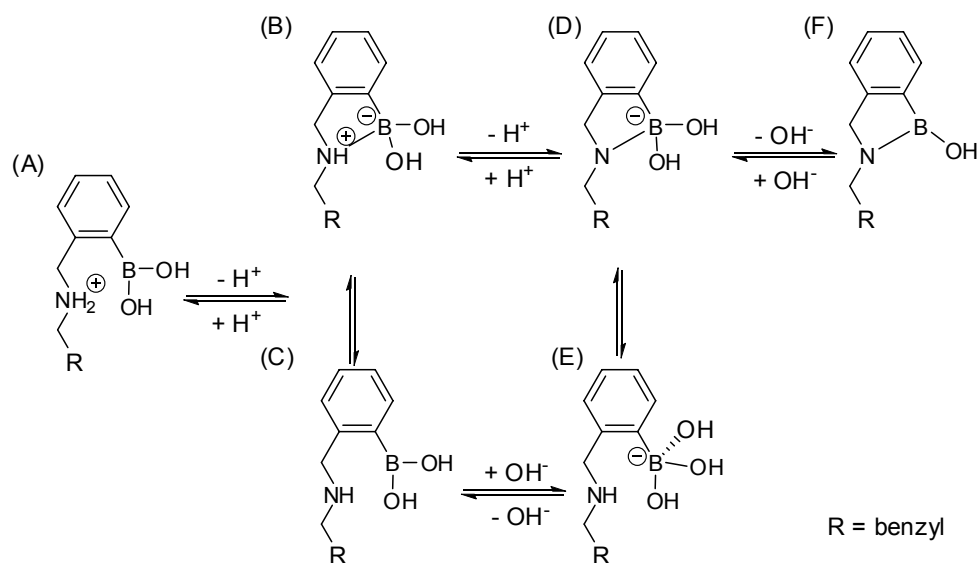
This so-called coordinative or dative bond was first demonstrated by Wulff [25] and although the amine base – boronic acid (N→B or B–N) interaction has been studied for more than 100 years, its exact nature is still under debate [7]. The strength of the B–N bond depends greatly on both the substituents at the nitrogen and the boron centre. The Lewis acidity of the boron centre is further increased by

electron withdrawing substituents, while the Lewis basicity of the nitrogen centre is increased by electron donating substituents. These electronic factors are balanced by counteracting steric requirements and ring strain (in the case of cyclic diesters) that can weaken and elongate the B–N bond [26]. These steric effects weaken the tetrahedral geometry of the boron centre, thereby increasing the pK_a [7]. In solution the B–N interaction is in equilibrium with insertion of protic solvent molecules (solvolyis) [26]. In protic media, solvent insertion instead of the B–N bond is more dominant, thereby resulting in a hydrogen bonded zwitterionic species, whereas in aprotic solvents the species with the full B–N interaction is dominant.

Table 2.1. pK_a values of different (phenyl)boronic acids.

 <p>boronic acid pK_a ~ 9 (BA)</p>	 <p>phenylboronic acid pK_a 8.8 (PBA)</p>	 <p>4-carboxyPBA pK_a 8.0</p>	 <p>2-methoxyPBA pK_a 9.0</p>
 <p>3-acetylPBA pK_a 8.0</p>	 <p>4-acetylPBA pK_a 7.7</p>	 <p>3-formylPBA pK_a 7.8</p>	 <p>4-formylPBA pK_a 7.6</p>
 <p>4-aminomethylPBA pK_a 8.3</p>	 <p>2-dimethylaminomethylPBA pK_a 6.7</p>	 <p>3-aminoPBA pK_a 8.9</p>	 <p>3-nitroPBA pK_a 7.1</p>
 <p>4-bromoPBA pK_a 8.8</p>	 <p>4-fluoroPBA pK_a 8.6</p>	 <p>3-chloro-4-fluoroPBA pK_a 7.8</p>	 <p>2-fluoro-5-nitroPBA pK_a 6.0</p>
 <p>2,4-dichloroPBA pK_a 8.5</p>	 <p>2,4-difluoroPBA pK_a 7.6</p>	 <p>2,5-difluoroPBA pK_a 7.0</p>	 <p>3,4,5-trifluoroPBA pK_a 6.8</p>
 <p>3-pyridinylBA pK_a 8.1</p>	 <p>4-pyridinylBA pK_a 8.0</p>	 <p>N-methyl-3-pyridiniumBA pK_a 4.4</p>	 <p>N-benzyl-3-pyridiniumBA pK_a 4.2</p>

Whiskur *et al.* found that the possibility of a B–N interaction raises the pK_a of the boronic acid by several units (typically to pH 11 – 12), while it reduces the pK_a of the corresponding ammonium ion significantly (typically to pH 5) [20]. The interaction between the amine and the boronic acid results in several equilibria of different geometries for the boron and nitrogen centers at varying pH in water. An example of a thoroughly investigated system, is 2-(*N*-benzylaminomethyl)phenylboronic acid [20]. The protonation equilibria are shown in Scheme 2.2, where the first transition (pK_a) from the deprotonation of the ammonium ion (A) results in the equilibrium between the cyclic (B) and acyclic (C) form, complete B–N interaction and no B–N interaction, respectively. The second transition (pK_a) from can be attributed to either another deprotonation of the amine (D) or hydroxyl addition to the boronic acid centre (E). If the second deprotonation is of the amine, this could lead to hydroxide elimination (F) under dehydrating conditions. The energy of the B–N interaction in 2-(*N*-benzylaminomethyl)phenylboronic acid has been determined from calculations of the stepwise formation constants of potentiometric titrations and found to be in the range of 15–25 kJ mol⁻¹, which is comparable to the energy of a hydrogen bond. [7, 20]

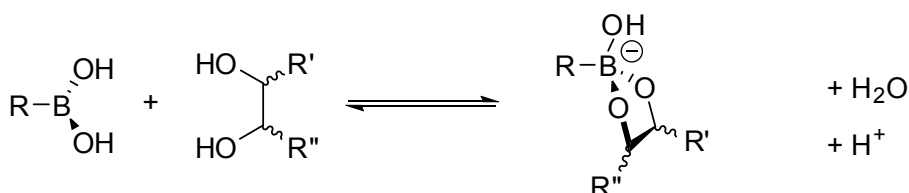


Scheme 2.2. Protonation equilibria in the 2-(*N*-benzylaminomethyl)phenylboronic acid system. The geometry of this compound changes as a function of the pH and the boron–nitrogen interaction. [20]

2.2 Complexation of boronic acids with diols

2.2.1. Diol complexation mechanism

The most important feature of boronic acids is their interaction with diols, resulting in complexation and boronic ester formation. This feature is most relevant for complexation of saccharides, which has a long history and several reviews have been written on this topic, including a recent overview by James [7]. Boronic acids form complexes in solution with hydroxyl groups, preferably with 2 hydroxyl groups in 1,2- and sometimes 1,3-configurations, thereby forming five- and six-membered cyclic esters, respectively. When both possibilities are available, like in many carbohydrates, experimental evidence by Pizer *et al.* [27] indicates that five-membered rings are favored over six-membered rings. Trivalent boronic esters are also acidic and can react with water to release a proton (Scheme 2.3).



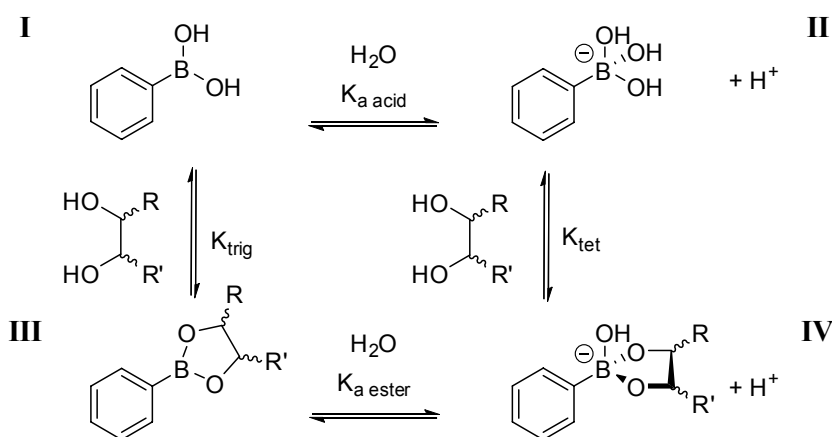
Scheme 2.3. Rapid and reversible formation of a cyclic boronate ester. R, R', and R'' can be alkyl, alkenyl, alkynyl, or aryl

Because of this unique feature, both boronic acids and boronic esters are acids. The rise in acidity upon boronate ester formation can be used to determine binding constants, which is known as the pH depression method. Springsteen and Wang [18, 28-29] reported that the pH-dependency of diol ester formation of a boronic acid is a complicated process and that, in contrast to previous assumptions by Lorand and Edwards [19], the optimal pH for the boronic ester formation is not necessarily above the pK_a of the boronic acid species, where most is in the tetrahedral boronate anion form II (Scheme 2.4).

Generally, a boronic ester is a stronger Lewis acid than a boronic acid, which implies that the equilibrium of addition of a water molecule to the boron center to form the tetrahedral boronate anion under release of a proton is more shifted to the proton production for boronic ester (*i.e.* pK_{a ester} < pK_{a acid}). Consequently, it was widely advocated that a higher pH of the system would result in higher complexation between a diol and a boronic acid, and the lower the pK_a of the boronic acid, the higher the affinity towards diol complexation [7].

The boronic/boronate ester formation is also related to the pK_a of the alcohol, as it was found that the optimal pH for complexation with a catechol (pH *ca.* 4) is much lower than for complexation with ethylene glycol (pH > 7) [30].

This difference is consistent with the relative pK_a of an alkyl alcohol (*ca.* 15.5) versus a phenol (10.0). Since the pH at optimal complexation of phenylboronic acid with a catechol ($pH \sim 4$) is much lower than the pH where formation of the boronate anion is observed ($pH > 6$), this suggests that the neutral phenylboronic acid is the reagent rather than the phenylboronate anion.



Scheme 2.4. The relationships between phenylboronic acid and its diol ester. R, and R', can be alkyl, alkenyl, alkynyl, or aryl

With respect to the B–N interaction, the presence of a vicinal amine group can function as an internal Lewis base and buffer the released proton after boronate ester formation, thereby stabilizing the anionic boronate ester. In general it was found that the presence of amines facilitates boronic/boronate ester formation with diols at reduced (physiological) pH [20, 31].

2.2.2. Complexation of boronic acids with saccharides

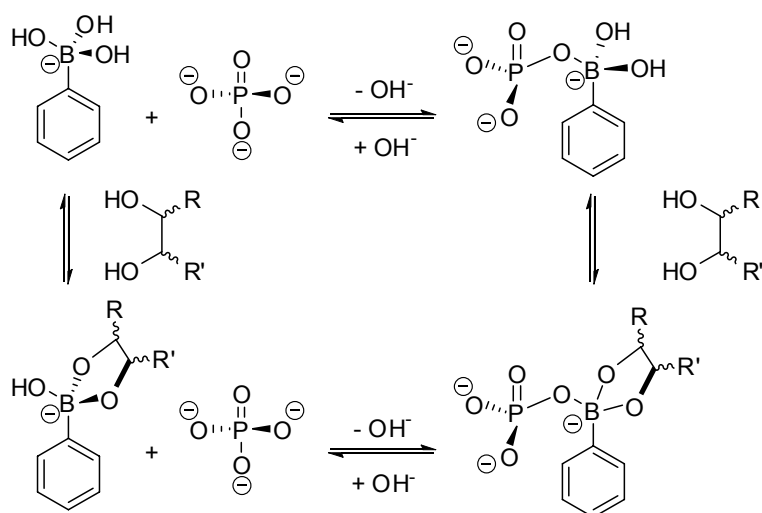
As many sugars bear multiple hydroxyl groups, the affinity of boronic acids to form boronic esters with different saccharides seems obvious. The group of Wang has determined the binding constants between phenylboronic acid (PBA) and many different sugars, using a competitive binding assay with Alizarin red S (ARS), since this compound forms a fluorescent PBA–ARS complex. [18, 28-29, 32-34]. Some saccharides, such as fructose and sorbitol were found to form tridentate complexes with boronic acids, explaining the high binding affinity of boronic acids for these sugars [32]. This method is adopted by other groups and many binding constants have been confirmed while the list is further completed. [35-36]

Since the 1990s, many fluorescent probes based on boronic acids have been developed, in most cases for the detection of saccharides [8, 37-41]. For an extensive overview of this area the reader is referred to the review of James [7].

In theory, a boronic acid can bind any molecule with a 1,2- or a 1,3-diol correctly positioned. This feature makes it possible to use boronic acids for binding and/or recognition of various drug molecules in drug delivery or sensor systems, respectively. Typical, well studied examples of drug molecules that have boronic acid affinity are catechol analogues such as catecholamines, including dopamine, and L-DOPA [42-43], relevant in the treatment of Parkinson's and Alzheimer's disease. All these examples suggest that the incorporation of (phenyl)boronic acids in bioactive polymers could prove very useful in the development of future drug delivery systems [17].

2.2.3. Effect of buffering species on the boronic acid – boronic ester equilibrium

For most applications, especially in the field of biomedical chemistry, boronic acid complexation is most relevant at physiological pH; hence most experiments are conducted in a buffer. It was found that the presence of certain buffer species or other Lewis bases (such as chlorides, bromides, fluorides, or the conjugate base of phosphate) could interfere with the boronic acid–polyhydroxyl complexation as stable complexes between boronic acids and Lewis bases are easily formed [18, 44]. Also ternary complexes can be formed in buffers in which the boronic acid is coordinated with the diol and the Lewis base present in the buffer (Scheme 2.5). These complexes can become significant under acidic conditions and in certain stoichiometric ratios. Since the equilibrium between diols and boronic acids can be heavily disturbed by buffering species, it should be taken into account that the obtained binding constants are strongly depending on the medium in which the experiments are performed.



Scheme 2.5. Interactions of phosphate buffer with phenylboronic acid, affecting the diol complexation.

2.3. Applications of boronic acids

A great variety of boronic acids have been studied for their inhibitory effect on hydrolytic enzymes such as proteases [6, 17]. The theory behind the application of boronic acid compounds as enzyme inhibitors originates from the fact that these compounds can rapidly undergo interconversion from the neutral trigonal planar sp^2 boron to the anionic tetrahedral sp^3 boron under the right conditions, which make these compounds suitable as transition state analogues for the inhibition of hydrolytic enzymes [45-47].

Another application of boronic acids can be found in membrane transport. Westmark *et al.* showed that phenylboronic acid functionalized compounds can be used to transport ribonucleosides through a lipid bilayer membrane [48], but also monosaccharides in and out of liposomes [49]. The boronic acid derivatives can form reversible complexes with diol moieties of sugars and ribonucleosides [50] and upon binding of the boronic acid with the hydrophilic diol compound a lipophilic covalent complex is formed that is extracted into the liquid organic membrane [48]. The selectivity towards transport of different monosaccharides through these membranes follows the known order of sugar-boronate complex stabilities: sorbitol > fructose > glucose >> maltose \geq sucrose [49].

Using boronic acid affinity chromatography, several important biological molecules have been analyzed and purified, including carbohydrates [51], catecholamines [52-53], ribonucleosides [54], proteins [55] and steroids [56-57].

Stolowitz *et al.* [58-59] used the interaction of phenylboronic acid (PBA) with salicylhydroxamic acid (SHA) in affinity column chromatography for protein immobilization. The chemical affinity of the PBA-SHA system was similar to an Avidin or *anti*-hapten antibody column, in which bioconjugates with appended PBA moieties were efficiently immobilized on a SHA-based chromatographic support. This strong PBA-SHA linkage has also been used for hydrogel formation, and will be discussed in more detail in sections 2.3.3 and 2.4.4 [60-62].

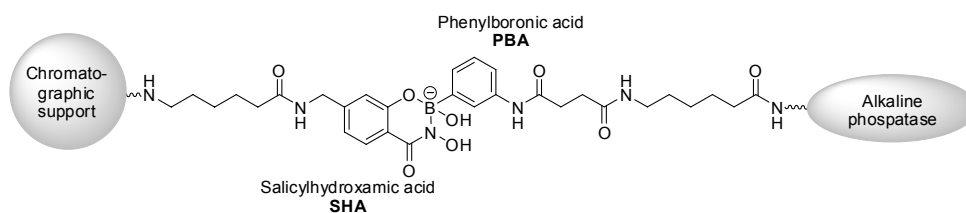


Figure 2.4. A chromatographic support is functionalized with salicylhydroxamic acid (SHA) that can form a reversible covalent ester with phenylboronic acid (PBA) functionalized alkaline phosphatase. The PBA-alkaline phosphatase can be efficiently immobilized over a wide pH-range with anti-body like properties.

2.3.1. Drug delivery systems

As boronic acid compounds were found to interact with cells and in particular with the diols and polyols of glycoproteins on the cell surface [89, 91], boronated materials can be used to develop new drug delivery systems that strongly interact with cells. In the field of drug delivery systems great focus is on development of bioresponsive materials, and especially on delivery systems that can release the drug in response to the presence of certain bioanalytes such as blood sugars or catechols [63]. Boronic acids have thus far played an interesting role in the development of these types of systems, since the equilibrium of complexes of boronic acids with diol compounds such as glucose is depending on temperature, pH, ionic strength, and the concentration of competing diols. As a result boronic acid containing materials are generally thermoresponsive, pH-responsive and chemoresponsive [17]. For example, many studies have been performed to design a boronic acid containing hydrogel that releases insulin in response to an increased blood glucose concentration [64-70]. In most of these cases boronic acids are simply used as sugar binding/sensing moieties, and the group of Kataoka is leading in this field. For example, Shiino *et al.* [64-65] developed a system in which insulin was glyconated, which enabled its binding to boronic acid moieties of gel beads. The glyconated insulin could be released upon the addition of glucose, which is in competition for the complexation with the boronic acid moieties. Another method to release insulin from gels by Kataoka *et al.* [66] makes use of the change in chemical properties of the boronic acid–sugar complex. Insulin was physically entrapped inside a gel with boronic acid moieties. Upon binding of glucose to the boronic acids, these boronate esters complexes become negatively charged and as a result the whole system obtains a more hydrophilic character, resulting in an increased swelling of the gel, thereby accommodating the release of insulin [66-68]. This concept of glucose-induced swelling based insulin release has been adopted by others [69-70], and despite the promising prospects of these stimuli-responsive drug delivery systems, these gels have not yet been used in clinical settings.

2.3.2. Polymeric applications of boronic acids

In the previous sections many interesting applications of (phenyl)boronic acid containing materials have been discussed, thereby focusing on the boronic chemistry. As the functionalization of polymeric materials with boronic acids is an art in itself, in this section more emphasis is on the polymer systems that have been functionalized with (phenyl)boronic acid moieties. For example, the boronic acid functionalized polymers used in glucose sensing typically are hydrophilic materials such as (cross-linked) polyurethanes, polyacrylamides, polyhydroxyethyl methacrylates, polyalcohols, and certain polysaccharides. A successful example is the highly selective

polymer-based fructose sensor by the group of Wang in 1999 [71-72] using a polymerizable methacrylic ester containing a boronic acid saccharide probe.

Boronic acid moieties can also be grafted on an existing polymer system. An example of the latter is given by Sebastian *et al.* [73] who end-capped phosphorhydrazone-based dendrimers with boronic acids, using the Schiff condensation. Also the group of Shinkai functionalized poly(L-lysine) by grafting of 4-chloroformyl phenylboronic acid to the pending amines in order to study conformational changes induced by the boronic acid functionalities in presence of glucose [74]. However, it has also been reported that introducing a high PBA content in polymers results in poor water-solubility [75].

2.3.3. Boronic acids in gene therapy

Until present, boronic acids are only rarely used in the field of gene therapy. To the best of our knowledge, the only relevant available example is a recent communication by Peng *et al.* [76] which describes the enhanced gene transfection capability of a phenylboronic acid functionalized polyethylenimine. Unfortunately, in this communication the PBA-PEI is only compared with the unmodified PEI and no satisfying explanation was provided for the higher transfection efficiency of the PBA-PEI vector due to the lack of a relevant control polymer or additional experiments.

In the work of Moffat *et al.* in 2005 [77] the strong affinity between phenyl(di)boronic acid (PDBA) and salicylhydroxamic acid (SHA) was used to develop a novel polyethylenimine (PEI)-DNA vector formulation that is capable of efficient tumor specific delivery after intravenous administration to nude mice. In their work the peptide CNGRC was attached to the vector, which is specific for aminopeptidase N (CD13), separated by a PEG linker to reduce steric hindrance between the vector and the peptide. *In vitro* assessment showed a 5-fold increase in transfection through targeting by the CNGRC/PEG/PEI/DNA vector carrying a β -galactosidase (β -Gal)-expressing plasmid in various cell lines, relative to the untargeted PEG/PEI/DNA vector. The PDBA-SHA linkage was sufficiently strong for successful intravenous administration of the CNGRC/PEG/PEI/DNA vector to nude mice bearing subcutaneous tumors. Moreover, the presence of the peptide CNGRC was found to result in a 12-fold increase in β -Gal expression in tumors as compared to expression in either lungs or tumors from animals treated with the original PEI/DNA vector. In their follow-up studies in 2006, similar systems based on this linkage were used to study p53-mediated gene therapy [78] and the uptake characteristics of NGR-coupled stealth PEI/DNA nanoparticles loaded with PLGA-PEG-PLGA tri-block copolymer for targeted delivery to human monocyte-derived dendritic cells [79], and to study for targeted delivery *in vitro* in human prostate cancer cells [80-81].

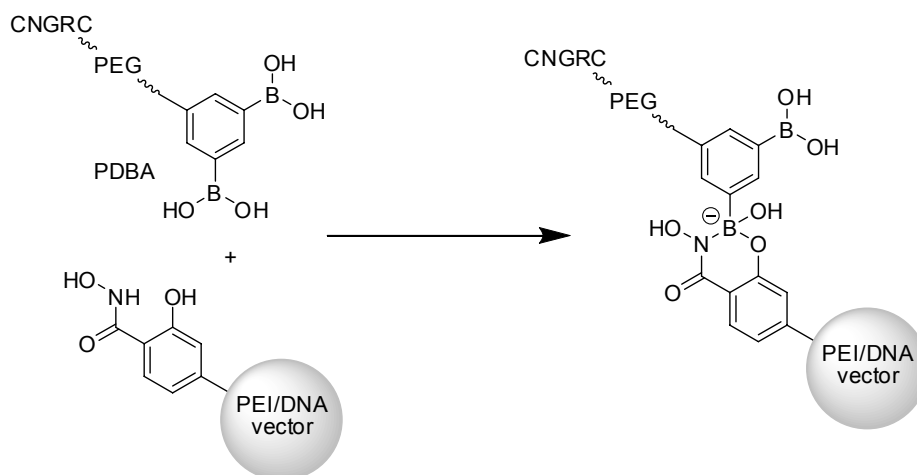


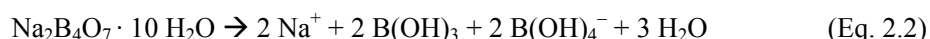
Figure 2.5. Post-PEGylation of a PEI/DNA vector using a phenyl(di)boronic acid (PDBA) functionalized PEG functionalized with the peptide CNGRC that is targeting aminopeptidase N (CD13). The PDBA can form a reversible covalent linkage with salicylhydroxamic acid functionalized PEI yielding a stable bioconjugate.

2.4. Boronic acid gel systems

Nowadays, there is a great attention for bioresponsive hydrogels, especially in the field of time/spatial controlled drug release [82-85]. In order to develop a bioresponsive drug delivery system a hydrogel needs to be either pH responsive [86], temperature responsive [87], and/or chemoresponsive [88]. Boronic acid containing hydrogels meet all these demands, as the boronic acid/diol equilibrium is pH-, temperature-, and chemoresponsive. Moreover, in these hydrogel systems the boronic acid–diol complexation results in the formation of dynamic covalent crosslinks, resulting in gels with “self-healing” properties. All these properties render boronated polymer systems very promising materials for biomedical applications [6]. The work done in this field, mainly involves poly(acrylamides) such as NIPAM, being boronic acid functionalized with peptide coupling techniques [69] or prepared using copolymerization of boronic acid containing monomers [67-68, 89]. Mixing of these boronic acid functionalized polymers with polyols, results in dynamic covalently crosslinked hydrogel systems that are often being employed as (components of) biomaterials. Poly(vinyl alcohol) (PVA) is an example of a frequently used polymeric polyol that interacts strongly with boronic acids. Although water-soluble (co)polymers bearing phenylboronate functions have a great potential in biomedical applications, this is a relatively immature field. In contrast, complex formation between PVA and sodium tetraborate (borax) has been studied extensively and many features that apply to borax–PVA gels also apply to a certain extent for phenylboronated polymer–PVA gels.

2.4.1. Borax PVA gels

At low concentrations in water, anhydrous sodium borate or borax ($\text{Na}_2\text{B}_4\text{O}_7 \cdot 10 \text{H}_2\text{O}$) completely dissociates into sodium ions, boric acid, and (mono)borate according to:



In water, boric acid and borate are in equilibrium with a pK_a of *ca.* 9.2 [90]. Borax can form gels with poly(vinyl alcohol) (PVA) [91-92] and other polyhydroxy macromolecules such as galactomannans (guar gum) [93-94]. The focus in this review will be on PVA as it is highly soluble in water, and it is non-toxic and biocompatible and hence it is FDA-approved for a variety of biomedical applications. The most interesting physical properties are due to the hydrogen bonding ability of the hydroxyl groups of PVA [92], and as a result concentrated aqueous PVA solutions are known to be capable of gelation by temperature quenching [91, 95-96]. Hydrogels from PVA have attracted considerable attention because of their high degree of swelling in water, inherent low toxicity, good biocompatibility, and other desirable properties such as transparency and easy handling. The chemistry involved in the crosslinking of PVA using borax consists of di-diol complexation that is originating from one monoborate and two adjacent diol groups of PVA [90, 97]. The formation of these complexes is very fast, which is unusual in the domain of gels and complexing polymers [98]. The crosslinking mechanism can be divided into two steps: the first step is the reaction in which monodiol complexation results in a six-membered monoborate ring, followed by the actual crosslinking after formation of a di-diol complex (Figure 2.6). This mechanism is also supported by other authors that used other polyhydroxy compounds than PVA to determine the complexation chemistry of borate ions [93] [99].

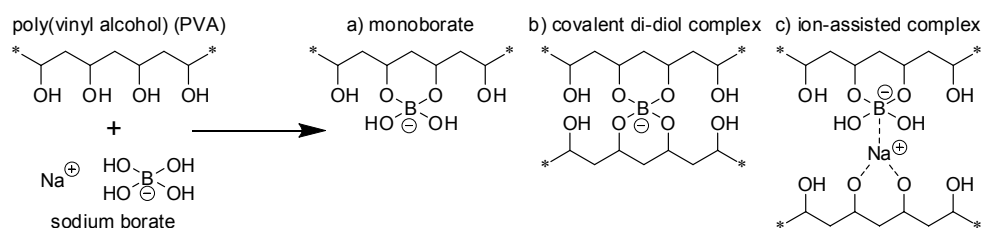


Figure 2.6. PVA can be crosslinked with sodium borate (borax). First a monoborate (a) is formed with the borate and a PVA chain, and then a covalent di-diol complex (b) or an ion-assisted complex (c) is responsible for the formation of a di-diol crosslink.

As opposed to the proposed covalent di-diol complex formation via borate ions directly linked to the PVA chains, it has been suggested by others that the mechanism for borate crosslinking is “ion-assisted” [91-92, 97]. In this scenario, free sodium ions also coordinate with PVA chains and act as counter ions that interact strongly with borate monodiol ions. In this case the crosslink is formed by the ionic interaction between the PVA-bound borate anion and the PVA-chelated sodium cation (Figure 2.6c). Although the mechanism is different, this type of network formation also occurs via di-diol complexation.

PVA-borax systems have found several biomedical applications. An example is described by Loughlin *et al.* [100]. They used a formulation of a PVA-borax gel containing the soluble hydrochloride salt of the anesthetic lidocaine that can be administered locally to sites of lacerations by using the unique flow properties of PVA-borate hydrogels. As the viscoelastic behavior depends on the shear rate, upon vigorous mixing the gel behaves as an elastic solid and can be easily molded into the outline of a wound. Next the gel is left to relax under low shear stress, and the material acts like a viscous liquid and thus completely fills the cavity of the wound during a period of *ca.* 10 minutes, thereby maximizing drug absorption by the surrounding tissue. Despite the viscoelastic behavior, the gel remains as a cohesive mass when it is extricated from the wound site and does not cause further tissue trauma. It was found that the gel demixed into a two-phased system due to the presence of the free ions originating from the HCl salt of the lidocaine, but the addition of a certain amount of the carbohydrate D-mannitol was found to improve the homogeneity of the system again. The release mechanism of the drug lidocaine from the borax–PVA gel was found to be highly dependent on the temperature and the presence of D-mannitol. As this type of gelation is completely reversible, resulting gels are of major interest for biomedical applications as drug delivery systems, especially since these gels are prepared from non-toxic and biocompatible materials, which make these reversible covalent borax-PVA systems superior to most other cross-linked networks.

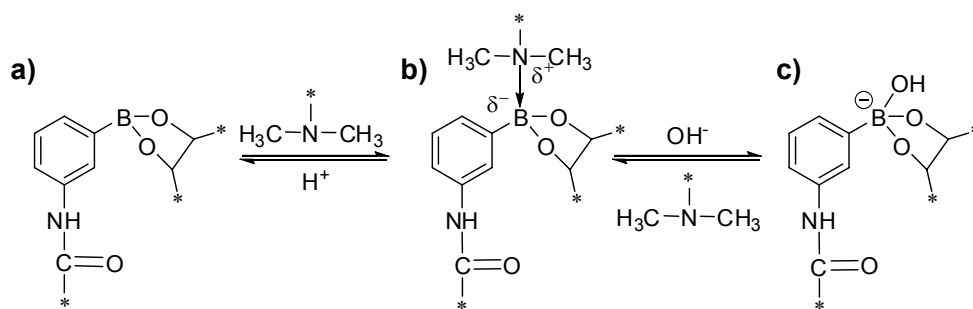
2.4.2. Polymeric boronate gel systems

In contrast to boric acid that functions as a divalent crosslinker of macromolecular polyols such as PVA at basic pH, simple arylboronic acids can form a stronger complex with PVA at lower (physiological relevant) pH. The addition of an arylboronic acid to PVA would only result in the formation of a monodiol complex instead of a productive crosslink, but the introduction of multiple arylboronic acid moieties onto a polymer chain results in the formation of strong hydrogels with PVA in aqueous medium. A single chain of the boronic acid containing polymer can interact with multiple chains of PVA via the formation of monodiol-boronate complexes

that result in productive crosslinks, and through cooperative binding and entanglement the shape-stability of polymeric systems is higher as compared to borax systems.

In 1992 Kitano *et al.* [101] reported a novel type of glucose-responsive drug delivery system based on a polymer complex between PVA and a phenylboronic acid functionalized poly(N-vinylpyrrolidone), abbreviated as p(NVP-co-PBA). The resulting hydrogel was developed for the preparation of a glucose-sensitive insulin delivery system, where the phenylboronic acid moieties incorporated in p(NVP) served as glucose sensors. Reversible exchange of boronate-diol complexes occurs when competing glucose is present that weakens the gel and eventually converts it to a sol at higher glucose concentrations. The insulin incorporated into the polymer gel can then be released from the viscous sol. Kitano *et al.* [101] also found that increasing the PVA molecular weight as well as increasing the polymer concentrations increased the viscosity of the system, and these parameters could be easily adjusted to control the rheological properties of the system.

In 1997 Hisamitsu *et al.* [102] continued the research on these glucose-responsive gel systems. The major drawback of the above described system studied by Kitano *et al.* was the fact that these gels and their glucose sensitive behavior were observed only under alkaline conditions (pH *ca.* 9.0). For biomedical applications, however, such systems are desired to operate under relevant physiological conditions (pH value of *ca.* 7.4). The phenylboronic acid derivative studied by Kitano *et al.* has a pK_a value of *ca.* 8.6, which is close to the pK_a of phenylboronic acid itself with a pK_a value of *ca.* 9 and as a result, the phenylboronate esters with glucose are relatively unstable at physiological pH (see section 2.2.2). In the study of Hisamitsu *et al.* this problem was tackled by incorporating flanking amino groups into the phenylborate polymer that stabilize the boronate-polyol complex by interaction of these amino groups with the boronic center, thereby preventing the nucleophilic attack of a water molecule, and thus protecting the boronic ester (Scheme 2.6).



Scheme 2.6. Phenylboronic ester equilibria in aqueous solution in the presence of flanking amino groups. Upon increasing the pH of the system, the boronic ester goes from the neutral trigonal form at relatively low pH (a) via the species experiencing the B–N interaction at intermediate pH (b) to the anionic form at high pH (c).

In recent work Ivanov *et al.* [103] described the preparation of three different phenylboronate containing constructs onto a silica surface, via chemisorption of epoxy-containing organosilane, graft polymerization, or polyacrylamide gel layer formation. All three constructs had phenylboronate moieties for the adhesion of murine cells through boronate ester formation with polyols at the cell surface. The cells were adhered efficiently after which they proliferated, and the cells could be easily removed after the addition of a fructose solution.

2.4.3. Encapsulation of cells with boronic acid gels

Another interesting PVA/boronic acid polymer system is described by Konno *et al.* [104]. The aim of the study by Konno *et al.* was to develop a gel system that can be used to (temporarily) encapsulate cells. To this purpose a water-soluble phospholipid polymer with pendant boronic acid groups was prepared. This polymer is abbreviated as PMBV (poly(2-methacryloyloxyethyl phosphorylcholine-co-n-butyl methacrylate-co-p-vinylphenylboronic acid)). Hydrogels were prepared under physiological conditions in cell culture medium by mixing of a PMBV solution with a PVA solution. The cells could be seeded uniformly due to the homogeneous hydrogel formation of PVA and PMBV in the cell culture medium. Cells could be encapsulated for one week, after which the gel was dissociated by the addition of excess di- or polyhydroxyl compounds, such as D-glucose. After this procedure the cells adhered and proliferated as usual on a conventional tissue culture plate. This shows that the PMBV–PVA hydrogel can be useful as a cell-container using reversible encapsulation, without any significant adverse effects on the entrapped cells.

2.4.4. PBA-SHA crosslinked gels

Recent literature also deals with other polyhydroxyl macromolecules instead of PVA that yield hydrogels with boronic acid containing polymers. For example, Roberts *et al.* [60-61] used the strong interaction between phenylboronic acids (PBA) and salicylhydroxamic acids (SHA) (also see section 2.3.3) to produce very strong hydrogels at pH 7.4 and weaker gels at low pH 4–6. The gels were formed after mixing of a PBA-functionalized poly(hydroxypropylacrylamide) with a SHA-functionalized poly(hydroxypropylacrylamide). Jay *et al.* [62] studied these materials for application as vaginal gels to reduce the transport of HIV-1 to susceptible tissues and thus prevent the first stage of male-to-female transmission of HIV-1. It was indeed observed that at pH 4.8 transport of the HIV-1 becomes significantly impeded by the matrix.

2.5. Perspectives

Reversible covalent chemistry, such as boronic ester formation, can provide a useful alternative for covalent or ionic interactions, especially in the preparation of

bioconjugates. As described in detail, boronic acids have strong interaction with polyols such as saccharides and PVA, and as a result boronic acid functionalized materials can be used to formulate saccharide-responsive materials, such as glucose-responsive hydrogels for the controlled release of insulin. However, the research of boronic acid containing biomaterials is an immature field, in particular in the field of gene therapy.

Our group has developed a broad range of disulfide containing poly(amido amine)s (SS-PAA)s [105-111]. PAAs are water-soluble and biodegradable polymers that can easily be synthesized from the stepwise polyaddition of primary or secondary aliphatic amines to bisacrylamides. The resulting *tert*-amino polymers have peptide mimicking structures and are known form helixes or random coils, promoting aggregation into nanoparticles, which make them ideal for drug and gene delivery including peptides, proteins, plasmid DNA and siRNA [112-113]. The relatively easy synthesis is compatible with the presence of many different functional groups, which allows for great structural variation, making PAAs ideal for investigation of structure-function relationships. Our group has demonstrated that the introduction of disulfide moieties facilitates rapid intracellular vector unpacking through disulfide degradation and several SS-PAA)s have been developed that combine high transfection efficiencies with low cytotoxicity profiles *in vitro* [105-111]. Also PBA moieties can be easily incorporated in these PAAs and this would in theory result in the development of a novel class of boronated biomaterials, capable of reversible covalent chemistries. Obviously, this would allow for the development of a novel class of glucose-responsive hydrogels, but the introduction of boronic acid functionalities would also be very interesting for the development of novel gene delivery agents. For example, the presence of pending amine or alcohol groups would allow for additional reversible covalent crosslink formation with the phenylboronate moieties within a polyplex nanoparticle formed after mixing with a therapeutic oligonucleotide. Such boronated particles may have additional stability, which is beneficial for the overall delivery process. In addition, it can be expected that boronated PAA nanoparticles have additional cell-adhesive properties as they can bind to glycoproteins on the cell surface, which could prove beneficial for particle uptake, thereby improving the overall delivery efficiency of the therapeutic content. Also the presence of phenylboronate moieties allows for the decoration (*post*-modification) of therapeutic nanoparticles with different mono- or polysaccharides to reduce the particle surface charge or invoke receptor mediated particle uptake altering the intracellular routing of the particles. And last but not least, the presence of the PBA groups would allow additional binding of drug molecules that can form complexes with PBA, like dopamine, which opens avenues for new drug delivery strategies as well as for combined drug and gene delivery.

2.6 References

- [1] M.B. Smith, J. March, *March's advanced organic chemistry: reactions, mechanisms, and structure*, 6 ed., John Wiley & sons, 2007.
- [2] W. Gerrard, *The Organic Chemistry of Boron*, Academic Press, London and New York, 1961.
- [3] H. Steinberg, *Organoboron Chemistry Vol 1: Boron-oxygen and boron-sulfur compounds* Interscience Publishers, John Wiley & Sons, London, 1964.
- [4] H. Steinberg, *Organoboron Chemistry Vol 2: Boron-nitrogen and boron-phosphorus compounds* Interscience Publishers, John Wiley & Sons, London, 1966.
- [5] H.C. Brown, *Boranes in Organic Chemistry*, Cornell University Press, London, 1972.
- [6] D.G. Hall, *Boronic Acids - Preparation and applications in organic synthesis and medicine*, John Wiley & Sons, 2005.
- [7] T.D. James, Saccharide-selective boronic acid based photoinduced electron transfer (PET) fluorescent sensors, *Top. Curr. Chem.*, 277 (2007) 107-152.
- [8] T.D. James, S. Shinkai, Artificial receptors as chemosensors for carbohydrates, *Top. Curr. Chem.*, 218 (2002) 159-200.
- [9] W.G. Woods, An Introduction to boron: history, sources, uses, and chemistry, *Environ. Health Perspect.*, 102 (1994) 5-11.
- [10] E. Bassil, H.N. Hu, P.H. Brown, Use of phenylboronic acids to investigate boron function in plants. possible role of boron in transvacuolar cytoplasmic strands and cell-to-wall adhesion, *Plant Physiol.*, 136 (2004) 3383-3395.
- [11] D.S. Matteson, Boronic esters in stereodirected synthesis, *Tetrahedron*, 45 (1989) 1859-1885.
- [12] N. Balucani, F. Zhang, R.I. Kaiser, Elementary Reactions of Boron Atoms with Hydrocarbons—Toward the Formation of Organo-Boron Compounds, *Chem. Rev.*, 110 (2010) 5107-5127.
- [13] N.R. Candéias, F. Montalbano, P.M.S.D. Cal, P.M.P. Gois, Boronic Acids and Esters in the Petasis-Borono Mannich Multicomponent Reaction, *Chem. Rev.*, 110 (2010) 6169-6193.
- [14] H. Jourdan, G. Gouhier, L. Van Hijfte, P. Angibaud, S.R. Pietre, On the use of boronates in the Petasis reaction, *Tetrahedron Lett.*, 46 (2005) 8027-8031.
- [15] T. Ohe, N. Miyaura, A. Suzuki, Palladium-catalyzed cross-coupling reaction of organoboron compounds with organic triflates, *J. Org. Chem.*, 58 (1993) 2201-2208.
- [16] G.A. Molander, N. Ellis, Organotrifluoroborates: Protected boronic acids that expand the versatility of the Suzuki coupling reaction, *Accounts Chem. Res.*, 40 (2007) 275-286.
- [17] W.Q. Yang, X.M. Gao, B.H. Wang, Boronic acid compounds as potential pharmaceutical agents, *Med. Res. Rev.*, 23 (2003) 346-368.
- [18] J. Yan, G. Springsteen, S. Deeter, B.H. Wang, The relationship among pK(a), pH, and binding constants in the interactions between boronic acids and diols - it is not as simple as it appears, *Tetrahedron*, 60 (2004) 11205-11209.
- [19] J.P. Lorand, J.O. Edwards, Polyol complexes and structure of the benzenboronate ion, *J. Org. Chem.*, 24 (1959) 769-774.
- [20] S.L. Wiskur, J.J. Lavigne, H. Ait-Haddou, V. Lynch, Y.H. Chiu, J.W. Canary, E.V. Anslyn, pK(a) values and geometries of secondary and tertiary amines complexed to boronic acids - Implications for sensor design, *Org. Lett.*, 3 (2001) 1311-1314.
- [21] B.E. Collins, S. Sorey, A.E. Hargrove, S.H. Shabbir, V.M. Lynch, E.V. Anslyn, Probing Intramolecular B-N Interactions in Ortho-Aminomethyl Arylboronic Acids, *J. Org. Chem.*, 74 (2009) 4055-4060.
- [22] A. Adameczyk-Wozniak, Z. Brzozka, M.K. Cyranski, A. Filipowicz-Szymanska, P. Klimentowska, A. Zubrowska, K. Zukowski, A. Sporzynski, ortho-(aminomethyl) phenyl boronic acids - synthesis, structure and sugar receptor activity, *Appl. Organomet. Chem.*, 22 (2008) 427-432.
- [23] E. Galbraith, A.M. Kelly, J.S. Fossey, G. Kociok-Kohn, M.G. Davidson, S.D. Bull, T.D. James, Dynamic covalent self-assembled macrocycles prepared from 2-formyl-aryl-boronic acids and 1,2-amino alcohols, *New J. Chem.*, 33 (2009) 181-185.
- [24] M. Biedrzycki, W.H. Scouten, Z. Biedrzycka, Derivatives of tetrahedral boronic acids, *J. Organomet. Chem.*, 431 (1992) 255-270.
- [25] G. Wulff, Selective binding to polymers via covalent bonds - the construction of chiral cavities as specific receptor-sites, *Pure Appl. Chem.*, 54 (1982) 2093-2102.
- [26] L. Zhu, S.H. Shabbir, M. Gray, V.M. Lynch, S. Sorey, E.V. Anslyn, A structural investigation of the N-B interaction in an o-(N,N-dialkylaminomethyl)arylboronate system, *J. Am. Chem. Soc.*, 128 (2006) 1222-1232.

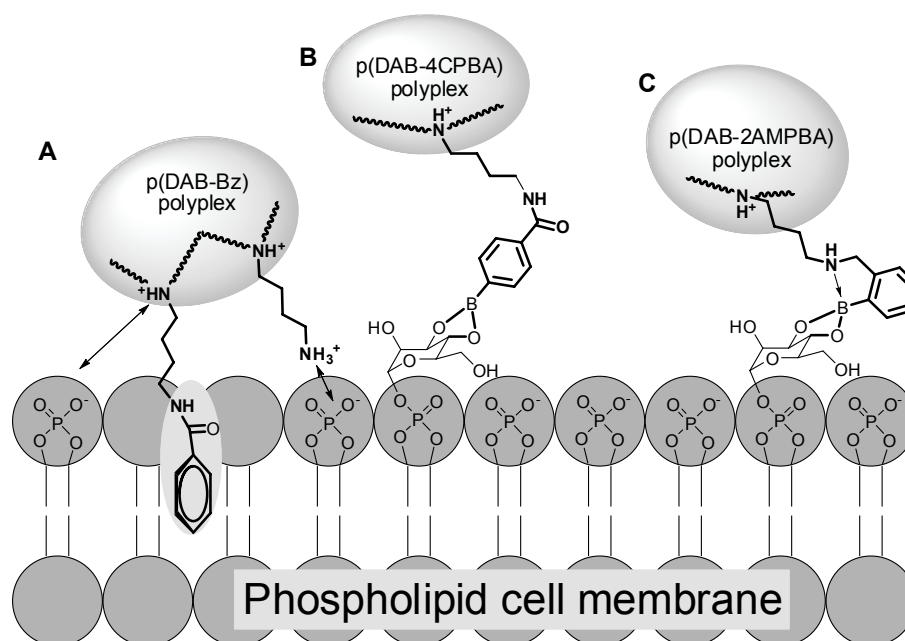
- [27] R. Pizer, C. Tihal, Equilibria and Reaction-Mechanism of the Complexation of Methylboronic Acid with Polyols, *Inorg. Chem.*, 31 (1992) 3243-3247.
- [28] G. Springsteen, B.H. Wang, Alizarin Red S. as a general optical reporter for studying the binding of boronic acids with carbohydrates, *Chem. Commun.*, (2001) 1608-1609.
- [29] G. Springsteen, B.H. Wang, A detailed examination of boronic acid-diol complexation, *Tetrahedron*, 58 (2002) 5291-5300.
- [30] M. Bishop, N. Shahid, J.Z. Yang, A.R. Barron, Determination of the mode and efficacy of the cross-linking of guar by borate using MAS B-11 NMR of borate cross-linked guar in combination with solution B-11 NMR of model systems, *Dalton T.*, (2004) 2621-2634.
- [31] H. Otsuka, E. Uchimura, H. Koshino, T. Okano, K. Kataoka, Anomalous binding profile of phenylboronic acid with N-acetylneuraminic acid (Neu5Ac) in aqueous solution with varying pH, *J. Am. Chem. Soc.*, 125 (2003) 3493-3502.
- [32] J. Yan, H. Fang, B.H. Wang, Boronolactins and fluorescent boronolactins: An examination of the detailed chemistry issues important for the design, *Med. Res. Rev.*, 25 (2005) 490-520.
- [33] W.Q. Yang, L. Lin, B.H. Wang, A new type of boronic acid fluorescent reporter compound for sugar recognition, *Tetrahedron Lett.*, 46 (2005) 7981-7984.
- [34] W.Q. Yang, J. Yan, G. Springsteen, S. Deeter, B.H. Wang, A novel type of fluorescent boronic acid that shows large fluorescence intensity changes upon binding with a carbohydrate in aqueous solution at physiological pH, *Bioorg. Med. Chem. Lett.*, 13 (2003) 1019-1022.
- [35] B. Elmas, S. Senel, A. Tuncel, A new thermosensitive fluorescent probe for diol sensing: Poly(N-isopropylacrylamide-co-vinylphenylboronic acid)-alizarin red S complex, *React. Funct. Polym.*, 67 (2007) 87-96.
- [36] Q.S. Wang, G.Q. Li, W.Y. Mao, H.X. Qi, G.W. Li, Glucose-responsive vesicular sensor based on boronic acid-glucose recognition in the ARS/PBA/DBBTAB covesicles, *Sensor Actuat. B-Chem.*, 119 (2006) 695-700.
- [37] B. Appleton, T.D. Gibson, Detection of total sugar concentration using photoinduced electron transfer materials: development of operationally stable, reusable optical sensors, *Sensor Actuat. B-Chem.*, 65 (2000) 302-304.
- [38] H.R. Mulla, N.J. Agard, A. Basu, 3-methoxycarbonyl-5-nitrophenyl boronic acid: high affinity diol recognition at neutral pH, *Bioorg. Med. Chem. Lett.*, 14 (2004) 25-27.
- [39] T.D. James, K.R.A.S. Sandanayake, S. Shinkai, A Glucose-Selective Molecular Fluorescence Sensor, *Angew. Chem. Int. Edit.*, 33 (1994) 2207-2209.
- [40] J. Boeseken, The Use of Boric Acid for the Determination of the Configuration of Carbohydrates, *Adv. Carbohydr. Chem.*, 4 (1949) 189-210.
- [41] H.S. Mader, O.S. Wolfbeis, Boronic acid based probes for microdetermination of saccharides and glycosylated biomolecules, *Microchim. Acta*, 162 (2008) 1-34.
- [42] A. Coskun, E.U. Akkaya, Three-point recognition and selective fluorescence sensing of L-DOPA, *Org. Lett.*, 6 (2004) 3107-3109.
- [43] J. Yoon, A.W. Czarnik, Fluorescent chemosensing of catechol and catecholamines in water, *Bioorg. Med. Chem.*, 1 (1993) 267-271.
- [44] L.I. Bosch, T.M. Fyles, T.D. James, Binary and ternary phenylboronic acid complexes with saccharides and Lewis bases, *Tetrahedron*, 60 (2004) 11175-11190.
- [45] I. Georgiou, G. Ilyashenko, A. Whiting, Synthesis of aminoboronic acids and their applications in bifunctional catalysis, *Accounts Chem. Res.*, 42 (2009) 756-768.
- [46] A. Minkkilä, S.M. Saario, H. Kašnañen, J. Leppänen, A. Poso, T. Nevalainen, Discovery of boronic acids as novel and potent inhibitors of fatty acid amide hydrolase, *J. Med. Chem.*, 51 (2008) 7057-7060.
- [47] S.J. Coutts, T.A. Kelly, R.J. Snow, C.A. Kennedy, R.W. Barton, J. Adams, D.A. Krolikowski, D.M. Freeman, S.J. Campbell, J.F. Ksiazek, W.W. Bachovchin, Structure-activity relationships of boronic acid inhibitors of dipeptidyl peptidase IV .1. Variation of the P-2 position of X(aa)-boroPro dipeptides, *J. Med. Chem.*, 39 (1996) 2087-2094.
- [48] P.R. Westmark, B.D. Smith, Boronic acids facilitate the transport of ribonucleosides through lipid bilayers, *J. Pharm. Sci.*, 85 (1996) 266-269.
- [49] P.R. Westmark, S.J. Gardiner, B.D. Smith, Selective monosaccharide transport through lipid bilayers using boronic acid carriers, *J. Am. Chem. Soc.*, 118 (1996) 11093-11100.
- [50] M.J. Karpa, P.J. Duggan, G.J. Griffin, S.J. Freudigmann, Competitive transport of reducing sugars through a lipophilic membrane facilitated by aryl boron acids, *Tetrahedron*, 53 (1997) 3669-3678.
- [51] A.E. Ivanov, H.A. Panahi, M.V. Kuzimenkova, L. Nilsson, B. Bergenstahl, H.S. Waqif, M. Jahanshahi, I.Y. Galaev, B. Mattiasson, Affinity adhesion of carbohydrate particles and yeast cells to boronate-containing polymer brushes grafted onto siliceous supports, *Chem-Eur. J.*, 12 (2006) 7204-7214.

- [52] B.M. Eriksson, M. Wikstrom, Determination of Vanilmandelic Acid in Urine by Coupled-Column Liquid-Chromatography Combining Affinity to Boronate and Separation by Anion-Exchange, *J. Chromatogr.-Biomed.*, 567 (1991) 1-9.
- [53] B.M. Eriksson, M. Wikstrom, Determination of Catecholamines in Urine by Liquid-Chromatography and Electrochemical Detection after Online Sample Purification on Immobilized Boronic Acid, *J. Chromatogr.*, 593 (1992) 185-190.
- [54] A.E. Ivanov, I.Y. Galaev, B. Mattiasson, Binding of adenosine to pendant phenylboronate groups of thermoresponsive copolymer: a quantitative study, *Macromol Biosci.*, 5 (2005) 795-800.
- [55] F. Frantzen, K. Grimsrud, D.E. Heggli, E. Sundrehagen, Protein-Boronic Acid Conjugates and Their Binding to Low-Molecular-Mass Cis-Diols and Glycated Hemoglobin, *J. Chromatogr. B*, 670 (1995) 37-45.
- [56] K. Gamoh, S. Takatsuto, A Boronic Acid-Derivative as a Highly Sensitive Fluorescence Derivatization Reagent for Brassinosteroids in Liquid-Chromatography, *Anal. Chim. Acta*, 222 (1989) 201-204.
- [57] V.D. Gildengorn, Reversed-phase affinity chromatography of ecdysteroids with boronic acid-containing eluents, *J. Chromatogr. A*, 730 (1996) 147-152.
- [58] M.L. Stollowitz, C. Ahlem, K.A. Hughes, R.J. Kaiser, E.A. Kesicki, G.S. Li, K.P. Lund, S.M. Torkelson, J.P. Wiley, Phenylboronic acid-salicylhydroxamic acid biconjugates. 1. A novel boronic acid complex for protein immobilization, *Bioconjugate Chem.*, 12 (2001) 229-239.
- [59] J.P. Wiley, K.A. Hughes, R.J. Kaiser, E.A. Kesicki, K.P. Lund, M.L. Stollowitz, Phenylboronic acid-salicylhydroxamic acid biconjugates. 2. Polyvalent immobilization of protein ligands for affinity chromatography, *Bioconjugate Chem.*, 12 (2001) 240-250.
- [60] M.C. Roberts, M.C. Hanson, A.P. Massey, E.A. Karren, P.F. Kiser, Dynamically restructuring hydrogel networks formed with reversible covalent crosslinks, *Adv. Mater.*, 19 (2007) 2503-2507.
- [61] M.C. Roberts, A. Mahalingam, M.C. Hanson, P.F. Kiser, Chemorheology of phenylboronate-salicylhydroxamate cross-linked hydrogel networks with a sulfonated polymer backbone, *Macromolecules*, 41 (2008) 8832-8840.
- [62] J.I. Jay, S. Shukair, K. Langheinrich, M.C. Hanson, G.C. Cianci, T.J. Johnson, M.R. Clark, T.J. Hope, P.F. Kiser, Modulation of viscoelasticity and HIV transport as a function of pH in a reversibly crosslinked hydrogel, *Adv. Funct. Mater.*, 19 (2009) 2969-2977.
- [63] S. Ganta, H. Devalapally, A. Shahiwala, M. Amiji, A review of stimuli-responsive nanocarriers for drug and gene delivery, *J. Control. Release*, 126 (2008) 187-204.
- [64] D. Shiino, Y. Murata, K. Kataoka, Y. Koyama, M. Yokoyama, T. Okano, Y. Sakurai, Preparation and characterization of a glucose-responsive insulin-releasing polymer device, *Biomaterials*, 15 (1994) 121-128.
- [65] D. Shiino, Y. Murata, A. Kubo, Y.J. Kim, K. Kataoka, Y. Koyama, A. Kikuchi, M. Yokoyama, Y. Sakurai, T. Okano, Amine containing phenylboronic acid gel for glucose-responsive insulin release under physiological pH, *J. Control. Release* 37 (1995) 269-276.
- [66] K. Kataoka, H. Miyazaki, M. Bunya, T. Okano, Y. Sakurai, Totally synthetic polymer gels responding to external glucose concentration: Their preparation and application to on-off regulation of insulin release, *J. Am. Chem. Soc.*, 120 (1998) 12694-12695.
- [67] A. Matsumoto, S. Ikeda, A. Harada, K. Kataoka, Glucose-responsive polymer bearing a novel phenylborate derivative as a glucose-sensing moiety operating at physiological pH conditions, *Biomacromolecules*, 4 (2003) 1410-1416.
- [68] A. Matsumoto, R. Yoshida, K. Kataoka, Glucose-responsive polymer gel bearing phenylborate derivative as a glucose-sensing moiety operating at the physiological pH, *Biomacromolecules*, 5 (2004) 1038-1045.
- [69] T. Hoare, R. Pelton, Engineering glucose swelling responses in poly(N-isopropylacrylamide)-based microgels, *Macromolecules*, 40 (2007) 670-678.
- [70] S.B. Zhang, L.Y. Chu, D. Xu, J. Zhang, X.J. Ju, R. Xie, Poly(N-isopropylacrylamide)-based comb-type grafted hydrogel with rapid response to blood glucose concentration change at physiological temperature, *Polym. Advan. Technol.*, 19 (2008) 937-943.
- [71] W. Wang, S.H. Gao, B.H. Wang, Building fluorescent sensors by template polymerization: The preparation of a fluorescent sensor for D-Fructose, *Org. Lett.*, 1 (1999) 1209-1212.
- [72] S.H. Gao, W. Wang, B.H. Wang, Building fluorescent sensors for carbohydrates using template-directed polymerizations, *Bioorg. Chem.*, 29 (2001) 308-320.
- [73] R.M. Sebastian, G. Magro, A.M. Caminade, J.P. Majoral, Dendrimers with N,N-disubstituted hydrazines as end groups, useful precursors for the synthesis of water-soluble dendrimers capped with carbohydrate, carboxylic or boronic acid derivatives, *Tetrahedron*, 56 (2000) 6269-6277.

- [74] H. Kobayashi, K. Nakashima, E. Ohshima, Y. Hisaeda, I. Hamachi, S. Shinkai, Novel saccharide-induced conformational changes in a boronic acid-appended poly(L-lysine) as detected by circular dichroism and fluorescence, *J. Chem. Soc. Perk. T. 2*, 5 (2000) 997-1002.
- [75] S.T. Camli, S. Senel, A. Tuncel, Nucleotide isolation by boronic acid functionalized hydrophilic supports, *Colloid Surface A*, 207 (2002) 127-137.
- [76] Q. Peng, F. Chen, Z. Zhong, R. Zhuo, Enhanced gene transfection capability of polyethylenimine by incorporating boronic acid groups, *Chem. Commun.*, 46 (2010) 5888-5890.
- [77] S. Moffatt, S. Wiehle, R.J. Cristiano, Tumor-specific gene delivery mediated by a novel peptide-polyethylenimine-DNA polyplex targeting aminopeptidase N/CD13, *Hum. Gene Ther.*, 16 (2005) 57-67.
- [78] S. Moffatt, S. Wiehle, R.J. Cristiano, A multifunctional PEI-based cationic polyplex for enhanced systemic p53-mediated gene therapy, *Gene Ther.*, 13 (2006) 1512-1523.
- [79] S. Moffatt, R.J. Cristiano, Uptake characteristics of NGR-coupled stealth PEI/pDNA nanoparticles loaded with PLGA-PEG-PLGA tri-block copolymer for targeted delivery to human monocyte-derived dendritic cells, *Int. J. Pharmaceut.*, 321 (2006) 143-154.
- [80] S. Moffatt, R.J. Cristiano, PEGylated J591 mAb loaded in PLGA-PEG-PLGA tri-block copolymer for targeted delivery: In vitro evaluation in human prostate cancer cells, *Int. J. Pharm.*, 317 (2006) 10-13.
- [81] S. Moffatt, C. Papasakelariou, S. Wiehle, R. Cristiano, Successful in vivo tumor targeting of prostate-specific membrane antigen with a highly efficient J591//PEI//DNA molecular conjugate, *Gene Ther.*, 13 (2006) 761-772.
- [82] S. Chaterji, I.K. Kwon, K. Park, Smart polymeric gels: Redefining the limits of biomedical devices, *Prog. Polym. Sci.*, 32 (2007) 1083-1122.
- [83] A.S. Hoffman, Hydrogels for biomedical applications, *Adv. Drug Deliv. Rev.*, 54 (2002) 3-12.
- [84] N.A. Peppas, P. Bures, W. Leobandung, H. Ichikawa, Hydrogels in pharmaceutical formulations, *Eur. J. Pharm. Biopharm.*, 50 (2000) 27-46.
- [85] N.A. Peppas, J.Z. Hilt, A. Khademhosseini, R. Langer, Hydrogels in biology and medicine: From molecular principles to bionanotechnology, *Adv. Mater.*, 18 (2006) 1345-1360.
- [86] P. Gupta, K. Vermani, S. Garg, Hydrogels: from controlled release to pH-responsive drug delivery, *Drug Discov. Today*, 7 (2002) 569-579.
- [87] W. Agut, A. Brulet, D. Taton, S. Lecommandoux, Thermoresponsive micelles from jeffamine-b-poly(L-glutamic acid) double hydrophilic block copolymers, *Langmuir*, 23 (2007) 11526-11533.
- [88] G.H. Deng, C.M. Tang, F.Y. Li, H.F. Jiang, Y.M. Chen, Covalent cross-linked polymer gels with reversible sol-gel transition and self-healing properties, *Macromolecules*, 43 (2010) 1191-1194.
- [89] P. Hazot, T. Delair, A. Elaissari, J.P. Chapel, C. Pichot, Functionalization of poly(N-ethylmethacryl-amide) thermosensitive particles by phenylboronic acid, *Colloid Polym. Sci.*, 280 (2002) 637-646.
- [90] S.W. Sinton, Complexation chemistry of sodium-borate with poly(vinyl-alcohol) and small diols - a B-11 NMR-study, *Macromolecules*, 20 (1987) 2430-2441.
- [91] M. Shibayama, Y. Hiroyuki, K. Hidenobu, F. Hiroshi, N. Shunji, Sol-gel transition of poly(vinyl alcohol)-borate complex, *Polymer*, 29 (1988) 2066-2071.
- [92] M. Shibayama, M. Sato, Y. Kimura, H. Fujiwara, S. Nomura, ¹¹B n.m.r. study on the reaction of poly(vinyl alcohol) with boric acid, *Polymer*, 29 (1988) 336-340.
- [93] E. Pezron, L. Leibler, A. Ricard, R. Audebert, Reversible gel formation induced by ion complexation .2. Phase-diagrams, *Macromolecules*, 21 (1988) 1126-1131.
- [94] S.J. Gao, J.M. Guo, L.L. Wu, S. Wang, Gelation of konjac glucomannan crosslinked by organic borate, *Carbohydr. Polym.*, 73 (2008) 498-505.
- [95] M. Shibayama, R. Moriwaki, F. Ikkai, S. Nomura, Viscosity Behavior of Weakly Charged Polymer Ion Complexes Comprising Poly(Vinyl Alcohol) and Congo Red, *Polymer*, 35 (1994) 5716-5721.
- [96] D. Mawad, R. Odell, L.A. Poole-Warren, Network structure and macromolecular drug release from poly(vinyl alcohol) hydrogels fabricated via two crosslinking strategies, *Int. J. Pharm.*, 366 (2009) 31-37.
- [97] H. Kurokawa, M. Shibayama, T. Ishimaru, S. Nomura, W.I. Wu, Phase-Behavior and Sol-Gel Transition of Poly(Vinyl Alcohol) Borate Complex in Aqueous-Solution, *Polymer*, 33 (1992) 2182-2188.
- [98] G. Keita, A. Ricard, R. Audebert, E. Pezron, L. Leibler, The Poly(Vinyl Alcohol) Borate System - Influence of Polyelectrolyte Effects on Phase-Diagrams, *Polymer*, 36 (1995) 49-54.
- [99] M. Vanduin, J.A. Peters, A.P.G. Kieboom, H. Vanbekkum, The Ph-Dependence of the Stability of Esters of Boric-Acid and Borate in Aqueous-Medium as Studied by B-11 Nmr, *Tetrahedron*, 40 (1984) 2901-2911.

- [100] R.G. Loughlin, M.M. Tunney, R.F. Donnelly, D.F. Murphy, M. Jenkins, P.A. McCarron, Modulation of gel formation and drug-release characteristics of lidocaine-loaded poly(vinyl alcohol)-tetraborate hydrogel systems using scavenger polyol sugars, *Eur. J. Pharm. Biopharm.*, 69 (2008) 1135-1146.
- [101] S. Kitano, Y. Koyama, K. Kataoka, T. Okano, Y. Sakurai, A novel drug delivery system utilizing a glucose responsive polymer complex between poly (vinyl alcohol) and poly (N-vinyl-2-pyrrolidone) with a phenylboronic acid moiety, *J. Control. Release*, 19 (1992) 161-170.
- [102] I. Hisamitsu, K. Kataoka, T. Okano, Y. Sakurai, Glucose-responsive gel from phenylborate polymer and poly(vinyl alcohol): Prompt response at physiological pH through the interaction of borate with amine group in the gel, *Pharmaceut. Res.*, 14 (1997) 289-293.
- [103] A.E. Ivanov, A. Kumar, S. Nilsang, M.R. Aguilar, L.I. Mikhalovska, I.N. Savina, L. Nilsson, I.G. Scheblykin, M.V. Kuzimenkova, I.Y. Galaev, Evaluation of boronate-containing polymer brushes and gels as substrates for carbohydrate-mediated adhesion and cultivation of animal cells, *Colloid Surface B*, 75 (2010) 510-519.
- [104] T. Konno, K. Ishihara, Temporal and spatially controllable cell encapsulation using a water-soluble phospholipid polymer with phenylboronic acid moiety, *Biomaterials*, 28 (2007) 1770-1777.
- [105] C. Lin, C.J. Blaauboer, M.M. Timoneda, M.C. Lok, M. van Steenberg, W.E. Hennink, Z.Y. Zhong, J. Feijen, J.F.J. Engbersen, Bioreducible poly(amido amine)s with oligoamine side chains: Synthesis, characterization, and structural effects on gene delivery, *J. Control. Release*, 126 (2008) 166-174.
- [106] C. Lin, Z.Y. Zhong, M.C. Lok, X.L. Jiang, W.E. Hennink, J. Feijen, J.F.J. Engbersen, Linear poly(amido amine)s with secondary and tertiary amino groups and variable amounts of disulfide linkages: Synthesis and in vitro gene transfer properties, *J. Control. Release*, 116 (2006) 130-137.
- [107] C. Lin, Z.Y. Zhong, M.C. Lok, X.L. Jiang, W.E. Hennink, J. Feijen, J.F.J. Engbersen, Novel bioreducible poly(amido amine)s for highly efficient gene delivery, *Bioconjugate Chem.*, 18 (2007) 138-145.
- [108] M.A. Mateos-Timoneda, M.C. Lok, W.E. Hennink, J. Feijen, J.F.J. Engbersen, Poly(amido amine)s as gene delivery vectors: Effects of quaternary nicotinamide moieties in the side chains, *Chemmedchem*, 3 (2008) 478-486.
- [109] M. Piest, C. Lin, M.A. Mateos-Timoneda, M.C. Lok, W.E. Hennink, J. Feijen, J.F.J. Engbersen, Novel poly(amido amine)s with bioreducible disulfide linkages in their diamino-units: Structure effects and in vitro gene transfer properties, *J. Control. Release*, 130 (2008) 38-45.
- [110] M. Piest, J.F.J. Engbersen, Effects of charge density and hydrophobicity of poly(amido amine)s for non-viral gene delivery, *J. Control. Release*, 148 (2010) 83-90.
- [111] L.V. Christensen, C.W. Chang, W.J. Kim, S.W. Kim, Z.Y. Zhong, C. Lin, J.F.J. Engbersen, J. Feijen, Reducible poly(amido ethylenimine)s designed for triggered intracellular gene delivery, *Bioconjugate Chem.*, 17 (2006) 1233-1240.
- [112] P. Ferruti, M.A. Marchisio, R. Duncan, Poly(amido-amine)s: Biomedical applications, *Macromol. Rapid Comm.*, 23 (2002) 332-355.
- [113] S.C.W. Richardson, N.G. Patrick, N. Lavignac, P. Ferruti, R. Duncan, Intracellular fate of bioresponsive poly(amidoamine)s in vitro and in vivo, *J. Control. Release*, 142 (2010) 78-88.

Role of boronic acid moieties in poly(amido amine)s for non-viral gene delivery



Abstract

The effects of the presence of two different types of phenylboronic acids as side groups in disulfide-containing poly(amido amine)s (SS-PAA) were investigated in their effectiveness to function as gene delivery vectors. To this purpose, a para-carboxyphenylboronic acid was grafted on a SS-PAA with pending aminobutyl side chains, resulting in p(DAB-4CPBA) and an ortho-aminomethylphenylboronic acid was incorporated through copolymerization, resulting in p(DAB-2AMPBA). Both polymers have 30% of phenylboronic acid side chains and 70% of residual aminobutyl side chains and were compared with a non-boronated benzoylated analogue p(DAB-Bz) of similar Mw. It was found that the presence of phenylboronic acid moieties improved polyplex formation with plasmid DNA as smaller and more monodisperse polyplexes were formed as compared to their non-boronated counterparts. The transfection efficiency of polyplexes of p(DAB-4CPBA) was approximately similar to that of p(DAB-Bz) and commercial PEI (Exgen), both in the absence and the presence of serum, indicating that p(DAB-4CPBA) and p(DAB-Bz) are potent gene delivery vectors. However, the polymers with phenylboronic acid functionalities showed increased cytotoxicity, which is stronger for the ortho-aminophenylboronic acid containing polyplexes of p(DAB-2AMPBA) than for the p(DAB-4CPBA) analog. The cytotoxic effect may be caused by increased membrane disruptive interaction as was indicated by the increased hemolytic activity observed for these polymers.

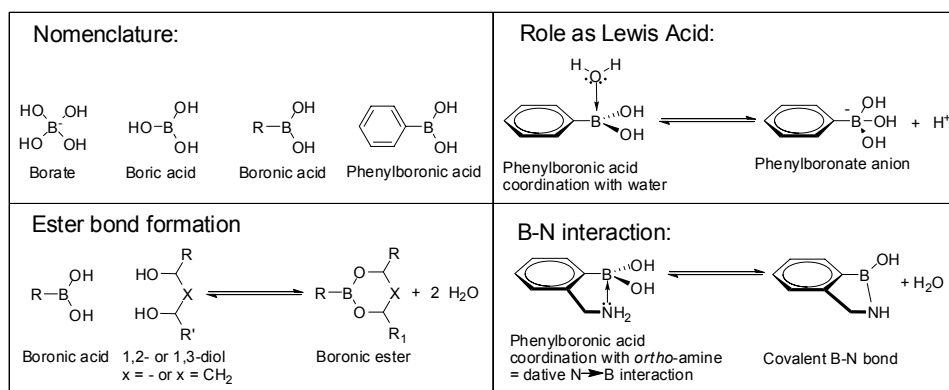
3.1 Introduction

Gene therapy is a promising technique to cure various metabolic diseases by administration of a therapeutic “healthy” gene to compensate for a malfunctioning gene in the body. The greatest challenge in gene therapy is delivery, which can be improved using vectors to efficiently transport therapeutic genes into target cells [1]. For example, adeno-associated or recombinant viral vectors are characterized by highly efficient transfection and long-term gene expression, but viral vectors are also plagued by potential risk on safety and immune responses [2]. In contrast, cationic polymeric vectors are considered to be safer, but generally show much lower efficiency [3-7]. One very interesting class of materials are poly(amido amine)s (PAAs), since their synthesis by poly Michael addition of primary or bis(secondary) amines to bis(acrylamides) allows for large structural variation of the main chain and side chains of the polymer. These polymers are typically well soluble in water and their structure can be tuned to form stable nanoparticles that can be used for delivery of a great variety of therapeutic molecules including peptides, plasmid DNA, and siRNA [8].

Previously, our group has developed a broad range of disulfide-based poly(amido amine)s (SS-PAAs) for the delivery of therapeutic plasmid DNA. We showed that the presence of repetitive disulfide bonds in the polymer main chain facilitated the DNA release in the reductive environment of the cytosol through disulfide bond reduction, causing fast degradation of the polymer [9-13]. The charge density of the polymer can be relatively tuned by introduction of aminobutyl side chains that can be partially acylated, as was shown in a recent study for poly(cystamine bisacrylamide/diaminobutane) (abbreviated as p(DAB)) [14]. In the present study we have investigated the effects of the presence of phenylboronic acids in the side chains of SS-PAAs on DNA condensation and transfection properties. Boronic acids are a class of compounds that have interesting binding properties to vicinal diols, notably carbohydrate moieties, and an overview of boronic acid chemistry is presented in Scheme 3.1.

Boronic acids are organic derivatives of boric acid and one of the most important properties is the possibility of reversible ester bond formation with alcohols, preferably *cis*-1,2- and 1,3-diols. The resulting boronic ester can be neutral sp^2 hybridized or anionic sp^3 hybridized and the equilibrium is depending on the pK_a of the alcohol moieties, the pK_a of the boronic acid (typical 10 for alkylboronic acids) and the local environment. It was found that phenylboronic acids can form boronic esters at lower pH (*ca.* 9), since the phenyl ring increases the electron deficiency of the boron centre and increases its role as Lewis acid [15]. In addition, an amine group in the *ortho* position with respect to the boronic acid can significantly increase the pK_a of the boronic acid (from *ca.* 9 to > 11) and decrease the pK_a of the secondary amine (from *ca.* 9 to 5) through formation of a dative boron nitrogen bond [16].

This so-called dative B–N (or N→B) interaction could enhance diol complexation at physiological pH.

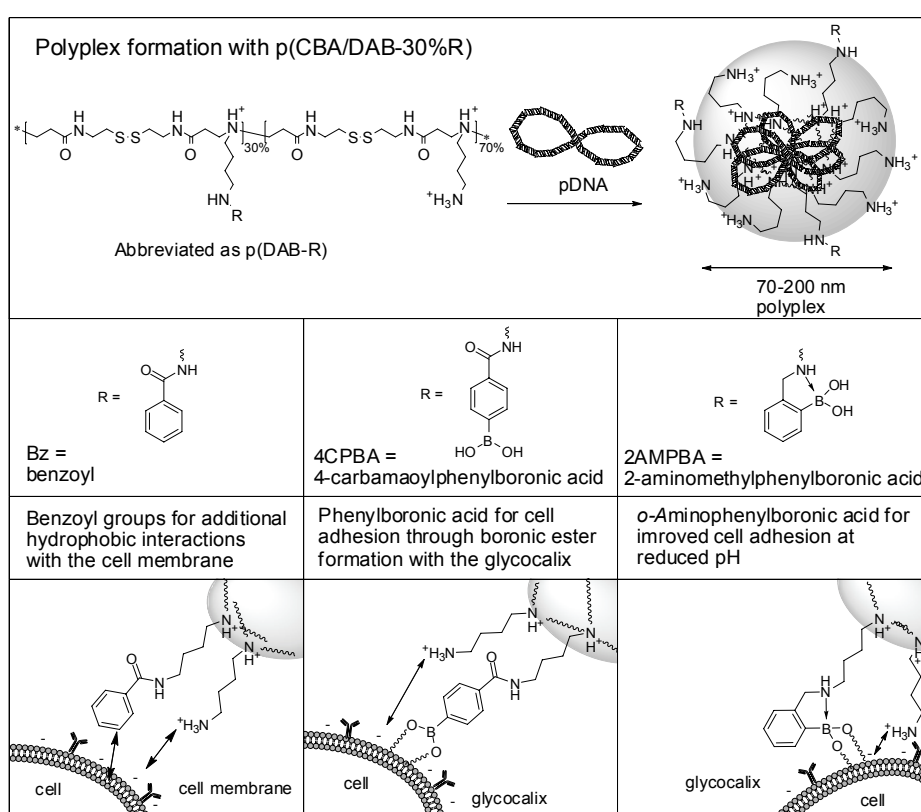


Scheme 3.1. Overview of boronic acid chemistry.

Over the years, phenylboronic acids have been widely applied in sensor technology for recognition of sugars [17-22], and for the purification of nucleotides and nucleic acids [23-27]. In the biomedical field phenylboronic acid containing polymers have been used for recognition of L-DOPA [28] and for glucose-responsive delivery of insulin [29-33]. Polymers with boronic acid functionalities have also been used for affinity chromatography [34] and some boronic acid containing compounds can act as enzyme inhibitors [35, 36]. In addition, boronic acid compounds are known to interact with cells [37-39] and more specifically with the glycoproteins on the cell surfaces [40]. However, boronic acids have been scarcely studied in the field of gene delivery; the only examples can be found in the work of Moffat *et al.*, who utilized the reversible boronic ester bond formation between a salicylhydroxamic acid functionalized PEI and a phenyl(di)boronic acid functionalized PEG for the *post*-PEGylation of PEI/DNA polyplexes [41, 42], and in very recent work of Peng *et al.* polyethyleneimine (PEI) with phenylboronic acid groups to improve the gene transfection [43]. However, no studies have been performed on the effects of boronic acids in poly(amido amine) gene delivery vectors in relation to cellular uptake and transfection efficiency of boronated polyplexes. Therefore, we aimed to explore the effects of boronic acids in SS-PAA for gene delivery, and a conceptual overview of our approach is given in Scheme 3.2.

In this approach *para*-carboxyphenylboronic acid was grafted on 30% of the aminobutyl side chains of SS-PAA from cystamine bisacrylamide and diaminobutane called p(DAB), resulting in p(DAB-4CPBA). Similarly a nonboronated analogue with 30% of the aminobutyl side chains benzoylated abbreviated as p(DAB-Bz) was prepared from the same parent batch of p(DAB) (Scheme 3.3). This 30% degree of functionalization was selected since higher degrees of benzoylation

were found to reduce the polymer solubility [14]. In parallel, a polymer with *ortho*-aminomethylphenylboronic acid moieties was synthesized through copolymerization of cystamine bisacrylamide with a mixture of 2-((4-aminobutylamino)methyl)phenylboronic acid (monomer 1) and mono-BOC protected 1,4-diaminobutane followed by deprotection (Scheme 3.4), resulting in polymer p(DAB-2AMPBA). Both boronated SS-PAAAs could be relevantly compared with the non-boronated analogue p(DAB-Bz), as their M_w and degree of functionalization were similar.



Scheme 3.2. Boronic acid containing SS-PAAAs for gene delivery. Top: polyplex formation with DNA. Bottom: different interactions of the benzoyl or phenylboronic acid groups in the polymer side chains.

From literature data it is known that the presence of an amine in the *ortho* position relative to the boronic acid as is present in p(DAB-2AMPBA) can give a B–N interaction that enhances the binding affinity of the boronic acid for vicinal diol groups as are present in carbohydrates [16, 32]. Therefore, it was hypothesized that possible effects of the presence of boronic acid moieties in SS-PAAAs would appear more dominant for p(DAB-2AMPBA) than for p(DAB-4CPBA).

3.2 Materials and methods

N,N'-cystamine bisacrylamide (CBA, Aldrich), N-BOC-1,4-diaminobutane (Aldrich), benzoylchloride (Aldrich), 2-formylphenylboronic acid (Aldrich) and 4-carboxyphenylboronic acid (Aldrich) were of commercial grade and used without further purification. All reagents and solvents were of reagent grade and were used without further purification.

NMR spectra were recorded on a Varian Unity 300 (^1H NMR 300 MHz) using the solvent residual peak as the internal standard. ES-TOF-MS spectra were recorded on a Waters/Micromas LCT mass spectrometer and MALDI-TOF spectra were recorded on a Applied biosystems Voyager DE-RP mass spectrometer.

3.2.1 Synthesis of the parent poly(amido amine) p(DAB).

N,N'-cystamine bisacrylamide (3.11 g, 11.6 mmol) and N-BOC-1,4-diaminobutane (2.25 g, 11.6 mmol) in 5.5 ml methanol/water 4/1 were polymerized by Michael type addition in a brown reaction flask. The reaction mixture became homogeneous in less than 1 h and the reaction was allowed to proceed for 6 days in the dark at 45 °C under an argon atmosphere, yielding a viscous solution. Subsequently, *ca.* 10 mol% excess of N-BOC-1,4-diaminobutane (0.29 g, 1.5 mmol) was added to consume any unreacted acrylamide groups and stirring was continued for 2 days at 45 °C. The resulting solution was diluted with water to about 45 ml, acidified with a few drops of 1 M HCl to pH \sim 4, and then purified using an ultrafiltration membrane ($M_w\text{CO}$ 3000 g/mol). After freeze-drying, the BOC-protected polymer p(N-BOC-DAB) was collected as the HCl-salt, yielding 1.8 g (34%) white foam-like material. The composition was established by ^1H NMR (D_2O , 300 MHz).

Next, the BOC-protected polymer p(N-BOC-DAB) was dissolved in about 30 ml methanol and fully deprotected by perfusion of dry HCl-gas through the solution for 30 min. The methanol was removed by rotational evaporation and the polymer was redissolved in about 30 ml water, the pH was adjusted to \sim 4 using 4 M NaOH (aq). The polymer was then purified again using an ultrafiltration membrane ($M_w\text{CO}$ 3000 g/mol). After freeze-drying, p(DAB) polymer was collected as the HCl-salt, yielding 0.45 g (25% recovery) transparent amorphous material. The complete removal of the *N*-tert-butoxycarbonyl groups (BOC-groups) was confirmed by ^1H NMR (D_2O , 300 MHz).

3.2.2. Synthesis of p(DAB-30%Bz)

Polymer p(DAB) (0.171 g, 0.45 mmol NH_2) was dissolved in 25 ml methanol, and triethylamine (0.045 g, 0.43 mmol) was added, followed by 0.3 equivalents of benzoylchloride (0.0175 g, 0.12 mmol). The solution was stirred overnight at ambient temperature, after which the methanol was evaporated and the resulting polymer

was redissolved in 20 ml water and purified using an ultrafiltration membrane (M_wCO 3000 g/mol) at pH 5. The isolated yield was 52% (0.099 g) and the degree of substitution was 32% according to 1H NMR (D_2O , 300 MHz). $M_n = 2432$ g/mol, and $M_w = 2729$ g/mol, PDI = 1.13 according to MALDI-TOF MS.

3.2.3. Synthesis of p(DAB-30%4CPBA

4-Carboxyphenylboronic acid (0.165 g, 1.00 mmol) was dissolved in 5 ml methanol by shortly increasing the temperature to 50 °C under magnetic stirring. About 2 equivalents of 1-ethyl-3-(3-dimethylaminopropyl)carbodiimide hydrochloride (EDC) (0.447 g, 2.33 mmol) dissolved in 5 ml millipore water were added to the reaction mixture at ambient temperature. After 10 min 2.55 equivalents of N-hydroxysulfosuccinimide (0.299 g, 2.54 mmol) dissolved in 5 ml millipore water were added. The mixture became a little turbid and 4 ml methanol was added. The pH dropped to 6 during the reaction. After another 30 min at ambient temperature the deprotected polymer p(DAB) (0.286 g, 0.75 mmol NH_2), dissolved in 12 ml millipore water was added to the reaction mixture. The reaction mixture was stirred for 6 h at ambient temperature at pH 6 under nitrogen in the dark. The polymer solution was then purified using an ultrafiltration membrane (M_wCO 3000 g/mol). After freeze-drying, the PAAs were collected as the HCl-salt. The isolated yield was 86% (0.284 g) and the degree of substitution was 34% according to 1H NMR (D_2O , 300 MHz). $M_n = 1753$ g/mol, and $M_w = 2151$ g/mol, PDI = 1.23 according to MALDI-TOF MS.

3.2.4. Synthesis of 2-((4-aminobutylamino)methyl)phenylboronic acid (monomer 1)

2-Formylphenylboronic acid (5.10 g, 34.0 mmol) was dissolved in 45 ml methanol, together with N-BOC-1,4-diaminobutane (6.69 g, 34.7 mmol) and 3 equivalents triethylamine (10.08 g, 99.6 mmol) and the mixture was stirred overnight under nitrogen at ambient temperature. The mixture turned yellow and 1H NMR confirmed the formation of the Schiff's base. Next, 3 equivalents $NaBH_4$ (3.91 g, 103.3 mmol) were added to the reaction mixture to reduce the Schiff's base and the solution turned colorless. The product was thrice extracted from water/chloroform. The organic layer was dried over $MgSO_4$ and evaporated under reduced pressure. The product was isolated as an off-white solid (8.78 g, 75% yield). The BOC-protected product was dissolved in 30 ml of methanol and deprotected by perfusion of HCl-gas through the reaction mixture for 30 min at ambient temperature. The solvent was evaporated to dryness and 1H NMR of the product showed complete deprotection. The product containing 50% of monomer **1** as based on 1H NMR using *p*-toluene sulfonic acid as internal standard was used without further purification. Residual mass was due to bound water to the boronic acid and counter ions (HCl-salt of the amines).

¹H-NMR (D₂O, 300 MHz): $\delta = 7.1\text{--}7.4$ (4H, m, ArH), $\delta = 3.950$ (2H, s, ArH-CH₂-NH); $\delta = 2.905$ (2H, t, 3J(H-H) = 7.2 Hz, NH-CH₂-CH₂), $\delta = 2.825$ (2H, t, 3J(H-H) = 7.5 Hz, CH₂-CH₂-NH₂), $\delta = 1.673$ (2H, q, 5J(H-H) = 7.7 Hz, CH₂-CH₂-CH₂-CH₂-NH₂), $\delta = 1.601$ (2H, q, 5J(H-H) = 8.4 Hz, CH₂-CH₂-CH₂-CH₂-NH₂). MS (ES⁺-TOF): $m/z = 239.3$ (100) ([M+OH+ H⁺], calculated for [C₁₁H₂₀BN₂O₃]: 239.16).

3.3.5. Synthesis of p(DAB-2AMPBA)

Polymer p(cystamine bisacrylamide / (diaminobutane_{70%} 2-((4-aminobutylamino)methyl)phenylboronic acid_{30%})), abbreviated as p(DAB-2AMPBA) was synthesized by the Michael addition of 0.8 equivalents N-BOC-1,4-diaminobutane (1.04 g, 5.40 mmol) and 0.2 equivalents 2-((4-aminobutylamino)methyl)phenylboronic acid (monomer **1**) (0.35 g, 1.36 mmol) to cystamine bisacrylamide (1.80 g, 6.78 mmol, 1.0 eq). Polymerization was performed in a brown reaction flask with 2.0 ml methanol and 0.5 ml water as the solvent. The polymerization was carried out in the dark at 45 °C in a nitrogen atmosphere and was left to proceed for 7 days, yielding a viscous solution. Subsequently, 9 mol% excess of monomer **1** (0.156 g, 0.62 mmol) dissolved in a mixture of 1.0 ml methanol and 0.25 ml water was added to consume any unreacted acrylamide groups and the reaction was left to proceed for 3 days at 45 °C. The resulting solution was diluted with water to about 30 ml, acidified with a few drops of 1 M HCl to pH ~ 4, and then purified using an ultrafiltration membrane (M_wCO 3000 g/mol). The product was obtained after freeze-drying as off-white foam like material (2.08 g). The composition of the polymer was established by ¹H NMR (D₂O, 300 MHz).

Next, the BOC-protected polymer was dissolved in 30 ml methanol and fully deprotected by perfusion of dry HCl-gas through the solution for 20 min. The methanol was removed by rotational evaporation and the polymer was redissolved in 30 ml water, the pH was adjusted to 4 using 1 M NaOH (aq). The polymer was then purified using an ultrafiltration membrane (M_wCO 3000 g/mol). After freeze-drying, the PAA was collected as the HCl-salt. The complete removal of the *N*-*tert*-butoxycarbonyl groups (BOC-groups) was confirmed by ¹H NMR (D₂O, 300 MHz) and boronic acid content was 30%. M_n = 2781 g/mol, and M_w = 4261 g/mol, PDI = 1.53 according to MALDI-TOF MS.

3.2.6. Determination of the buffer capacity of the polymers

The buffer capacity of the SS-PAAAs was determined by recording the pH change during the automated titration of a concentrated acidic polymer solution with 0.1 M NaOH solution. Therefore, 0.05 g of polymer (0.25 mmol of protonable nitrogens) was dissolved in 5 ml of 150 mM NaCl solution and the pH was set to 2.0 with a few drops of 1.0 M HCl. This solution was titrated with 0.1 M NaOH solution

(0.4 ml/min) and the pH was recorded as a function of the added sodium hydroxide solution.

The buffer capacity is defined as the percentage of (protonable) nitrogen atoms in PAA that becomes protonated in the pH interval from 7.4 to 5.1, being the pH change the polyplexes experience upon change from the extracellular environment (pH 7.4) to the late endosomal environment (pH 5.1). The buffer capacity can be calculated as the mol OH⁻ added per mol of protonable N-atoms of the polymer, according to Equation 3.1.

$$\text{BufferCapacity}(\%) = \frac{(\Delta V_{pol} - \Delta V_{NaCl}) \times 0.1M}{mol N} * 100\% \quad (\text{Equation 3.1})$$

Where ΔV_{pol} and ΔV_{NaCl} are the volumes of 0.1M NaOH added to change the pH from 5.1 to 7.4 in the polymer solution and pure 150 mM NaCl solution, respectively. ΔV_{NaCl} was measured and found to be negligible in this pH range. Mol N is the total amount of protonable nitrogen atoms.

3.2.7. Polyplex preparation

The DNA plasmid solution (1 mg/ml) as supplied by manufacturer was diluted to a final concentration of 0.075 mg/ml in HEPES buffer solution (50 mM, set to pH 7.4). A series of polymer solutions of different concentrations was prepared by dilution of a solution of 0.9 mg/ml in HEPES buffer solution repeatedly 1:1 with HEPES buffer solution. To prepare polyplexes at 48/1, 24/1, and 12/1 polymer/DNA weight ratio 0.80 ml of each polymer solution was added to 0.20 ml of DNA solution in a 1.5 ml Eppendorf tube. The polyplex solutions were vortexed for 5 s and incubated for 30 min at ambient temperature prior to use.

3.2.8. Determination of polyplex properties by Dynamic Light Scattering (DLS)

Size and zeta potential of the nanoparticles formed by spontaneous self assembly of the poly(amido amine) nanoparticles and of the poly(amido amine)/plasmid DNA polyplexes were measured at 25 °C on a Zetasizer Nano (Malvern Instruments Ltd, Malvern, UK) and the dynamic light scattering results were processed using Dispersion Technology Software V5.0.

3.2.9. Atomic Force Microscopy (AFM) analysis of polyplex formation

Samples were prepared on freshly cleaved mica using a mixed solution of DNA (0.015 mg/ml final concentration) and polymer (0.72 mg/ml final concentration) resulting in polyplexes of 48/1 polymer/DNA weight ratio in HEPES (20 mM, pH 7.4). The solution was mixed on the mica surface and a total volume of 0.5 μ l was used. Polyplex formation was studied using a Veeco Nanoscope III controller in tapping

mode. Tapping mode imaging was performed *in situ* in HBS, using a standard liquid cell and a standard Veeco NP cantilever. The polyplex solution was prepared directly on the sample surface and after temperature stabilization imaging was started. The formation was monitored for 3 h and partial DNA condensation took place, next the substrate was left to dry overnight while the DNA condensation process was finalized. After drying overnight the polyplexes on mica were studied using tapping mode in air (Nanosensors PPP-NCH-W cantilever). Images were recorded using a scan rate of 1 Hz.

3.2.10 Determination of DNA condensation using ethidium bromide fluorescence

The efficiency of DNA condensation was measured using the ethidium bromide fluorescence assay as previously described, using a Varian Eclipse fluorescence spectrophotometer, with excitation and emission wavelength of 520 and 600 nm, respectively [13]. Briefly, the fluorescence intensity of a solution of ethidium bromide (5×10^{-6} M) in the presence of uncondensed DNA (0.015 mg/ml) in HEPES buffer (20 mM, pH 7.4) was determined by fluorescence spectroscopy. The molar ratio of ethidium bromide to the DNA phosphates in this solution is 1:10, resulting in intercalation and strong fluorescence of the ethidium cation. Similarly, ethidium fluorescence is measured in the presence of the appropriate polyplex solutions, using the same concentrations of ethidium bromide and DNA. The relative fluorescence (F_r) represents a relative measure for the degree of shielding of DNA in the polyplex, and was determined from the equation: $F_r = (F_{\text{obs}} - F_e) / (F_0 - F_e)$. Here F_{obs} is the fluorescence of the polyplex dispersion, F_e is the fluorescence of ethidium bromide in the absence of DNA, and F_0 is the initial fluorescence of DNA/ethidium bromide in the absence of polymer.

3.2.11. In vitro transfection and cell viability

Transfection and cell viability studies were carried out with COS-7 cells (SV-40 transformed African Green monkey kidney cells). Plasmid pCMV-GFP DNA was used as the reporter gene. Two parallel transfection series, one in the presence of serum and one in the absence of serum, were carried out in separate 96-well plates, $n = 6$. The determination of reporter gene expression (GFP) and the evaluation of the cell viability by XTT assay were carried out with the same samples. Polyplexes with polymer/DNA weight ratios 6/1, 12/1, 24/1 and 48/1 were used in the transfection experiments and compared with polyplexes of linear PEI (Exgen 500) at its optimal 6/1 N/P ratio as reference.

In a typical transfection experiment, cells were plated with 10,000 cells per well 24 h prior to use and were > 80% confluent. The next day, the cells were incubated

with the desired amount of polyplexes (100 μ l dispersion with 1 μ g plasmid DNA per well) for 2 h at 37 $^{\circ}$ C in a humidified 5% CO₂-containing atmosphere. Next, the polyplex solution was removed, and the cells were washed with 100 μ l PBS before 100 μ l of fresh culture medium was added and the cells were cultured for another 48 h. The fluorescent intensity of the cells was measured on a TECAN Safire² plate reader using SW Magellan Software V6.4. Excitation was at 480 nm and optimal emission was determined at 503 nm.

The cell viability was measured using an XTT assay, in which the XTT value for untreated cells (cells not exposed to the transfection agents) was taken as 100% cell viability. XTT measurements were performed in triplicate using the Perkin Elmer LS50B luminescence spectrometer and analyzed in Kineticalc for Windows V2.0. The absorbance was measured at 490 nm with a reference at 655 nm.

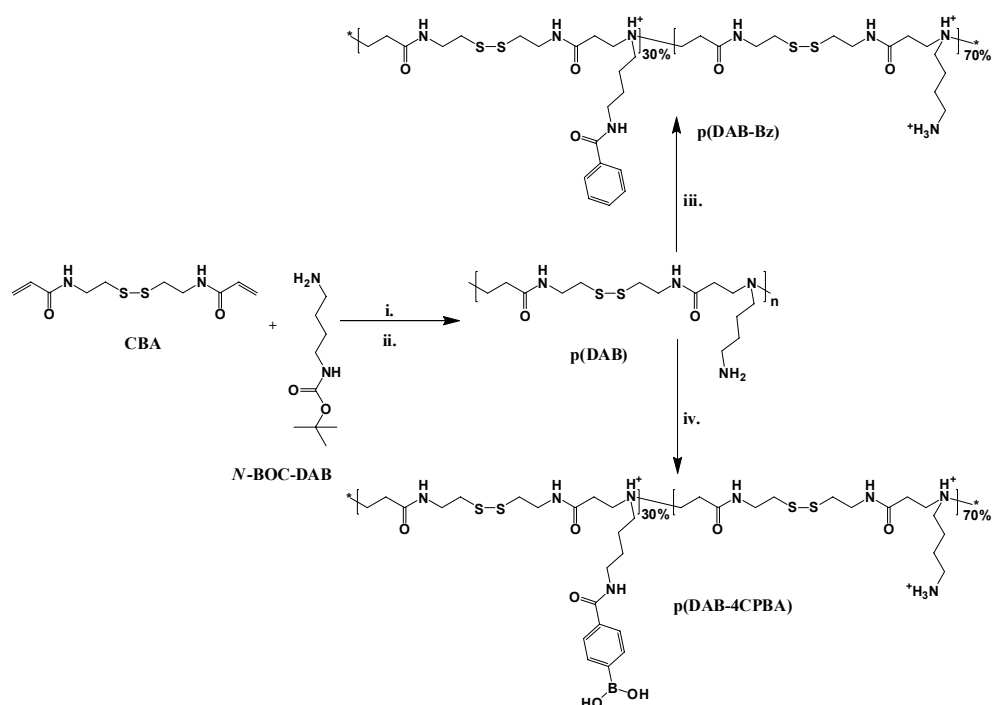
3.2.12 Erythrocyte leakage

The hemolytic activity of polymers was measured according to literature procedure [14]. A polymer dilution series in HBS (20 mM HEPES, 130 mM NaCl, pH 7.4) was prepared, starting from 1.25 mg/ml to 2.44 μ g/ml (10 dilutions). Buffer solution containing 1% Triton X-100 was used as positive control; buffer only was used as a negative control. Polymer and control solutions were filled out in a V-bottom 96-well plate, 100 μ l per well. Human erythrocytes were isolated from fresh citrate treated blood, washed in phosphate-buffered saline (PBS) by four centrifugation cycles, each at 800 g for 10 min at 4 $^{\circ}$ C. The erythrocyte pellet was diluted 10-fold in 150 mM NaCl and 25 μ l erythrocyte suspension was added to each well. The plates were incubated at 37 $^{\circ}$ C for 30 min under constant shaking and the plates were centrifuged at 300 g for 10 min. Next, 60 μ l of the supernatant was transferred to a new flat bottom 96-well plate and analyze for hemoglobin content at 405 nm on a TECAN Safire² plate reader using SW Magellan Software V6.4.

3.3. Results and discussion

3.3.1. Polymer synthesis

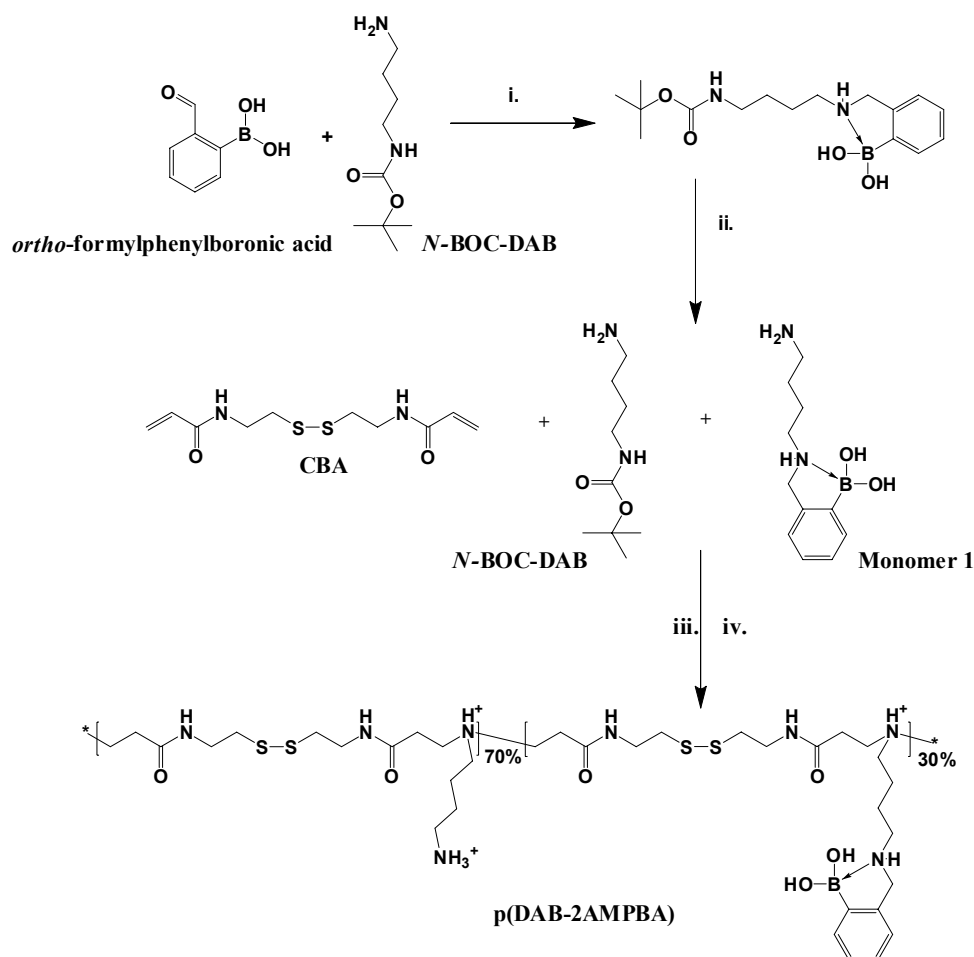
In our previous studies of disulfide containing poly(amido amine)s (SS-PAA)s as gene delivery vectors, it was shown that the presence of bioreducible disulfide linkages in these polymers results in significant increases in transfection efficiency together with a reduction in cytotoxicity [9-13]. In this study two SS-PAA)s with different phenylboronic acid functionalized side chains were compared with the benzoylated reference polymer p(DAB-Bz). The synthesis routes for these polymers are given in Scheme 3.3 and Scheme 3.4, respectively.



Scheme 3.3 i) Michael addition polymerization of CBA with N-BOC-1,4-DAB and ii) deprotection with HCl (g) resulting in p(DAB) followed by iii) functionalization with benzoyl chloride or iv) functionalization with 4-CPBA through EDC/NHS coupling resulting in p(DAB-Bz) and p(DAB-4CPBA), respectively.

The polymers p(DAB-Bz) and p(DAB-4CPBA) as given in Scheme 3.3 were synthesized from the same parent batch of p(DAB), which was synthesized by Michael addition polymerization of N,N'-cystamine bisacrylamide and N-BOC protected 1,4-diaminobutane followed by deprotection of the pending amines. From this parent p(DAB) with M_w of 3.5 kDa 30% of the aminobutyl groups were benzoylated, resulting in the non-boronated reference polymer p(DAB-Bz). From the same parent

polymer p(DAB) 30% of the aminobutyl groups were functionalized using an EDC/NHS coupling with 4-carboxyphenylboronic acid, resulting in p(DAB-4CPBA).



Scheme 3.4. i) Reductive amination of 2-formylphenylboronic acid to *N*-BOC-1,4-DAB and ii) deprotection with HCl (g) resulting in **Monomer 1**. iii) Michael addition polymerization of CBA with *N*-BOC-1,4-DAB and **Monomer 1** followed by iv) deprotection with HCl (g), resulting in p(DAB-2AMPBA).

It was observed from the ^1H NMR data given in Figure 3.1 that the EDC/NHS coupling of 4-carboxyphenylboronic acid resulted in a significantly lower degree of substitution (30%) than the feed ratio (1.3 eq relative to primary amines). The yield after the functionalization step and ultrafiltration was 86%. It was attempted to graft higher levels of 4CPBA, but this proved to be difficult. From our previous work [14], it was found that hydrophobic modifications of the p(DAB) promote self-aggregation, which reduces the accessibility of the free amines.

The introduction of the *ortho*-(aminomethyl)phenylboronic acid moieties according to Scheme 3.4 was achieved by the copolymerization of *N,N'*-cystamine bisacrylamide with the boronated monomer **1** (20%) and *N*-BOC 1,4-diaminobutane (80%). The polymer was end-capped with excess monomer **1**, followed by a deprotection step with HCl (g), resulting in polymer p(DAB-2AMPBA). Monomer **1** could be easily synthesized by reductive amination of *N*-BOC 1,4-diaminobutane and 2-formyl phenylboronic acid, followed by a deprotection step, according to Scheme 3.4. Although *post*-modification from the same parent batch p(DAB) would be advantageous to minimize batch differences (i.e. M_w , PDI), copolymerization was selected since the *post*-modification of p(DAB) by reductive amination of *ortho*-formylphenylboronic acid to the pending aminobutyl groups would also reduce the repetitive disulfide bonds, thereby breaking up the polymer backbone. The resulting polymer p(DAB-2AMPBA) had a M_w of 4261 g/mol that is somewhat higher than the other two polymers p(DAB-Bz) and p(DAB-4CPBA) (2729 and 2151 g/mol, respectively). The structural composition of the polymers was confirmed by ^1H NMR (Figure 3.1). Polymer p(DAB-2AMPBA) was a linear polymer, formed by Michael addition polymerization of the primary amine of monomer **1**. No addition reaction has occurred by the secondary amine, as was confirmed by ^1H NMR (Figure 3.1). The sterically hindered secondary amine in the *ortho* position with respect to the boronic acid can form a dative B–N interaction thereby reducing the nucleophilicity of this secondary amine (Scheme 3.1).

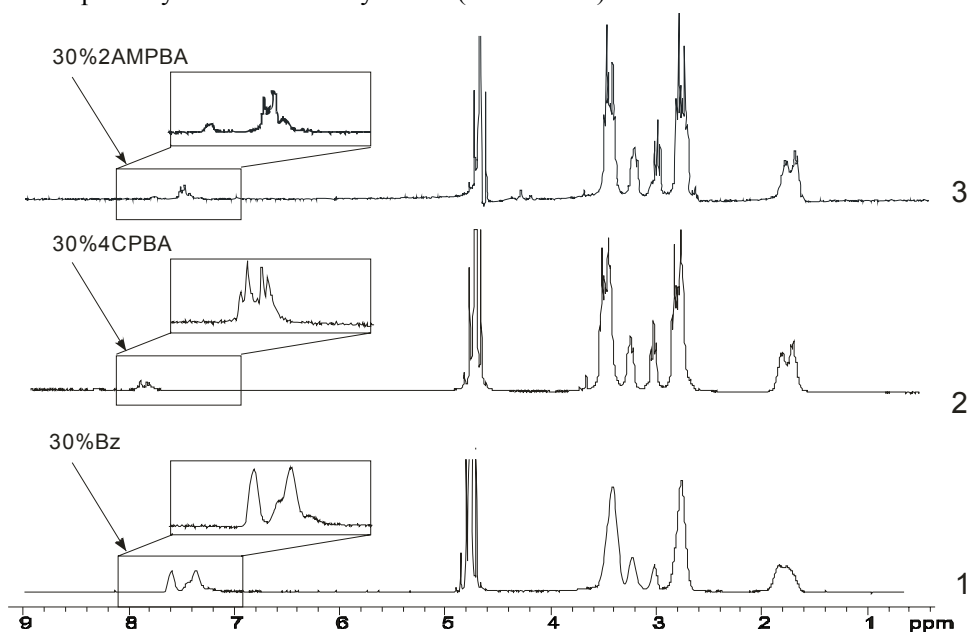


Figure 3.1. ^1H NMR of the different SS-PAA. Line 1 is p(DAB-Bz); line 2 is p(DAB-4CPBA); and line 3 is p(DAB-2AMPBA).

3.3.2. Influence of boronic acid groups on the polymer properties

For all three polymers both the M_w and the degree of functionalization are approximately similar, therefore differences in the polymer behavior such as solubility, pH profile, and the tendency for self-aggregation can be ascribed primarily to differences in the side group functionality. The pH profiles of the polymers were determined by pH titration experiments and it was observed that all three polymers had a similar pH profile, as is shown in Figure 3.2. It has been observed in our previous studies on SS-PAAAs that the buffer capacity of the polymers positively correlates with the transfection efficiency [11]. It is assumed that polymers with a high content of tertiary and secondary amines can buffer the endosomal acidification (proton sponge theory). This results in additional polymer protonation invoking increased charge interactions that can destabilize the endosomal membrane, thereby facilitating endosomal escape [44-46]. The buffer capacity is defined as the percentage of titratable amines that becomes protonated upon the pH change from 7.4 (physiological pH) to 5.1 (pH of the late endosome/lysosome).

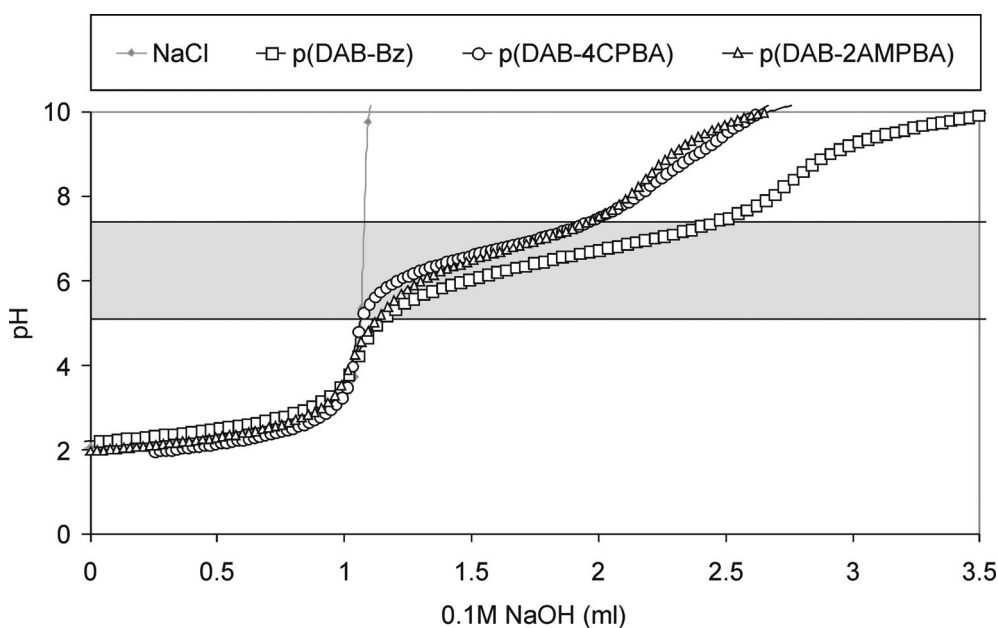


Figure 3.2. pH titration curves of 150 mM NaCl (grey diamonds), p(DAB-Bz) (squares), p(DAB-4CPBA) (circles), and p(DAB-2AMPBA) (triangles). Relevant endosomal pH interval between pH 7.4 and 5.1 is marked grey for clarity.

From the upper part of the curves in Figure 3.2 it is apparent that the pK_a values of the primary amine groups in the side chains of the p(DAB) derivatives are typically

around 10, as expected for primary amines. Therefore these groups do not contribute to the buffering of the polymers in the endosomal pH range. In contrast, the tertiary amines in the backbone of these polymers have pK_a values in the range of 6.5–7.0 and consequently the relative percentage of protonation/deprotonation of these amines is determining the buffer capacity of the polymer in the endosomal pH range. Since the degree of grafting is similar, differences in buffer capacity between p(DAB-Bz) and p(DAB-4CPBA) can be contributed solely to the presence of the boronic acid functionality in the latter polymer.

Table 3.1. Polymer properties

Polymer	M_w (g/mol)	Buffer capacity	Average Size (nm) ^a	Derived count rate (kCps)	PDI ^a	ζ -Potential (mV) ^a
p(DAB-Bz)	2730	62%	227 ± 8	13420 ± 60	0.15 ± 0.02	40 ± 2
p(DAB-4CPBA)	2150	44%	72 ± 3	944 ± 5	0.47 ± 0.05	43 ± 3
p(DAB-2AMPBA)	4260	36%	133 ± 65*	97 ± 2	0.22 ± 0.04	10 ± 3

^a Nanoparticles formed at a polymer concentration of 0.9 mg/ml in HEPES (pH 7.4, 20 mM)

* Poor data due to low signal

As is shown Table 3.1, the buffer capacities of the boronated polymers p(DAB-4CPBA) and p(DAB-2AMPBA) are significantly lower than that of p(DAB-Bz) (44% and 36% compared to 62% respectively). The relatively high buffer capacity of p(DAB-Bz) can be attributed to the spontaneous formation of nanoparticles in solution that induce differences in the microenvironment of the tertiary amino groups in the main chain of the polymer. The spontaneous formation of nanoparticles by these polymers in neutral aqueous solution was confirmed by dynamic light scattering (DLS) experiments (*vide infra*, Table 3.1). It may be assumed that at neutral pH most of the tertiary amino groups are buried in an unprotonated form in the hydrophobic microenvironment of the nanoparticles. At decreasing pH the protonation of the polymer backbone induces an increasing hydrophilicity in the nanoparticles and the increase in hydration of the polymer further shifts the tertiary amines towards increasing protonation.

The lower buffer capacity of the boronated polymers p(DAB-4CPBA) and p(DAB-2AMPBA) indicates that the presence of boronic acids affects the protonation equilibrium of the tertiary amino groups in the main chain. As is shown in Scheme 3.1, boronic acids are in equilibrium with their boronate anions after coordination with a molecule of water and release of a proton. The pK_a of phenylboronic acid for this equilibration is reported to be 8.8 [15], and the presence of a dative B–N interaction is reported to further decrease the pK_a to *ca.* 5 [16]. However, in the titration curves of

solutions of both p(DAB-4CPBA) and p(DAB-2AMPBA) no additional buffering is observed in the range pH 7–9, indicating that apparently no free boronic acid is present. A possible explanation for this phenomenon is that the boronic acid groups form a dative B–N interaction with vicinal unprotonated amines (primary, secondary or tertiary) resulting in decrease of pK_a of the amines and an increase of pK_a of the boronic acids to values above 11 [16]. The enhanced pK_a is further based on the possibility of the boronate anion to form an ion pair with protonated amines.

DLS experiments showed that when a solution of p(DAB-Bz) (0.9 mg/ml) was vortexed for 5 seconds and left standing for 30 minutes a high amount of nanoparticles (13420 kCps) were formed with sizes in the range of 227 nm and small polydispersity index (PDI). This self-aggregation was much less apparent for the boronic acid containing polymers p(DAB-4CPBA) and p(DAB-2AMPBA) where count rates were tenfold and hundredfold lower, respectively. The lower tendency for self-aggregation is most likely due to a more hydrophilic polymer architecture as the boronic acid groups can form additional hydrogen bonds. Although the presence of the boronic acid moieties apparently reduces the tendency for self-aggregation, the surface charge of the nanoparticles of p(DAB-Bz) and p(DAB-4CPBA) is almost the same with zeta potentials of 40 mV and 43 mV, respectively. This could indicate that in both types of nanoparticles the positively charged outer sphere is primarily composed of protonated primary aminobutyl side groups of the polymer.

3.3.3. Polyplex formation

Polyplexes were prepared by adding a polymer solution to a DNA solution at different polymer/DNA weight ratios. It was found that polyplex formation occurred rapidly within the first 5 minutes and that the polyplexes are stable in time. This is demonstrated in Figure 3.3 for polyplexes of p(DAB-2AMPBA) at 48/1 polymer/DNA weight ratio where both size and count rate were monitored. The first measurement was obtained 5 minutes after vortexing and it was observed that the size and the normalized count rate (representing the number of particles) remained essentially constant during the next 2 hours.

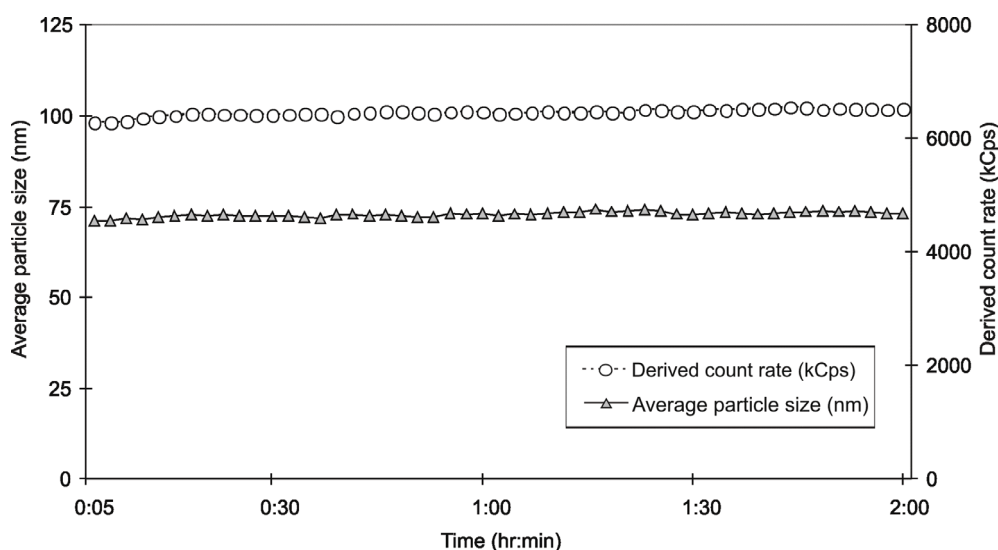


Figure 3.3. Particle size (triangles) and derived count rate (circles) of polyplexes of p(DAB-2AMPBA) with pDNA at 48/1 weight ratio as a function of time. First measurement was performed 5 minutes after mixing.

Both size and surface potential were determined by dynamic light scattering, and the results are presented in Figure 3.4. From Figure 3.4A it can be observed that the size of polyplexes of p(DAB-Bz) increased with increasing polymer/DNA weight ratio and thus with increasing polymer concentration. This is not observed for the boronic acid polymers; both p(DAB-4CPBA) and p(DAB-2AMPBA) form stable and monodisperse nanoparticles smaller than 100 nm at all polymer/DNA weight ratios studied. From Figure 3.4B it can be observed that the polydispersity index for polyplexes of p(DAB-Bz) is significantly higher than for the boronic acid containing polymers p(DAB-4CPBA) and p(DAB-2AMPBA). Moreover the number of particles represented by the derived count rate is approximately twice as high for polyplexes of p(DAB-Bz) compared to polyplexes of p(DAB-4CPBA) and p(DAB-2AMPBA), indicating that boronic acid contributes to well defined monodisperse particles whereas the non-boronated p(DAB-Bz) shows a much broader dispersity. As was already discussed in section 3.2 (Table 3.1), p(DAB-Bz) has a strong tendency for self-aggregation to form nanoparticles with average size of 227 nm. Therefore, it is likely that the higher particle size polydispersity index for p(DAB-Bz) is due to the co-existence of these nanoparticles with smaller p(DAB-Bz)/DNA polyplexes.

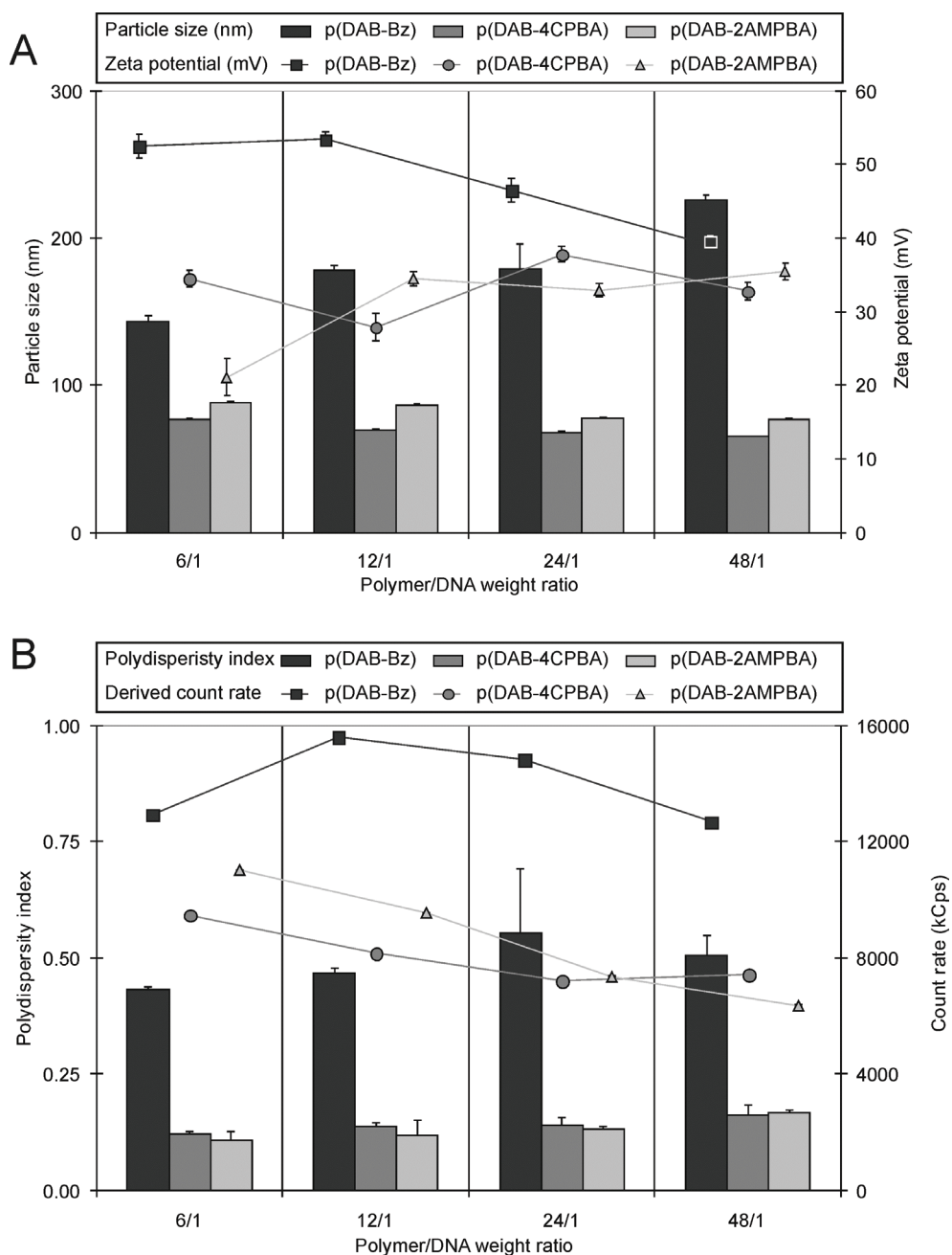


Figure 3.4. Polyplexes formed by the different polymers with pDNA. In Figure **A** polyplex sizes are given in bars and the zeta potentials of the same polyplexes are given in symbols for polyplexes of p(DAB-Bz) (dark grey and squares), p(DAB-4CPBA) (grey and circles), and p(DAB-2AMPBA) (light grey and triangles). In Figure **B** polydispersity indices are given in bars and the derived count rates (kCps) of the same polyplexes are given in symbols for polyplexes of p(DAB-Bz) (dark grey and squares), p(DAB-4CPBA) (grey and circles), and p(DAB-2AMPBA) (light grey and triangles). Lines are added for clarity.

In order to obtain further information on the contribution of the boronic acid moieties to the DNA condensation, polyplexes formed at a 6/1, 12/1, 24/1 and 48/1 polymer/DNA weight ratio were subjected to the ethidium bromide assay (Figure 3.5). The ethidium cation gives an increased fluorescence upon intercalation with DNA; therefore the relative decrease in fluorescent signal gives a measure for the fraction of DNA that is not accessible and thus shielded in the polyplex. DNA condensation is a function of the polymer/DNA charge ratio as well as polymer flexibility and molecular weight of the polymer. Since the polymer backbone is the same and the degrees of functionalization of the aminobutyl side chains as well as the M_w of the polymers are similar, differences can be ascribed to the functional groups in the side chains.

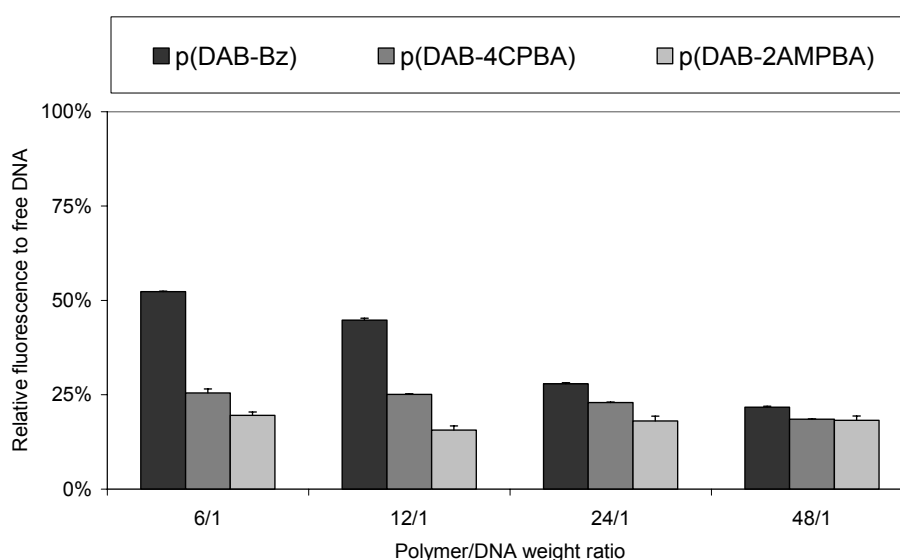


Figure 3.5. Fluorescence resulting from ethidium bromide DNA intercalation relative to free pDNA for polyplexes of p(DAB-Bz) (dark grey), p(DAB-4CPBA) (grey), and p(DAB-2AMPBA) (light grey).

At high polymer/DNA weight ratio of 48/1 all three p(DAB) derivatives showed residual ethidium fluorescence of less than 25%, suggesting that >75% of the DNA is effectively shielded from ethidium intercalation inside the polyplex. At lower polymer/DNA weight ratios of 6/1 and 12/1 the boronic acid containing polymers p(DAB-4CPBA) and p(DAB-2AMPBA) were better capable of DNA shielding than p(DAB-Bz), suggesting a more condensed packing of DNA in these boronated polyplexes. From this it is concluded that the introduction of boronic acid moieties favorably contributes to the DNA condensation.

3.3.4. AFM study of polyplexes formed with p(DAB-2AMPBA)

The polyplexes formed with p(DAB-2AMPBA) at 48/1 polymer/DNA weight ratio were further investigated with atomic force microscopy (AFM). This polymer was selected in this study, since it gave the best condensed polyplexes according to DLS and ethidium bromide fluorescence measurements. A freshly prepared solution polymer/DNA at 48/1 weight ratio in HEPES buffer was added onto a freshly cleaved mica surface and the sample was probed by AFM in tapping mode *in situ* for 3 hours. Next, the sample was dried overnight and measured again the day after in the dry state.

At the start of the measurement, predominantly plasmid DNA was visible at the surface and after 2 to 3 hours an increasing number of polyplex aggregates could be observed (Figure 3.6). This slow polyplex formation at the surface is significantly different from that observed for the polyplexes formed in solution, as studied by DLS. This may be due to the adsorption of the positively charged polymer on the negatively charged mica surface. In Figure 3.6A,B predominantly uncondensed plasmid DNA is visible. By following the same DNA plasmids for 2 hours it was observed that the DNA gradually condensed into spherical particles with heights up to 40–80 nm. At first, loosely packed particles with uncondensed DNA coils at the periphery of the polyplexes and much denser packed material (DNA and polymer) on the inside were visible and progressing in time the polyplexes became more homogeneously densely packed. In Figure 3.6C a semi condensed or “immature” polyplex with a height of 10 nm is depicted, which slowly became more condensed with a height of 48 nm after another 30 minutes (inset in Figure 3.6C). In the phase image (Figure 3.6D) the softer “free” DNA appears light and the more rigid core appears as darker spots (inset in Figure 3.6D). When the sample was rinsed with HEPES buffer and left drying overnight spherical particles could be observed in Figure 3.6E and Figure 3.6F, where no phase contrast was observed, indicating that the particles were homogeneously packed.

Cross section analysis of 15 polymer/DNA particles on the mica surface gave an average diameter of 138 ± 64 nm. For comparison, also polymer in absence of DNA was measured. It was found that the polymer slowly adsorbed to the mica surface forming aggregates with a much smaller averaged diameter of 28 ± 6 nm (cross section analysis of 10 particles) (data not shown).

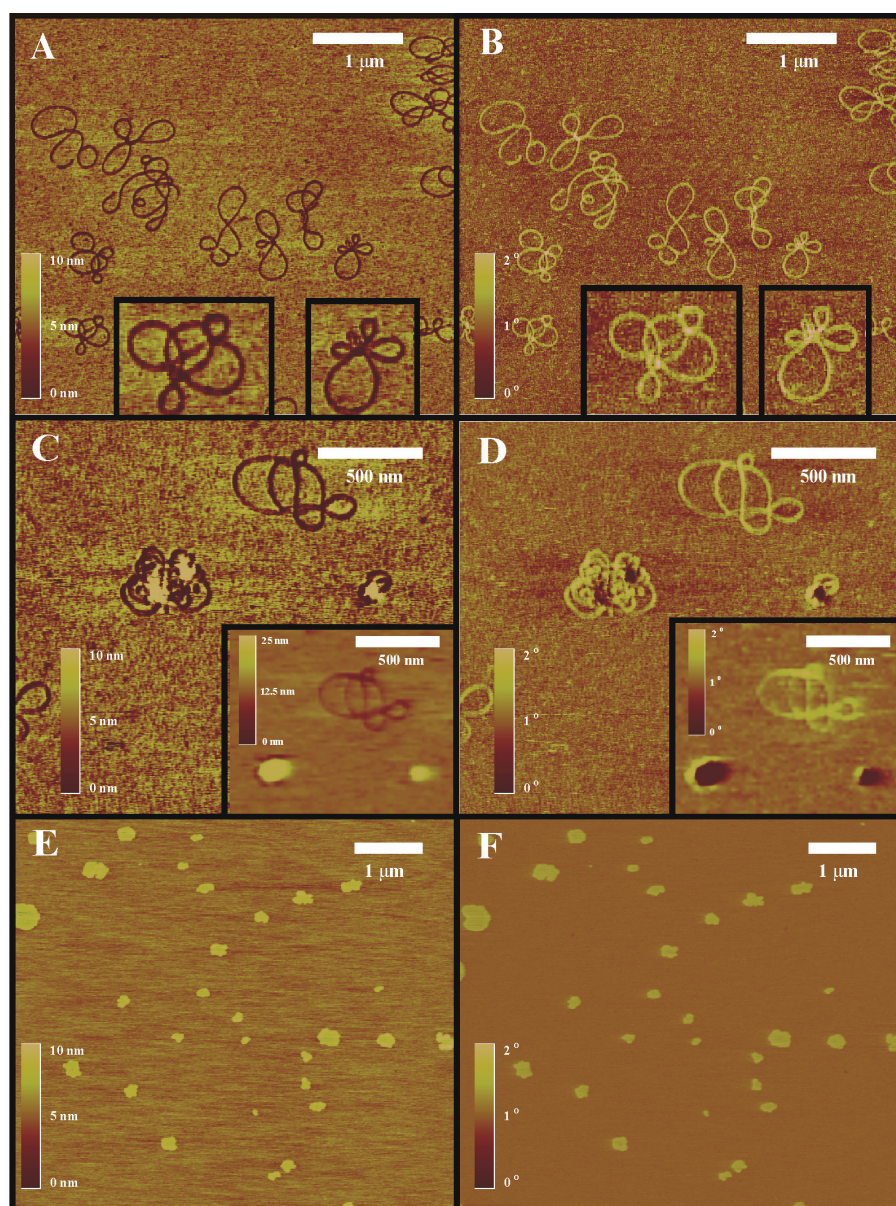


Figure 3.6. Atomic force microscopy images of polyplexes with p(DAB-2AMPBA) in tapping mode. (A, B) Overview of particle formation of DNA polyplexes on mica, using tapping mode AFM in HEPES buffer showing the onset of particle formation, with (A) height image and (B) phase image. (C, D) Second stage (after 1.5 hours) of DNA polyplex wrapping process, with (C) height image and (D) phase image. Note the condensed particles that have been formed in the insets after 2 hours. The outsides of the particles show clear phase contrast indicating less dense and more adhesive material. (E, F) Final stage of the condensed particles after 1 day measured in dry air, with (E) height image and (F) phase image. Cross section analysis of 15 condensed particles provided an average particle size of 138 ± 64 nm.

3.5. pH dependant polyplex properties

The effects of the different boronic acid functionalities on polyplex properties were further investigated. To mimic the polyplex response upon endosomal acidification, a solution of 10 ml of polyplexes at 48/1 polymer/DNA weight ratio (0.72 mg/ml polymer and 0.015 mg/ml DNA) was titrated with 0.25 M NaOH (aq) from pH 5.1 to 7.4 and then back from pH 7.4 to 5.1 with 0.25 M HCl (aq) while monitoring the particle size using a Zetasizer Nano (Malvern, UK) with a MPT-2 Autotitrator. The pH response of the particle size proved to be reversible and the results for polyplexes of the three polymers are shown in Figure 3.7.

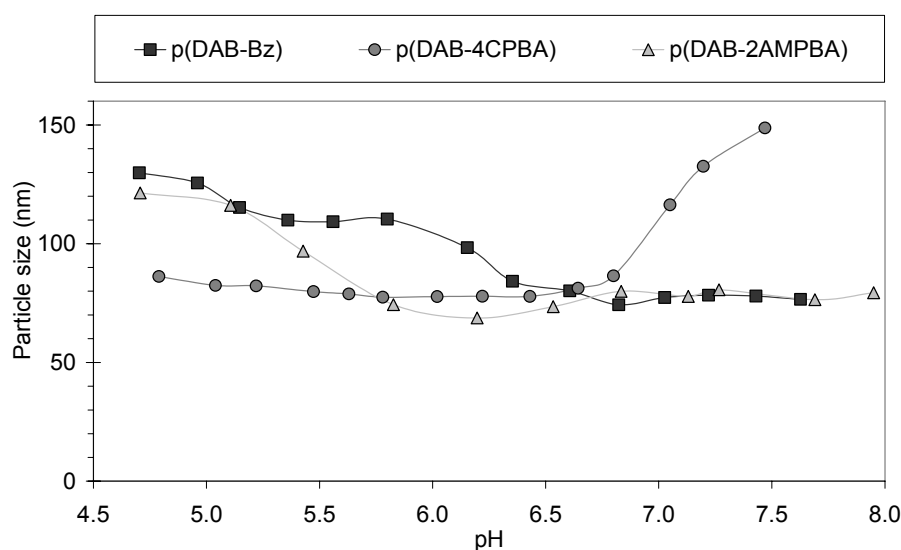


Figure 3.7. Titration of polyplexes prepared at 48/1 polymer/DNA weight ratio with polymer p(DAB-Bz) (dark squares), p(DAB-4CPBA) (grey circles) and p(DAB-2AMPBA) (light grey triangles), lines are added for clarity.

Considering the pH decrease from pH 7.4 to 5.1 it can be seen that the polyplexes from reference polymer p(DAB-Bz) start to increase in size at pH \sim 6.5 and gradually increase in size upon further acidification. The difference in particle size with previous data in Figure 3.4 can be explained by the setup using the flow-cell with constant perfusion using the MPT-2 autotitrator. As the sample is subjected to shear forces in between measurements (circulation of the sample while adjusting the pH) the polymer-only aggregates (of *ca.* 227 nm) are disrupted and only the more stable polyplexes of with pDNA (*ca.* 80 nm) are detected. The increase in polyplex size upon acidification can be explained by the increasing protonation of the tertiary amines of the polymer backbone that are present in the more hydrophobic core of the particle (with pK_a values in the range of 6.5–7.0). Protonation of these tertiary amines will increase the charge repulsion between polymer chains explaining the increase in

particle size observed. Polyplexes from p(DAB-4CPBA) showed quite different behavior. These polyplexes were significantly larger at pH 7.4 than those of p(DAB-Bz) (80 nm vs 150 nm, respectively), but became smaller upon acidification with a sharp transition in the pH range 6.8–7.2 (Figure 3.7). This different behavior can be attributed to hydroxyl addition to the boron centre, under the premise that this boron centre is part of an intermolecular dative B–N bond in this pH regime 5–7, that result in the dissociation of the dative B–N bonds. This different behavior can be attributed to protonation of the secondary amines that result in the dissociation of intermolecular dative B–N bonds in this pH regime. The pK_a of phenylboronic acid itself is typically around 8.8, but in this case the phenylboronic acid groups in the side chains of the polymer are in the proximity of the protonated primary amine side groups and this cationic microenvironment can stabilize the boronate anion, thereby decreasing the pK_a of the boronic acid within the polyplex particle. The protonated amine and the boronate acid can form a dative B–N bond after release of a molecule of water. Oppositely, it is rationalized that the hydrolysis of the dative B–N bond above *ca.* pH 7.2 can be viewed as the breaking of crosslinks in the polyplexes formed by p(DAB-4CPBA) resulting in larger particles.

For polyplexes of polymer p(DAB-2AMPBA) above pH 5.5 small polyplexes of *ca.* 80 nm were formed, whereas in more acidic environment particles increase in size to *ca.* 120 nm. Polymer p(DAB-2AMPBA) contains *ortho*-aminophenylboronic acid side groups which form an intramolecular dative B–N bond that exists between pH 5–7 [16]. This type of B–N interaction decreases the pK_a of the *ortho*-amino groups to a value as low as *ca.* 5.5. At decreasing pH the B–N interaction will be broken through protonation of the amine (besides the protonation of the tertiary amines in the polymer main chain) and the additional amount of protonated amines in the polyplex may lead to extra charge repulsion, resulting in the relatively strong increase in polyplex size that is observed for this polymer at pH < 5.5.

3.3.6. Transfection studies

Transfection efficiencies of polyplexes of the polymers with DNA encoding for green fluorescent protein (GFP) were determined by measuring the fluorescent intensities in COS-7 cells both in the absence and in the presence of serum. The cell viabilities of the corresponding polyplexes were determined by XTT-assay. Figure 3.8A shows the transfection and cell viabilities in the absence of serum. From this figure it is clear that polyplexes of p(DAB-Bz) showed the highest transfections with 2–3 times higher than those obtained with polyplexes from the reference polymer linear PEI (Exgen) at its optimal N/P ratio 6. Polyplexes of p(DAB-4CPBA) showed similar transfection efficiencies as Exgen, whereas polyplexes of p(DAB-2AMPBA) were not very efficient in the transfection. The results show that the boronic acid

containing polyplexes of p(DAB-4CPBA) under these conditions, in the absence of serum, are less effective in transfection than polyplexes of the non-boronated analog p(DAB-Bz). This may be mainly caused by the higher cytotoxicity that is observed for these polyplexes. Whereas p(DAB-Bz) shows almost no cytotoxicity at 6/1, 12/1 and 24/1 polymer/DNA weight ratios, the cell viabilities of p(DAB-4CPBA) and p(DAB-2AMPBA) dramatically decrease with increasing polymer/DNA weight ratio.

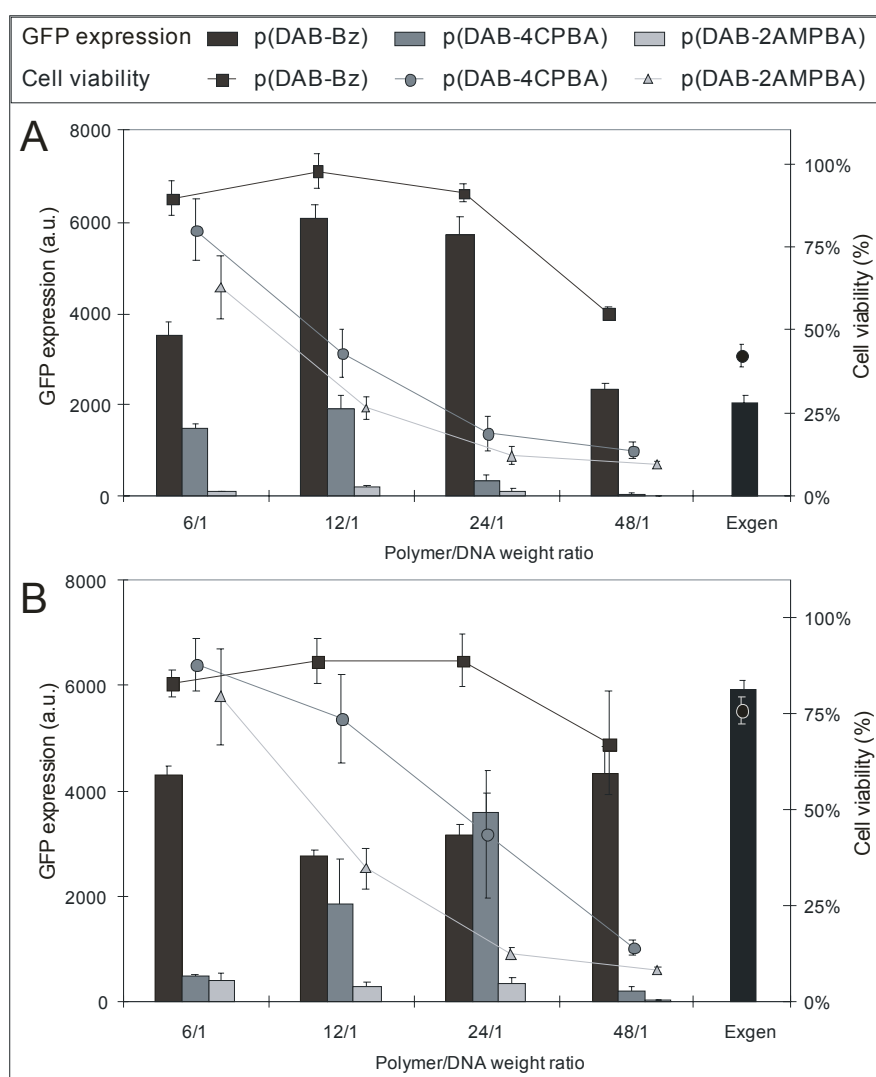


Figure 3.8. Transfection efficiencies were determined in COS-7 cells (fluorescence from GFP expression is shown in bars) and cell viabilities of the same polyplexes (metabolic activity by XTT relative to untreated cells is shown in symbols) in the absence of serum (A) and in the presence of serum (B). Polyplexes were prepared with p(DAB-Bz) (dark grey and squares), p(DAB-4CPBA) (grey and circles), and p(DAB-2AMPBA) (light grey and triangles). Lines are added for clarity.

Figure 3.8B shows the transfection and cell viabilities in the presence of serum. For Exgen a higher GFP expression is observed in the presence of serum than in the absence of serum, which is expected as this polymer at N/P ratio of 6/1 is optimized for use in presence of serum according to the manufacturer. Quite remarkably, the presence of serum has almost no negative effect on the transfection efficiency of polyplexes of p(DAB-Bz). Generally, the presence of serum impedes the transfection efficiency of cationic polyplexes. Therefore, p(DAB-Bz) can be considered as a potent gene delivery vector, with an efficiency that is comparable to that of Exgen in the presence of serum. For polyplexes of p(DAB-4CPBA) a significant increase in transfection efficiency was observed in the presence of serum. At a 24/1 polymer/DNA weight ratio transfection efficiency in presence of serum is close to that of polyplexes of p(DAB-Bz). However, polyplexes prepared with p(DAB-2AMPBA) only gave a marginal increase in transfection efficiency in presence of serum. For p(DAB-4CPBA) the increase in GFP expression can be explained by the improved cell viability in the presence of serum. Although the presence of serum improves the cell viability for both polyplexes of p(DAB-4CPBA) and p(DAB-2AMPBA) also in this medium significant cytotoxicity was observed at the higher 24/1 and 48/1 polymer/DNA weight ratios.

3.3.7. Hemolytic activity of the polymers using erythrocyte leakage

The presence of boronic acid moieties in the p(DAB-4CPBA) and p(DAB-2AMPBA) polymers showed to induce an increase in cytotoxic effect, especially for polyplexes of p(DAB-2AMPBA). Since boronic acids bind to vicinal diols, as are present in carbohydrates, it is likely that the boronated polyplexes interact with glycoproteins on the cell surface [37-39]. Boronic ester formation with the glycocalyx of the cells could improve membrane adhesion and consequently could promote particle uptake, as is schematically illustrated in Figure 3.9. However, the increased membrane interaction caused by the presence of the boronic acid moieties could also promote membrane disruption and thereby induce toxicity.

In order to obtain more information about the membrane disrupting activity of the polymers, a hemolytic red blood cell (RBC) assay was performed. In this assay the concentration of hemoglobin that is leaked out of the erythrocytes due to the presence of polymer that disrupt the erythrocyte cell membrane is determined. This hemolytic activity of polymers can serve as a measure for the membrane disruptive properties of the polymer. To investigate the role of the presence of boronic acid moieties on the membrane disruption of the p(DAB) derivatives, polymer dilution series were prepared of the non-boronated p(DAB-Bz) as well as of the boronated polymers p(DAB-4CPBA) and p(DAB-2AMPBA). The polymer solutions were added to erythrocytes and the hemoglobin concentration of the supernatant was measured using UV-absorption and compared to complete lysis with Triton X-100.

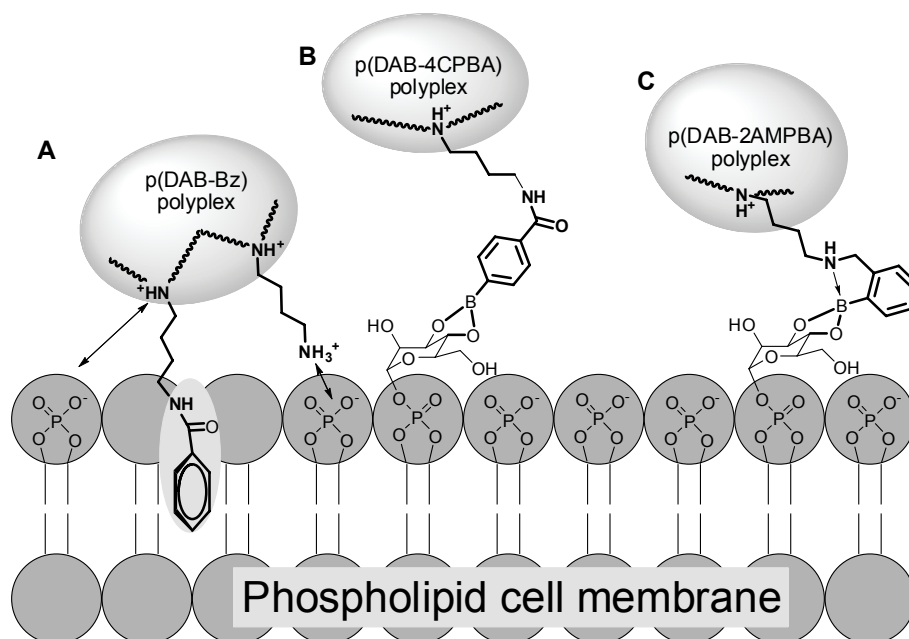


Figure 3.9. Schematic representation of the different interactions between polyplexes and cells possible. **A)** Hydrophobic interaction of the benzoylated side chains with the hydrophobic phospholipids of the cell membrane in combination with charge attraction between protonated aminobutyl side chains with the negatively charge phospholipid membrane. **B)** Boronic ester formation of 4-carbamoylphenylboronic acid side chains with a glucose residue of the cell surface. **C)** Improved boronic ester formation of 2-aminomethylphenylboronic acid side chains with a glucose residue of the cell surface, through a dative B–N interaction.

The data points for the non-boronated polymer p(DAB-Bz) show that significant hemolytic activity becomes apparent at polymer concentration above 0.05 mg/ml (Figure 3.10). The hemolytic activity may originate from cationic interactions of the protonated aminobutyl side chains and/or from hydrophobic interactions of the benzoyl groups with the cell membrane. Remarkably, the boronated polymer p(DAB-4CPBA) has significantly less hemolytic activity which was unexpected based on the cell viabilities of the polyplexes. A possible reason for the lower hemolytic activity could be the reduced hydrophobicity of the 4-carbamoylphenylboronic acid group (4CPBA) as compared to the benzoyl group. Polymer p(DAB-2AMPBA) with the *ortho*-aminophenylboronic acid (2AMPBA) exhibits significantly higher hemolytic activity, which is already starting at a much lower polymer concentration. This observation may serve as an indication that the 2AMPBA groups induce stronger membrane interactions than the 4CPBA groups, which is in accordance with higher propensity of the 2AMPBA groups for boronic ester formation. These stronger membrane interactions could then be well responsible for the high cytotoxicity of the polyplexes formed with p(DAB-2AMPBA) as observed by the XTT assay.

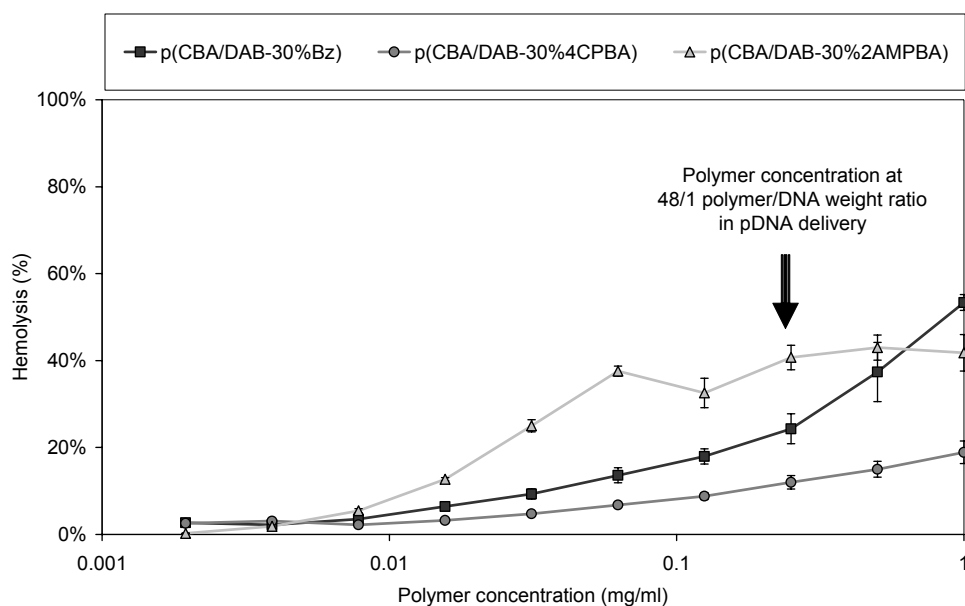


Figure 3.10. Hemolytic activity of the polymer p(DAB-Bz) (squares), p(DAB-4CPBA) (circles) and p(DAB-2AMPBA) (triangles) as determined by the RBC assay. Positive control triton X-100 (1 mg/ml) was set to 100% and negative control HBS was set to 0%. Lines are added for clarity and the arrow represents the highest polymer concentration used in the transfection assay (at 48/1 polymer/DNA weight ratio).

3.4. Conclusions

Boronic acid functionalities could be introduced in the side chains of poly(amido amine)s by functionalization of a disulfide containing poly(amido amine) with pending aminobutyl side chains p(DAB). For this purpose 4-carboxyphenylboronic acid was grafted on the aminobutyl side chains through EDC/NHS coupling, resulting in p(DAB-4CPBA) which was compared with a non-boronated benzoyl-grafted polymer p(DAB-Bz) from the same parent p(DAB). A similar polymer containing *ortho*-(aminomethyl)phenylboronic acid moieties on the aminobutyl side chains was prepared by copolymerization of a boronated monomer, resulting in p(DAB-2AMPBA). The presence of boronic acid moieties in the side chains of these polymers results in the formation of smaller and more monodisperse polyplexes with plasmid DNA compared to that of the non-boronated p(DAB-Bz) as was shown by dynamic light scattering experiments. At low polymer/DNA weight ratios DNA shielding against ethidium bromide intercalation proved to be more efficient for the boronated polymers p(DAB-4CPBA) and p(DAB-2AMPBA) than for the non-boronated reference p(DAB-Bz). This indicates a more efficient condensation and packing of DNA by the boronated polymers.

In the absence of serum, the transfection efficiency of polyplexes of the non-boronated polymer p(DAB-Bz) at a 12/1 and 24/1 polymer/DNA weight ratio was 2–3 times higher than polyplexes of commercial PEI (Exgen), whereas polyplexes of p(DAB-4CPBA) gave about equal transfection efficiencies. In the presence of serum, a medium in which the transfection efficiencies of most cationic polymers are significantly diminished, the transfection efficiency of polyplexes of p(DAB-4CPBA) at 24/1 polymer/DNA weight ratio was considerably improved compared to the serum-free medium.

Ortho-(aminomethyl)phenylboronic acid (2AMPBA) binds stronger to diols than 4CPBA at physiological pH, and higher cellular adhesion might be expected for polyplexes of p(DAB-2AMPBA). Remarkably, low cell viabilities were observed for COS-7 cells exposed to polyplexes of p(DAB-2AMPBA) compared to p(DAB-4CPBA). In addition, significantly higher hemolytic activity was observed for this polymer than for p(DAB-Bz) and p(DAB-4CPBA). These results serve as an indication that the presence of the 2AMPBA moieties induces stronger membrane interactions leading to membrane disruption or interference with essential cellular processes.

In conclusion, by grafting of phenylboronic acid moieties onto the pending aminobutyl side chains of p(DAB) small and monodisperse polyplexes can be formed. However, the concentration and the polymer/DNA ratio of the polyplexes have to be carefully optimized since the boronated polymers are less tolerable to cytotoxicity than the non-boronated analog. In serum the boronic acid groups are probably (partially) shielded, giving rise to lower cytotoxicity. An interesting feature of the presence of boronic acid moieties in the polymer and polyplexes is the possibility for decoration of polyplexes with a variety of polyols such as saccharides providing stealth properties and for glycotargeting.

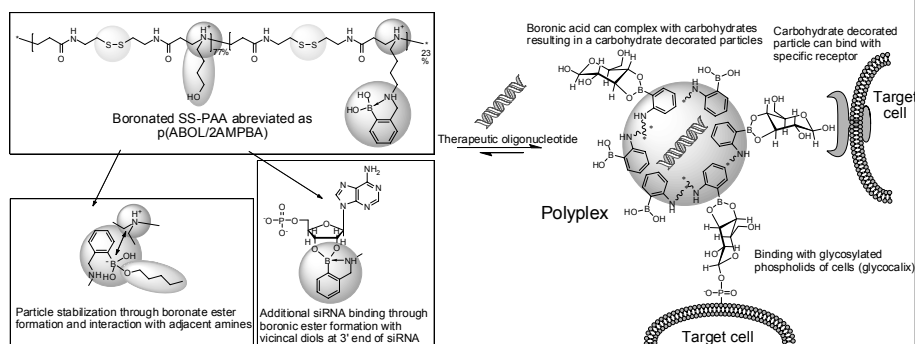
3.5 References

- [1] I.M. Verma, N. Somia, Gene therapy - promises, problems and prospects, *Nature*, 389 (1997) 239-242.
- [2] O. Singer, I.M. Verma, Applications of lentiviral vectors for shRNA delivery and transgenesis, *Curr. Gene Ther.*, 8 (2008) 483-488.
- [3] S.Y. Wong, J.M. Pelet, D. Putnam, Polymer systems for gene delivery-past, present, and future, *Prog. Polym. Sci.*, 32 (2007) 799-837.
- [4] E. Wagner, J. Kloeckner, Gene delivery using polymer therapeutics, *Adv. Polym. Sci.*, 192 (2006) 135-173.
- [5] S.B. Zhang, Y.M. Xu, B. Wang, W.H. Qiao, D.L. Liu, Z.S. Li, Cationic compounds used in lipoplexes and polyplexes for gene delivery, *J. Control. Release*, 100 (2004) 165-180.
- [6] J. Luten, C.F. van Nostruin, S.C. De Smedt, W.E. Hennink, Biodegradable polymers as non-viral carriers for plasmid DNA delivery, *J. Control. Release*, 126 (2008) 97-110.
- [7] T.G. Park, J.H. Jeong, S.W. Kim, Current status of polymeric gene delivery systems, *Adv. Drug Deliver. Rev.*, 58 (2006) 467-486.
- [8] P. Ferruti, M.A. Marchisio, R. Duncan, Poly(amido-amine)s: Biomedical applications, *Macromol. Rapid Comm.*, 23 (2002) 332-355.

- [9] C. Lin, Z.Y. Zhong, M.C. Lok, X.L. Jiang, W.E. Hennink, J. Feijen, J.F.J. Engbersen, Linear poly(amido amine)s with secondary and tertiary amino groups and variable amounts of disulfide linkages: Synthesis and in vitro gene transfer properties, *J. Control. Release*, 116 (2006) 130-137.
- [10] C. Lin, Z.Y. Zhong, M.C. Lok, X.L. Jiang, W.E. Hennink, J. Feijen, J.F.J. Engbersen, Novel bioreducible poly(amido amine)s for highly efficient gene delivery, *Bioconjugate Chem.*, 18 (2007) 138-145.
- [11] M. Piest, C. Lin, M.A. Mateos-Timoneda, M.C. Lok, W.E. Hennink, J. Feijen, J.F.J. Engbersen, Novel poly(amido amine)s with bioreducible disulfide linkages in their diamino-units: Structure effects and in vitro gene transfer properties, *J. Control. Release*, 130 (2008) 38-45.
- [12] C. Lin, C.J. Blaauboer, M.M. Timoneda, M.C. Lok, M. van Steenberg, W.E. Hennink, Z.Y. Zhong, J. Feijen, J.F.J. Engbersen, Bioreducible poly(amido amine)s with oligoamine side chains: Synthesis, characterization, and structural effects on gene delivery, *J. Control. Release*, 126 (2008) 166-174.
- [13] M.A. Mateos-Timoneda, M.C. Lok, W.E. Hennink, J. Feijen, J.F.J. Engbersen, Poly(amido amine)s as gene delivery vectors: Effects of quaternary nicotinamide moieties in the side chains, *Chemmedchem*, 3 (2008) 478-486.
- [14] M. Piest, J.F.J. Engbersen, Effects of charge density and hydrophobicity of poly(amido amine)s for non-viral gene delivery, *J. Control. Release*, 148 (2010) 83-90.
- [15] W.Q. Yang, X.M. Gao, B.H. Wang, Boronic acid compounds as potential pharmaceutical agents, *Med. Res. Rev.*, 23 (2003) 346-368.
- [16] S.L. Wiskur, J.J. Lavigne, H. Ait-Haddou, V. Lynch, Y.H. Chiu, J.W. Canary, E.V. Anslyn, pK(a) values and geometries of secondary and tertiary amines complexed to boronic acids - Implications for sensor design, *Org. Lett.*, 3 (2001) 1311-1314.
- [17] H. Kitano, M. Kuwayama, N. Kanayama, K. Ohno, Interfacial recognition of sugars by novel boronic acid-carrying amphiphiles prepared with a lipophilic radical initiator, *Langmuir*, 14 (1998) 165-170.
- [18] A. Matsumoto, S. Ikeda, A. Harada, K. Kataoka, Glucose-responsive polymer bearing a novel phenylborate derivative as a glucose-sensing moiety operating at physiological pH conditions, *Biomacromolecules*, 4 (2003) 1410-1416.
- [19] T. Hoare, R. Pelton, Engineering glucose swelling responses in poly(N-isopropylacrylamide)-based microgels, *Macromolecules*, 40 (2007) 670-678.
- [20] B. Appleton, T.D. Gibson, Detection of total sugar concentration using photoinduced electron transfer materials: development of operationally stable, reusable optical sensors, *Sensor Actuat. B-Chem.*, 65 (2000) 302-304.
- [21] S.H. Gao, W. Wang, B.H. Wang, Building fluorescent sensors for carbohydrates using template-directed polymerizations, *Bioorg. Chem.*, 29 (2001) 308-320.
- [22] M. Di Luccio, B.D. Smith, T. Kida, C.P. Borges, T.L.M. Alves, Separation of fructose from a mixture of sugars using supported liquid membranes, *J. Membrane Sci.*, 174 (2000) 217-224.
- [23] A.E. Ivanov, I.Y. Galaev, B. Mattiasson, Binding of adenosine to pendant phenylboronate groups of thermoresponsive copolymer: a quantitative study, *Macromol Biosci.*, 5 (2005) 795-800.
- [24] A. Ozdemir, A. Tuncel, Boronic acid-functionalized HEMA-based gels for nucleotide adsorption, *J. Appl. Polym. Sci.*, 78 (2000) 268-277.
- [25] H. Cicek, Nucleotide isolation by boronic acid functionalized hydrogel beads, *J. Bioact. Compat. Pol.*, 20 (2005) 245-257.
- [26] S. Senel, S.T. Camli, M. Tuncel, A. Tuncel, Nucleotide adsorption-desorption behaviour of boronic acid functionalized uniform-porous particles, *J. Chromatogr. B*, 769 (2002) 283-295.
- [27] B. Elmas, M.A. Onur, S. Senel, A. Tuncel, Temperature controlled RNA isolation by N-isopropylacrylamide-vinylphenyl boronic acid copolymer latex, *Colloid Polym. Sci.*, 280 (2002) 1137-1146.
- [28] A. Coskun, E.U. Akkaya, Three-point recognition and selective fluorescence sensing of L-DOPA, *Org. Lett.*, 6 (2004) 3107-3109.
- [29] S. Kitano, Y. Koyama, K. Kataoka, T. Okano, Y. Sakurai, A novel drug delivery system utilizing a glucose responsive polymer complex between poly (vinyl alcohol) and poly (N-vinyl-2-pyrrolidone) with a phenylboronic acid moiety, *J. Control. Release*, 19 (1992) 161-170.
- [30] C. Young Kweon, J. Seo Young, K. Young Ha, A glucose-triggered solubilizable polymer gel matrix for an insulin delivery system, *Int. J. Pharm.*, 80 (1992) 9-16.
- [31] D. Shiino, Y. Murata, K. Kataoka, Y. Koyama, M. Yokoyama, T. Okano, Y. Sakurai, Preparation and characterization of a glucose-responsive insulin-releasing polymer device, *Biomaterials*, 15 (1994) 121-128.

- [32] D. Shiino, Y. Murata, A. Kubo, Y.J. Kim, K. Kataoka, Y. Koyama, A. Kikuchi, M. Yokoyama, Y. Sakurai, T. Okano, Amine containing phenylboronic acid gel for glucose-responsive insulin release under physiological pH, *J. Control. Release* 37 (1995) 269-276.
- [33] V. Lapeyre, C. Ancla, B. Catargi, V. Ravaine, Glucose-responsive microgels with a core-shell structure, *J. Colloid Interface Sci.*, 327 (2008) 316-323.
- [34] T. Koyama, K. Terauchi, Synthesis and application of boronic acid-immobilized porous polymer particles: A novel packing for high-performance liquid affinity chromatography, *J. Chromatogr. B*, 679 (1996) 31-40.
- [35] S.J. Coutts, T.A. Kelly, R.J. Snow, C.A. Kennedy, R.W. Barton, J. Adams, D.A. Krolkowski, D.M. Freeman, S.J. Campbell, J.F. Ksiazek, W.W. Bachovchin, Structure-activity relationships of boronic acid inhibitors of dipeptidyl peptidase IV .1. Variation of the P-2 position of X(aa)-boroPro dipeptides, *J. Med. Chem.*, 39 (1996) 2087-2094.
- [36] P. Hazot, T. Delair, A. Elaissari, J.P. Chapel, C. Pichot, Functionalization of poly(N-ethylmethacryl-amide) thermosensitive particles by phenylboronic acid, *Colloid Polym. Sci.*, 280 (2002) 637-646.
- [37] N.D. Winblade, H. Schmokel, M. Baumann, A.S. Hoffman, J.A. Hubbell, Sterically blocking adhesion of cells to biological surfaces with a surface-active copolymer containing poly(ethylene glycol) and phenylboronic acid, *J Biomed Mater Res*, 59 (2002) 618-631.
- [38] Y.R. Vandenburg, Z.Y. Zhang, D.J. Fishkind, B.D. Smith, Enhanced cell binding using liposomes containing an artificial carbohydrate-binding receptor, *Chem. Commun.*, (2000) 149-150.
- [39] A.E. Ivanov, I.Y. Galaev, B. Mattiasson, Interaction of sugars, polysaccharides and cells with boronate-containing copolymers: from solution to polymer brushes, *J. Mol. Recognit.*, 19 (2006) 322-331.
- [40] A.E. Ivanov, K. Shiomori, Y. Kawano, I.Y. Galaev, B. Mattiasson, Effects of polyols, saccharides, and glycoproteins on thermoprecipitation of phenylboronate-containing copolymers, *Biomacromolecules*, 7 (2006) 1017-1024.
- [41] S. Moffatt, S. Wiehle, R.J. Cristiano, Tumor-specific gene delivery mediated by a novel peptide-polyethylenimine-DNA polyplex targeting aminopeptidase N/CD13, *Hum. Gene Ther.*, 16 (2005) 57-67.
- [42] S. Moffatt, R.J. Cristiano, Uptake characteristics of NGR-coupled stealth PEI/pDNA nanoparticles loaded with PLGA-PEG-PLGA tri-block copolymer for targeted delivery to human monocyte-derived dendritic cells, *Int. J. Pharmaceut.*, 321 (2006) 143-154.
- [43] Q. Peng, F. Chen, Z. Zhong, R. Zhuo, Enhanced gene transfection capability of polyethylenimine by incorporating boronic acid groups, *Chem. Commun.*, 46 (2010) 5888-5890.

Boronic acid functionalized poly(amido amine) with improved polyplex stability for pDNA and siRNA delivery in vitro

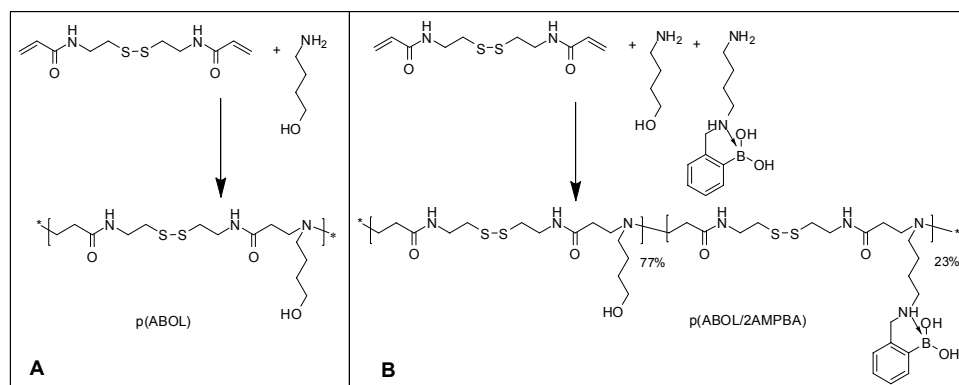


Abstract

The effects of the presence of *ortho*-aminomethylphenylboronic acid moieties as side groups in disulfide containing poly(amido amines) were investigated in their effectiveness to function as gene delivery vectors. To this purpose, a boronated polymer was prepared by Michael-type polyaddition of a 3:1 mixture of 4-aminobutanol (ABOL) and 2-((4-aminobutylamino)methyl)phenyl boronic acid (2AMPBA) to an equimolar amount of *N,N'*-cystamine bisacrylamide. The resulting polymer, p(ABOL/2AMPBA), incorporating 23% of *ortho*-aminophenylboronic acid comonomers, forms polyplexes with pDNA and siRNA of *ca.* 100 nm and 40 mV. The presence of the boronic acid moieties strongly enhances the stability of the polyplexes, and no aggregation was observed after storage of 4 days at 37 °C. The nanoparticles release their nucleotide cargo completely in a reductive environment due to rapid cleavage of the disulfide bonds in the main chain of the polymer. DNA transfection in different cell lines (COS-7, HUH-6 and H1299-Fluc) using p(ABOL/2AMPBA) as polymeric vector gave transfection efficiencies that were approximately similar to commercial PEI, whereas p(ABOL) lacking the boronic acid moieties was *ca.* two times more effective than PEI. For siRNA transfection the use of p(ABOL) and p(ABOL/2AMPBA) as polymeric vectors results in knockdown efficiencies of luciferase expression in H1229-Fluc cells of *ca.* 28% and 35%, respectively. Most importantly, whereas addition of different monosaccharides to polyplexes of p(ABOL) have only marginal effects, the knockdown of efficiency of siRNA polyplexes of p(ABOL/2AMPBA) could be significantly enhanced (up to 67%) in the presence of these carbohydrates.

4.1. Introduction

Most of the metabolic diseases have a genetic component. Therefore administration of a therapeutic “healthy” gene or silencing of a malfunctioning gene in the body is suggested as a promising technique to cure various metabolic diseases [1]. In gene therapy, the greatest challenge is the delivery of therapeutic genes in the target cells. Although viral vectors have shown some success, inherent disadvantages like immunoresponse and mutagenity direct expectations to further progress toward cationic polymeric vectors to transport therapeutic nucleotides (DNA or siRNA) into target cells [2-6]. However, using these non-viral systems, the efficiency of transfection has to be significantly improved. We previously developed a broad range of poly(amido amine)s with repetitive disulfide linkages in the main chain (SS-PAA) that combine high transfection efficiencies with low cytotoxicity profiles [7-13]. Amongst these polymers, the polymer derived from the Michael-type polyaddition of 4-aminobutanol to cystamine bisacrylamide (p(ABOL)), having pending hydroxybutyl side chains, was the most successful *in vitro* gene delivery vector to date [10]. The synthesis of p(ABOL) and its boronated analogue p(ABOL/2AMPBA) are given in Scheme 4.1.



Scheme 4.1. **A** Michael addition polymerization of *N,N'* cystamine bisacrylamide and 4-aminobutanol resulting in p(ABOL), **B** Michael addition polymerization of *N,N'* cystamine bisacrylamide and 75% 4-aminobutanol and 25% of monomer 1 resulting in the boronated analogue p(ABOL/2AMPBA) containing 23% of *ortho*-aminomethylphenylboronic acid groups.

In more recent work we have incorporated boronic acid moieties into SS-PAAAs [12]. Boronic acids are Lewis acids that are known to reversibly form boronic esters with vicinal diols [14-18], including carbohydrates [20-24]. Incorporation of boronic acids in various materials is known to improve adhesion of cells to these materials [19-21] and allows for new strategies of drug conjugation [17] and *post*-PEGylation of polyplexes [27-28]. From literature data it is known that the presence of an aminomethyl group in the *ortho* position relative to the phenylboronic acid can give a

dative B–N (or N→B) interaction that enhances the binding affinity of the boronic acid for vicinal diols, as present in carbohydrates, at neutral pH [29-30]. Since carbohydrates play a pivotal role in many cellular processes, like cell adhesion and molecular recognition processes by membrane glycoconjugates, it is of particular interest to gain information about the effect of introduction of carbohydrate binding boronic acid moieties in the polymeric gene vector. Therefore, we have developed an SS-PAA copolymer based on p(ABOL) and an aminobutyl comonomer with terminal *ortho*-aminomethylphenylboronic acid (2AMPBA) moieties. This copolymer, abbreviated as p(ABOL/2AMPBA) was obtained by Michael-type polyaddition of a 3:1 mixture of 4-aminobutanol and 2AMPBA butylamine to an equimolar amount of *N,N'*-cystamine bisacrylamide (Scheme 4.1B). The structure of p(ABOL/2AMPBA) has several special features, that makes this polymer of interest to evaluate its properties as potential vector for gene (and drug) delivery (Figure 4.1).

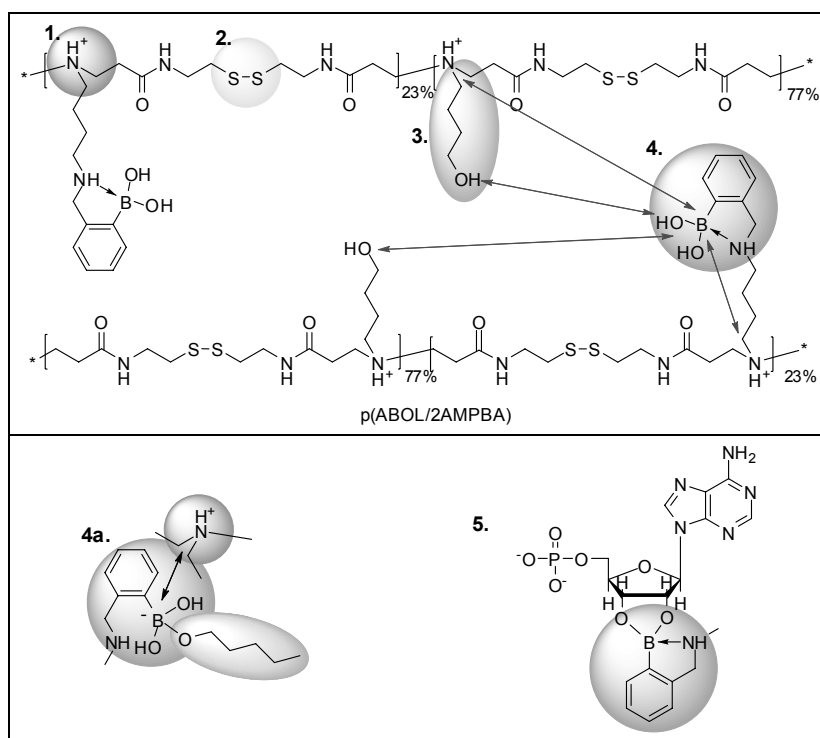
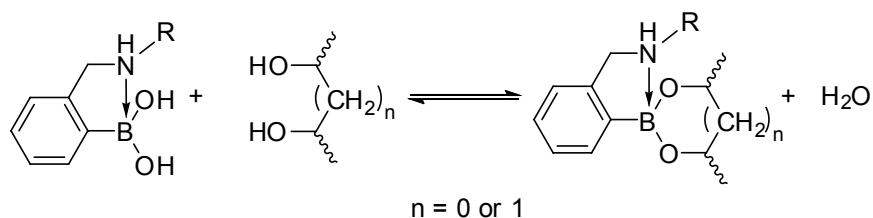


Figure 4.1. Overview of the special features of p(ABOL/2AMPBA).

1. Protonable tertiary amines for DNA condensation and endosomal pH buffering. **2.** Repetitive disulfide linkages for fast intracellular polymer degradation through disulfide reduction. **3.** Hydroxybutyl side chains have proven to favorably contribute to the transfection efficiency of polyplexes with DNA. **4.** *Ortho*-aminomethylphenylboronic acid (2AMPBA) that can interact with Lewis bases such as amines and alcohols of the same polymer chain or a polymer chain in the close vicinity. **4a.** 2AMPBA can form a boronate ester with the hydroxybutyl side chains and the anion can be stabilized by proximal cationic amines. **5.** 2AMPBA can form a boronic ester with the vicinal diols of ribose present in nucleotides, such as at the 3' ribose end of RNA.

First, the tertiary amino groups in the PAA main chain give the polymer buffer capacity in the pH range 7.4–5.1, the pH region where endosomal acidification occurs [10]. This buffering effect favorably contributes to the endosomal escape of PAA polyplexes. Second, the repetitive disulfide moieties in the main chain make the polymer readily degradable in the reductive intracellular environment. This enables rapid unpacking of the therapeutic payload once the polymer is taken up by the cell. Third, the presence of hydroxybutyl groups in the side chains of SS-PAA has shown to favorably contribute to the transfection efficiency. Although the specific influence of this side group has not yet been elucidated, it is assumed that this group provides additional endosomolytic properties to the polymer through a beneficial influence on the hydrophilic/hydrophobic balance. Fourth, the presence of the 2AMPBA moieties provides the polymer carbohydrate-binding properties by reversible boronate ester formation (see Scheme 4.2).



Scheme 4.2. Stabilization of boronic ester bond formation due to possibility of a dative B–N interaction.

It is speculated that the presence of the 2AMPBA in the polyplexes will result in increased cell membrane interactions by binding affinity to the glycocalyx of the cell membrane. Moreover, carbohydrates present in a p(ABOL/2AMPBA) polyplex solution can bind to the polyplex surface which can lead to increased polyplex stability, stealth properties, or increased cell specificity (targeting). In addition, since the boron center in 2AMPBA has Lewis acid properties, the 2AMPBA moieties in the SS-PAA polymer may also interact with tertiary amino groups in the main chain and hydroxybutyl side groups of the polymer. This may give rise to non-covalent crosslinking interactions and increased stability of polyplexes of this polymer, since high local concentrations of tertiary amines and hydroxybutyl side chains in the proximity of boronic acid moieties inside a polyplex result in increased Lewis acid (boronic acid) - Lewis base (amine, alcohol) interactions and eventually boronic ester bond formation. Fifth, by the presence of the *ortho*-aminophenylboronic acid moieties the siRNA binding in the polyplex and polyplex formation can be improved. It is known that boronic acids have a strong interaction with RNA due to reversible boronic ester formation with the vicinal diols of the 3' ribose endgroups [22-23]. It can be expected that this reversible ester formation gives additional stabilization to p(ABOL/2AMPBA)/siRNA polyplexes which will be very advantageous for siRNA delivery, where usually polyplex stability poses a problem.

4.2. Materials and methods

N,N'-cystamine bisacrylamide (CBA, Aldrich), N-BOC-1,4-diaminobutane (Aldrich), benzoylchloride (Aldrich), 2-formylphenylboronic acid (Aldrich) and 4-aminobutanol (Aldrich) were of commercial grade and used without further purification. All reagents and solvents were of reagent grade and were used without further purification.

NMR spectra were recorded on a Varian Unity 300 (¹H NMR 300 MHz) using the solvent residual peak as the internal standard. ES-TOF-MS spectra were recorded on a Waters/Micromas LCT mass spectrometer.

4.2.1. Synthesis of 2-((4-aminobutylamino)methyl)phenyl boronic acid (monomer 1)

2-Formylphenylboronic acid (5.10 g, 34.0 mmol) was dissolved in 45 ml methanol, together with N-BOC-1,4-diaminobutane (6.69 g, 34.7 mmol) and 3 equivalents triethylamine (10.08 g, 99.6 mmol) and the mixture was stirred overnight under nitrogen at ambient temperature. The mixture turned yellow and ¹H NMR confirmed the formation of the Schiff's base. Next, 3 equivalents NaBH₄ (3.91 g, 103.3 mmol) were added to the reaction mixture to reduce the Schiff's base and the solution turned colorless. The product was thrice extracted from water/chloroform. The organic layer was dried over MgSO₄ and evaporated under reduced pressure. The product was isolated as an off-white solid (8.78 g, 75% yield). The BOC-protected product was dissolved in 30 ml of methanol and deprotected by perfusion of HCl-gas through the reaction mixture for 30 min at ambient temperature. The solvent was evaporated to dryness and ¹H NMR of the product showed complete deprotection. The product contained 50% of monomer **1** according to ¹H NMR using *p*-toluene sulfonic acid as internal standard and was used without further purification. Residual mass was due to bound water to the boronic acid and counter ions (HCl-salt of the amines).

¹H-NMR (D₂O, 300 MHz): δ = 7.1–7.4 (4H, m, ArH), δ = 3.950 (2H, s, ArH-CH₂-NH); δ = 2.905 (2H, t, 3J(H-H) = 7.2 Hz, NH-CH₂-CH₂), δ = 2.825 (2H, t, 3J(H-H) = 7.5 Hz, CH₂-CH₂-NH₂), δ = 1.673 (2H, q, 5J(H-H) = 7.7 Hz, CH₂-CH₂-CH₂-CH₂-NH₂), δ = 1.601 (2H, q, 5J(H-H) = 8.4 Hz, CH₂-CH₂-CH₂-CH₂-NH₂). MS (ES⁺-TOF): m/z = 239.3 (100) ([M+OH+ H⁺], calculated for [C₁₁H₂₀BN₂O₃]: 239.16).

4.2.2 Synthesis of p (ABOL/2AMPBA)

The polymer was synthesized by the Michael addition of N,N'-cystamine bisacrylamide (1.18 g, 4.37 mmol), 78% of 4-aminobutanol (0.31 g, 3.41 mmol) and 22% of monomer **1** (0.23 g, 0.96 mmol). The reactants were dissolved in a mixture of methanol (1.6 ml), water (0.4 ml) and triethylamine (0.5 ml). After 8 days reacting at 45 °C under nitrogen in the dark, the reaction was terminated by addition of excess of

monomer **1** (0.33 g, 1.47 mmol) dissolved in methanol (0.9 ml), water (0.6 ml) and triethylamine (0.23 ml). The termination reaction was left to proceed for another 5 days and the polymer was isolated using an ultrafiltration membrane (M_w CO 3000 g/mol), yielding 1.14 g of off-white solid (66.5% yield). The composition of the polymer was established by ^1H NMR (D_2O , 300 MHz) and the content of boronic acid side groups was 23% with respect to the total amount of side groups.

^1H NMR (p(ABOL/2AMPBA), HCl salt, D_2O , 300 MHz):

δ 7.7–7.8 (0.23H, m, ArH), δ = 7.4–7.5 (0.69H, m, ArH), δ = 4.2–4.4 (0.46H, m, ArH- CH_2 -NH), δ = 3.65 (4H, t, (2H, t, NHCO- CH_2 - CH_2 -N), δ = 3.55 (4H, t, SS- CH_2 - CH_2 -N), δ = 3.30 (1.64H, t, CH_2 - CH_2 -OH), δ = 3.30 (0.46H, t, CH_2 - CH_2 -NH- CH_2 -Ar), δ = 3.15 (2H, t, R_2 -N- CH_2 - CH_2), δ = 2.90 (4H, t, NHCO- CH_2 - CH_2 -N), δ = 2.75 (4H, t, CH_2 -SS- CH_2), δ = 1.75 (2H, m, N- CH_2 - CH_2 - CH_2 - CH_2), δ = 1.55 (2H, m, N- CH_2 - CH_2 - CH_2 - CH_2)

4.2.3. Determination of the molecular weight of the polymer

Molecular weight information was obtained using a TDA302 system (operated without a column) equipped with a TDA302 triple detector array, consisting of a refractive index (RI) detector, a light scattering detector (7° and 90°) and a viscosity detector, together with the OmniSec 4.1 software provided by Viscotec (Oss, The Netherlands). First, the samples were dried overnight over siccant, and subsequently stirred to dissolve for 24 h at a concentration of 5 mg/ml in a mixture of water/methanol 1/4 (v/v). Next, 20 μl of the sample was injected and dn/dc was calculated based on the RI response using the flow injection polymer analysis (FIPA) method.

4.2.4. Determination of the buffer capacity of the polymer

The buffer capacity of the SS-PAAAs was determined by recording the pH change during the automated titration of a concentrated acidic polymer solution with 0.1 M NaOH solution. Therefore, 0.05 g of polymer (0.25 mmol of protonable nitrogens) was dissolved in 5 ml of 150 mM NaCl solution and the pH was set to 2.0 with a few drops of 1.0 M HCl. This solution was titrated with 0.1 M NaOH solution (0.4 ml/min) and the pH was recorded as a function of the added sodium hydroxide solution.

The buffer capacity is defined as the percentage of (protonable) nitrogen atoms in PAA that becomes protonated in the pH interval from 7.4 to 5.1, being the pH change the polyplexes experience upon change from the extracellular environment (pH 7.4) to the late endosomal environment (pH 5.1). The buffer capacity can be calculated as the mol OH^- added per mol of protonable N-atoms of the polymer, according to Equation 4.1.

$$BufferCapacity(\%) = \frac{(\Delta V_{pol} - \Delta V_{NaCl}) \times 0.1M}{mol\ N} * 100\% \quad (\text{Equation 4.1})$$

Where ΔV_{pol} and ΔV_{NaCl} are the volumes of 0.1 M NaOH added to change the pH from 5.1 to 7.4 in the polymer solution and pure 150 mM NaCl solution, respectively. ΔV_{NaCl} was measured and found to be negligible in this pH range. Mol N is the total amount of protonable nitrogen atoms.

4.2.5. Polyplex preparation

The DNA plasmid solution (1 mg/ml) as supplied by manufacturer (PlasmidFactory, Bielefeld) was diluted to a final concentration of 0.075 mg/ml in HEPES buffer solution (50 mM, set to pH 7.4). A series of polymer solutions of different concentrations was prepared by dilution of a solution of 0.9 mg/ml in HEPES buffer solution repeatedly 1:1 with HEPES buffer solution. To prepare polyplexes at 48/1, 24/1, and 12/1 polymer/DNA weight ratio 0.80 ml of each polymer solution was added to 0.20 ml of DNA solution in a 1.5 ml Eppendorf tube. The polyplex solutions were vortexed for 5 s and incubated for 30 min at ambient temperature prior to use.

Polyplexes with siRNA (Anti-Firefly Luciferase, Eurogentec; AllStars Negative Control siRNA, Qiagen) were prepared using a 1:1 dilution series of polymer, starting from 0.375 mg/ml in Hepes buffer. Next, 16 μ l of polymer solution was added to 4 μ l of siRNA (31.25 μ g/ml), resulting in polyplexes with polymer/siRNA weight ratios of 48/1, 24/1, and 12/1 respectively. The polyplexes were vortexed for 5 s and incubated 30 min at ambient temperature.

For the transfection experiments in the presence of sugars, 100 μ l of different carbohydrate stock solutions (10% w/v) were added to 1.0 ml of polyplexes to a final concentration of 0.9% w/v and the samples were incubated for another 30 min at ambient temperature prior to use.

4.2.6. Determination of polyplex properties by Dynamic Light Scattering (DLS)

Size and zeta-potential of the nanoparticles formed by spontaneous self-assembly of the poly(amido amine)s, of poly(amido amine)/plasmid DNA polyplexes and of poly(amido amine)/plasmid siRNA polyplexes were measured at 25 °C with a Zetasizer Nano (Malvern Instruments Ltd, Malvern, UK) and the dynamic light scattering results were processed using Dispersion Technology Software V5.0. For the stability measurements polyplexes were stored at 37 °C and measured at 25 °C.

4.2.7 Determination of DNA or siRNA condensation using ethidium bromide fluorescence

The efficiency of DNA (or siRNA) condensation was measured using the ethidium bromide fluorescence assay as previously described in section 2.5, using a Varian Eclipse fluorescence spectrophotometer, with excitation and emission wavelength of 520 and 600 nm, respectively [11]. Briefly, the fluorescence intensity of a solution of ethidium bromide (5×10^{-6} M) in the presence of uncondensed DNA (or siRNA) (0.015 mg/ml) in HEPES (20 mM, pH 7.4) was determined by fluorescence spectroscopy. The molar ratio of ethidium bromide to the DNA (or siRNA) phosphates in this solution is 1:10, resulting in intercalation and strong fluorescence of the ethidium cation. Similarly, ethidium fluorescence is measured in the presence of the appropriate polyplex solutions, using the same concentrations of ethidium bromide and DNA (or siRNA). The relative fluorescence (F_r) represents a relative measure for the degree of shielding of DNA (or siRNA) in the polyplex, and was determined from the equation: $F_r = (F_{\text{obs}} - F_e) / (F_0 - F_e)$. Here F_{obs} is the fluorescence of the polyplex dispersion, F_e is the fluorescence of ethidium bromide in the absence of DNA (or siRNA), and F_0 is the initial fluorescence of DNA/ethidium bromide (or siRNA/ethidium bromide) in the absence of polymer.

4.2.8 Agarose gel retardation

Polyplex solutions at different polymer/DNA weight ratios were prepared as described in section 2.5, followed by vortexing for 5 s and incubation at ambient temperature for 30 min. DTT was used to mimic glutathione reduction and was added to a final concentration of 2.5 mM to the appropriate samples. After another 30 min (with or without DTT incubation), polyplexes were loaded on a 0.8% w/v agarose gel containing 1.25 μ M ethidium bromide. Electrophoresis was performed for 60 min at 90 V in a TAE running buffer (40 mM tris(hydroxymethyl)aminomethane, 20 mM acetic acid, 10 mM EDTA, pH 8.0) supplemented with 1.25 μ M ethidium bromide. After electrophoresis, pictures were taken on a Biorad Gel Doc 2000 under UV illumination and analyzed using Biorad Multi Analyst software version 1.1.

4.2.9. In vitro transfection and cell viability

The cell culture medium consisted of Dulbecco's Modified Eagle Medium (invitrogen) with 1 g/l D-glucose, completed with L-glutamine (1% v/v of GlutaMAX 200 mM) and penicillin-streptomycin solution (2% v/v of stock solution).

Transfection and cell viability studies were performed with COS-7 cells (SV-40 transformed African Green monkey kidney cells), HUH-6 cells (human hepatoblastoma cells) and H1299-Fluc (non-small cell human lung carcinoma cell line stably transfected with firefly luciferase) in the absence and the presence of

10% calf bovine serum in separate 96-well plates, $n = 4$. Cells were plated 24 h prior to transfection (COS-7 at 10,000 cells/well, HUH-6 at 8,000 cells/well and H1299-Fluc at 12,000 cells/well) and were 60–80% confluent after 24 h. Plasmid pCMV/GFP was used as reporter gene. Two parallel transfection series, one for the determination of reporter gene expression (GFP) and the other for the evaluation of the cell viability by XTT assay, were carried out in separate 96-well plates. Different polymer/DNA weight ratios were used to prepare the polyplexes. In a typical transfection experiment, the cells were incubated with the desired amount of polyplexes (100 μ l dispersion or 110 μ l after addition of a sugar solution of 10% w/v resulting in 1 μ g plasmid DNA per well) for 2 h at 37 °C in a humidified 5% CO₂-containing atmosphere. Next, the polyplex solution was removed, 100 μ l of fresh culture medium was added and the cells were cultured for another 48 h. Transfection efficiencies (TE) were compared to the transfection of linear PEI (Exgen 500, Fermentas) at its optimal 6/1 N/P ratio (TE was set at 1.0). In all transfection studies p(ABOL/2AMPBA) was compared with the non-boronated analog p(ABOL), that has shown excellent transfection efficiencies in our previous studies [10]. The TE was determined by measuring the GFP expression by fluorescence spectroscopy, using a TECAN Safire² plate reader using SW Magellan Software V6.4 with 4 readings per well at different positions. Excitation was at 480 nm and optimal emission was determined at 503 nm. The percentage of GFP positive cells was determined after fixation of the cells with 4% formaldehyde in PBS, followed by a DAPI staining according to manufacturer (Sigma). The 96-well plates were analyzed using a BD Pathway 435 bioimaging system operated with AttoVisionTM Software and the percentage of GFP positive cells was calculated using Cellprofiler 2.0 Software.

The cell viability was measured using an XTT assay, in which the XTT value for untreated cells (cells not exposed to transfection agents) was taken as 100 % cell viability. XTT measurements were performed in quadruplicate using the Perkin Elmer LS50B luminescence spectrometer and analyzed in Kineticalc for Windows V2.0. For the XTT absorbance was measured at 490 nm with a reference at 655 nm.

4.2.10 Luciferase knockdown using siRNA

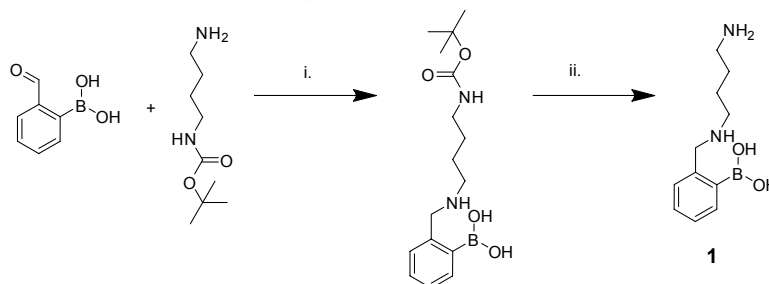
Anti-luciferase siRNA was used to knockdown luciferase expression in H1299-Fluc cells. H1299-Fluc is a non-small cell lung carcinoma cell line derived from the lymph node, stably expressing firefly luciferase. Cells were cultured in completed RPMI 1640 medium completed with L-glutamine (1% v/v of GlutaMAX 200 mM) and penicillin-streptomycin solution (2% v/v of stock solution) and 10 % v/v FBS). The cells were plated at 8,000 cells/well in a 96-well plate 24 h prior to the experiment and incubation at 37 °C in a humidified 5% CO₂-containing atmosphere. Cells were 40–50 % confluent.

Polyplexes were prepared using a 1:1 dilution series of polymer, starting from 0.375 mg/ml in Hepes buffer. Next, 16 μ l of polymer solution was added to 4 μ l of siRNA (31.25 μ g/ml), resulting in polyplexes with polymer/siRNA weight ratios of 48/1, 24/1, and 12/1 respectively. Next, 2.0 μ l of 10% w/v of the appropriate sugar solution was added to the polyplexes. The polyplexes were vortexed for 5 s and incubated 30 min at ambient temperature. Two parallel series were prepared, the first using Allstars Negative Control siRNA (Qiagen) to determine the cell viability and the second using anti-luciferase siRNA (Eurogentec) to determine the knockdown. Medium was replaced with 100 μ l plain RPMI 1640 medium. After 30 min of incubation in the refreshed medium, 20 μ l of the polyplexes were added to the corresponding wells. After 2 h incubation at 37 °C and 5% CO₂, the medium/polyplex mixture was removed from the cells, cells were washed once with 100 μ l PBS and finally 100 μ l completed medium (with FBS) was added. The cells were incubated for 48 h at 37 °C and 5% CO₂ before lysis of the cells. The cell lysates were treated with Luciferase Assay Reagent (Promega) at ambient temperature and the luciferase activity was measured within the next 10 min, using a VICTOR3TM 1420 multilabel counter (Perkin-Elmer) analyzed with Wallac 1420 Software. Polyplexes of Lipofectamine2000 (Invitrogen) and Exgen500 (N/P ratio = 5, Fermentas) were used as positive control and prepared according to manufacturers protocol with the same amount of siRNA as the SS-PAA polyplexes. The relative knockdown was corrected using the non-coding siRNA transfected samples, compared to untreated cells.

4.3. Results and discussion

4.3.1 Synthesis of p(ABOL/2AMPBA)

The boronic acid containing amine monomer **1** was synthesized by the Schiff's condensation of *o*-formylphenylboronic acid with *N*-BOC-diaminobutane, followed by the reduction with sodium borohydride [12].

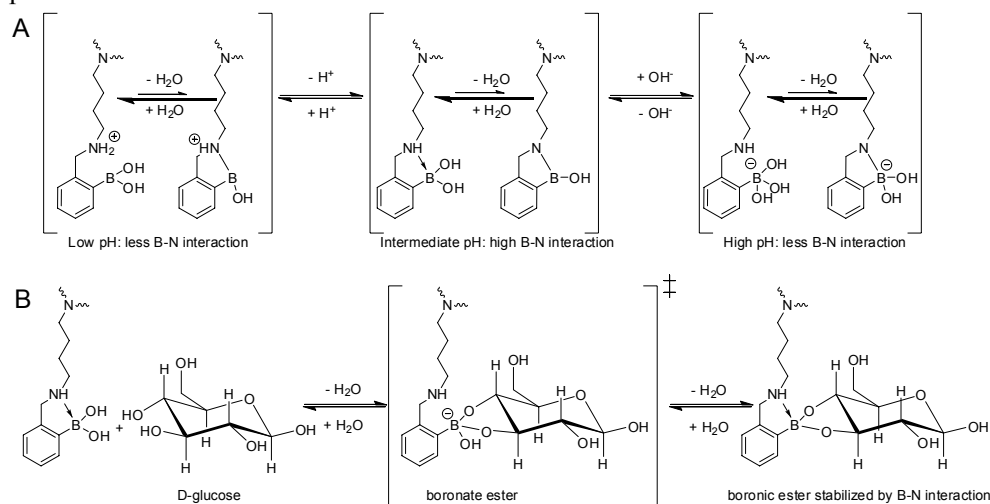


Scheme 4.3. Synthesis of monomer **1**. i.) Schiff's base formation in methanol followed by reduction with NaBH₄. ii.) deprotection with HCl (g) in methanol.

It was found that among the SS-PAA's developed by our group, the polymer based on cystamine bisacrylamide and 4-aminobutanol abbreviated as p(ABOL) is one of the most effective vectors for *in vitro* delivery of pDNA [10]. Therefore, the 4-aminobutanol was selected as the comonomer in the copolymer containing the boronic acid moieties. Copolymer p(ABOL/2AMPBA) was synthesized by reacting *N,N'*-cystamine bisacrylamide with 78% of 4-aminobutanol and 22% of monomer **1** according to Scheme 4.1. The copolymer was obtained in 67% yield and the amount of boronic acid containing aminobutyl units was found to be *ca.* 23% according to ¹H NMR. The weight average M_w was determined to be 4.2 kDa, which is similar to the M_w of p(ABOL) of 4.1 kDa [24] used in this study. From the M_w it was calculated that the polymer chains contain *ca.* 12 repeating units; therefore on average each polymer chain has approximately 3 *ortho*-aminomethylphenylboronic acid moieties.

By comparing the gene delivery properties of p(ABOL/2AMPBA) and p(ABOL), possible effects of the presence of *ortho*-aminomethylphenylboronic acid groups in the polymer can be evaluated. Binding of phenylboronic acids with diols to form phenylboronic esters is generally optimal at the pH that is equal to the pK_a of the phenylboronic acids. The parent compound phenylboronic acid (PBA) has a pK_a of 8.8, and therefore boronic ester formation at physiological relevant pH is poor [18]. However this situation is profoundly different in 2AMPBA. Due to the presence of the *ortho*-aminomethyl group in 2AMPBA a dative B–N (or N→B) bond can be formed that reduces the energy for the transition of the sp² hybridized boronic center to the sp³ hybridized boronate which is beneficial for diol binding (e.g. glucose) and ester formation (Scheme 4.4). As a result, polymer p(ABOL/2AMPBA)

can form reversible covalent esters with diols at physiological pH, including sugars and glycoproteins of the cell membrane. It was hypothesized that this property would also affect the transfection properties of polyplexes formed with this polymer and pDNA or siRNA.



Scheme 4.4. Figure A shows pH-dependant formation of a dative B–N bond in the side chains of p(ABOL/2AMPBA). Figure B shows binding of 2AMPBA side chains with glucose, thereby disrupting the B–N interaction and formation of a labile anionic boronate ester that is stabilized by the reformation of the dative B–N interaction, resulting in the loss of H_2O

4.3.2 The buffer capacity of p(ABOL/2AMPBA) compared to p(ABOL)

Typically, SS-PAA with tertiary amines in the polymer backbone have high buffering capacity which is assumed to favorably contribute to endosomal escape. For example p(ABOL) has a buffer capacity of 72% in the pH range of 7.4 to 5.1 as determined by acid - base titration [10]. Such a high buffer capacity indicates a large increase in the degree of protonation upon endosomal acidification from pH 7.4 (bloodstream) to pH 5.1 (late endosome), resulting in an increase in charge density of the polyplexes which is believed to cause endosomal membrane disruption [25-26]. Compared to p(ABOL), the copolymer p(ABOL/2AMPBA) possesses 23% of *ortho*-aminomethylphenylboronic acid groups and protonation of the secondary aminogroup in this moiety is occurring in the pH range 5–6 [27]. Consequently, this protonation also contributes to the buffering action of the polymer. The buffer capacities as calculated from the pH titration curves (Figure 4.2) are 69% for p(ABOL/2AMPBA) and 72% for p(ABOL). These almost similar data suggest that the boronic acid moiety does not add to the buffer capacity. It has been reported by Whiskur *et al.* that the pK_a of the secondary amine group in 2AMPBA is *ca.* 5.3 (protonation step in Scheme 4.4A), and the B–N interaction raises the boronic acid's pK_a from *ca.* 8.8 in PBA to *ca.* 12 in 2AMPBA (OH^- addition step in Scheme 4.4A) [27].

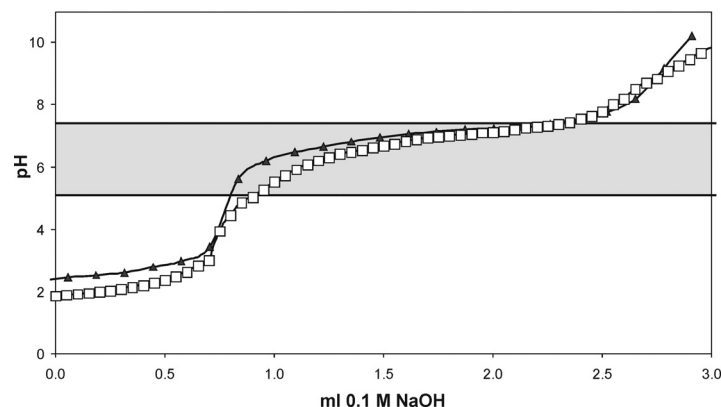


Figure 4.2. pH-titration curves of p(ABOL) (triangles) and p(ABOL/2AMPBA) (squares). Relevant endosomal pH interval between pH 7.4 and 5.1 is marked grey for clarity.

4.3.3 Particle formation and characterization

Upon standing at ambient temperature solutions of 0.18 to 0.72 mg/ml of p(ABOL) in 20 mM HEPES buffer tend to aggregate and eventually form precipitate on a timescale of 4–10 hours. Therefore always fresh solutions were prepared that were vigorously vortexed prior to polyplex formation. However, p(ABOL/2AMPBA) under identical circumstances forms stable solutions that were slightly opaque. Dynamic light scattering (DLS) measurements showed that self-assembled nanoparticles were formed in the polymer concentration range from 0.18 to 0.72 mg/ml. These self-assembled nanoparticles were stable in time and have particle sizes of *ca.* 100 nm with a narrow size distribution (PDI = 0.2–0.3) and zeta potentials of *ca.* 40 mV. As the boron atom in boronic acids is a Lewis acid center that can bind with alcohols and amines, the stability of these nanoparticles can be most likely attributed to boronic ester bond formation of the *ortho*-aminomethylphenylboronic acid groups with proximate hydroxybutyl side chains, resulting in the dynamically covalently crosslinking of the polymer chains in the spontaneously formed nanoparticles. In addition the interaction of boronic acid moieties with tertiary amino groups in the main chain of the polymer can also contribute to the stability of the nanoparticles.

The formation of polyplexes with pDNA and siRNA with cationic polymers primarily occurs by electrostatic interactions. In the boronated polymer it is likely that also the intra- and intermolecular forces as described above contributes to the stability of the polyplex. Moreover, in case of siRNA additional stabilization could occur through ester bond formation between the *ortho*-aminomethylphenylboronic acid groups and the 3' ribose endgroups of the siRNA. The particle sizes and zeta potentials of polyplexes of p(ABOL) and p(ABOL/2AMPBA) with pDNA and siRNA are shown in Figure 4.3.

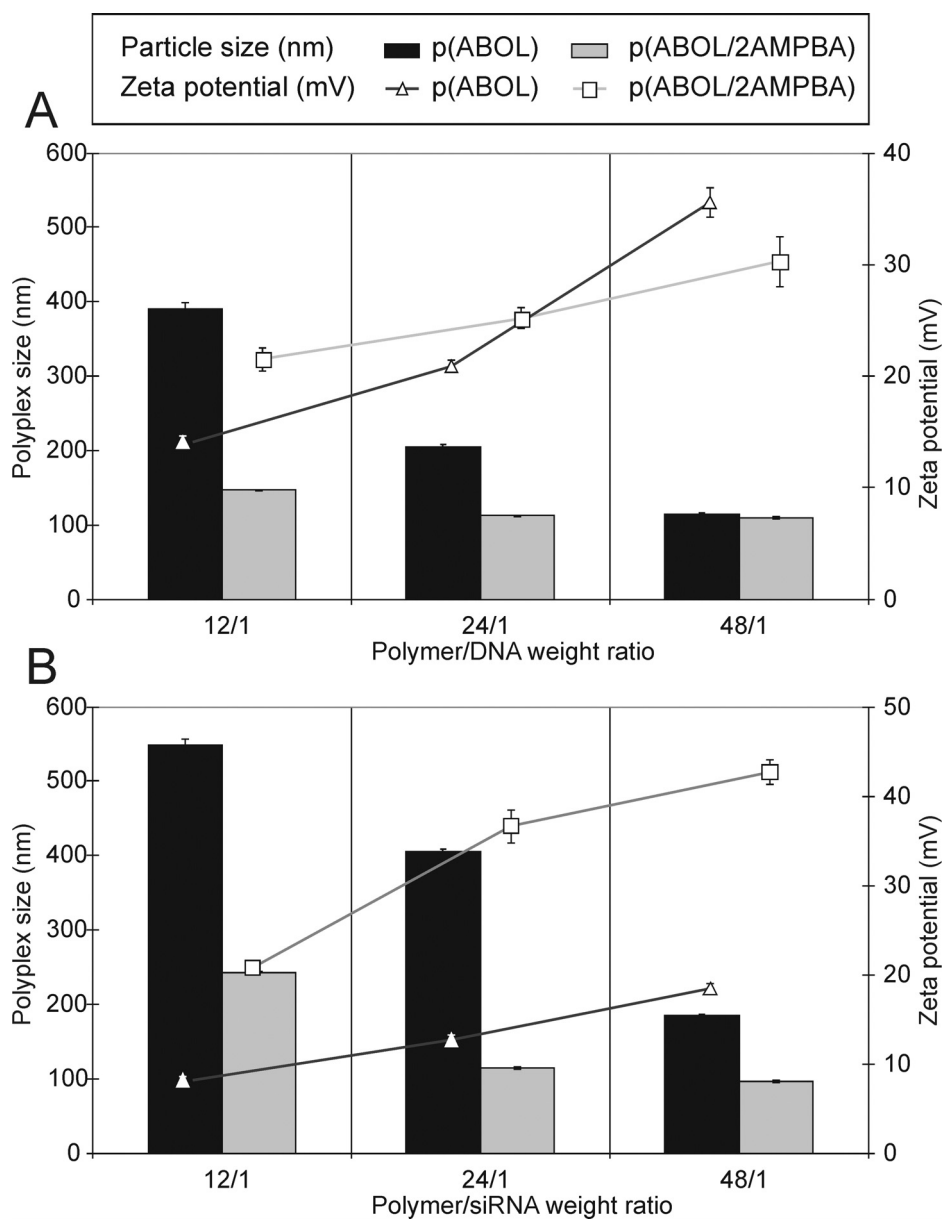


Figure 4.3. Polyplexes formed in HEPES buffer (20 mM, pH 7.4) for polyplexes in presence of pDNA (A) and siRNA (B). Particle sizes are shown in bars for the with polymer p(ABOL) (dark grey) and p(ABOL/2AMPBA) (light grey). The particle surface potentials are shown in connecting lines for clarity for p(ABOL) (triangles) and for p(ABOL/2AMPBA) (squares).

Figure 4.3A shows the sizes of polyplexes of p(ABOL) and p(ABOL/2AMPBA) with pDNA at different polymer/DNA weight ratios. For p(ABOL) at polymer/DNA weight ratio 12/1 no stable polyplexes are formed. Increase in p(ABOL) concentration

to 24/1 and 48/1 yields polyplexes of *ca.* 200 and *ca.* 100 nm respectively. However, for p(ABOL/2AMPBA) already at 12/1 polymer/DNA weight ratio stable polyplexes were formed with size of *ca.* 150 nm and the size decreases to *ca.* 100 nm at polymer/DNA ratio of 24/1. No further decrease of polyplex size was observed at higher polymer/DNA weight ratio. These data show that p(ABOL/2AMPBA) is more efficient in the condensation of pDNA, resulting in stable polyplexes smaller than 200 nm (Figure 4.3A).

For polyplexes with siRNA a similar behavior was observed. p(ABOL/2AMPBA) gives with siRNA significantly smaller particles than p(ABOL). At polymer/siRNA weight ratios increasing from 12/1 to 48/1, particle size decreased from *ca.* 240 nm to 100 nm with a narrow size distribution (PDI = *ca.* 0.2) and a concomitant increase in zeta potential from 21 to 43 mV, respectively. In contrast, p(ABOL) did not form small polyplexes at 12/1 and 24/1 polymer/siRNA weight ratios and only at p(ABOL)/siRNA 48/1 weight ratio polyplexes are formed of *ca.* 185 nm in size and a zeta potential of 18 mV (Figure 4.3B). DLS experiments showed that polyplexes from p(ABOL/2AMPBA) with both pDNA and siRNA were stable at 37 °C for at least 4 days, see Table 4.1. This is a very advantageous property of this polymer; since polyplexes of p(ABOL) tend to gradually aggregate upon standing. Figure 4.3 shows that polyplexes of p(ABOL/2AMPBA) generally have higher zeta potentials than those of p(ABOL). This higher positive surface charge is most likely due to the extra secondary amino group that is present in the 2-AMPBA moiety. The pK_a of this secondary amino group is about 5 in the single 2-AMPBA molecule [27] but it is likely that in the vicinity of the negative charges of the nucleotides in the polyplex this pK_a value is shifted to more neutral pH value and (partial) protonation of the secondary nitrogen is responsible for the increased positive surface charge of the p(ABOL/2AMPBA) polyplexes compared to p(ABOL).

Table 4.1. Polyplex properties of p(ABOL/2AMPBA) with DNA and siRNA

Oligo-nucleotide	Weight ratio	ζ -potential (mV) ^b 0 hr	Size (nm) ^a 0 hr	Size (nm) ^a 24 hr	Size (nm) ^a 96 hr	F (EtBr) ^c (%)
pDNA	24/1	27	105	148	185	56
pDNA	48/1	32	89	91	101	55
siRNA	24/1	37	115	115	119	81
siRNA	48/1	43	97	97	98	69

^a Determined by dynamic light scattering with ± 2 nm accuracy. Samples were stored at 37 °C and measured at 25 °C.

^b Determined by dynamic light scattering with ± 3 mV accuracy at 25 °C.

^c Ethidium bromide intercalation in polyplexes determined by fluorescence, relative to intercalation of EtBr with uncondensed pDNA or siRNA (100%) with ± 1.6 % accuracy.

The encapsulation efficiency of p(ABOL/2AMPBA) for pDNA and siRNA was studied by the ethidium bromide assay (Table 4.1). The ethidium cation gives an increased fluorescence upon intercalation with DNA (or siRNA), therefore the relative decrease in fluorescent signal gives a measure for the fraction of DNA (or siRNA) that is not accessible and thus shielded in the polyplex. Polyplexes prepared with pDNA at 24/1 and 48/1 polymer/DNA weight ratio showed a fluorescence of *ca.* 55% of the original intensity relative to the fluorescence of ethidium bromide in free DNA solution (100%), indicating that a significant fraction of DNA is shielded in the polyplex. The ethidium bromide fluorescence with 24/1 and 48/1 p(ABOL/2AMPBA)/siRNA weight ratio polyplexes was only reduced to 81% and 69% compared to free siRNA solution (100%) respectively, indicating that a higher fraction of siRNA is still accessible to the ethidium cation intercalation. Polyplexes of the non-boronated p(ABOL) showed similar behavior in the shielding of the ethidium ion. For DNA polyplexes of p(ABOL) values of 59% and 53% were obtained and for siRNA polyplexes the residual fluorescence was 75% and 71% at a 24/1 and 48/1 polymer/oligonucleotide weight ratio, respectively [24].

4.3.4 Disulfide reduction

The presence of the disulfide moieties in the polymer backbone allows for rapid vector unpacking and release of therapeutic content in a reductive environment such as the cytosol. This special property of SS-PAAAs was previously demonstrated for p(ABOL) [10], and it was verified whether vector unpacking through disulfide reduction was similar for p(ABOL/2AMPBA).

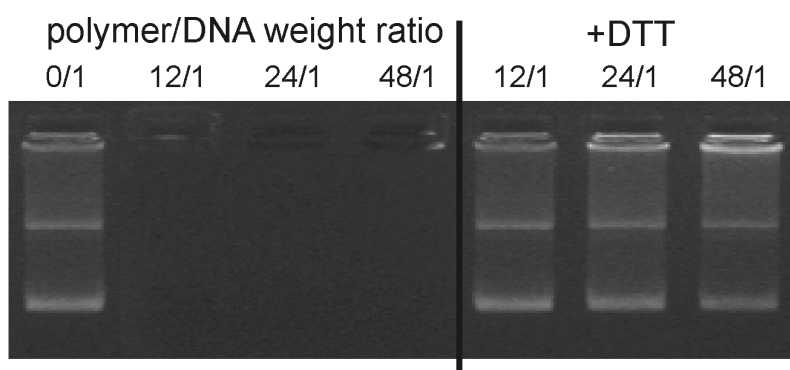


Figure 4.4. Agarose gel retardation of free DNA (first lane) followed by polyplexes of p(ABOL/2AMPBA) at 12/1 24/1 and 48/1 polymer/DNA weight ratio in absence of DTT (left) and after treatment with 2.5 mM DTT for 30 min (right).

The results from electrophoresis experiments with p(ABOL/2AMPBA)/DNA polyplexes as displayed in Figure 4.4 show complete DNA retardation at polymer/DNA weight ratios 12/1, 24/1, and 48/1. This indicates that DNA is highly

packed in these polyplexes. However, after treatment with 2.5 mM DTT for 30 minutes complete release of DNA was observed. These data suggest that although a considerable increase in particle stability is observed for polyplexes of p(ABOL/2AMPBA), complete polymer degradation still occurs after disulfide reduction by DTT.

4.3.5. Transfection properties of p(ABOL/2AMPBA)

In order to evaluate whether the presence of the *ortho*-aminomethylphenylboronic acid moieties in the polymer have effect on the transfection properties, polyplexes of p(ABOL) and p(ABOL/2AMPBA) with pDNA were measured both in the absence and in the presence of serum. Initial experiments with COS-7 cells using pDNA encoding for green fluorescent protein (GFP) showed that polyplexes of p(ABOL) at 48/1 polymer/DNA weight ratio in the absence of serum yield approximately 2 times higher gene expression than polyplexes of commercial linear poly(ethyleneimine) (Exgen500 at optimal N/P ratio of 6/1). For p(ABOL/2AMPBA) the transfection efficiency under these conditions was similar to that of poly(ethyleneimine) (PEI) (Figure 4.5A). In the presence of serum (Figure 4.5B), both polymers showed a reduction in transfection efficiency to *ca.* 0.5 times that of PEI. Polyplexes of both p(ABOL/2AMPBA) and p(ABOL) showed no or only low cytotoxicity with cell viabilities of 80–100% both in the absence and in the presence of serum.

Besides the COS-7 cells, also the transfections in HUH-6 and H1299-Fluc cell lines were investigated. All three cell lines are cancer cells, but are derived from different organs, thereby expressing different glycoproteins at the cell surface. COS-7 is a kidney derived cell line from simians (green African monkey), HUH-6 is a human hepatoblastoma cell line, and H1299-Fluc is a human lung carcinoma cell line which is stably expressing firefly luciferase. In Table 4.2 the transfection efficiencies are shown for the three cell lines (COS-7, HUH-6, and H1299-Fluc) under serum free conditions, relative to p(ABOL) (set to 100%).

Table 4.2. Transfection efficiency relative to p(ABOL)

Polymer/Cell line	COS-7 cells	HUH-6 cells	H1299-Fluc cells
p(ABOL/2AMPBA)	50 ± 13% ^a	21 ± 13% ^a	61 ± 11% ^a

^a Gene expression (GFP) of different cells, measured 48 hours after incubation for 2 hours in serum free conditions with polyplexes of p(ABOL/2AMPBA) at a 48/1 polymer/DNA weight ratio. GFP expression of p(ABOL) under identical circumstances was set to 100%.

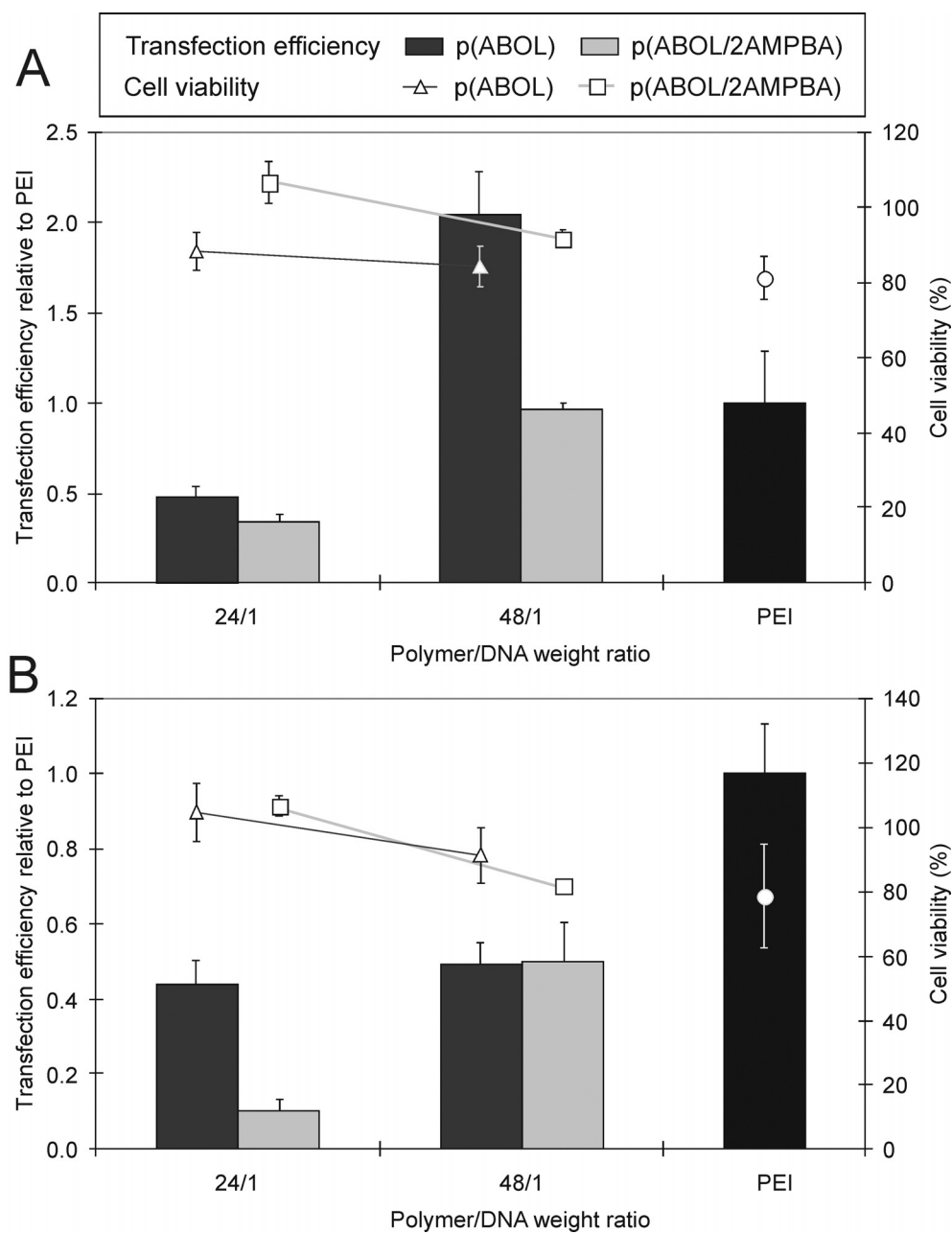


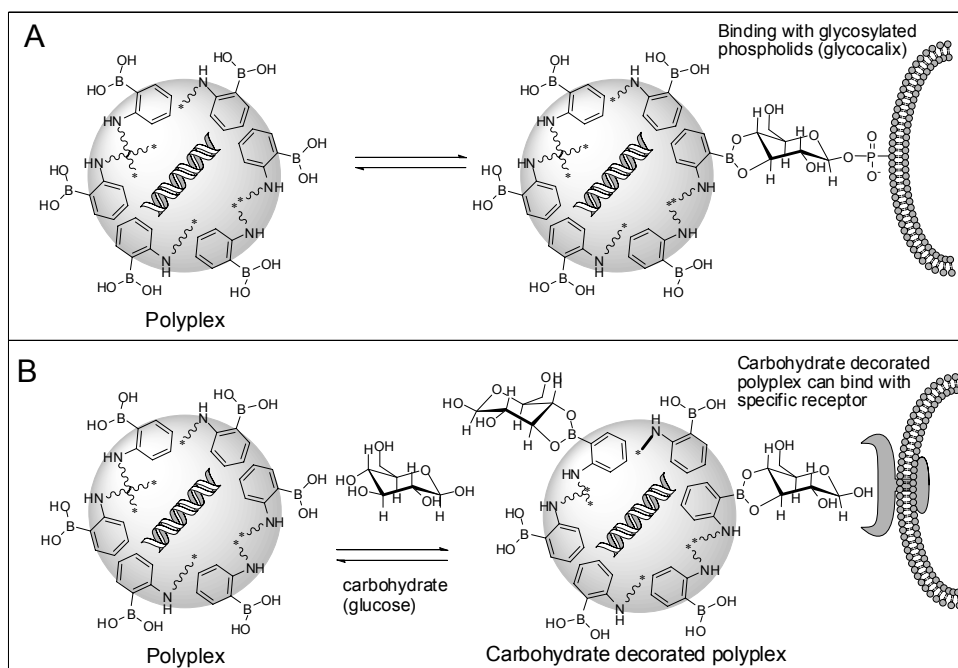
Figure 4.5. Transfection efficiency of polyplexes p(ABOL) (dark grey bars) and p(ABOL/2AMPBA) (light grey bars) at 24/1 and 48/1 polymer/DNA weight ratio of in COS-7 cells in the absence of serum (**A**) and in the presence of serum (**B**) given relative to linear PEI (Exgen at N/P = 6). Corresponding cell viabilities are shown in symbols with connecting lines for clarity for p(ABOL) (triangles) and for p(ABOL/2AMPBA) (squares). Cell viability for PEI is included (circles).

It can be seen that p(ABOL/2AMPBA) gave a transfection efficiency relative to p(ABOL) of *ca.* $50 \pm 13\%$ for COS-7 cells, $21 \pm 13\%$ for HUH-6 cells, and $61 \pm 11\%$ for H1299-Fluc cells. No significant cytotoxicity was observed in any of the different cell lines (data not shown). The relative transfection data indicate that the presence of *ortho*-aminomethylphenylboronic acid moieties in the polymer decreases the transfection efficiency and that the effect is to a certain extent cell specific. As transfection is a complicated process involving many different steps, possible explanations can range from different interactions with the glycocalix, altering particle uptake and intracellular routing as each cell type has a different glycocalix composition to the idea that the presence of boronic acid moieties could interfere with metabolic pathways that are cell type dependant. In the next section additional experiments are described in which the boronic acid moieties were partially converted to boronic esters by the addition of different carbohydrates to the transfection solution.

4.3.6 Effects of the presence of carbohydrates on the transfection efficiency

From the previous results the role of the boronic acid moieties remains unclear. As boronic acids are well known to bind with carbohydrates [18], it is of particular interest to see whether it is possible to decorate the formed polyplexes of p(ABOL/2AMPBA) with sugars by *post*-modification. New strategies for glycotargeting are currently being investigated, since it has been shown that both endosomal uptake and intracellular trafficking of nucleic acids are influenced by glycosylated polymeric vectors, and that glycolysation has a beneficial effect on the transfection efficiency [28-29]. Decoration of boronated polyplexes with carbohydrates would result in particles with altered cellular interactions. A schematic overview of the possible mechanism by which polyplexes with boronic acid moieties at the surface can interact with cells in the presence of carbohydrates is given in Scheme 4.5.

Surface-orientated *ortho*-aminomethylphenylboronic acid groups of polyplexes of p(ABOL/2AMPBA) could be used for boronic ester formation with glycosylated phospholipids present in the glycocalix (Scheme 4.5A). Similarly, surface-oriented *ortho*-aminomethylphenylboronic acid groups of polyplexes of p(ABOL/2AMPBA) can form boronic esters with carbohydrates (*e.g.* glucose in Scheme 4.5B). Theoretically, boronic ester formation with carbohydrates present in the transfection medium could compete for boronic ester formation with the glycocalix. Alternatively, decoration of polyplexes with different saccharides could allow for an easy strategy alternative to glycolysation of polyplexes that in turn could facilitate receptor-mediated uptake.



Scheme 4.5. Possible binding mechanisms of binding of boronated polyplexes. In Figure **A** surface-oriented boronic acid moieties can bind with glycosylated phospholipids. In Figure **B** surface-oriented boronic acid moieties can bind a carbohydrate (e.g. glucose) and subsequently bind with a specific receptor present on the cell membrane.

In order to evaluate the effect of different sugars on the transfection properties, first the effects of the presence of several monosaccharides on the size and stability of polyplexes formed with p(ABOL/2AMPBA) and pDNA were investigated. D-glucose was selected because of its presence in most cell culture media. D-mannose was selected, since mannosylated polyplexes are also known to be taken up efficiently by the mannose receptor present on many types of cancer cells [30-32], and D-galactose was selected since galactosylated polyplexes have been described to be taken up by the galactose receptor present on liver and kidney cells [33-36]. Finally, D-sorbitol was selected since it is a compound that is relatively strongly binding to boronic acids [18] and thus in case of interaction of boronic acid functionalities with glycoproteins present on cell membranes this carbohydrate might display the strongest inhibiting effect.

Polyplexes were prepared with p(ABOL/2AMPBA) and pDNA at 24/1 and 48/1 ratio in HEPES buffer (pH 7.4). When the different sugars were added to the polyplex solutions to a final concentration of 0.9% w/v the polyplex size and zeta potential was not significantly affected (data not shown). The sizes of the polyplexes in the absence and the presence of D-glucose and D-sorbitol were monitored in time at 37 °C.

Polyplexes prepared at a 48/1 polymer/DNA weight ratio remained stable for up to 6 days at 37 °C (Figure 4.6). Gradual particle destabilization was only observed for polyplexes at a 24/1 polymer/DNA weight ratio in the presence of 0.9% w/v of D-sorbitol. This observation supports the idea that the *ortho*-aminomethylphenylboronic acid moieties present in the polyplex interact with proximal hydroxybutyl side chains and/or tertiary amino groups in the main chain, thereby stabilizing the polyplex by dynamic covalent crosslinking. Addition of the strongly binding D-sorbitol to the polyplexes then results in competition with these groups for binding to the boronic acid center and eventual boronic ester formation which is more dominant at the 24/1 polymer/DNA weight ratio than at the 48/1 polymer/DNA weight ratio due to the higher polymer concentration in the polyplex.

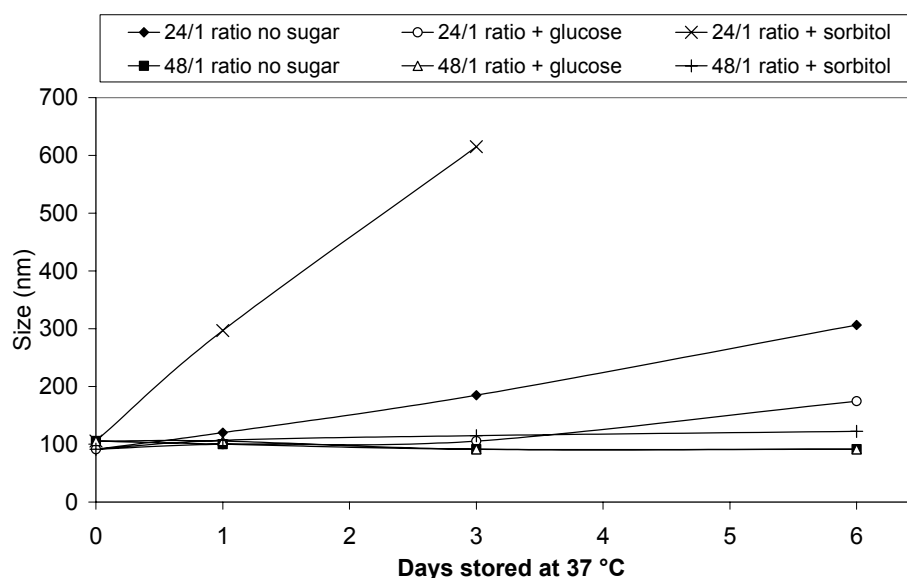


Figure 4.6. Polyplex size as a function of time in HEPES (pH 7.4, 20 mM, kept at 37 °C). Data is shown for polyplexes of p(ABOL/2AMPBA) in absence of sugar (dark diamonds and squares); and in the presence of 0.9% w/v D-glucose (open circles and triangles); and 0.9% w/v D-sorbitol (crosses and vertical lines) at 24/1 and 48/1 polymer/DNA weight ratio, respectively.

Transfection studies were performed in presence of the different sugars with polyplexes of p(ABOL) and p(ABOL/2AMPBA) containing a plasmid encoding for green fluorescent protein (GFP) at a 48/1 polymer/DNA weight ratio in COS-7 cells. The results are depicted in Figure 4.7. Both the GFP expression and the percentage of GFP positive cells in these samples as determined by automated fluorescent microscopy are shown for the conditions with different saccharides added. The corresponding pictures of the transfected cells are shown in Figure 4.7B.

Figure 4.7A shows that polyplexes of p(ABOL) generally give 3–4 times higher GFP expression than polyplexes of p(ABOL/2AMPBA). From the fluorescence microscopy pictures it was calculated that the percentage of transfected cells by p(ABOL) polyplexes ranged from 29–43% in the presence of different sugars. However, for polyplexes from p(ABOL/2AMPBA) the percentage of transfected cells in the absence of sugars was only *ca.* $5 \pm 1\%$. This again shows that the presence of boronic acid has an inhibitory effect on the overall transfection. Addition of sugars to p(ABOL/2AMPBA) resulted in an increase of the percentage of positive cells to 16–19% for the weaker binding sugars glucose, mannose, and galactose, whereas it was 26% for the stronger binding sorbitol.

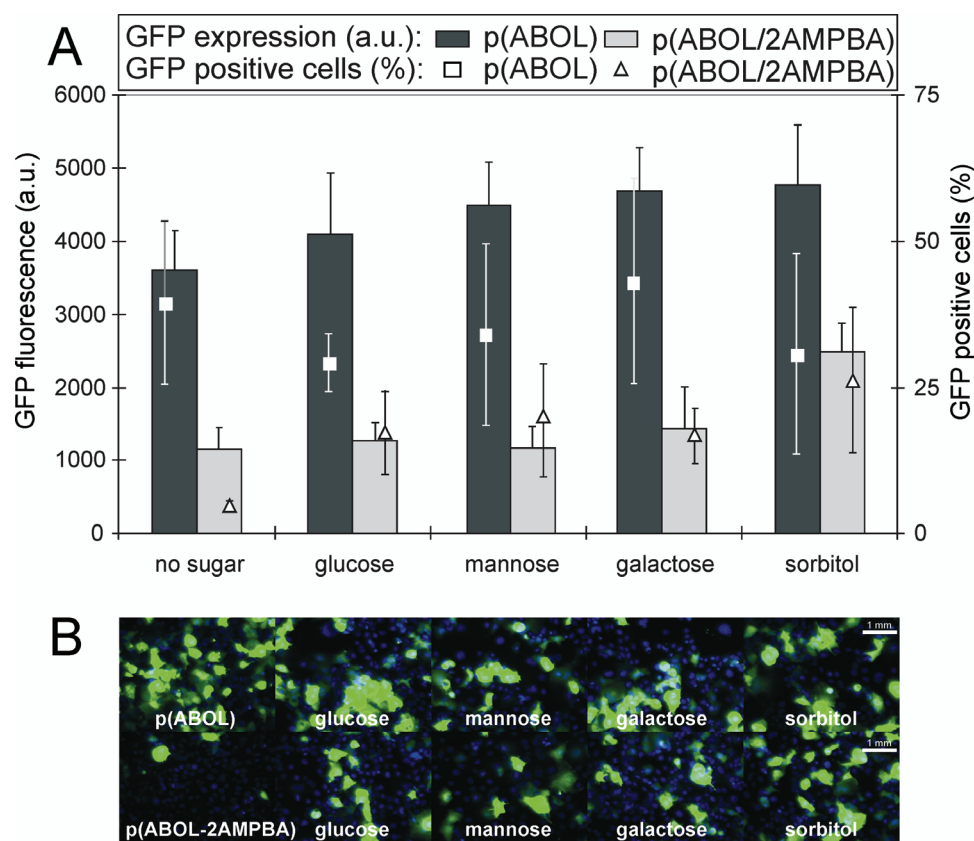


Figure 4.7. GFP expression in COS-7 cells after transfection with p(ABOL) or P(ABOL/2AMPBA) at a 48/1 polymer/DNA weight ratio. Figure **A** shows the fluorescent intensities in bars depending on the sugar added resulting from GFP expression measured with a TECAN plate reader and the corresponding percentage of GFP positive cells in lines as determined by automatic fluorescence microscopy. Figure **B** shows the corresponding fluorescent microscopy pictures representative for the GFP expression (green) in the cell culture, with a DAPI staining of the cell nuclei (blue). The upper row corresponds to p(ABOL) samples and the lower row corresponds to p(ABOL/2AMPBA). From left to right are polyplexes in absence of sugar, followed by polyplexes in presence of 0.9% w/v of D-glucose, D-mannose, D-galactose, and D-sorbitol, respectively.

It appears that the binding of the sugars and especially the strongest binding D-sorbitol masks the boronic acid functionality of p(ABOL/2AMPBA), resulting in a higher transfection efficiency. This observation supports the idea that the presence of free boronic acids to glycoproteins of the cell membrane acts inhibitory in the gene delivery and/or gene expression. Moreover, since the addition of D-mannose and D-galactose did not result in significant higher transfection efficiencies, these sugars apparently do not promote receptor mediated endocytosis as was posed as a possible mechanism in Scheme 4.5B. The addition of the different sugars to the transfection medium did not significantly affect the cell viability, which remained 90–100% (data not shown).

4.3.7 Luciferase knockdown using siRNA polyplexes in the presence of sugars

The polymers p(ABOL) and p(ABOL/2AMPBA) were also evaluated for their ability to deliver siRNA for gene silencing both in the absence and in the presence of different sugars. Polyplexes of p(ABOL) and siRNA are larger as compared to polyplexes of p(ABOL) and pDNA (Figure 4.3). In contrast to DNA, siRNA has a vicinal diol group at the 3' ribose end that can form a reversible boronate ester with boronic acids [22]. Therefore it was of interest to investigate whether the boronated p(ABOL/2AMPBA) could be more efficient in siRNA delivery than its structural analogue p(ABOL). To test this hypothesis anti-luciferase siRNA was used to knockdown luciferase expression in H1299-Fluc cells. In previous work by our group, for p(ABOL) the highest knockdown of *ca.* 70% was observed at polymer/siRNA weight ratios of 48/1, while luciferase expression remained around 90–100% for polyplexes with a non-coding siRNA, indicating good cell viability [24]. In the experiments presented here, the cells were incubated under serum free conditions for 2 hours with polyplexes at 48/1 polymer/siRNA weight ratio in presence of 0.9% w/v of different sugars. Figure 4.8 shows that the luciferase expression is only $28 \pm 8\%$ reduced using p(ABOL) ($72 \pm 8\%$ luciferase expression) and the presence of different sugars did not significantly improve gene silencing for polyplexes of p(ABOL). The luciferase expression is more significantly reduced using polyplexes of p(ABOL/2AMPBA) (35% knockdown), indicating that the presence of the 2AMPBA groups in this case apparently is beneficial for the gene silencing. Moreover, for polyplexes of p(ABOL/2AMPBA) in the presence of different carbohydrates the gene silencing is further improved (up to 67% knockdown). Apparently the binding of boronic acid to carbohydrates has a positive effect on the overall gene silencing. The cell viability for both p(ABOL) and p(ABOL/2AMPBA), as can be seen from the relative luciferase expression for polyplexes with non-coding siRNA (depicted in symbols in Figure 4.8), was approximately 100% and

the presence of the different carbohydrates did not significantly alter the cell viability for both polymers. For comparison, lipofectamine which is known as an excellent vector for siRNA transfection was used as a positive control and showed a knockdown of $84 \pm 7\%$ without cytotoxicity. In contrast, the commercial PEI (Exgen at N/P ratio 5) did not show any significant downregulation but shows significantly reduced cell viability ($82 \pm 11\%$). The hypothesis that incorporation of boronic acid moieties into SS-PAA could improve the gene silencing properties with siRNA seemed to be supported from this experimental data, although the exact role of the sugars is not clear.

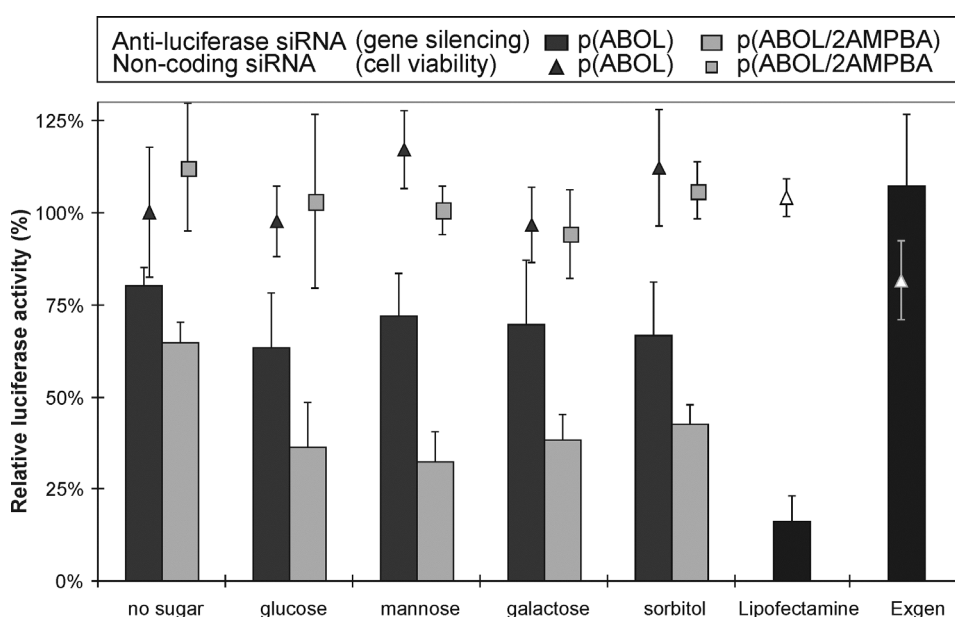


Figure 4.8. Luciferase expression shown in symbols for polyplexes of p(ABOL) (dark grey triangles) or p(ABOL/2AMPBA) (light grey squares) with non-coding siRNA at a 48/1 polymer/siRNA weight ratio relative to uncreated cells. Luciferase expression shown in bars for polyplexes of p(ABOL/2AMPBA) (light grey) or p(ABOL) (dark grey) with anti-luciferase siRNA at a 48/1 polymer/siRNA weight ratio relative to non-coding siRNA samples. Lipofectamine is included as positive control and Exgen (IPEI at N/P ratio 5) as negative control.

4.5 Conclusions

A boronated disulfide-containing poly(amido amine) (SS-PAA) with a structure similar to the efficient polymer p(ABOL) for *in vitro* gene delivery was synthesized by copolymerization of *N,N'*-cystaminebisacrylamide, 4-aminobutanol and the boronated monomer 2-((4-aminobutylamino)methyl)phenyl boronic acid (**1**). This monomer **1** contains a dative B–N interaction which promotes diol binding at physiological pH. The resulting polymer p(ABOL/2AMPBA) was able to form polyplexes with pDNA

and siRNA that were stable for at least 4 days at 37 °C, which is considerably more stable than polyplexes of p(ABOL). It was hypothesized that the additional stability was due to the interaction or even boronic ester formation of the *ortho*-aminomethylphenylboronic acid moieties with proximal hydroxybutyl side chains in the polymer and/or interaction with tertiary amino groups in the main chain, resulting in dynamic covalent crosslinking of polymer chains in the polyplex. The stability of the p(ABOL/2AMPBA) polyplexes was not significantly influenced by the addition of different sugars, except for the relatively strong complexing D-sorbitol that has a destabilizing effect, suggesting that the competing boronic ester formation reduces the crosslinking interactions in the polyplexes.

Polyplexes of p(ABOL) gave higher transfection than those of p(ABOL/2AMPBA) in the three different cell lines COS-7, HUH-6, and H1299-Fluc, suggesting that the presence of *ortho*-aminomethylphenylboronic acid moieties had an unfavorable effect on the eventual transfection efficiency. It was found that the addition of the strong binding D-sorbitol had a positive effect on the gene expression of polyplexes of p(ABOL/2AMPBA), most probably by formation of boronic esters that mitigate the effect of the boronic acid moieties that otherwise would bind to the glycoproteins on the cell surface. These observations may serve as an indication that binding of boronic acid moieties of the polyplex to the glycocalyx of the cell membrane is unfavorable for obtaining high transfection efficiencies.

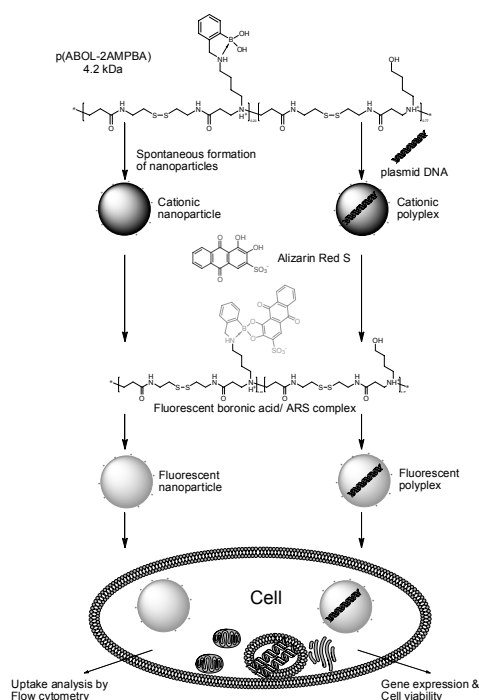
Since boronic acids can bind to vicinal diol groups as present in siRNA p(ABOL/2AMPBA)/siRNA polyplexes were evaluated for gene knockdown in H1299-Fluc cells. It was hypothesized that boronic ester formation with the 3' ribose end of siRNA, together with the crosslinking interactions of the boronic acid groups with pending hydroxybutyl side chains and tertiary amino groups in the main chain of the polymer could improve siRNA binding and polyplex stabilization, resulting in more efficient siRNA delivery and eventually in higher knockdown. Indeed, a higher knockdown was observed for polymer p(ABOL/2AMPBA) than for p(ABOL), lacking the boronic acid moieties. Surprisingly, knockdown was further enhanced in the presence of sugars. This enhanced gene silencing together with the increased stability of the siRNA polyplexes makes p(ABOL/2AMPBA) a promising candidate for siRNA delivery. The role of the presence of sugars remains illusive, but these boronated polymers open new possibilities for glycotargeting that could prove both beneficial *in vitro* and *in vivo*.

4.6 References

- [1] I.M. Verma, N. Somia, Gene therapy - promises, problems and prospects, *Nature*, 389 (1997) 239-242.
- [2] S.Y. Wong, J.M. Pelet, D. Putnam, Polymer systems for gene delivery-past, present, and future, *Prog. Polym. Sci.*, 32 (2007) 799-837.
- [3] E. Wagner, J. Kloeckner, Gene delivery using polymer therapeutics, *Adv. Polym. Sci.*, 192 (2006) 135-173.
- [4] S.B. Zhang, Y.M. Xu, B. Wang, W.H. Qiao, D.L. Liu, Z.S. Li, Cationic compounds used in lipoplexes and polyplexes for gene delivery, *J. Control. Release*, 100 (2004) 165-180.
- [5] J. Luten, C.F. van Nostruin, S.C. De Smedt, W.E. Hennink, Biodegradable polymers as non-viral carriers for plasmid DNA delivery, *J. Control. Release*, 126 (2008) 97-110.
- [6] T.G. Park, J.H. Jeong, S.W. Kim, Current status of polymeric gene delivery systems, *Adv. Drug Deliver. Rev.*, 58 (2006) 467-486.
- [7] L.V. Christensen, C.W. Chang, W.J. Kim, S.W. Kim, Z.Y. Zhong, C. Lin, J.F.J. Engbersen, J. Feijen, Reducible poly(amido ethylenimine)s designed for triggered intracellular gene delivery, *Bioconjugate Chem.*, 17 (2006) 1233-1240.
- [8] C. Lin, C.J. Blaauboer, M.M. Timoneda, M.C. Lok, M. van Steenberg, W.E. Hennink, Z.Y. Zhong, J. Feijen, J.F.J. Engbersen, Bioreducible poly(amido amine)s with oligoamine side chains: Synthesis, characterization, and structural effects on gene delivery, *J. Control. Release*, 126 (2008) 166-174.
- [9] C. Lin, Z.Y. Zhong, M.C. Lok, X.L. Jiang, W.E. Hennink, J. Feijen, J.F.J. Engbersen, Linear poly(amido amine)s with secondary and tertiary amino groups and variable amounts of disulfide linkages: Synthesis and in vitro gene transfer properties, *J. Control. Release*, 116 (2006) 130-137.
- [10] C. Lin, Z.Y. Zhong, M.C. Lok, X.L. Jiang, W.E. Hennink, J. Feijen, J.F.J. Engbersen, Novel bioreducible poly(amido amine)s for highly efficient gene delivery, *Bioconjugate Chem.*, 18 (2007) 138-145.
- [11] M.A. Mateos-Timoneda, M.C. Lok, W.E. Hennink, J. Feijen, J.F.J. Engbersen, Poly(amido amine)s as gene delivery vectors: Effects of quaternary nicotinamide moieties in the side chains, *Chemmedchem*, 3 (2008) 478-486.
- [12] M. Piest, J.F.J. Engbersen, Role of boronic acid moieties in disulfide containing poly(amido amine)s for non-viral gene delivery, See chapter 3 of this thesis, (2010).
- [13] M. Piest, C. Lin, M.A. Mateos-Timoneda, M.C. Lok, W.E. Hennink, J. Feijen, J.F.J. Engbersen, Novel poly(amido amine)s with bioreducible disulfide linkages in their diamino-units: Structure effects and in vitro gene transfer properties, *J. Control. Release*, 130 (2008) 38-45.
- [14] N. Fujita, S. Shinkai, T.D. James, Boronic acids in molecular self-assembly, *Chem-Asian J.*, 3 (2008) 1076-1091.
- [15] D.G. Hall, *Boronic Acids - Preparation and applications in organic synthesis and medicine*, John Wiley & Sons, 2005.
- [16] D.S. Matteson, Boronic esters in stereodirected synthesis, *Tetrahedron*, 45 (1989) 1859-1885.
- [17] W.Q. Yang, X.M. Gao, B.H. Wang, Boronic acid compounds as potential pharmaceutical agents, *Med. Res. Rev.*, 23 (2003) 346-368.
- [18] J. Yan, G. Springsteen, S. Deeter, B.H. Wang, The relationship among pK(a), pH, and binding constants in the interactions between boronic acids and diols - it is not as simple as it appears, *Tetrahedron*, 60 (2004) 11205-11209.
- [19] H. Kitano, M. Kuwayama, N. Kanayama, K. Ohno, Interfacial recognition of sugars by novel boronic acid-carrying amphiphiles prepared with a lipophilic radical initiator, *Langmuir*, 14 (1998) 165-170.
- [20] A.E. Ivanov, I.Y. Galaev, B. Mattiasson, Interaction of sugars, polysaccharides and cells with boronate-containing copolymers: from solution to polymer brushes, *J. Mol. Recognit.*, 19 (2006) 322-331.
- [21] N.D. Winblade, H. Schmokel, M. Baumann, A.S. Hoffman, J.A. Hubbell, Sterically blocking adhesion of cells to biological surfaces with a surface-active copolymer containing poly(ethylene glycol) and phenylboronic acid, *J. Biomed. Mater. Res.*, 59 (2002) 618-631.
- [22] B. Elmas, M.A. Onur, S. Senel, A. Tuncel, Temperature controlled RNA isolation by N-isopropylacrylamide-vinylphenyl boronic acid copolymer latex, *Colloid Polym. Sci.*, 280 (2002) 1137-1146.
- [23] E. Uguzdogan, H. Kayi, E.B. Denkbaz, S. Patir, A. Tuncel, Stimuli-responsive properties of aminophenylboronic acid-carrying thermosensitive copolymers, *Polym. Int.*, 52 (2003) 649-657.
- [24] L.J. van der Aa, P. Vader, G. Storm, R.M. Schiffelers, J.F.J. Engbersen, Optimization of poly(amido amine)s as vectors for siRNA delivery, *J. Control. Release*, In Press, Corrected Proof doi: DOI: 10.1016/j.jconrel.2010.1011.1030.
- [25] N. Lavignac, M. Lazenby, P. Foka, B. Malgesini, I. Verpilio, P. Ferruti, R. Duncan, Synthesis and endosomolytic properties of poly(amidoamine) block copolymers, *Macromol. Biosci.*, 4 (2004) 922-929.
- [26] E. Ranucci, P. Ferruti, E. Lattanzio, A. Manfredi, M. Rossi, P.A. Mussini, F. Chiellini, C. Bartoli, Acid-base properties of poly(amidoamine)s, *J. Polym. Sci. Pol. Chem.*, 47 (2009) 6977-6991.

- [27] S.L. Wiskur, J.J. Lavigne, H. Ait-Haddou, V. Lynch, Y.H. Chiu, J.W. Canary, E.V. Anslyn, pK(a) values and geometries of secondary and tertiary amines complexed to boronic acids - Implications for sensor design, *Org. Lett.*, 3 (2001) 1311-1314.
- [28] M. Monsigny, P. Midoux, R. Mayer, A.C. Roche, Glycotargeting: Influence of the sugar moiety on both the uptake and the intracellular trafficking of nucleic acid carried by glycosylated polymers, *Bioscience Rep.*, 19 (1999) 125-132.
- [29] H.B. Yan, K. Tram, Glycotargeting to improve cellular delivery efficiency of nucleic acids, *Glycoconjugate J.*, 24 (2007) 107-123.
- [30] I.Y. Park, I.Y. Kim, M.K. Yoo, Y.J. Choi, M.H. Cho, C.S. Cho, Mannosylated polyethylenimine coupled mesoporous silica nanoparticles for receptor-mediated gene delivery, *Int. J. Pharm.*, 359 (2008) 280-287.
- [31] T.H. Kim, H. Jin, H.W. Kim, M.H. Cho, C.S. Cho, Mannosylated chitosan nanoparticle-based cytokine gene therapy suppressed cancer growth in BALB/c mice bearing CT-26 carcinoma cells, *Mol. Cancer Ther.*, 5 (2006) 1723-1732.
- [32] W. Wijagkanalan, S. Kawakami, M. Takenaga, R. Igarashi, F. Yamashita, M. Hashida, Efficient targeting to alveolar macrophages by intratracheal administration of mannosylated liposomes in rats, *J. Control. Release*, 125 (2008) 121-130.
- [33] G.Y. Wu, C.H. Wu, Receptor-mediated in vitro gene transformation by a soluble DNA carrier system, *J. Biol. Chem.*, 262 (1987) 4429-4432.
- [34] J.S. Remy, A. Kichler, V. Mordvinov, F. Schuber, J.P. Behr, Targeted gene-transfer into hepatoma-cells with lipopolyamine-condensed DNA particles presenting galactose ligands - a stage toward artificial viruses, *P. Natl. Acad. Sci. USA*, 92 (1995) 1744-1748.
- [35] J. Han, Y.I. Yeom, Specific gene transfer mediated by galactosylated poly-L-lysine into hepatoma cells, *Int. J. Pharm.*, 202 (2000) 151-160.
- [36] M. Hashida, S. Takemura, M. Nishikawa, Y. Takakura, Targeted delivery of plasmid DNA complexed with galactosylated poly(L-lysine), *J. Control. Release*, 53 (1998) 301-310.

A boronic acid functionalized poly(amido amine) for drug delivery and combined drug and gene delivery



Abstract

A disulfide-based poly(amido amine) copolymer p(ABOL/2AMPBA) containing *ortho*-aminomethylphenylboronic acid moieties was prepared by Michael-type polyaddition of a mixture of 1,4-aminobutanol (ABOL) and 2-((4-aminobutylamino)methyl)phenylboronic acid (2AMPBA) to cystamine bisacrylamide (CBA). This copolymer spontaneously forms stable nanoparticles in HEPES buffer solution (pH 7.4) and the presence of the 2AMPBA moieties in the nanoparticles allows for drug conjugation by dynamic covalent boronic ester formation with compounds containing vicinal diols (like dopamine and L-dopa) enabling new strategies for drug delivery. Moreover, with pDNA the copolymer readily forms nanosized polyplexes, which makes this copolymer excellently suitable for combined drug and gene delivery. In this study alizarin red S (ARS) was selected as a model drug, as ARS forms a fluorescent complex with boronic acids enabling the visualization of the uptake of boronic acid-ARS complexed nanoparticles. p(ABOL/2AMPBA) nanoparticles loaded with 12.5% ARS with respect to the PBA moieties, as well as ARS loaded polyplexes with pDNA were internalized up to 70–90% in COS-7 and H1299-Fluc cells, demonstrating efficient drug delivery and combined drug and gene delivery with this polymeric vector. The ARS-loaded polyplexes showed transfection efficiencies of 1.3–1.7 times that of PEI in COS-7 cells, while retaining almost full cell viability.

This chapter is prepared for publication as: M. Piest, K. Göeken, and J.F.J. Engbersen. *A boronic acid functionalized poly(amido amine) for drug delivery and combined drug and gene delivery.*

5.1. Introduction

With the advent of nanotechnology new strategies are available for disease prevention, diagnosis and therapy. Therapeutic nanoparticles have great promises to deliver bioactive molecules to target areas in the body maximizing their therapeutic potential and minimizing side-effects [1-3]. Of particular interest are stimuli-responsive nanocarriers for drug and gene delivery in which the delivery system plays an active role in transporting the content across the different barriers [4]. For example we previously developed poly(amido amine)s with repetitive disulfide bonds (SS-PAA) that are capable of efficient intracellular delivery of plasmid DNA *in vitro* [5-11]. These SS-PAA are stimuli-responsive in respect that they can rapidly release their therapeutic content through disulfide reduction upon exposure to a reducing environment, such as the cytosol where glutathione levels are 10–100 folds higher than in the blood [4, 6-7]. The SS-PAA are also pH-responsive in respect that protonation of tertiary amines in the polymer backbone results in increased charge density and membrane interactions upon acidification, which favorably contributes to endosomal escape [11-12]. Recently, we developed a boronated SS-PAA that forms well-defined nanoparticles through spontaneous self-assembly as well as nanosized polyplexes with pDNA and siRNA [10]. Boronic acids can reversibly form boronate esters with compounds containing vicinal diol groups [13], like carbohydrates, ribonucleotides, and catecholamines such as dopamine and L-dopa [14]. For phenylboronic acid the optimum in dynamic covalent binding of diols is above physiological pH, but the presence of an *ortho*-aminomethyl group gives a dative N→B (N–B) interaction which shifts the pH for optimal diol binding towards the pH 7.5–5.0 range [15]. Therefore, the presence of *ortho*-aminomethylphenylboronic acid moieties in the polymeric nanoparticles offers new possibilities for decoration of these therapeutic carriers with sugar moieties and the boronic acid can bind therapeutic compounds relevant in e.g. Parkinson's and Alzheimer's disease. For example, it has been shown that boronated nanoparticles can effectively transport ribonucleosides across lipophilic membranes [16-17]. Since the stability of boronic esters is dependent on the pH environment and the binding equilibrium is sensitive towards competing diols, pH and glucose responsive behavior is an inherent property of this type of systems [18-20]. As a result boronic acid functionalized materials are of therapeutic interest, for example for glucose-responsive insulin delivery [19].

To demonstrate the potential of boronated SS-PAA for new drug delivery strategies we have developed the polymer p(ABOL/2AMPBA). In recent studies this polymer showed to be an efficient vector for pDNA and siRNA delivery *in vitro* [10]. In this study we aimed to investigate whether the multifunctional properties of this polymer could be advantageously exploited for drug delivery and combined drug and gene delivery. The latter is of particular interest in view of possible synergetic effects

of e.g. gene therapy with anticancer drug delivery [21-24]. Moreover, the fact alone that boronic acids can bind with glycoproteins on the cell surfaces renders a boronated polymer a potential candidate for drug delivery vehicles [25-27].

In this study we demonstrate that alizarin red S (ARS) can be efficiently loaded into spontaneously formed polymeric nanoparticles of p(ABOL/2AMPBA) as well as into polyplexes of p(ABOL/2AMPBA) with pDNA, giving rise to fluorescent nanoparticles and polyplexes that enable visualization of intracellular uptake. Moreover, ARS serves as a model for different catecholamines such as L-DOPA and dopamine, relevant in treatment of Alzheimer's or Parkinson's disease. The binding of a boronic moiety to ARS eliminates fluorescent quenching of free ARS, which allows for the determination of association constants and the loading efficiency into the nanoparticles [28]. In the second part of this study we demonstrate the intracellular delivery of ARS loaded polymeric nanoparticles of p(ABOL/2AMPBA) as well as polyplexes of p(ABOL/2AMPBA) (Figure 5.1).

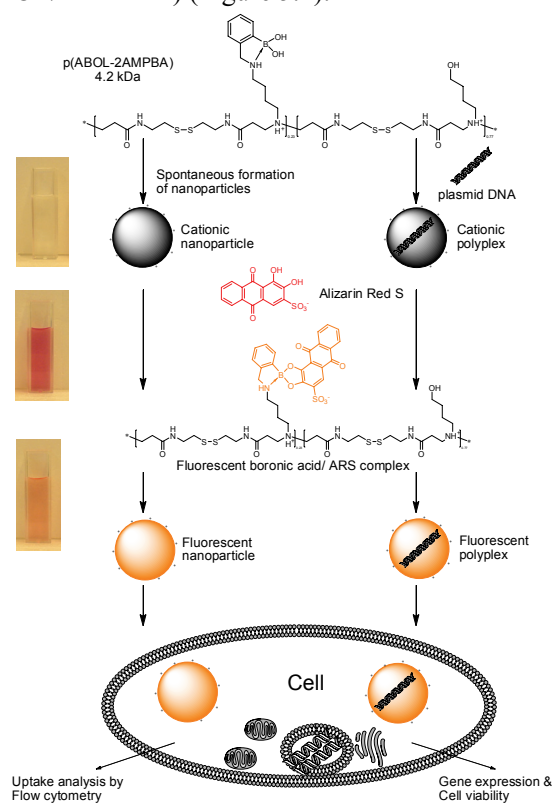


Figure 5.1. A transparent solution of p(ABOL/2AMPBA) spontaneously forms nanosized particles that can be loaded with ARS to form a fluorescent boronic-ARS ester. Alternatively, p(ABOL/2AMPBA) in the presence of plasmid DNA assembles to nanosized polyplexes. Also these polyplexes can be loaded with ARS to form the fluorescent boronic-ARS ester. Uptake of fluorescent nanoparticles into cells can be determined by flow cytometry. In addition, transfection (for polyplexes) and cell viability in COS-7 cells were evaluated by β -galactosidase activity (ONPG-assay) and XTT assay, respectively.

5.2. Materials and methods

Alizarin red S (ARS) was of commercial grade (Aldrich) and used without further purification. All reagents and solvents were of reagent grade and were used without further purification. Polymer p(ABOL/2AMPBA) was synthesized as described previously [10]. The composition of the polymer was established by ^1H NMR (D_2O , 300 MHz) and the content of *ortho*-aminomethylphenylboronic acid (2AMPBA) side groups in p(ABOL/2AMPBA) was 23% with respect to the total amount of side groups. The polymer was found to have a M_w of *ca.* 4.2 kDa and a buffer capacity of 69% [10].

5.2.1. Determination of the binding constant K_{ARS}

The binding constant of the ARS with 2AMPBA moieties in p(ABOL/2AMPBA) was determined according to the protocol described by Springsteen *et al.* [28-29]. To this purpose a polymer stock solution of p(ABOL/2AMPBA), containing 1 mM of 2AMPBA moieties in HEPES (20 mM, pH 7.4) was prepared. A dilution series was prepared from this polymer stock solution ranging in 2AMPBA concentrations from 1.0×10^{-3} to 1.0×10^{-4} M. A stock solution of 1.30×10^{-4} M ARS was prepared in HEPES buffer (20 mM, pH 7.4). Next, 0.1 ml of ARS stock solution was added to 1.0 ml of the polymer solutions with fixed $[\text{ARS}]_0 = 1.18 \times 10^{-5}$ M and $[\text{2AMPBA}]_0/[\text{ARS}]_0$ ratios ranging from 10–100. The fluorescence was measured using a Varian Eclipse fluorescence spectrophotometer with excitation at 468 nm and the emission at 572 nm was analyzed using Cary Eclipse scan application v2002 software.

The relationship between the increase in fluorescent intensity (ΔI_f) and the boronic acid concentration is expressed in Equation 5.1 [28]. The double reciprocal of Equation 5.1 yields the Benesi-Hildebrand Equation 5.2. The binding constant of the 2AMPBA-ARS complex (K_{ARS}) is the quotient of the intercept and the slope of a plot of $1/[\text{2AMPBA}]$ vs. $1/\Delta I_f$.

$$\Delta I_f = \frac{(\Delta k p_0 K_{\text{ARS}}) \times [\text{2AMPBA}] \times [\text{ARS}]}{1 + K_{\text{ARS}} \times [\text{2AMPBA}]} \quad (\text{Equation 5.1})$$

$$\frac{1}{\Delta I_f} = \frac{1}{\Delta k p_0 \times K_{\text{ARS}} \times [\text{2AMPBA}]} + \frac{1}{\Delta k p_0 \times [\text{ARS}]} \quad (\text{Equation 5.2})$$

Where $\Delta k p_0$ is a constant derived from the intrinsic fluorescence and the laser power.

2.2. ARS binding to the polymer p(ABOL/2AMPBA) using thin layer chromatography

A polymer stock solution of 2.4 mg/ml p(ABOL/2AMPBA) (1.71 mM of 2AMPBA moieties) in HEPES buffer (20 mM, pH 7.4) was prepared. Dilution series in HEPES buffer (20 mM, pH 7.4) was prepared ranging in 2AMPBA concentration of 0 to 1.7×10^{-3} M. Next, 100 μ l ARS stock (1.75×10^{-4} M) was added to 140 μ l of polymer solution, resulting in a series with molar ratios of $[2AMPBA]_0/[ARS]_0$ ranging from 0 (= ARS only) to *ca.* 14. Next, 4 μ l of each sample was placed on a cellulose thin layer chromatography (TLC) plate and dried in air. The samples were eluted using acetate buffer (20 mM, pH 5.0). The fluorescent complex was analyzed by eye under daylight or under an UV light source of 366 nm. Pictures were obtained using a Nikon D60 digital camera with a Tampon 18–200 lens.

5.2.3. Polymer and polyplex properties measured by dynamic light scattering

A 0.9 mg/ml polymer stock solution of p(ABOL/2AMPBA) was prepared in HEPES buffer solution (20 mM, pH 7.4). From this stock solution a dilution series in HEPES was prepared ranging from 0.18–0.72 mg/ml polymer and the solutions were vortexed for 5 s and equilibrated for at least 30 min at ambient temperature. During this time period the polymer spontaneously formed nanoparticles in solution.

To prepare polyplexes, DNA plasmid solution (1 mg/ml) as supplied by manufacturer (PlasmidFactory, Bielefeld) was diluted to a final concentration of 0.075 mg/ml in HEPES buffer solution (20 mM, pH 7.4). The polymer stock solution of 0.9 mg/ml of p(ABOL/2AMPBA) was used to prepare polyplexes at polymer/DNA weight ratios 6/1, 12/1, 24/1 and 48/1, respectively. For example, for the preparation of polyplexes at 48/1 polymer/DNA weight ratio, 0.80 ml of the polymer stock solution was added to 0.20 ml of DNA solution in a 1.5 ml Eppendorf tube. The polyplex solutions were vortexed for 5 s and incubated for 30 min at ambient temperature prior to use.

ARS was loaded into the p(ABOL/2AMPBA) nanoparticles or polyplexes by adding 0.1 ml of ARS (9×10^{-5} M in HEPES pH 7.4) to 1.0 ml solution of the self-assembled nanoparticle solution or the polyplex solution. The samples were incubated for another 30 min at ambient temperature prior to use. Size and zeta potential of the self-assembled nanoparticles of p(ABOL/2AMPBA) and p(ABOL/2AMPBA)/plasmid DNA polyplexes were measured at 25 or 37 °C on a Zetasizer Nano (Malvern Instruments Ltd, Malvern, UK) and the dynamic light scattering results were processed using Dispersion Technology Software V5.0. During the stability measurements, samples were stored at 37 °C in between the measurements.

5.2.4. Visualization of ARS uptake by confocal microscopy

COS-7 cells were cultured in Dulbecco's Modified Eagle Medium (Invitrogen) with 1 g/l D-glucose, completed with L-glutamine (1% v/v of GlutaMAX 200 mM) and penicillin-streptomycin solution (2% v/v of stock solution) and 10% v/v fetal bovine serum. Cells were seeded with a density of 56×10^3 cells per well on fibronectin-coated glass coverslips in a 24-well plate (0.56 ml / well of a stock solution of 10^5 cells per ml). The next day, cells were incubated with 0.56 ml of self-assembled nanoparticles of p(ABOL/2AMPBA) (0.24 mg/ml in 20 mM HEPES, pH 7.4) or 0.56 ml of polyplexes of p(ABOL/2AMPBA) prepared at a 24/1 polymer/DNA ratio (0.01 mg/ml DNA final concentration) as described in section 2.3. Cells were incubated with the ARS loaded nanoparticles and with unloaded nanoparticles as a control. A solution of ARS (0.56 ml of 9×10^{-6} M) was used as a negative control. After 2 hour incubation, the cells were washed 3 times with PBS, and fixated with 4% (w/v) formaldehyde/PBS for 15 min at ambient temperature.

Next, coverslips were washed with PBS and a 100 ng/ml solution of 4',6-diamidino-2-phenylindole (DAPI) was applied for 5 min to stain nuclei. After three times rinsing with PBS, coverslips were mounted on microscope slides using Mowiol (CalBiochem, Darmstadt, Germany) and stored at 4 °C in the dark until they were imaged with a Zeiss LSM 510 confocal microscope using Zen2008 software. ARS fluorescence was analyzed after a long pass 560 nm filter using a 488 nm laser excitation. DAPI fluorescence was analyzed after a band pass 435–485 nm IR filter using a 760 nm laser excitation. Images had up to 40 times zoom with a pinhole of 0.1–1.0 mm.

5.2.5. Determination of ARS positive cells by flow cytometry

COS-7 cells and H1299-Fluc were plated in a 96-well plate at 10,000 cells per well 24 h prior to the experiment. A 1:1 dilution series of self-assembled nanoparticles of p(ABOL/2AMPBA) in HEPES buffer (pH 7.4, 20 mM) was prepared starting from 0.48 mg/ml to 0.015 mg/ml. Similarly a 1:1 dilution series of polyplexes at 48/1 p(ABOL/2AMPBA)/DNA weight ratio was prepared starting from 0.48 mg/ml to 0.015 mg/ml. Next, particles were loaded with ARS by addition of ARS (10 μ l, 9×10^{-5} M) to each sample (100 μ l) of self-assembled nanoparticles of p(ABOL/2AMPBA) and polyplexes at 48/1 p(ABOL/2AMPBA)/DNA weight ratio and the samples were incubated for 30 min at ambient temperature. COS-7 cells were incubated with the samples for 2 h in serum free medium (110 μ l of ARS loaded polymer nanoparticle or polyplexes per well). Cells were 4 times rinsed with PBS buffer, trypsinated and stored on ice until fluorescence of individual cells was measured by flow cytometry, using a Becton-Dickinson FACSCalibur. Excitation was elicited at 488 nm with the argon laser and emission was subsequently analyzed by the fluorescence detector after

a 585 nm band-pass filter. For each sample at least 1,000 events were measured. Data were analyzed by FACSComp Software. Untreated cells showed little fluorescence (*ca.* 6 ± 2 units) and cells with fluorescence intensity above 10.5 units were gated as positive cells.

5.2.6. In vitro transfection and cell viability

COS-7 cells were plated 24 h prior to transfection at 10,000 cells/well and were 60–80% confluent after 24 h. Cell medium was changed to serum free medium 2 h prior to transfection. Plasmid pCMV/LacZ DNA was used as reporter gene. Two parallel transfection series, one for the determination of reporter gene expression (β -galactosidase) and the other for the evaluation of the cell viability by XTT assay, were carried out in separate 96-well plates, $n = 4$. Different polymer/DNA weight ratios were used to prepare the polyplexes. In a typical transfection experiment, the cells were incubated with the desired amount of polyplexes (100 μ l dispersion or 110 μ l after addition of 10 μ l ARS solution of 9.0×10^{-5} M, resulting in 1 μ g plasmid DNA per well) for 2 h at 37 °C in a humidified 5% CO₂-containing atmosphere. Next, the polyplex solution was removed, 100 μ l of fresh culture medium was added and the cells were cultured for another 48 ± 2 h. The transfection efficiency was determined by measuring the enzyme activity of β -galactosidase using the ONPG assay. Linear PEI (Exgen 500, Invitrogen) at its optimal 6/1 N/P ratio, was used as reference. The cell viability was measured using an XTT assay, in which the XTT value for untreated cells (cells not exposed to transfection agents) was taken as 100% cell viability. Measurements were performed in quadruplicate using the Perkin Elmer LS50B luminescence spectrometer and analyzed in Kineticalc for Windows V2.0. For the ONPG assay the absorbance was measured at 415 nm with a reference at 655 nm and for the XTT absorbance was measured at 490 nm with a reference at 655 nm.

5.3. Results and discussion

5.3.1. Binding of alizarin red S in self-assembled nanoparticles of p(ABOL/2AMPBA)

The boronated polymer p(ABOL/2AMPBA) was synthesized according to the procedure as described earlier [10]. p(ABOL/2AMPBA) had a weight average M_w of 4.2 kg/mol, representing *ca.* 12 repeating units, with a *ortho*-aminomethylphenylboronic acid (2AMPBA) content of 23% according to ^1H NMR. This indicates that on average each polymer chain contained *ca.* 3 boronic acid functionalities for binding with vicinal diols. Dynamic light scattering measurements showed that over the concentration range of 0.09–0.72 mg/ml p(ABOL/2AMPBA) polymer in solution, corresponding with a 2AMPBA concentration range from 5.9×10^{-5} M to 4.7×10^{-4} M, this polymer spontaneously formed self-assembled nanoparticles of *ca.* 140 nm with a narrow PDI of *ca.* 0.2 and zeta potential of *ca.* 25 mV. The addition of ARS (8.2×10^{-6} M) to the solution, and the subsequent uptake of ARS in the nanoparticles, did not significantly affect the size and the zeta potential (data not shown).

In order to evaluate the potency to use dynamic covalent boronic ester formation in the p(ABOL/2AMPBA) nanoparticles for binding therapeutic diol compounds it was desired to determine the binding constants of the 2AMPBA group in the polymer with a representative model compound. For this purpose alizarin red S (ARS) was selected, because it has a catechol unit that binds relatively strongly to boronic acids and its structure has similarity with dopamine and L-dopa. Most importantly, ARS forms a fluorescent complex upon binding to the phenylboronic acid moiety and the appearance of fluorescence upon boronic ester formation enables the determination of the binding constant, as depicted in Figure 5.2.

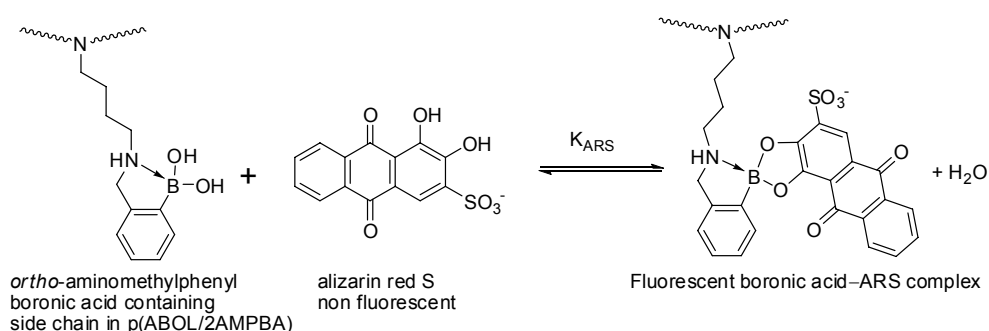


Figure 5.2. The *ortho*-aminomethylphenylboronic acid containing side chains of polymer p(ABOL/2AMPBA) can form a fluorescent reversible covalent boronic ester with alizarin red S.

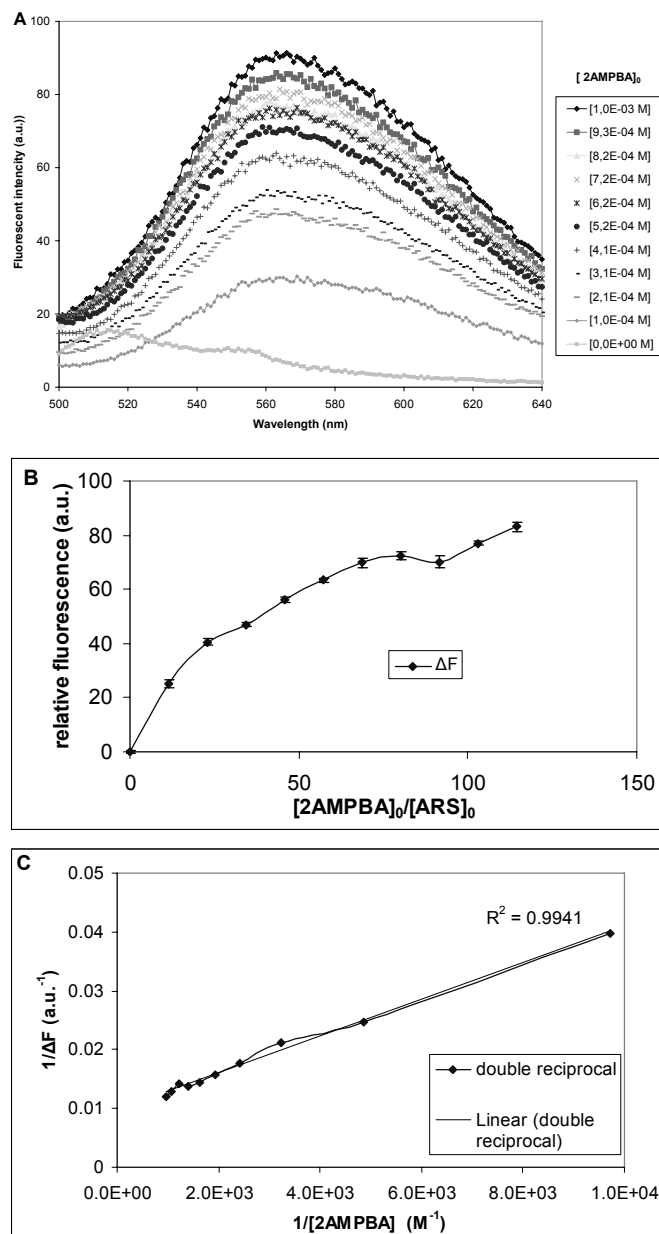


Figure 5.3. Figure A shows the fluorescent data obtained upon increasing [2AMPBA]₀, Figure B shows the relative increase in fluorescence as a function of increasing [2AMPBA]₀/[ARS]₀, and Figure C shows the data plotted as 1/ΔF versus 1/[2AMPBA].

The association constant K_{ARS} for binding of ARS to the 2AMPBA moieties in the polymer nanoparticles was determined with by measuring the increase in fluorescence intensity of solutions of ARS (1×10^{-5} M) at increasing p(ABOL/2AMPBA)

concentrations. An example of a binding curve experiment is shown in Figure 5.3. In Figure 5.3A an increase in fluorescent intensity can be observed upon increasing the concentration of 2AMPBA in the sample from 1.0×10^{-4} M to 1.0×10^{-3} M. These data were used to plot the increase in fluorescent intensity measured at 472 nm as a function of the stoichiometric ratio of $[2AMPBA]_0/[ARS]_0$, see Figure 5.3B. After plotting the reciprocal of the relative increase in fluorescent intensity versus the reciprocal of the 2AMPBA concentration depicted in Figure 5.3C, the binding constant could be determined according to Equation 2. From three individual series of experiments an average binding constant for the binding of ARS to the p(ABOL/2AMPBA) nanoparticles of $K_{ARS} = 2400 \pm 270 \text{ M}^{-1}$ was determined. This value is significantly higher compared to the K_{ARS} of 1300 M^{-1} for phenylboronic acid as determined by Springsteen *et al.* [28-29], suggesting efficient ARS complexation by the p(ABOL/2AMPBA) nanoparticles.

The loading and release of ARS to the polymeric nanoparticles could be visualized using thin layer chromatography (TLC) using acetate buffer (20 mM, pH 5) as eluent and cellulose as stationary phase. As the fluorescent complex could be visualized using an UV light source of 366 nm, this technique can give an indication of the binding capacity of ARS by the polymeric nanoparticles. An increasing polymer concentration (0 to 9.9×10^{-4} M 2AMPBA) was used in order to fully immobilize 1.75×10^{-8} mol of ARS and the corresponding stoichiometric 2AMPBA/ARS ratio ($[2AMPBA]_0/[ARS]_0$) was increased from 0 (ARS only) to *ca.* 14 (complexed ARS).

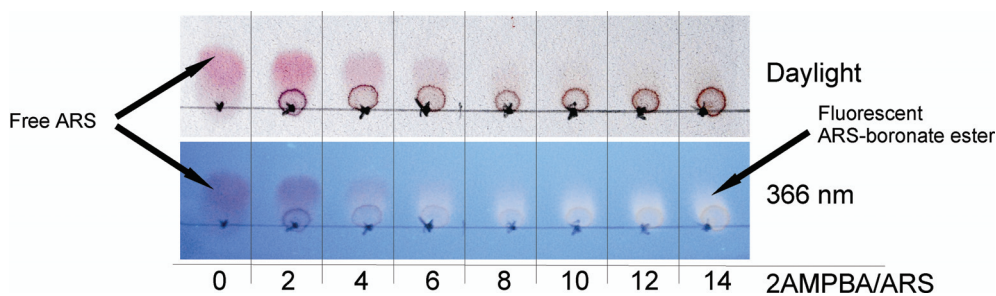


Figure 5.4. Thin layer chromatography plate of p(ABOL/2AMPBA)-ARS solutions at different stoichiometric phenylboronic acid/alizarin ratios (2AMPBA/ARS). Cellulose was used as stationary phase and acetate buffer (20 mM, pH 5) was used as eluent. The pictures were taken using a digital photo camera under daylight (top) or under a UV lamp of 366 nm (bottom) illuminating the fluorescent boronic ester formed with ARS, visible from 2AMPBA/ARS ratio of 4.

The polymer was able to completely retain the ARS from molar ratios of $2AMPBA/ARS > 8$, demonstrating strong and efficient complexation. The fluorescent complexes were clearly visible under the UV lamp of 366 nm at $2AMPBA/ARS > 4$. This result indicates that 1.75×10^{-8} mol ARS can be fully retained into the

p(ABOL/2AMPBA) nanoparticles at 2AMPBA/ARS = 8 (5.8×10^{-4} M 2AMPBA), which corresponds to *ca.* 12.5% loading of the 2AMPBA moieties.

5.3.2. Properties of ARS loaded p(ABOL/2AMPBA) polyplexes with DNA

As we demonstrated successful loading of ARS onto p(ABOL/2AMPBA) self-assembled nanoparticles we were interested whether ARS influenced the properties of p(ABOL/2AMPBA) polyplexes with plasmid DNA (pDNA), as a model for combined drug and gene therapy. In preliminary experiments it was found that the particle size of polyplexes formed at 48/1 p(ABOL/2AMPBA)/DNA weight ratio was not significantly influenced by the presence of ARS up to concentrations of 5×10^{-4} M ARS. However, at higher ARS concentrations the polyplex size rapidly increased to > 1000 nm, and the onset of precipitation was observed (data not shown). Apparently, the addition of higher concentration of ARS results in a hydrophobically driven aggregation of the polyplexes, which may become dominant due to boronic ester formation and the reduction in charge repulsion between the polyplexes caused by the presence of the anionic sulfate groups of ARS.

At polymer concentrations identical to those used in the study of the self-assembled nanoparticles, e.g. at polymer concentrations ranging from 0.09 to 0.72 mg/ml of p(ABOL/2AMPBA), polyplexes with pDNA (0.015 mg/ml) were prepared with polymer/DNA weight ratio 6/1, 12/1, 24/1 and 48/1, respectively. These polyplexes could be loaded with ARS (8.2×10^{-6} M) as was observed by a color change from red to yellow orange in absence of precipitation (Figure 5.1). The solutions of these polyplexes were measured by DLS, and it was observed that the size distributions of these polyplexes was somewhat larger (PDI = 0.4) than that of the polyplexes in the absence ARS (PDI < 0.2). The ARS loaded polyplexes were monitored for several days, and the results are depicted in Figure 5.5.

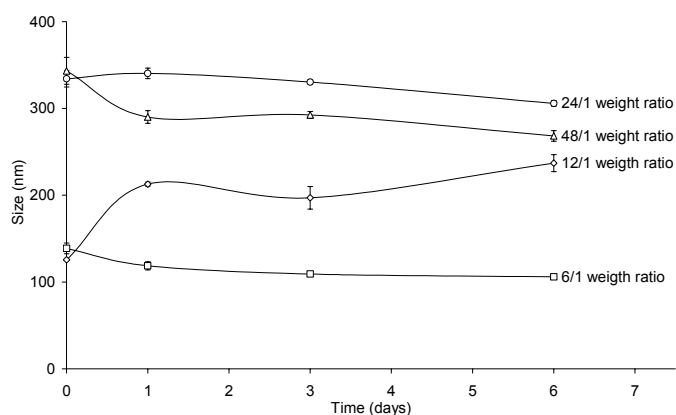


Figure 5.5. Polyplex stability in HEPES (20 mM, pH 7.4) at 37 °C of polyplexes prepared at polymer/DNA weight ratios of 6/1 (-□-), 12/1 (-◇-), 24/1 (-○-), and 48/1 (-△-) that were loaded with ARS (8.2×10^{-6} M). Lines are added for clarity.

As is shown in Figure 5.5 the polyplexes with lowest polymer/DNA weight ratio 6/1 and thus the lowest polymer concentration (6.4×10^{-5} M 2AMPBA) have the smallest particle size (120–140 nm), and are stable in time. Particle size increased with increasing concentration of p(ABOL/2AMPBA), to *ca.* 340 nm at 24/1 and 48/1 polymer/DNA weight ratio. Once formed, these particles remained stable for up to six days at 37 °C without any precipitation observed (both PDI and count rate did not significantly change in time, data not shown).

5.3.3. ARS delivery with the boronated p(ABOL/2AMPBA) nanoparticles

To demonstrate the drug delivery potential of the p(ABOL/2AMPBA) nanoparticles we selected two different cell lines: COS-7 cells, an African green monkey derived kidney cell line that is frequently used in transfection studies using plasmid DNA, and H1299-Fluc cells, a human non-small carcinoma cell line stably expressing firefly luciferase that is frequently used in gene silencing experiments. To this purpose, COS-7 and H1299-Fluc cells were incubated 1 hour with p(ABOL/2AMPBA) nanoparticles loaded with ARS (8.2×10^{-6} M). After 3 times washing with PBS and trypsination of the cells, the percentage of cells that show fluorescence due to uptake of the nanoparticles containing the 2AMPBA-ARS ester was determined by flow cytometry and the results are shown in Figure 5.6.

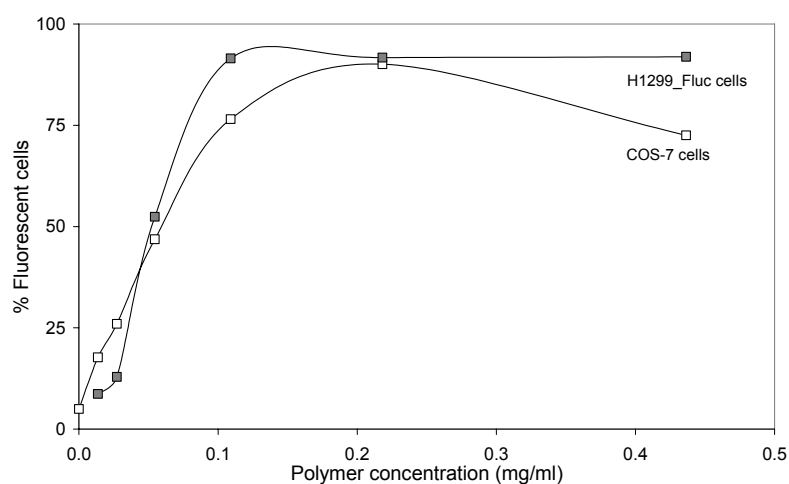


Figure 5.6. Uptake of ARS-loaded p(ABOL/2AMPBA) nanoparticles as determined by flow cytometry. The fluorescence of the boronic acid / alizarin complex was measured as the percentage of fluorescent (gated) cells. COS-7 cells are shown in white squares and H1299-Fluc cells shown in grey squares. Lines are added for clarity.

With increasing p(ABOL/2AMPBA) concentration the percentage of fluorescent positive cells increases. This increase is approximately linear up to a polymer

concentration of 0.12 mg/ml at which the majority of the cells have taken up the polymer-ARS particles (72–92% gated fluorescent cells). Further increase of the polymer concentration does not significantly increase the percentage of fluorescent cells and a plateau is reached at *ca.* 0.12 mg/ml in both cell lines. These results demonstrate that p(ABOL/2AMPBA) is an efficient vector for the delivery of therapeutics containing vicinal diols, and that uptake can be controlled by the doses of ARS-p(ABOL/2AMPBA) complex administered. Moreover, the release of the ARS from the nanoparticles can be triggered by both changes in pH or glucose concentration since the boronate ester binding of these drugs in the nanoparticles is both pH-sensitive and carbohydrate (glucose) responsive.

5.3.4. Uptake of ARS loaded polyplexes

In order to evaluate the potential of combined drug and gene therapy, ARS uptake was also investigated for polyplexes of p(ABOL/2AMPBA) with plasmid DNA at 48/1 polymer/DNA weight ratio in COS-7 and H1299-Fluc cells as a function of the polymer concentration. To this purpose, COS-7 and H1299-Fluc cells were incubated 1 hour with polyplexes of p(ABOL/2AMPBA)/DNA at 48/1 polymer/DNA weight ratio loaded with ARS (8.2×10^{-6} M). After 3 times washing with PBS and trypsination, the percentage of cells that show fluorescence due to uptake of the polyplexes with the 2AMPBA-ARS ester was determined by flow cytometry and the results are shown in Figure 5.7.

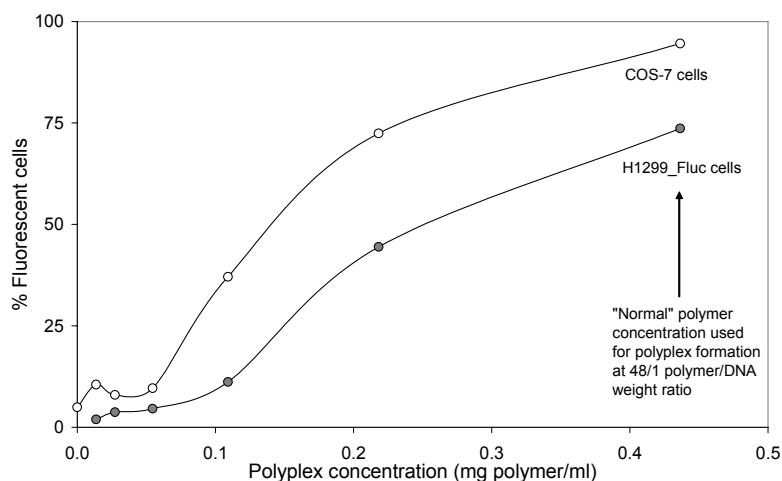


Figure 5.7. Uptake of ARS-loaded p(ABOL/2AMPBA) polyplexes as determined by flow cytometry. The fluorescence of the boronic acid-alizarin complex was measured as the percentage of fluorescent (gated) cells. COS-7 cells are shown in white circles and H1299-Fluc cells shown in grey circles. Lines are added for clarity.

It can be observed at very low polymer concentrations almost no fluorescent cells are measured. In contrast to the self-assembled nanoparticles, the percentage of fluorescent cells does not significantly increase with increasing concentration up to 0.06 mg/ml of p(ABOL/2AMPBA) polyplexes. From polymer concentration above 0.1 mg/ml the percentage of fluorescent cells gradually increases with the p(ABOL/2AMPBA) polyplex concentration. At 0.44 mg p(ABOL/2AMPBA), being the polymer concentration that is normally used in transfection experiments for polyplexes at 48/1 polymer/DNA weight ratio, 94.6% of the COS-7 cells and 73.6% of the H1299-Fluc cells were gated as fluorescent positive, indicating that they have taken up the fluorescent 2AMPBA-ARS containing polyplexes.

The loading of ARS to polyplexes of p(ABOL/2AMPBA) not only allows for the demonstration of the concept of combined drug and gene delivery, but can also be used as an analytical tool to study uptake kinetics of these polyplexes in which the fluorescent ARS-2AMPBA ester can be regarded as fluorescent label. Therefore, COS-7 cells were incubated with polyplexes at 24/1 p(ABOL/2AMPBA)/DNA weight ratio loaded with ARS (8.2×10^{-6} M) and uptake was investigated as function of the incubation time between the polyplexes and the cells before the washing procedure.

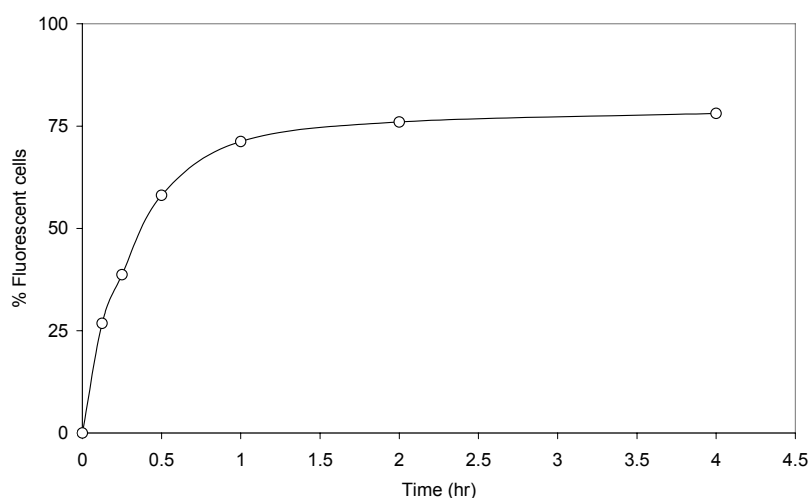


Figure 5.8. Percentage of fluorescent COS-7 cells as a function of the incubation time with polyplexes from p(ABOL/2AMPBA) and DNA at 24/1 polymer/DNA weight ratio loaded with 9×10^{-6} M ARS. Data points are shown a white circles and line is added for clarity.

The results in Figure 5.8 show that uptake of the polyplexes had occurred already in *ca.* 71% of the cells after *ca.* 1 hour contact time, after which a gradual increase up to *ca.* 78% fluorescent cells was reached after 4 hours incubation time, indicating that the majority of the polyplexes are taken up by the cells during the first hour.

5.3.5. Comparison of the uptake of self-assembled p(ABOL/2AMPBA) nanoparticles with the uptake of p(ABOL/2AMPBA)/DNA polyplexes

COS-7 cells were incubated for 1 hour with the ARS-loaded polymer nanoparticles formed by self-assembly as well as with polyplexes formed with pDNA. After washing, fixation and DAPI staining, the COS-7 cells were analyzed by confocal microscopy and representative pictures are shown in Figure 5.9.

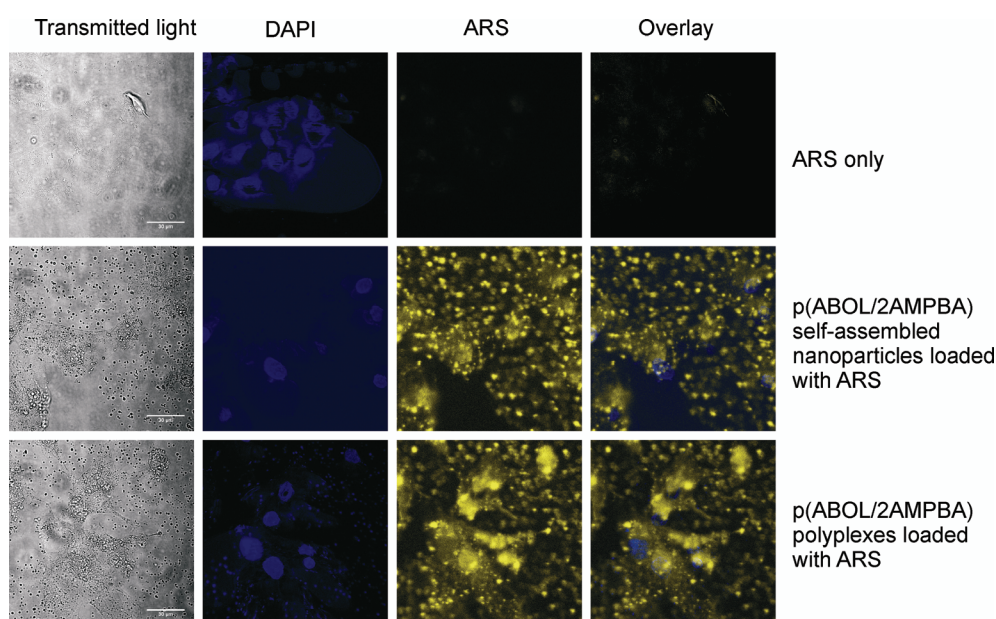


Figure 5.9. COS-7 cells incubated for 1 hour with a solution 9×10^{-6} M ARS (top row); 0.24 mg/ml self-assembled nanoparticle solution loaded with ARS (8.2×10^{-6} M) (middle row); and polyplexes of p(ABOL/2AMPBA) at 24/1 weight ratio (0.24 mg/ml polymer) loaded with ARS (8.2×10^{-6} M) (bottom row). From left to right pictures of transmitted light, double photon excitation of DAPI at 718 nm, excitation of ARS at 488 nm and an overlay picture of DAPI and ARS fluorescence is shown. The scale bar is 30 μ m.

For the sample without polymer (ARS only) no fluorescence was observed. For the self-assembled nanoparticles loaded with ARS a fluorescent layer was observed on top of the cells. Although the samples were washed several times with PBS, the self-assembled nanoparticles could not be completely removed from the cell membrane, indicating strong cell adhesion of these p(ABOL/2AMPBA) polymeric particles. Moreover, highly fluorescent clusters can be observed, which were reasoned to originate from endocytosed nanoparticles. These observations indicate that the cell membrane is loaded with p(ABOL/2AMPBA) nanoparticles, but not (yet) all polymer nanoparticles were efficiently internalized after 1 hour.

The p(ABOL/2AMPBA) polyplexes loaded with ARS also formed a fluorescent layer of polyplexes on the cell surface. Also here larger fluorescent aggregates can be

observed, and in comparison to the self-assembled nanoparticles the polyplexes appear to form larger fluorescent aggregates. These larger fluorescent polyplexes were in many cases co-localizing with DAPI fluorescence, originating from stained plasmid DNA, whereas the smaller fluorescent particles did not show DAPI staining. This observation indicates that the larger aggregates are mainly formed by the polyplexes loaded with pDNA, whereas the smaller particles are self-assembled nanoparticles. In addition, it was observed that the larger particles were found to accumulate in the epi-nuclear region. This epi-nuclear accumulation was observed for the self-assembled nanoparticles and to an even larger extent for the polyplexes. Therefore, it is concluded that the intracellular pathway is different for the polyplexes containing pDNA than for the self-assembled nanoparticles. Depending on where the therapeutic diol has to fulfill its therapeutic role within the cell, it could prove beneficial to add either therapeutic or non-coding DNA to p(ABOL/2AMPBA) to be able to optimize the intracellular routing of therapeutic diols.

5.3.6. Cell viability and transfection of COS-7 cells with ARS-loaded polyplexes

The effects of the presence of alizarin red S on the transfection properties of p(ABOL/2AMPBA)/DNA polyplexes was investigated in COS-7 cells. Due to the presence of ARS the density of hydrophobic moieties in the polyplex increases and, most importantly, the boronic acid groups are converted into boronic/boronate ester groups. To evaluate the effect of these changes in the polyplex the transfection properties of ARS-loaded polyplexes of p(ABOL/2AMPBA) with plasmid DNA encoding for β -galactosidase at 24/1 and 48/1 ratio were compared with unloaded control polyplexes of p(ABOL/2AMPBA) with pDNA. DNA encoding for β -galactosidase was selected above GFP encoding DNA as the β -galactosidase gene expression can be measured with the ONPG-assay which does not interfere with the 2AMPBA-ARS fluorescence. Both the gene expression and the cell viability by XTT assay were determined 48 hours after transfection and the results are shown in Figure 5.10.

It was found that the presence of ARS slightly reduced the transfection efficiency, although the difference was not significant. The transfection efficiency at the 24/1 polymer/DNA weight ratio was lower than the positive control PEI (Exgen at N/P ratio 6), but the transfection efficiency at the 48/1 polymer/DNA weight ratio was *ca.* 1.3–1.7 times that of PEI. The cell viability was slightly decreased at 48/1 ratio ($92 \pm 8\%$) in the absence of ARS, but in the presence of ARS complete cell viability was observed, whereas transfection with the control PEI resulted in a reduced cell viability ($67 \pm 15\%$) under identical circumstances. These transfection results again demonstrate the potential of p(ABOL/2AMPBA) for gene delivery. Importantly,

the presence of alizarin does not decrease the transfection efficiency, thereby paving the road for combined drug and gene therapies using boronated SS-PAAAs.

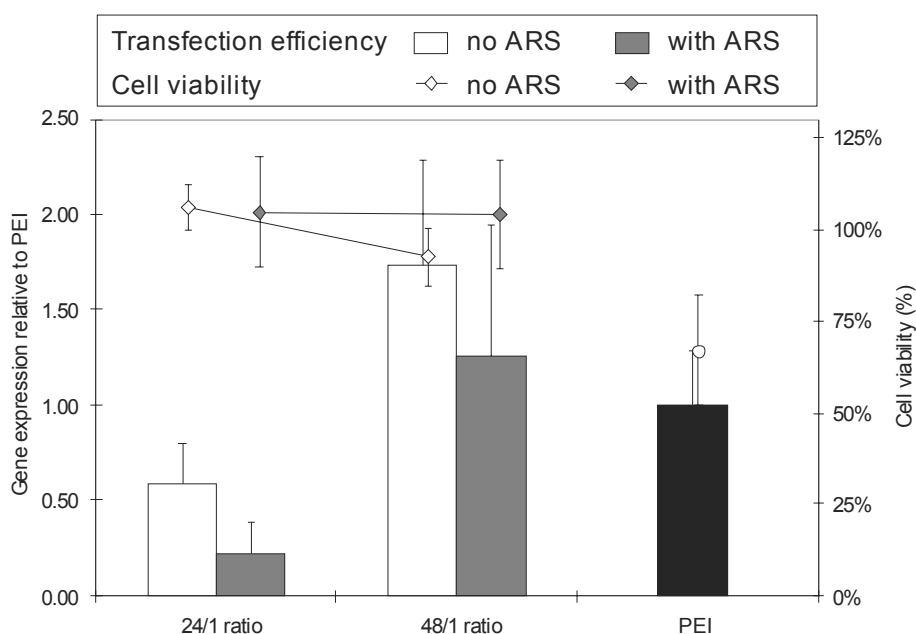


Figure 5.10. Transfection of p(ABOL/2AMPBA) polyplexes in COS-7 cells without (white) or with (grey) loading of 8.2×10^{-6} M ARS, relative to PEI (Exgen at N/P ratio 6). The transfection efficiency is shown in bars and the cell viability in symbols, lines are added for clarity.

5.4. Conclusions

We have developed a poly(amido amine) p(ABOL/2AMPBA) containing *ortho*-aminomethylphenylboronic acid (2AMPBA) functionalities which spontaneously forms nanoparticles as well as polyplexes with plasmid DNA. Moreover, both types of nanoparticles can effectively incorporate alizarin red S (ARS) that was selected as model drug compound for catecholamines such as L-DOPA and dopamine. Incorporation of ARS in the nanoparticles results in a fluorescent drug delivery system allowing both imaging and therapy.

The spontaneously formed nanoparticles of p(ABOL/2AMPBA) are capable of intracellular delivery of alizarin red S. Similar to polymeric nanoparticles, ARS-loaded polyplexes of p(ABOL/2AMPBA) with plasmid DNA were efficiently taken up COS-7 cells (up to 95%) and H1299-Fluc cells (up to 74%) during 1 hour incubation. Moreover, it was demonstrated that the fluorescent boronic/boronate ester formation of ARS with the 2AMPBA moieties inside polyplexes of p(ABOL/2AMPBA) with pDNA allows for monitoring of polyplex uptake by confocal microscopy. In a transfection experiment in COS-7 cells, it was found that ARS-loaded polyplexes

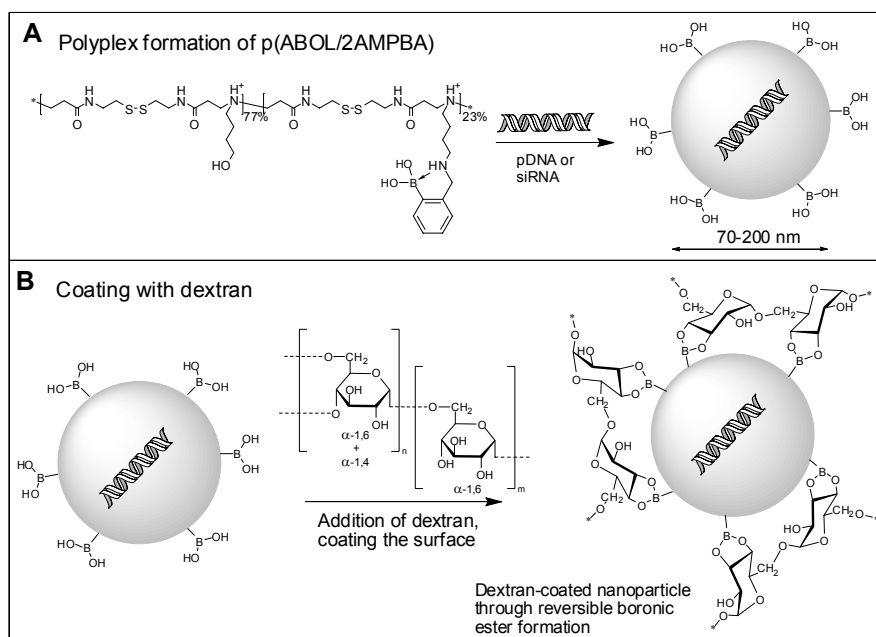
of p(ABOL/2AMPBA) had transfection efficiencies of 1.3–1.7 times that of PEI (comparable to the unloaded polyplexes). This study demonstrates the potential of boronic acid functionalized SS-PAAAs for drug delivery using therapeutics molecules with vicinal diols and combined drug and gene delivery of drug-loaded polyplexes with (therapeutic) DNA.

5.5. References

- [1] R. Duncan, H. Ringsdorf, R. Satchi-Fainaro, Polymer therapeutics: Polymers as drugs, drug and protein conjugates and gene delivery systems: Past, present and future opportunities, *Adv. Polym. Sci.*, 192 (2006) 1-8.
- [2] T.G. Park, J.H. Jeong, S.W. Kim, Current status of polymeric gene delivery systems, *Adv. Drug Deliver. Rev.*, 58 (2006) 467-486.
- [3] E. Wagner, J. Kloeckner, Gene delivery using polymer therapeutics, *Adv. Polym. Sci.*, 192 (2006) 135-173.
- [4] S. Ganta, H. Devalapally, A. Shahiwala, M. Amiji, A review of stimuli-responsive nanocarriers for drug and gene delivery, *J. Control. Release*, 126 (2008) 187-204.
- [5] C. Lin, C.J. Blaauboer, M.M. Timoneda, M.C. Lok, M. van Steenberg, W.E. Hennink, Z.Y. Zhong, J. Feijen, J.F.J. Engbersen, Bioreducible poly(amido amine)s with oligoamine side chains: Synthesis, characterization, and structural effects on gene delivery, *J. Control. Release*, 126 (2008) 166-174.
- [6] C. Lin, Z.Y. Zhong, M.C. Lok, X.L. Jiang, W.E. Hennink, J. Feijen, J.F.J. Engbersen, Linear poly(amido amine)s with secondary and tertiary amino groups and variable amounts of disulfide linkages: Synthesis and in vitro gene transfer properties, *J. Control. Release*, 116 (2006) 130-137.
- [7] C. Lin, Z.Y. Zhong, M.C. Lok, X.L. Jiang, W.E. Hennink, J. Feijen, J.F.J. Engbersen, Novel bioreducible poly(amido amine)s for highly efficient gene delivery, *Bioconjugate Chem.*, 18 (2007) 138-145.
- [8] M.A. Mateos-Timoneda, M.C. Lok, W.E. Hennink, J. Feijen, J.F.J. Engbersen, Poly(amido amine)s as gene delivery vectors: Effects of quaternary nicotinamide moieties in the side chains, *Chemmedchem*, 3 (2008) 478-486.
- [9] M. Piest, C. Lin, M.A. Mateos-Timoneda, M.C. Lok, W.E. Hennink, J. Feijen, J.F.J. Engbersen, Novel poly(amido amine)s with bioreducible disulfide linkages in their diamino-units: Structure effects and in vitro gene transfer properties, *J. Control. Release*, 130 (2008) 38-45.
- [10] M. Piest, J.F.J. Engbersen, Boronic acid functionalized disulfide containing poly(amido amine) with improved polyplex stability for pDNA and siRNA delivery in vitro, See chapter 4 of this thesis, (2010).
- [11] M. Piest, J.F.J. Engbersen, Effects of charge density and hydrophobicity of poly(amido amine)s for non-viral gene delivery, *J. Control. Release*, 148 (2010) 83-90.
- [12] E. Ranucci, P. Ferruti, E. Lattanzio, A. Manfredi, M. Rossi, P.A. Mussini, F. Chiellini, C. Bartoli, Acid-base properties of poly(amidoamine)s, *J. Polym. Sci. Pol. Chem.*, 47 (2009) 6977-6991.
- [13] W.Q. Yang, X.M. Gao, B.H. Wang, Boronic acid compounds as potential pharmaceutical agents, *Med. Res. Rev.*, 23 (2003) 346-368.
- [14] A. Coskun, E.U. Akkaya, Three-point recognition and selective fluorescence sensing of L-DOPA, *Org. Lett.*, 6 (2004) 3107-3109.
- [15] S.L. Wiskur, J.J. Lavigne, H. Ait-Haddou, V. Lynch, Y.H. Chiu, J.W. Canary, E.V. Anslyn, pK(a) values and geometries of secondary and tertiary amines complexed to boronic acids - Implications for sensor design, *Org. Lett.*, 3 (2001) 1311-1314.
- [16] P.R. Westmark, S.J. Gardiner, B.D. Smith, Selective monosaccharide transport through lipid bilayers using boronic acid carriers, *J. Am. Chem. Soc.*, 118 (1996) 11093-11100.
- [17] P.R. Westmark, B.D. Smith, Boronic acids facilitate the transport of ribonucleosides through lipid bilayers, *J. Pharm. Sci.*, 85 (1996) 266-269.
- [18] S. Kitano, Y. Koyama, K. Kataoka, T. Okano, Y. Sakurai, A novel drug delivery system utilizing a glucose responsive polymer complex between poly (vinyl alcohol) and poly (N-vinyl-2-pyrrolidone) with a phenylboronic acid moiety, *J. Control. Release*, 19 (1992) 161-170.
- [19] D. Shiino, Y. Murata, A. Kubo, Y.J. Kim, K. Kataoka, Y. Koyama, A. Kikuchi, M. Yokoyama, Y. Sakurai, T. Okano, Amine containing phenylboronic acid gel for glucose-responsive insulin release under physiological pH, *J. Control. Release* 37 (1995) 269-276.
- [20] C. Young Kweon, J. Seo Young, K. Young Ha, A glucose-triggered solubilizable polymer gel matrix for an insulin delivery system, *Int. J. Pharm.*, 80 (1992) 9-16.

- [21] C.H. Zhu, S. Jung, S.B. Luo, F.H. Meng, X.L. Zhu, T.G. Park, Z.Y. Zhong, Co-delivery of siRNA and paclitaxel into cancer cells by biodegradable cationic micelles based on PDMAEMA-PCL-PDMAEMA triblock copolymers, *Biomaterials*, 31 (2010) 2408-2416.
- [22] L. Chen, D.J. Waxman, Intratumoral activation and enhanced chemotherapeutic effect of oxazaphosphorines following cytochrome-P-450 gene-transfer - Development of a combined chemotherapy cancer gene-therapy strategy, *Cancer Res.*, 55 (1995) 581-589.
- [23] L.Y. Qiu, Y.H. Bae, Self-assembled polyethylenimine-graft-poly(epsilon-caprolactone) micelles as potential dual carriers of genes and anticancer drugs, *Biomaterials*, 28 (2007) 4132-4142.
- [24] J.L. Zhu, H. Cheng, Y. Jin, S.X. Cheng, X.Z. Zhang, R.X. Zhuo, Novel polycationic micelles for drug delivery and gene transfer, *J. Mater. Chem.*, 18 (2008) 4433-4441.
- [25] A.E. Ivanov, I.Y. Galaev, B. Mattiasson, Interaction of sugars, polysaccharides and cells with boronate-containing copolymers: from solution to polymer brushes, *J. Mol. Recognit.*, 19 (2006) 322-331.
- [26] A.E. Ivanov, K. Shiomori, Y. Kawano, I.Y. Galaev, B. Mattiasson, Effects of polyols, saccharides, and glycoproteins on thermoprecipitation of phenylboronate-containing copolymers, *Biomacromolecules*, 7 (2006) 1017-1024.
- [27] Y.R. Vandenburg, Z.Y. Zhang, D.J. Fishkind, B.D. Smith, Enhanced cell binding using liposomes containing an artificial carbohydrate-binding receptor, *Chem. Commun.*, (2000) 149-150.
- [28] G. Springsteen, B.H. Wang, A detailed examination of boronic acid-diol complexation, *Tetrahedron*, 58 (2002) 5291-5300.
- [29] G. Springsteen, B.H. Wang, Alizarin Red S. as a general optical reporter for studying the binding of boronic acids with carbohydrates, *Chem. Commun.*, (2001) 1608-1609.

The presence of dextran improves the transfection efficiency of a boronic acid functionalized poly(amido amine)



Abstract

We have developed a disulfide containing poly(amido amine) with *ortho*-aminomethylphenylboronic acid (2AMPBA) functionalities for reversible boronic ester formation with vicinal diols, including polycarbohydrates such as dextran. This polymer, abbreviated as p(ABOL/2AMPBA) spontaneously forms self-assembled nanoparticles that are stabilized by reversible interactions of the Lewis-acidic boronic acid groups with tertiary amine groups in the main chain and pending hydroxybutyl groups in the side chains of the polymer. Moreover, p(ABOL/2AMPBA) forms polyplexes with pDNA that were stable for at least up to 6 days at 37 °C in HEPES buffer. Dynamic light scattering showed that the presence of dextran did not significantly affect the size (100–140 nm) and the zeta potential (*ca.* 25 mV) of the polyplexes; however a clear indication of the shielding of the polyplexes by the presence of dextran was obtained from AFM pictures showing that only in the presence of dextran the spreading of the disulfide containing polyplexes on a gold surface is prevented. The presence of dextran was found to improve the transfection efficiencies of p(ABOL/2AMPBA) in COS-7 cells and SH-SY5Y neuroblastoma cells. Confocal studies showed that FITC-labeled dextran colocalized with polyplexes of p(ABOL/2AMPBA) and not with the non-boronated control polymer p(ABOL), suggesting that the dextran is bound to p(ABOL/2AMPBA) polyplexes through reversible boronic ester formation. Addition of dextran to siRNA- p(ABOL/2AMPBA) polyplexes also significantly improved the knockdown of luciferase expression in H1299-Fluc cells.

This chapter is being prepared for publication as: M. Piest, T.A.M. Groothuis, M.J.K. Ankoné, A. Embrechts and J.F.J. Engbersen. *The presence of dextran improves the transfection efficiency of a boronic acid functionalized poly(amido amine).*

6.1. Introduction

Non-viral DNA vehicles form an attractive alternative for viral vectors in the delivery of therapeutic genes in order to cure various metabolic diseases [1-2]. Most non-viral vectors investigated thus far are cationic polymers and although they are quite successful *in vitro*, their clinical breakthrough is hampered due to their lower transfection efficiency and limited stability *in vivo* [3]. Cationic polymers, such as poly(L-lysine), poly(amido amine) dendrimers and poly(ethylenimine) (PEI) can condense DNA into nanosized polyplexes through electrostatic interactions, especially at higher polymer/DNA ratios. The resulting cationic polyplexes can interact non-specifically with negatively charged cell-surfaces, originating from negatively charged proteoglycans [4]. Although the positive surface charge of the polyplexes is beneficial for cellular uptake, intravenous delivery of such cationic polyplexes leads to opsonization, thus inducing particle clearance by the reticuloendothelial system (RES) [5-6]. A number of chemical modifications of cationic polymers with hydrophilic polymers that shield the particle surface charge have been introduced [7-10]. Most common is the grafting of poly(ethylene glycol) (PEG) to cationic polymers to form neutral polyplexes that show improved circulation in the bloodstream and significantly reduced toxicity of these polyplexes [11-13]. Similarly, grafting of dextran could be used, as according to the work of Illum *et al.* [14], simply the presence of dextran in the transfection formulation could reduce RES clearance of model particles.

Boronic acids are well known to form boronic esters with cis-diols [15-19] like carbohydrates [20-26], including dextran, and in our previous work we have developed a boronated poly(amido amine) that can form reversible boronate esters with carbohydrates. This polymer was based on the disulfide-containing poly(amido amine) formed by Michael-type polyaddition of 4-aminobutanol to *N,N'*-cystaminebisacryl amide, abbreviated as p(ABOL), that combines high transfection efficiencies with good cell viability profiles *in vitro* [27]. The boronated analogue of this polymer was synthesized by the copolymerization of 2-((4-aminobutylamino)methyl)phenylboronic acid and 4-aminobutanol with *N,N'*-cystaminebisacrylamide. This polymer contained 23% of *ortho*-aminomethylphenylboronic acid moieties (2AMPBA) and is abbreviated as p(ABOL/2AMPBA). It was found that p(ABOL/2AMPBA) spontaneously forms polymeric nanoparticles in solution. Moreover, with pDNA p(ABOL/2AMPBA) forms polyplexes that are stable for at least up to 6 days at 37 °C in HEPES buffer [28]. Since the transfection efficiency of polymer p(ABOL/2AMPBA) was improved in the presence of different monosaccharides [28], it was of particular interest whether a polysaccharide such as dextran, which can form reversible boronic ester linkages with the p(ABOL/2AMPBA) polyplexes, would have effect on the gene delivery properties. It was hypothesized that the interaction of dextran with surface exposed boronic acid could provide a dextran coating on the nanoparticles.

A conceptual overview is given in Figure 6.1. p(ABOL/2AMPBA) can form polyplexes with pDNA and siRNA. Therefore DLS and SEM studies were performed in order to investigate whether the addition of dextran to a polyplex solution was resulting in a formation of a dextran layer around the boronated polyplexes. Moreover, transfection studies with p(ABOL/2AMPBA) polyplexes containing GFP encoding pDNA or antiluciferase siRNA were performed in order to elucidate whether the presence of dextran could improve the transfection efficiency of p(ABOL/2AMPBA)/pDNA polyplexes or luciferase knockdown of p(ABOL/2AMPBA)/siRNA polyplexes.

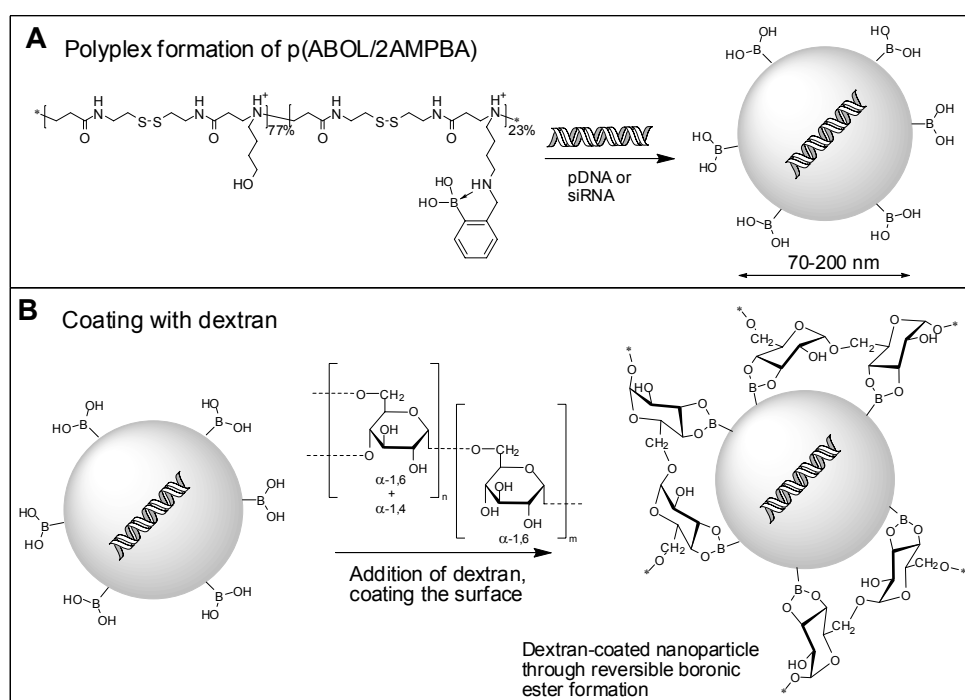


Figure 6.1. **A)** Conceptual overview of polyplex formation by electrostatic interactions with pDNA or siRNA. **B)** Coating of the polyplexes with dextran by reversible boronic ester formation of the *ortho*-aminomethylphenylboronic side group with the multiple hydroxyl groups of the dextran polymer.

6.2. Materials and methods

All reagents and solvents were of reagent grade and were used without further purification. Polymer p(ABOL/2AMPBA) was synthesized as described previously [28]. The composition of the polymer was established by ^1H NMR (D_2O , 300 MHz) and the content of boronic acid side groups in p(ABOL/2AMPBA) was 23% with respect to the total amount of side groups. The polymer was found to have a M_w of *ca.* 4.2 kDa and a buffer capacity of 69% [28].

6.2.1. Polyplex preparation

The DNA plasmid solution (1 mg/ml) as supplied by manufacturer (PlasmidFactory, Bielefeld) was diluted to a final concentration of 0.075 mg/ml in HEPES buffer solution (20 mM, set to pH 7.4). A series of polymer solutions of different concentrations was prepared by dilution of a solution of 0.9 mg/ml in HEPES buffer solution repeatedly 1:1 with HEPES buffer solution. To prepare polyplexes at 48/1, 24/1, and 12/1 polymer/DNA weight ratio 0.80 ml of the appropriate polymer solution was added to 0.20 ml of DNA solution in a 1.5 ml Eppendorf tube. The polyplex solutions were vortexed for 5 s and incubated for 30 min at ambient temperature prior to use. For the dextran coated polyplexes 100 μl of dextran (15–25 kDa, Sigma) solution (10% w/v) was added to 1.0 ml of polyplexes to a final concentration of 0.9% w/v and the samples were incubated for another 30 min at ambient temperature prior to use. Polyplexes with siRNA (Anti-Firefly Luciferase, Eurogentec) (AllStars Negative Control siRNA, Qiagen) were prepared in a similar manner using identical concentrations of polymer and siRNA as described above.

6.2.2. Determination of polyplex properties by Dynamic Light Scattering (DLS)

Polyplex size and surface (zeta) potential of the poly(amido amine)/plasmid DNA polyplexes and of the poly(amido amine)/plasmid siRNA polyplexes were stored at 37 °C and measured at 25 °C and/or 37 °C on a Zetasizer Nano series (Malvern Instruments Ltd, Malvern, UK) and the dynamic light scattering results were processed using Dispersion Technology Software V5.0.

6.2.3 Agarose gel retardation

Polyplexes at different polymer/DNA weight ratios were prepared in the absence and the presence of 0.9% w/v of dextran as described in 6.2.1, followed by vortexing for 5 s and incubation at ambient temperature for 30 min. DTT was used to mimic glutathione reduction and was added to a final concentration of 2.5 mM. After another 30 min (with or without DTT incubation), polyplexes were loaded on a 0.8% w/v agarose gel containing 1.25 μM ethidium bromide. Electrophoresis was performed for

60 min at 90 V in a TAE running buffer (40 mM tris(hydroxymethyl)aminomethane, 20 mM acetic acid, 10 mM EDTA, pH 8.0) supplemented with 1.25 μ M ethidium bromide. After electrophoresis, pictures were taken on a Biorad Gel Doc 2000 under UV illumination and analyzed using Biorad Multi Analyst software version 1.1.

6.2.4. Atomic force microscopy (AFM) study of dextran-coated polyplexes

One drop of polyplex solution of p(ABOL/2AMPBA) as prepared following the procedure in 6.2.1 were placed on a clean gold surface with 4 drops of milliQ water for good spreading. Next, the surface washed several times and dried to the air, before probing in air by a Veeco Nanoscope III controller in tapping mode equipped with a Nanosensors PPP-NCH-W cantilever. Images were recorded using a scan rate of 1 Hz.

6.2.5. Scanning electron microscopy (SEM) analysis of dextran-coated polyplexes

SEM imaging was performed with the samples described in 6.2.4, using an EMRAM MCS-A1 scanning electron microscope (FEI Systems) and any pretreatment (e.g., gold sputtering) was avoided. A 1-10 KeV protocol was applied (average working distance 10 mm; range 6-12 mm sample dependent). Samples were examined at low magnifications followed by further assessment at higher magnifications to characterize the particles present on the surface.

Polyplexes with p(ABOL/2AMPBA) and DNA at 24/1 and 48/1 weight ratio (1.0 ml) were prepared following the procedure described at 6.2.1. Both dextran-containing and dextran-free samples were rapidly frozen in liquid nitrogen and lyophilized. Part of the white “fluffy” polyplex samples was transferred to a SEM sample holder and gold sputtered for 50 seconds (40 μ A). SEM imaging was performed with an EMRAM MCS-A1 scanning electron microscope (FEI Systems). A 10 KeV protocol was applied (average working distance 10 mm; range 6-12 mm sample dependent). Representative images were obtained at different areas of the sample at low magnifications, followed by further assessment at higher magnifications to characterize the polyplex morphology and their dimensions. It was observed that the sample became damaged after longer exposure to the electron beam.

6.2.6. Cell culturing

COS-7 cells (SV-40 transformed African Green monkey kidney cells), HUH-6 cells (human hepatoblastoma cells) and H1299-Fluc (non-small cell human lung carcinoma cell line stably transfected with firefly luciferase) were cultured in Dulbecco's Modified Eagle Medium (Invitrogen) with 1 g/l D-glucose, completed with L-glutamine (1% v/v of GlutaMAX 200 mM) and penicillin-streptomycin solution (2% v/v of stock solution) and 10% v/v fetal bovine serum. SH-SY5Y neuroblastoma cells were cultured in RPMI 1640 medium (Invitrogen), completed with L-glutamine

(1% v/v of GlutaMAX 200mM) and penicillin-streptomycin solution (2% v/v of stock solution) and 10% v/v fetal bovine serum. Cells were cultured to 60–80% confluence and used in experiments below passage 20.

6.2.7. In vitro transfection and cell viability

Transfection and cell viability studies were performed with COS-7 cells, HUH-6 cells and H1299-Fluc in the absence and in the presence of 10% v/v fetal calf bovine serum in separate 96-well plates, $n = 4$. Cells were plated 24 h prior to transfection (COS-7 at 10,000 cells/well, and SH-SY5Y neuroblastoma at 20,000 cells per well) and were 60–80% confluent after 24 h. Plasmid pCMV/GFP was used as reporter gene. Two parallel transfection series, one for the determination of reporter gene expression (GFP) and the other for the evaluation of the cell viability by XTT assay, were carried out in separate 96-well plates. A polymer dilution series was prepared and 4 volume parts of the corresponding solutions were added to 1 volume part of DNA solution of 0.05 mg/ml to yield polyplexes with different polymer/DNA weight ratios. In a typical transfection experiment, the cells were incubated with the desired amount of polyplexes (100 μ l dispersion or 110 μ l in presence of 0.9% w/v dextran, resulting in 1 μ g plasmid DNA per well) for 2 h at 37 °C in a humidified 5% CO₂-containing atmosphere. Next, the polyplex solution was removed, 100 μ l of fresh culture medium was added and the cells were cultured for another 48 h. The transfection efficiency was determined by measuring the GFP expression by fluorescence microscopy. Linear PEI (Exgen 500, Invitrogen) at its optimal 6/1 N/P ratio, was used as reference. The cell viability was measured using an XTT assay, in which the XTT value for untreated cells (cells not exposed to transfection agents) was taken as 100% cell viability. XTT measurements were performed in quadrato using the Perkin Elmer LS50B luminescence spectrometer and analyzed in Kineticalc for Windows V2.0. For the XTT absorbance was measured at 490 nm with a reference at 655 nm. GFP expression was measured using a TECAN Safire² plate reader using SW Magellan Software V6.4 with 4 readings per well at different positions. Excitation was at 480 nm and optimal emission was determined at 503 nm. GFP expression was confirmed after fixation of the cells with 4% formaldehyde in PBS, followed by a DAPI staining according to manufacturer (Sigma). The plates were analyzed using a BD Pathway 435 bioimaging system operated with AttoVisionTM Software and the percentage of GFP positive cells was calculated using Cellprofiler 2.0 Software.

6.2.8. Confocal microscopy studies

Polyplexes were prepared from p(ABOL) and p(ABOL/2AMPBA) with plasmid DNA encoding for red fluorescent protein (RFP mCherry, Clontech) at a 48/1 polymer/DNA weight ratio. FITC-labeled dextran (4.0 kDa, Sigma) was added to a final concentration of 0.9% w/v. COS-7 cells were seeded in a μ -Slide 8-well at 2000 cells/well 24 h prior to the experiment. Medium was replaced with serum free medium (100 μ l) and polyplexes with and without dextran (110 and 100 μ l, respectively) were added to the cells for 2 h. Next, medium was replaced and the cells were monitored periodically using a Zeiss LSM 510 confocal microscope and images were obtained using Zen2008 software. FITC-dextran was analyzed after a band pass 500–550 nm IR filter using a 488 nm laser excitation. Red fluorescent protein was analyzed after a long pass 560 nm filter using a 543 nm laser excitation. Images had up to 40 times zoom with a pinhole of 100 μ m.

6.2.9. Luciferase knockdown using siRNA

Anti-luciferase siRNA was used to knockdown luciferase expression in H1299 Fluct cells. The cells were plated at 8000 cells/well in a 96-well plate 24 h prior to the experiment and incubation at 37 °C in a humidified 5% CO₂-containing atmosphere. Cells were 60–80 % confluent.

Polyplexes were prepared by addition of 16 μ l of polymer solution (0.375 mg/ml in HEPES buffer) to 4 μ l of siRNA (31.25 μ g/ml), resulting in polyplexes with polymer/siRNA weight ratio of 48/1. Next, 2.0 μ l of 10% w/v of dextran (25–40 kDa, Sigma) was added to the polyplexes, respectively. The polyplexes were vortexed for 5 s and incubated 30 min at ambient temperature. Two parallel series were prepared, the first using Allstars Negative Control siRNA (Qiagen) to determine the cell viability and the second using anti-luciferase siRNA (Eurogentec) to determine the knockdown. Medium was replaced with 100 μ l medium, without additives. After 30 min of incubation in the refreshed medium, 20 μ l of the polyplexes were added to the corresponding wells. After 2 h incubation at 37 °C and 5% CO₂, the medium/polyplex mixture was removed from the cells, cells were washed once with 100 μ l PBS and finally 100 μ l completed medium (with FBS) was added. The cells were incubated with for 48 h at 37 °C and 5% CO₂ before lysis of the cells. The cell lysates were treated with Luciferase Assay Reagent at ambient temperature and the luciferase activity was measured within the next 10 minutes, using a VICTOR³_{TM} 1420 multilabel counter (Perkin-Elmer) analyzed with Wallac 1420 Software. Lipofectamine (at optimal formulation) and Exgen500 (N/P ratio 5) were used as positive control. The relative knockdown was corrected using the non-coding siRNA transfected samples, compared to untreated cells.

6.3. Results and discussion

6.3.1. Effects of the presence of dextran on polyplex formation and stability

The polymer p(ABOL/2AMPBA) was synthesized with a M_w of 4.2 kDa and buffer capacity of 69%, thereby closely resembling p(ABOL) with M_w of 4.1 kDa and buffer capacity of 72% [28]. The presence of *ortho*-aminomethylphenylboronic acid moieties in p(ABOL/2AMPBA) resulted in the formation of more stable polyplexes with pDNA and siRNA than its non-boronated analogue p(ABOL). Polyplexes of p(ABOL/2AMPBA) were stable at 37 °C for more than 4 days, while polyplexes of p(ABOL) slowly formed a precipitate during 4–10 hours. The stabilization of the polyplexes is attributed to the reversible interaction and eventual boronate ester formation between the 2AMPBA moieties and the pending hydroxybutyl side chains, resulting in reversible crosslinking between the polymer chains [28]. In this study, the effect of dextran on the stability of polyplexes was investigated as the presence of dextran could in principle cause two effects. First, it is possible that dextran forms a coating layer around the nanoparticles by interaction with boronic acid moieties that are exposed to the surface of the polyplexes. Second, dextran could break up the crosslinks formed between the polymer chains in the polyplex by competing boronic ester formation leading to a transesterification reaction. DLS experiments at room temperature showed that the addition of 0.9% w/v dextran to polyplexes of p(ABOL/2AMPBA) at 24/1 polymer/DNA weight ratio did not significantly affect the particle size (*ca.* 120 nm) and no decrease in surface potential (*ca.* 26 mV) was observed. For polyplexes at 48/1 polymer/DNA weight ratio the addition of 0.9% w/v dextran did result in a minor increase of the particle size from 105 nm to *ca.* 120 nm, and the surface charge decreased from 32 mV to 25 mV. In order to evaluate whether the presence of dextran has influence on the long-term stability, the polyplexes were stored at 37 °C and monitored with DLS for 6 days. The results of this experiment are shown in Figure 6.2.

For the polyplexes at 24/1 polymer/DNA weight ratio a gradual increase in particle size during the storage of 6 days can be observed. However, in the presence dextran increase in size of the polyplexes is much slower indicating a stabilizing effect of dextran on the polyplexes. Polyplexes at 48/1 polymer/DNA weight ratio appeared to be more stable. No increase in size is observed during the 6 days storage at 37 °C, both in the absence and in the presence of dextran.

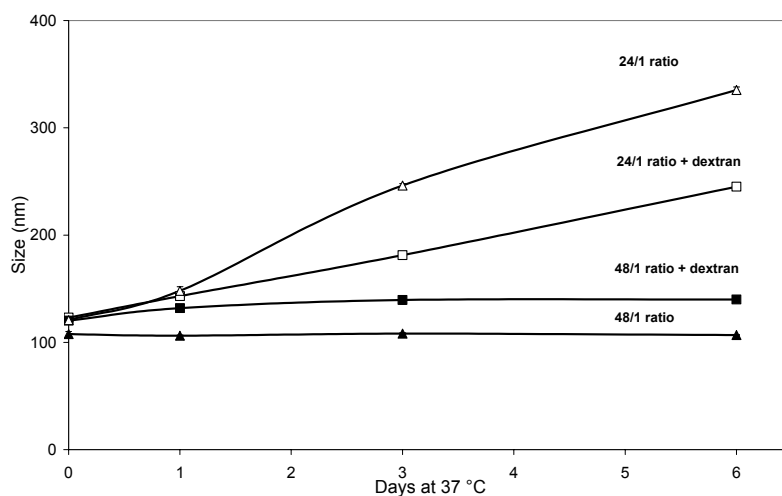


Figure 6.2. Particle size of polyplexes at 24/1 and 48/1 p(ABOL/2AMPBA)/DNA weight ratio as a function of time. Polyplexes in absence of dextran are shown in triangles and polyplexes in presence of dextran in squares, at 24/1 polymer/DNA weight ratio in open symbols and at 48/1 ratio in closed symbols. Samples were stored and measured at 37 °C at day 0 and again after 1, 3 and 6 days, respectively.

6.3.2. Effects of dextran on polyplex morphology

In order to gain additional insight on the effects of dextran on the polyplex properties, scanning electron microscopy (SEM) was used to study the morphology of 24/1 polymer/DNA weight ratio polyplexes in the absence and the presence of dextran. At higher magnification particles of 100–200 nm were observed, see Figure 6.3.

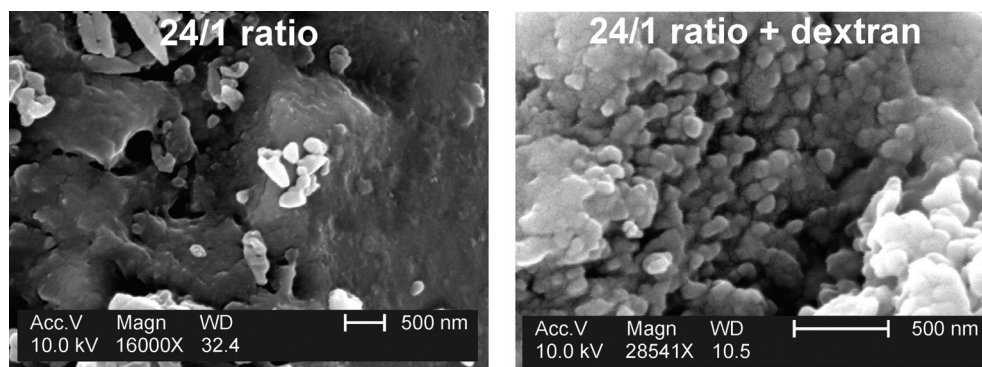


Figure 6.3. SEM pictures of lyophilized polyplexes at 24/1 p(ABOL/2AMPBA)/DNA weight ratio in absence (left) or presence (right) of dextran (scale bar is 500 nm).

From Figure 6.3 it appears that the nanosized polyplexes that were observed by DLS have a tendency to aggregate upon lyophilization. In the absence of dextran only few nanosized polyplexes are visible whereas the majority of the material appears as fused particles. In the presence of dextran, a significantly higher number of nanosized

particles can be observed. Moreover, the darker color of the aggregated polyplexes in absence of dextran suggests a more densely packed material than for the brighter polyplexes in the presence of dextran. These data suggest that the presence of dextran may serve as a lyoprotectant and the coating of the polyplexes with dextran prevents aggregation. Upon closer investigation of individual nanoparticles of 100-200 nm, no significant differences were observed between the polyplexes in the absence and polyplexes in the presence of dextran, except for the observation that the polyplexes in the absence of dextran appear to have sharper edges, whereas the polyplexes in the presence of dextran have a more spherical morphology.

6.3.3. Polyplex degradation in the presence of dextran

The disulfide linkages in the polymer backbone allows for rapid vector unpacking by disulfide cleavage in the reductive environment of the cytosol. The susceptibility of polyplexes of p(ABOL/2AMPBA) towards disulfide degradation has been demonstrated by the DNA release using agarose gel electrophoresis after treatment with DTT [28]. It was found that the presence of dextran did not interfere with the disulfide degradation in the polyplexes, since the DNA release after treatment with DTT was complete both in the absence and in the presence of dextran (Figure 6.4).

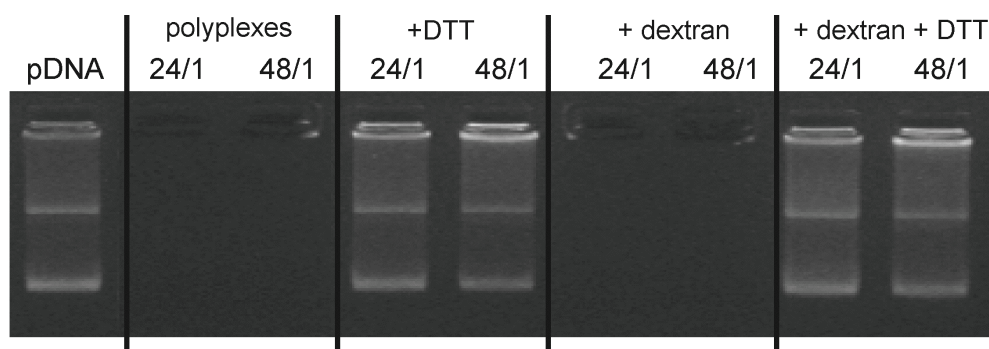


Figure 6.4. Agarose gel retardation of p(ABOL/2AMPBA) with pDNA at 24/1 and 48/1 polymer/DNA weight ratios in absence or presence of 5 mM DTT and/or 0.9% w/v dextran.

6.3.4. Addition of dextran prevents adsorption of cationic polyplexes to a gold surface

The subtle effects of the addition of dextran on the polyplex properties were further investigated. From atomic force microscopy (AFM) experiments, it was generally observed that polyplexes prepared with disulfide containing poly(amido amine)s have a tendency to spread on a gold surface, while this does not happen on a MICA surface. This is most probably due to binding of the disulfide moieties in the polymer backbone to the gold surface, causing the polyplexes to spread. It was investigated whether the presence of dextran, interacting with the boronated

polyplexes, could reduce the disulfide interaction with the gold surface. AFM experiments with polyplexes from p(ABOL/2AMPBA) at a 48/1 polymer/DNA weight ratio in the absence of dextran showed that a sticky smear was formed on the gold surface, and also tip-imaging was observed, whereas polyplexes in the presence of dextran were more spherical. Representative pictures are shown in Figure 6.5.

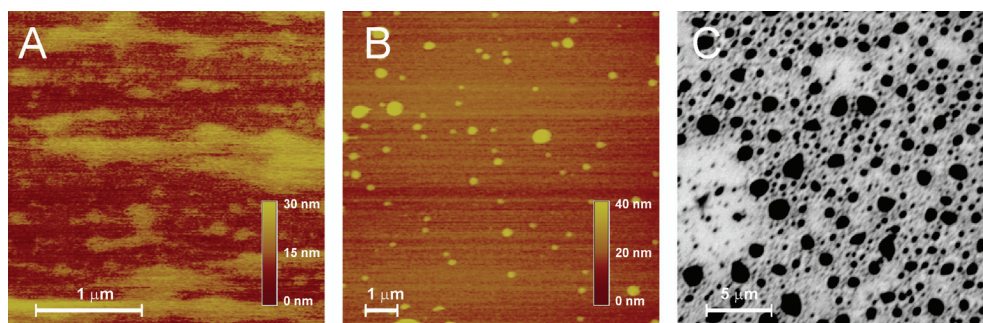


Figure 6.5. Polyplexes at 48/1 p(ABOL/2AMPBA)/DNA weight ratio in absence (A) or in presence of dextran (B, C). A) displays a 3x3 μm height image by AFM of polyplexes in absence of dextran where no polyplexes but “sticky layers” are formed on the surface. B) displays a 10x10 μm height image by AFM of polyplexes in presence of dextran where polyplexes of 100–250 nm are observed together with larger particles of 1–2 μm. C) displays the surface of polyplexes in the presence of dextran by SEM as only in the presence of dextran polyplexes of 80–150 nm and particles of ca. 1–2 μm can be observed (scale bar is 1 μm in A and B, and 5 μm in C).

In Figure 6.5A the height image of polyplexes in the absence of dextran is depicted. It can be observed that a “sticky” layer on the surface is formed that was frequently resulting in “tip-imaging” (*i.e.* sticking of material to the AFM tip resulting in artifacts in the obtained AFM picture, not shown). In contrast, Figure 6.5B shows the height image of polyplexes in the presence of dextran where particles of ca. 100–200 nm are visible. The same samples were also probed by SEM (Figure 6.5C). Only in the presence of dextran polyplexes could be observed. The SEM picture furthermore confirms that polyplexes of ca. 100–200 nm were present in large number besides larger particles of 1–2 μm. It was unclear whether the occurrence of the larger microparticles was due to the drying process or if they were resulting from the formation of microgels with dextran.

6.3.5. Effect of the presence of dextran on the transfection efficiency

The effect of the presence of dextran on the transfection efficiency of the polyplexes was investigated with COS-7 cells. To verify whether possible effects of dextran are indeed originating from specific interactions with the 2AMPBA moieties in the p(ABOL/2AMPBA)/DNA polyplexes, also polyplexes of the non-boronated polymer p(ABOL) were included in these experiments as a control. Polyplexes from p(ABOL/2AMPBA) and p(ABOL) at a 48/1 polymer/DNA weight ratio, both in the

absence and in the presence of 0.9% w/v dextran, were used to transfect COS-7 cells with pDNA encoding for GFP, allowing for the analysis by automated fluorescence microscopy. The results are shown in Figure 6.6.

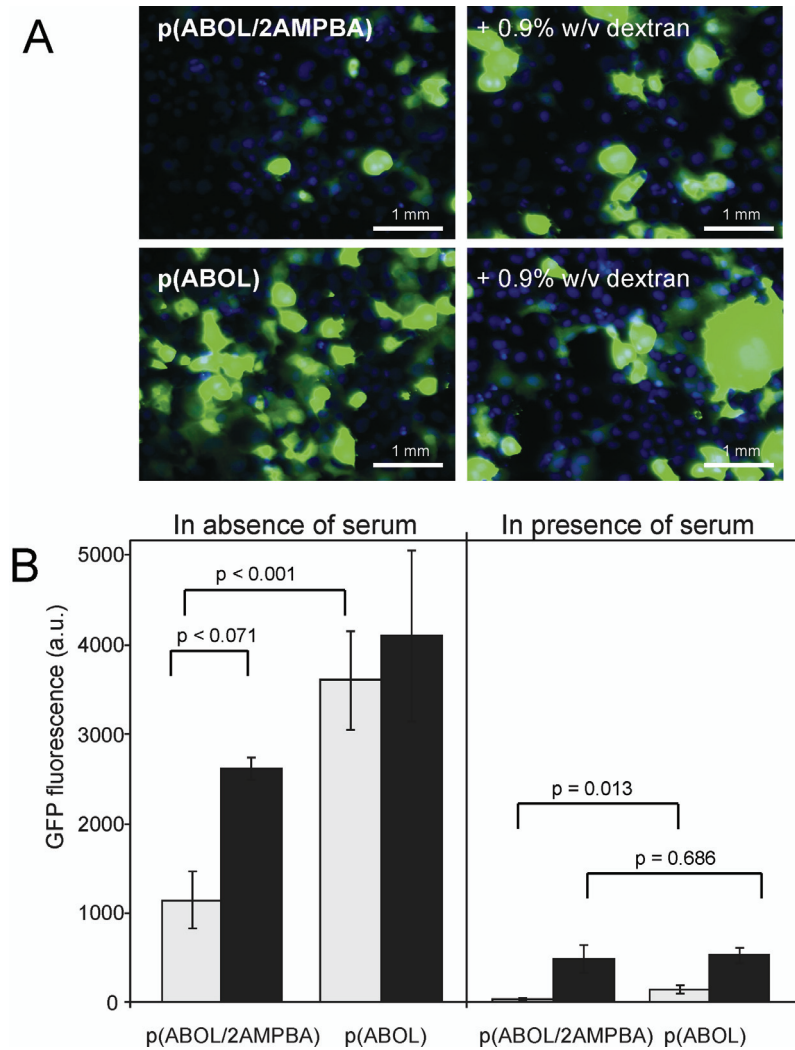


Figure 6.6. A Representative pictures of COS-7 cells transfected with polyplexes of p(ABOL/2AMPBA) (top row) and p(ABOL) (bottom row) at 48/1 polymer/DNA weight ratio in the absence (left) and in the presence of 0.9% w/v dextran (right), obtained by automated fluorescence microscopy. The percentage of GFP positive cells was determined by automated software analyzing colocalization of DAPI staining and GFP expression.

B Left panel: GFP fluorescence intensity of COS-7 cells treated in the absence of serum with p(ABOL/2AMPBA) in the absence (light grey) and in the presence of dextran (dark grey). For comparison p(ABOL) in the absence (light grey) and in the presence 0.9% w/v dextran is shown. Right panel: GFP fluorescence in the presence of serum. Statistic differences were determined by Student's t-Test (p values) and included for clarity.

Figure 6.6A gives some representative pictures of the transfection in the absence of serum. The percentage of GFP positive cells was determined from these pictures through automated analysis of the colocalization of DAPI staining and GFP fluorescence. It was found that polyplexes of p(ABOL/2AMPBA) in the absence of dextran resulted in only *ca.* 5% of the COS-7 cells expressing GFP. The presence of dextran was found to improve the percentage of GFP positive cells to *ca.* 31%, which is a significant improvement ($p = 0.003$). For the non-boronated control p(ABOL) in the absence of dextran it was found that *ca.* 40% of the COS-7 cells were expressing GFP, and in the presence of dextran the percentage of GFP-positive COS-7 cells reduces to *ca.* 25%. Thus, it appears that the presence of dextran has an inhibitory effect on polyplexes of p(ABOL), although difference between the presence and absence of dextran was less significant ($p = 0.109$).

Figure 6.6B shows the effect of dextran on the absolute GFP expression of COS-7 cells treated with polyplexes of p(ABOL/2AMPBA) and p(ABOL). It is apparent that the transfection efficiency in the absence of serum of p(ABOL/2AMPBA) is significantly lower than that of p(ABOL). Most likely, the stronger binding of p(ABOL/2AMPBA) with serum proteins more severely hampers interaction and uptake with the cells. The presence of dextran, which shields the p(ABOL/2AMPBA) polyplexes, results in a clear increase of the transfection efficiency of p(ABOL/2AMPBA), but not of that of p(ABOL) that has no interaction with dextran. In the presence of serum, the fluorescence due to GFP expression was almost completely reduced for both p(ABOL/2AMPBA) and p(ABOL), but the presence of dextran results in a significant increase in GFP expression for both polyplexes of p(ABOL/2AMPBA) and p(ABOL). It appears that the typical decrease in gene expression for cationic polymers in serum containing medium can be somewhat mitigated by the addition of dextran, although transfection is still far from that of polyplexes in serum free conditions.

6.3.6. Transfection of neuroblastoma cells

It has been reported that the neuroblastoma cell line SH-SY5Y is notoriously difficult to transfect, as this cell line is very sensitive towards cationic transfection agents, resulting in low viability [29-30]. Moreover the SH-SY5Y cells are growing in clusters, which make them more difficult to transfect compared to *e.g.* COS-7 cells as less surface area is available (and less cells are accessible) for polyplex uptake. Therefore, it was of particular interest whether the boronated polymer p(ABOL/2AMPBA) was capable of transfecting SH-SY5Y cells, especially in the presence of dextran. With the protocol used to transfect COS-7 cells under serum free conditions, it was observed that transfection of SH-SY5Y cells with polyplexes of both p(ABOL) and p(ABOL/2AMPBA) at 48/1 polymer/DNA weight ratio indeed resulted

in reduced cell viabilities (64–81%). However, although the cell viability is somewhat reduced, this is a promising result as polyplexes of the control PEI (Exgen at N/P ratio of 6) were very toxic towards these cells (cell viability < 50%). It is obvious that reduced cell viabilities result in reduced gene expression, hence transfection experiments were repeated with these polyplexes at the 24/1 p(ABOL/2AMPBA)/DNA weight ratio where optimal transfection efficiency of SH-SY5Y cells was observed while no decrease in cell viability was observed (cell viabilities were 90–100%). Analysis by automated microscopy showed that *ca.* 21% of the SH-SY5Y cells have expressed GFP, which can be considered as relatively efficient compared to other transfection agents (for example Westmark *et al.* report approximately 10–20% of SH-SY5Y cells transfected with lipofectamine [31]). Representative pictures are shown in Figure 6.7.

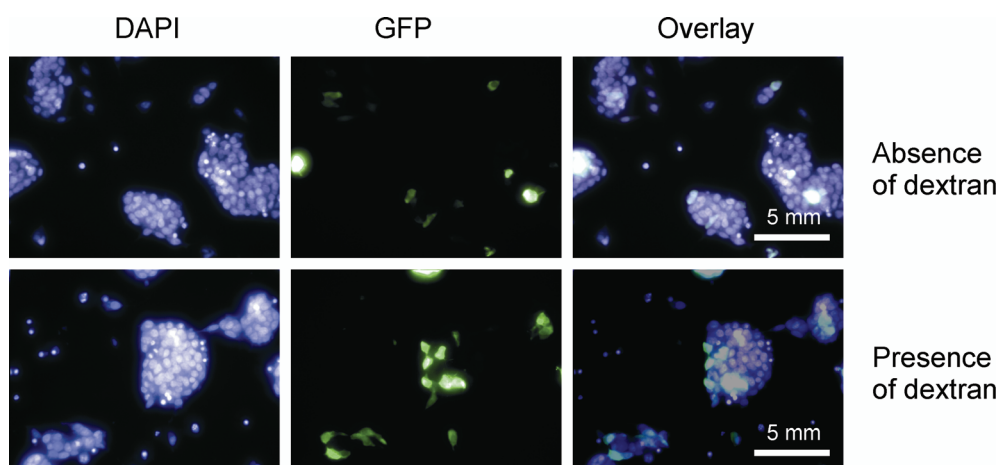


Figure 6.7. GFP expression in neuroblastoma cells (SH-SY5Y). From left to right is shown clusters of cells with a DAPI staining, GFP fluorescence and the overlay of the GFP expression with the DAPI staining of polyplexes formed with p(ABOL/2AMPBA) at a 24/1 polymer/DNA weight ratio in absence (top row) or presence of 1.0% w/v dextran (bottom row).

This remarkably high transfection of SH-SY5Y cells could be further improved in the presence of dextran, as the percentage of transfected cells then improved from *ca.* 21% to even *ca.* 41%.

6.3.7. Investigating the role of boronic acid in the uptake of the nanoparticles

In the absence of serum, it was observed that the presence of 0.9% w/v of dextran to polyplexes of p(ABOL/2AMPBA) results in higher gene expression, while it had much lower effect on polyplexes of p(ABOL). In the presence of serum, the presence of dextran leads to improved transfection by polyplexes of both polymers, raising the question if the effect of dextran is due to the assumed specific interactions of dextran

with the boronic acid moieties or to a non-specific effect. In order to obtain more evidence that the dextran is forming a coating around the boronated polyplexes and/or that dextran is only co-transported into the cells together with the boronated polyplexes, additional confocal experiments were performed using FITC-labeled dextran. Therefore, fluorescent microscopy pictures were taken 15 minutes after addition of polyplexes of p(ABOL/2AMPBA) in the presence of FITC-dextran to COS-7 cells. As FITC-dextran may be endocytosed independently, control experiments with FITC-dextran only were performed under all conditions applied. The results are given in Figure 6.8, showing the FITC fluorescence microscopy pictures, a transmitted light picture showing the outlines of the cells, and overlay pictures in order to confirm whether the FITC-fluorescence is inside or outside of the cells.

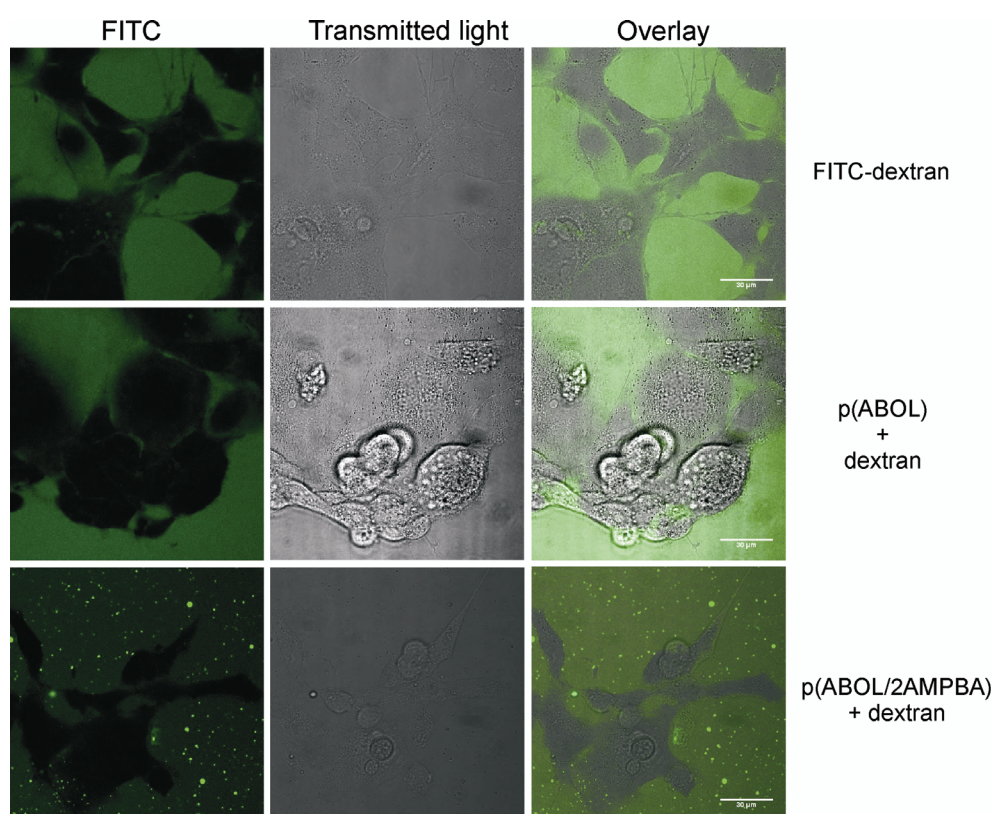


Figure 6.8. Fluorescent microscopy pictures of FITC-dextran (top row), polyplexes of p(ABOL) in presence of FITC-dextran (middle row), and polyplexes of p(ABOL/2AMPBA) in presence of FITC-dextran (bottom row). Pictures were taken 15–30 minutes after addition of the polyplexes to the cells, before removal of the polyplexes. The cells appear non-fluorescent (dark) and the surrounding medium was fluorescent (green). In case of polyplexes of p(ABOL/2AMPBA) fluorescent aggregates outside of the cells were visible (scale bar is 30 μm).

For both polyplexes of p(ABOL) and P(ABOL/2AMPBA) and FITC-dextran only, it was observed that a fluorescent background was visible around the cells originating from the FITC-dextran (intensity of 76-78 a.u.), whereas the cells themselves were non-fluorescent (the dark areas in the pictures). Moreover, the pictures show that free FITC-dextran is not endocytosed independently. However, under the same conditions FITC-dextran in presence of polyplexes of p(ABOL/2AMPBA) yielded some highly fluorescent aggregates outside the cells, whereas the fluorescent background signal was decreased to 48 a.u. This clearly shows that p(ABOL/2AMPBA) interacts with dextran under the formation of condensed fluorescent particles. After 2 hours of incubation, and subsequent washing with PBS, the cells were kept in culture for another 5 hours in serum-containing medium before the cells were monitored again (see Figure 6.9).

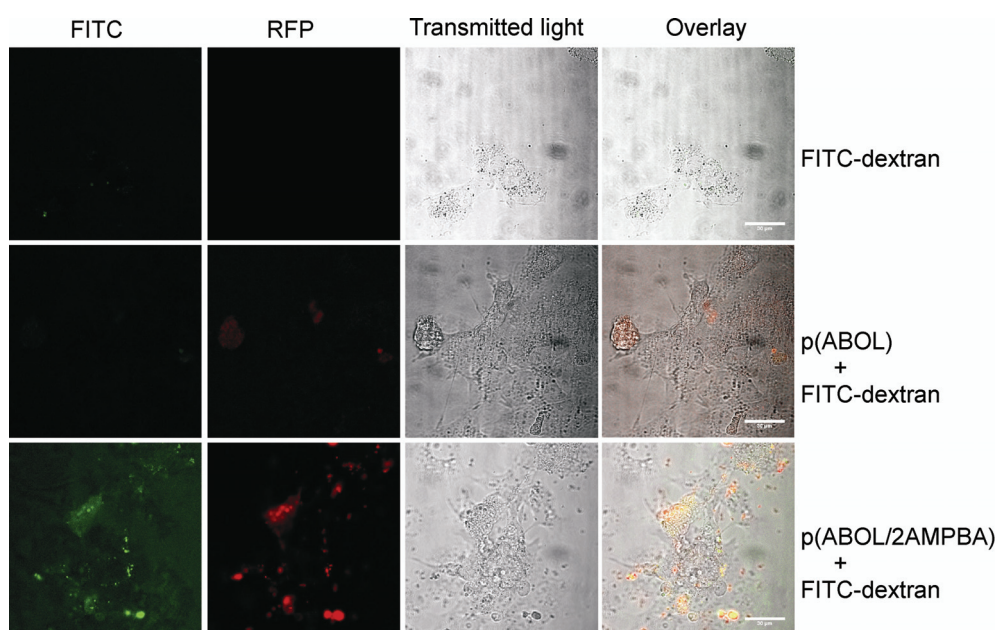


Figure 6.9. Fluorescent microscopy pictures of COS-7 cells 7 h after transfection with 0.9% w/v FITC-dextran, p(ABOL), p(ABOL/2AMPBA), p(ABOL) in the presence of 0.9% w/v FITC-dextran, and p(ABOL/2AMPBA) in the presence of 0.9% w/v FITC-dextran. In the left column fluorescence of FITC is depicted in green, in the second column fluorescence of RFP expression is depicted in red, in the third column a transmitted light picture is depicted and in the fourth column an overlay of the previous columns is shown. (Scale bar = 30 μ m).

After this period, no fluorescence of FITC-dextran could be observed in the absence of polymer, and also in the presence of p(ABOL) no fluorescence of FITC-dextran was observed, indicating that all FITC-dextran was removed in the washing step and not internalized by the cells together with p(ABOL) polyplexes. However, for FITC-dextran in the presence of p(ABOL/2AMPBA) residual fluorescence and green aggregates were still visible, predominantly inside the cells.

This indicates that the FITC-dextran is only internalized when p(ABOL/2AMPBA) is present, supporting the idea that dextran has coated the polyplexes. This was also supported by the expression of red fluorescent protein (RFP) in the cells with FITC-dextran fluorescence. These results suggest that the onset of gene expression in the presence of FITC-dextran was faster and the expression efficiency in the individual cells was slightly higher than observed for polyplexes of p(ABOL/2AMPBA) than for polyplexes of p(ABOL).

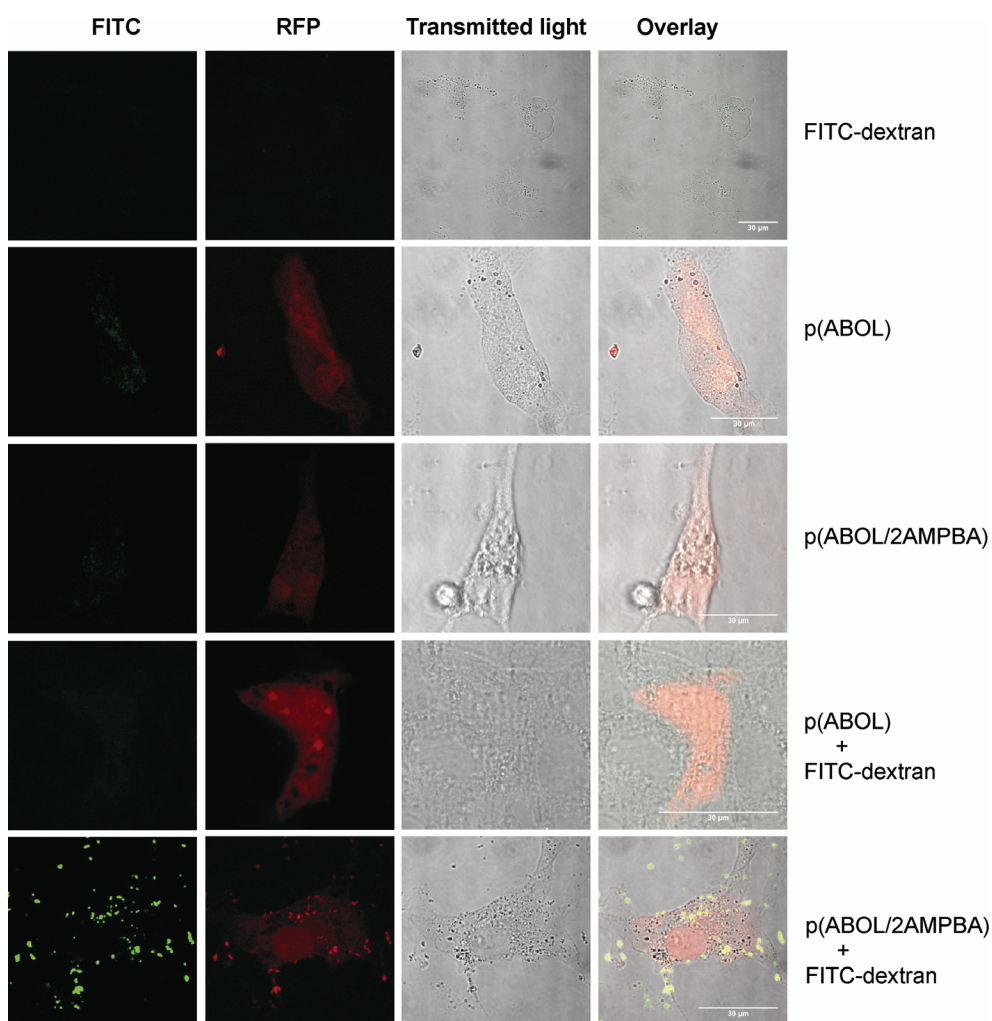


Figure 6.10. Fluorescent microscopy pictures of COS-7 cells 48 h after transfection with 0.9% w/v FITC-dextran, p(ABOL), p(ABOL/2AMPBA), p(ABOL) in the presence of 0.9% w/v FITC-dextran, and p(ABOL/2AMPBA) in the presence of 0.9% w/v FITC-dextran. In the left column fluorescence of FITC is depicted in green, in the second column fluorescence of RFP expression is depicted in red, in the third column a transmitted light picture is depicted and in the fourth column an overlay of the previous columns is shown. (Scale bar is 30 μ m)

The cells were monitored again 2 days after transfection, using identical fluorescent microscopy settings for all samples (Figure 6.10). In the samples treated with only FITC-dextran, a large number of viable cells were observed. Samples treated with with polyplexes of p(ABOL) in the presence of FITC-dextran showed only few remaining cells, but several of these cells showed high gene expression. Compared to p(ABOL), for cells treated with polyplexes of p(ABOL/2AMPBA) in the presence of FITC-dextran a larger number of viable cells were visible, and with a similar high RFP-expression. Similar to the observation after 5 hours of additional culture, also after this two-day additional culture period samples treated with polyplexes of p(ABOL/2AMPBA) in the presence of FITC-dextran showed many fluorescent particles in the FITC-channel, both outside as well as inside the cells (also see Figure 6.11). This clearly demonstrates that there is an interaction between the boronated polyplexes of p(ABOL/2AMPBA) with dextran that is not observed for p(ABOL).

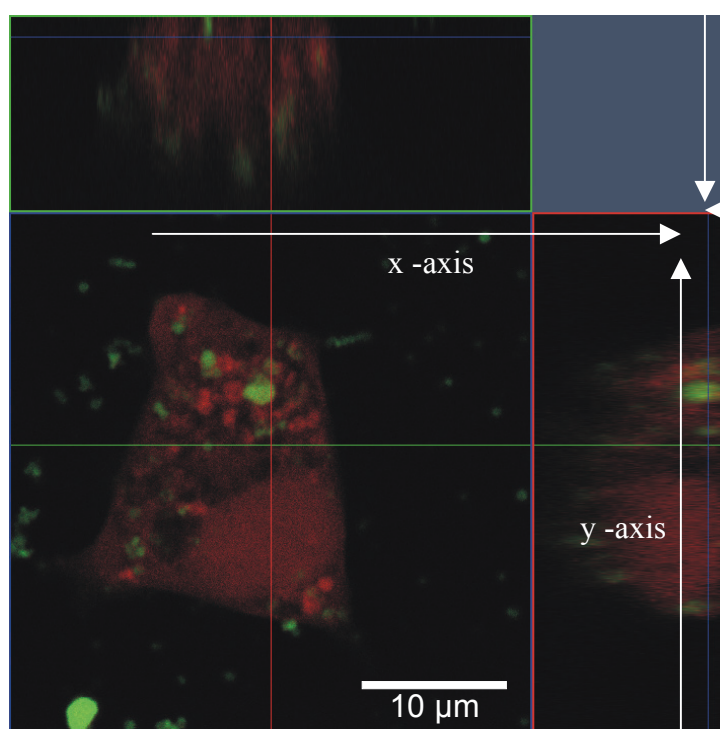


Figure 6.11. COS-7 cell treated with polyplexes of p(ABOL/2AMPBA) in the presence of FITC-dextran. The picture shows a cross-section based on a z-stack, clearly demonstrating the internalization of FITC-dextran (Scale bar = 10 μm).

6.3.8. Effect of dextran on gene silencing using siRNA polyplexes of p(ABOL/2AMPBA)

In our previous work it was found that the presence of different sugars to the boronic acid-containing polyplexes of p(ABOL/2AMPBA) resulted in increased gene silencing of luciferase in H1299-Fluc cells as compared to polyplexes of p(ABOL) [28]. Therefore it was of interest to study the effect of the presence of dextran on the luciferase knockdown of polyplexes at 48/1 polymer/siRNA weight ratio compared to the non-boronated analogues of p(ABOL). It was previously found that the siRNA polyplexes of p(ABOL/2AMPBA) had similar sizes and zeta potentials as polyplexes with pDNA [28]. H1299-Fluc cells were incubated under serum free conditions with polyplexes with non-coding siRNA and anti-luciferase siRNA in the absence or the presence of dextran for 2 hours and subsequent washing and the luciferase expression of the cells was determined after 48 hours. Cells treated with non-coding siRNA polyplexes showed a luciferase expression that was approximately equal to non-treated cells (negative control, 100% luciferase activity) indicating that there was no cytotoxicity for any of these polyplexes. For the cells treated with anti-luciferase siRNA polyplexes of p(ABOL/2AMPBA) and p(ABOL) the luciferase expression was reduced to 69% and 80%, respectively (Figure 6.12), indicating that p(ABOL/2AMPBA) is more efficient in the siRNA-mediated gene silencing than p(ABOL).

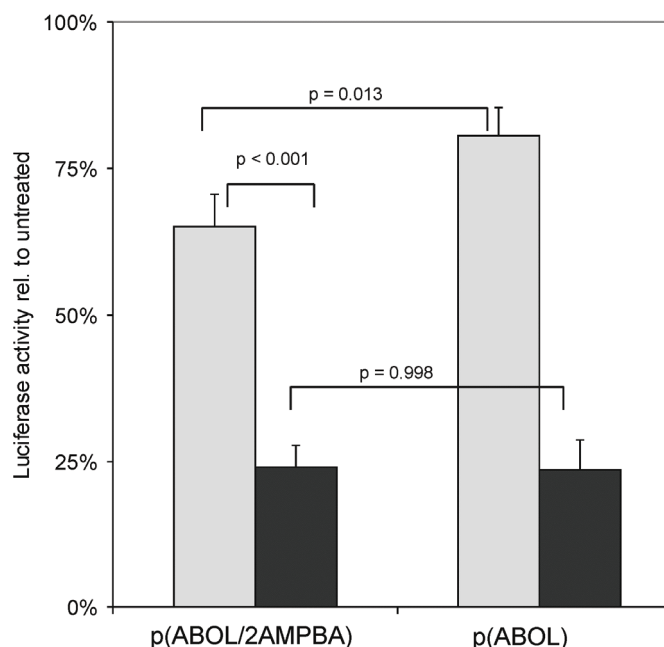


Figure 6.12. Gene silencing for polyplexes of p(ABOL/2AMPBA) and p(ABOL) at 48/1 polymer/siRNA weight ratio in the absence (light grey) and in the presence (dark grey) of 0.9% w/v dextran. (p was determined by Student's t-Test.)

In the presence of 0.9 % w/v dextran the luciferase expression significantly reduced further to *ca.* 24% for both polymers. To the best of our knowledge, this remarkable result has not been reported by others. An explanation could be that dextran binds with the cell surface thereby preventing or altering the endosomal uptake pathways. It is known that the endocytotic pathway is determining the intracellular fate of the particles [32-34] and it is conceivable that the presence of dextran direct the uptake to a more favorable pathway for gene silencing. For the boronated polyplexes, reversible boronic ester formation between boronic acid groups at the surface of polyplexes of p(ABOL/2AMPBA) and the hydroxyl groups of dextran may result in the surface coating, as observed in the confocal microscopy experiments. This reversible boronate ester formation may also prove to be beneficial upon further dilution, such as during *in vivo* siRNA delivery.

6.4. Conclusions

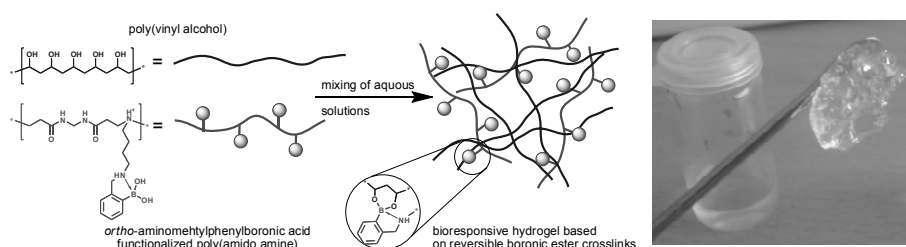
It was found that the presence of dextran favorably contributes to the overall gene expression of the boronated polyplexes of p(ABOL-2AMPBA) in COS-7 cells and SH-SY5Y cells. The boronated polymer p(ABOL/2AMPBA) was developed to reversibly form boronic esters with the hydroxyl groups of dextran and in this way to form stable polyplexes. In transfection studies with COS-7 cells it was observed that the transfection efficiency in serum containing medium was improved by the addition of dextran to polyplexes of both p(ABOL) and p(ABOL-2AMPBA). Remarkably, for transfection of SH-SY5Y cells with boronic acid polyplexes a doubling of the transfection efficiency from 21% to 41 % transfected cells was observed in the presence of dextran. Also gene silencing was significantly improved by addition of dextran to polyplexes of both p(ABOL) and p(ABOL-2AMPBA), suggesting that a reduction in interaction of the polyplexes with the cell membranes results in a higher siRNA gene silencing. Confocal microscopy demonstrated co-localization of FITC-labeled dextran and polyplexes of p(ABOL-2AMPBA) both outside and inside the cells, showing that p(ABOL/2AMPBA) polyplexes and the dextran are associated. Moreover, it further shows that the presence of boronic acid functionalities enable the transport of FITC-dextran into cells. These phenomena were not observed for polyplexes of p(ABOL). No colocalization with FITC-dextran is observed, giving evidence that the p(ABOL/2AMPBA)-FITC colocalization is due to binding of the boronic acid moieties with dextran.

6.5 References

- [1] E. Wagner, J. Kloeckner, Gene delivery using polymer therapeutics, *Adv. Polym. Sci.*, 192 (2006) 135-173.
- [2] S.Y. Wong, J.M. Pelet, D. Putnam, Polymer systems for gene delivery-past, present, and future, *Prog. Polym. Sci.*, 32 (2007) 799-837.
- [3] I.M. Verma, N. Somia, Gene therapy - promises, problems and prospects, *Nature*, 389 (1997) 239-242.
- [4] K.A. Mislick, J.D. Baldeschwieler, Evidence for the role of proteoglycans in cation-mediated gene transfer, *P. Natl. Acad. Sci. USA*, 93 (1996) 12349-12354.
- [5] S.S. Davis, L. Illum, Polymeric Microspheres as Drug Carriers, *Biomaterials*, 9 (1988) 111-115.
- [6] C. Plank, K. Mechtler, F.C. Szoka, E. Wagner, Activation of the complement system by synthetic DNA complexes: A potential barrier for intravenous gene delivery, *Hum. Gene Ther.*, 7 (1996) 1437-1446.
- [7] Z. Liu, Z. Zhang, C. Zhou, Y. Jiao, Hydrophobic modifications of cationic polymers for gene delivery, *Progr. Pol. Sci.*, 35 (2010) 1144-1162.
- [8] L. Illum, I.M. Hunneyball, S.S. Davis, The effect of hydrophilic coatings on the uptake of colloidal particles by the liver and by peritoneal-macrophages, *Int. J. Pharm.*, 29 (1986) 53-65.
- [9] H. Otsuka, Y. Nagasaki, K. Kataoka, PEGylated nanoparticles for biological and pharmaceutical applications, *Adv. Drug Delivery Rev.*, 55 (2003) 403-419.
- [10] A.V. Kabanov, Taking polycation gene delivery systems from in vitro to in vivo, *Pharm. Sci. Technol. To.*, 2 (1999) 365-372.
- [11] H. Petersen, P.M. Fechner, A.L. Martin, K. Kunath, S. Stolnik, C.J. Roberts, D. Fischer, M.C. Davies, T. Kissel, Polyethylenimine-graft-poly(ethylene glycol) copolymers: Influence of copolymer block structure on DNA complexation and biological activities as gene delivery system, *Bioconjugate Chem.*, 13 (2002) 845-854.
- [12] S.R. Mao, M. Neu, O. Germershaus, O. Merkel, J. Sitterberg, U. Bakowsky, T. Kissel, Influence of polyethylene glycol chain length on the physicochemical and biological properties of poly(ethylene imine)-graft-poly(ethylene glycol) block copolymer/SiRNA polyplexes, *Bioconjugate Chem.*, 17 (2006) 1209-1218.
- [13] R.S. Burke, S.H. Pun, Extracellular barriers to in vivo PEI and PEGylated PEI polyplex-mediated gene delivery to the liver, *Bioconjugate Chem.*, 19 (2008) 693-704.
- [14] L. Illum, N.W. Thomas, S.S. Davis, Effect of a selected suppression of the reticuloendothelial system on the distribution of model carrier particles, *J. Pharm. Sci.*, 75 (1986) 16-22.
- [15] N. Fujita, S. Shinkai, T.D. James, Boronic acids in molecular self-assembly, *Chem-Asian J.*, 3 (2008) 1076-1091.
- [16] D.G. Hall, *Boronic Acids - Preparation and applications in organic synthesis and medicine*, John Wiley & Sons, 2005.
- [17] J. Yan, G. Springsteen, S. Deeter, B.H. Wang, The relationship among pK(a), pH, and binding constants in the interactions between boronic acids and diols - it is not as simple as it appears, *Tetrahedron*, 60 (2004) 11205-11209.
- [18] D.S. Matteson, Boronic esters in stereodirected synthesis, *Tetrahedron*, 45 (1989) 1859-1885.
- [19] H.R. Mulla, N.J. Agard, A. Basu, 3-methoxycarbonyl-5-nitrophenyl boronic acid: high affinity diol recognition at neutral pH, *Bioorg. Med. Chem. Lett.*, 14 (2004) 25-27.
- [20] T.D. James, S. Shinkai, Artificial receptors as chemosensors for carbohydrates, *Top. Curr. Chem.*, 218 (2002) 159-200.
- [21] B. Appleton, T.D. Gibson, Detection of total sugar concentration using photoinduced electron transfer materials: development of operationally stable, reusable optical sensors, *Sensor Actuat. B-Chem.*, 65 (2000) 302-304.
- [22] T. Hoare, R. Pelton, Engineering glucose swelling responses in poly(N-isopropylacrylamide)-based microgels, *Macromolecules*, 40 (2007) 670-678.
- [23] H. Kitano, M. Kuwayama, N. Kanayama, K. Ohno, Interfacial recognition of sugars by novel boronic acid-carrying amphiphiles prepared with a lipophilic radical initiator, *Langmuir*, 14 (1998) 165-170.
- [24] A. Matsumoto, S. Ikeda, A. Harada, K. Kataoka, Glucose-responsive polymer bearing a novel phenylborate derivative as a glucose-sensing moiety operating at physiological pH conditions, *Biomacromolecules*, 4 (2003) 1410-1416.

- [25] M. Di Luccio, B.D. Smith, T. Kida, C.P. Borges, T.L.M. Alves, Separation of fructose from a mixture of sugars using supported liquid membranes, *J. Membrane Sci.*, 174 (2000) 217-224.
- [26] S.H. Gao, W. Wang, B.H. Wang, Building fluorescent sensors for carbohydrates using template-directed polymerizations, *Bioorg. Chem.*, 29 (2001) 308-320.
- [27] C. Lin, Z.Y. Zhong, M.C. Lok, X.L. Jiang, W.E. Hennink, J. Feijen, J.F.J. Engbersen, Novel bioreducible poly(amido amine)s for highly efficient gene delivery, *Bioconjugate Chem.*, 18 (2007) 138-145.
- [28] M. Piest, J.F.J. Engbersen, Boronic acid functionalized disulfide containing poly(amido amine) with improved polyplex stability for pDNA and siRNA delivery in vitro, See chapter 4 of this thesis, (2010).
- [29] E. Lavenius, C. Gestblom, I. Johansson, E. Nanberg, S. Pahlman, Transfection of Trk-a into human neuroblastoma-cells restores their ability to differentiate in response to nerve growth-factor, *Cell Growth Differ.*, 6 (1995) 727-736.
- [30] R.R. Smith, E.R. Dimayuga, J.N. Keller, W.F. Maragos, Enhanced toxicity to the catecholamine tyramine in polyglutamine transfected SH-SY5Y cells, *Neurochem. Res.*, 30 (2005) 527-531.
- [31] P.R. Westmark, H.C. Shin, C.J. Westmark, S.R. Soltaninassab, E.K. Reinke, J.S. Malter, Decoy mRNAs reduce beta-amyloid precursor protein mRNA in neuronal cells, *Neurobiol Aging*, 27 (2006) 787-796.
- [32] G.J. Doherty, H.T. McMahon, Mechanisms of endocytosis, *Annu. Rev. Biochem.*, 78 (2009) 857-902.
- [33] G. Sahay, D.Y. Alakhova, A.V. Kabanov, Endocytosis of nanomedicines, *J. Control. Release*, 145 (2010) 182-195.
- [34] D. Vercauteren, M. Piest, L.J. van der Aa, M. Al Soraj, A.T. Jones, J.F.J. Engbersen, S.C. De Smedt, K. Braeckmans, Flotillin-dependent endocytosis and a phagocytosis-like mechanism for cellular internalization of disulfide-based poly(amido amine)/DNA polyplexes, 32 (2011) 3072-3084.

Boronic acid functionalized poly(amido amine)s form bioresponsive, restructuring hydrogels with poly(vinyl alcohol) by reversible covalent crosslinking



Abstract

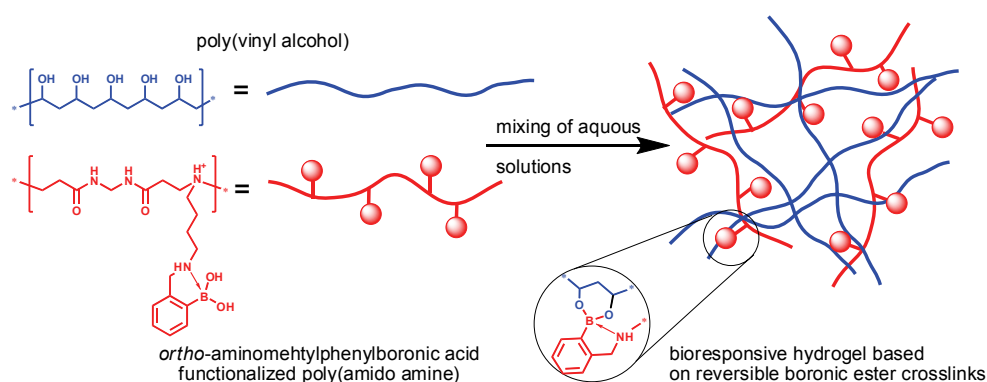
A water-soluble poly(amido amine) (PAA) with a high density of *ortho*-aminomethyl substituted phenylboronic acids was developed. Due to the possibility of a dative B–N interaction, the pK_a value of the *ortho*-aminomethylphenylboronic acid is significantly reduced and diol complexation is facilitated at lower pH. The boronated PAA readily formed dynamically restructuring strong hydrogels by reversible covalent crosslinking with poly(vinyl alcohol) (PVA) already at low concentrations of 5–10% w/v, with gel strengths G'_{\max} up to 20 kPa, whereas the non-boronated control PAA did not form a gel. The formed gels were transparent, thermoresponsive and this response to temperature changes was instantaneous and completely reversible. These dynamically crosslinked hydrogels have self-healing capacities and slowly degrade in a large excess of water within several hours, which make them suitable for controlled drug delivery applications. Addition of D-glucose solutions to these gels resulted in a significant increase of the degradation rate as a function of glucose concentration. The pH-, thermo-, and glucose-responsive behaviors of these types of gel systems render them ideal candidates for development of new glucose-responsive controlled drug delivery devices.

7.1 Introduction

Poly(amido amine)s (PAAs) are an interesting class of polymers with peptide-mimicking structures, due to the repetitive amide bonds in their main chain [1-2]. Their biodegradability, water-solubility and biocompatibility, and generally low cytotoxicity and low hemolytic activity are all factors that make them ideal for application as biomaterials [3]. The versatile synthesis by Michael-type addition polymerization of primary or secondary aliphatic amines to bisacrylamides allows for great structural variation [4-8]. For example, water-soluble PAAs have been designed with potential for use as polymeric drugs and polymer drug carriers [1-2]. In addition, pH-responsive PAAs show potential as non-viral vectors, as their endosomolytic characteristics enable the cytoplasmic delivery of genes and proteins [8-11]. PAA hydrogels are not often described in literature. They can be synthesized by using multifunctional aminomonomers in the Michael addition polymerization with bisacrylamides, resulting in network formation as has been exemplified by Ferutti *et al.* using primary bisamines as crosslinkers [12-15]. Typically, PAA hydrogels with a modest degree of crosslinking can absorb great amounts of water and show significant swelling behavior [16-17]. These PAA hydrogels have been studied predominantly by Ferutti's group as synthetic materials for cell culturing and tissue engineering [13-15, 18]. The field of applications for PAA hydrogels has still to be explored, as PAAs have possibilities to adjust and optimize the properties for specific purposes by the incorporation of a diversity of chemical functionalities.

Incorporation of boronic acid moieties in PAAs is of particular interest to introduce specific interactions with biological substrates, as boronic acids are known to rapidly and reversibly interact with dicarboxylic acids, α -hydroxy carboxylic acids and diols to form boronic esters in aqueous media [19]. We have recently developed a number of PAAs with disulfide groups in the main chain and boronic acid groups in the side chain (SS-PAAs) in order to study the effect of the presence of boronic acids in these polymers on their properties as gene delivery vectors [20-21]. We have demonstrated that boronated SS-PAAs can be used for drug delivery and combined drug and gene delivery [22]. The most common interactions of boronic acids are with 1,2- and 1,3-diols to form five- and six-membered rings, respectively [19, 23]. In this work we have specifically focused on the interaction of boronic acid functionalized PAAs with poly(vinyl alcohol) (PVA) as the reversible cross-linking of these PAAs with PVA results in a new class of bioresponsive hydrogels [24-25]. Since the structure of the PAAs allows large variation, these hydrogels may have high potential for biomedical application, especially in the field of controlled release of bioactive agents [26-27]. Since the parent phenylboronic acid compound forms stable boronic esters with diol functions only at relatively high pH (typically pH > 7.5) [23] we searched for a phenylboronic acid derivative that gives good binding with diol moieties at

physiological pH. To this purpose we identified the phenylboronic acid possessing an *ortho*-aminomethyl group as being a suitable compound to be incorporated in the PAAs. The *ortho*-aminomethyl group forms dative B–N (or N→B) interaction, which reduces the boronic acid pK_a by several units and strongly promotes boronic ester formation with the vicinal 1,3 diols of PVA at reduced pH. [28]. A conceptual overview of the crosslinking and formation of a PAA-PVA hydrogel is given in Scheme 7.1.



Scheme 7.1. Conceptual overview of a bioresponsive hydrogels based on the reversible crosslinking of poly(vinyl alcohol) by an *ortho*-aminophenylboronic acid containing poly(amido amine).

For the synthesis of the *ortho*-aminomethylphenylboronic acid containing poly(amido amine), we have developed the boronic acid containing monomer 2-((4-aminobutylamino)methyl)phenylboronic acid (M1, Scheme 7.3) by the reductive amination reaction of *ortho*-formylphenylboronic acid with N-BOC-diaminobutane, and subsequent deprotection with HCl (g) [20]. The resulting water-soluble monomer M1 possesses a primary amino group that is reactive in the Michael addition polymerization with *N,N'*-methylenebisacrylamide. As the secondary methylamino group in the *ortho*-position forms an *intra*-molecular B–N interaction and the bulky phenylboronic acid provides steric hindrance, branching is not occurring during this polymerization [20]. A nonboronated control PAA with benzyl moieties was prepared by Schiff condensation of benzaldehyde to a parent polymer p(MBA-DAB) prepared by Michael addition polymerization of methylene bisacrylamide and N-BOC-diaminobutane followed by deprotection of the BOC-protected aminobutyl side chains.

7.2. Materials and methods

N-BOC-1,4-diaminobutane (BOC-DAB, Aldrich), benzaldehyde (Aldrich), 2-formylphenylboronic acid (2-FPBA, Aldrich), 4-formylphenylboronic acid (4-FPBA, Aldrich), N,N'-methylene bisacrylamide (MBA, Aldrich), triethylamine (TEA, Aldrich), sodium borohydride (NaBH₄, Aldrich), poly(vinyl alcohol) (PVA, M_w 27, 47, 125, 195 kDa, Aldrich, 72 kDa, Merck), and D-glucose (Aldrich) were purchased in the highest purity and used without further purification.

NMR spectra were recorded on a Varian Unity 300 (¹H NMR 300 MHz) using the solvent residual peak as the internal standard.

7.2.1. Synthesis of monomer M1

The boronated monomer 2-((4-aminobutylamino)methyl)phenylboronic acid (monomer M1) was synthesized by reductive amination of 2-formylphenylboronic acid (3.92 g, 25.4 mmol) with N-BOC-1,4-diaminobutane (4.92 g, 25.4 mmol) in 20 ml methanol. The solution was stirred overnight under nitrogen at ambient temperature, during which the mixture turned dark yellow. ¹H NMR confirmed the formation of the Schiff base. Next, 1.6 equivalents NaBH₄ (1.56 g, 40.8 mmol) were added to the reaction mixture and the solution turned colorless. After 1 h no hydrogen gas evolution was observed anymore and the solvent was removed to dryness. The residue was dissolved in 75 ml MilliQ water and 5 times extracted with 75 ml dichloromethane. The organic layer was dried over MgSO₄ and evaporated under reduced pressure. The product was an off-white solid (7.50 g, 92% yield) and ¹H NMR showed complete reduction of the Schiff base. The BOC-protected product was dissolved in 30 ml of methanol and deprotected by perfusion of HCl-gas through the reaction mixture for 30 min at ambient temperature. The solvent was evaporated to dryness and the HCl-salt of the deprotected boronic acid monomer was obtained as a sticky off-white powder (6.65 g, 89% yield) and ¹H NMR showed complete deprotection.

¹H NMR (HCl salt, CD₃OD): 1.71–1.88 (m, –CH₂–CH₂–CH₂–), 1.71–1.88 (m, –CH₂–CH₂–CH₂–), 2.97 (t, –CH₂–CH₂–NH₃⁺), 3.11 (t, –NH–CH₂–CH₂–), 4.28 (s, –NH–CH₂–Ar), 7.40–7.50 (m, Ar(3 H)), 7.70–7.80 (m, Ar(1 H)). 1.40 (s, –CH₂–CH₂–NH₃⁺), 1.44–1.54 (m, –CH₂–CH₂–CH₂–), 1.65–1.75 (m, –CH₂–CH₂–CH₂–), 2.80–2.86 (t, –NH–CH₂–CH₂–), 3.02–3.08 (t, –NH–CH₂–CH₂–), 3.97 (s, –NH–CH₂–Ar), 7.09–7.19 (m, Ar(3 H)), 7.39–7.41 (m, Ar(1 H)).

The product was dissolved in MilliQ water and the pH was adjusted to 11 with 1M NaOH. Evaporation of the solution under reduced pressure yielded a mixture of salt (NaCl) and the product (free amine). The residue was suspended in DCM, dried with NaSO₄ after which the salts were filtered-off. Next, the clear solution was evaporated *in vacuo* resulting in a sticky off-white solid (ca 60% recovery).

^1H NMR (free amine, CD_3OD): 1.44–1.54 (m, $-\text{CH}_2-\text{CH}_2-\text{CH}_2-$), 1.65–1.75 (m, $-\text{CH}_2-\text{CH}_2-\text{CH}_2-$), 2.63–2.69 (t, $\text{NH}_2-\text{CH}_2-\text{CH}_2-$), 2.80–2.85 (t, $-\text{NH}-\text{CH}_2-\text{CH}_2-$), 3.97 (s, $-\text{NH}-\text{CH}_2-\text{Ar}$), 7.09–7.19 (m, Ar(3 *H*)), 7.39–7.41 (m, Ar(1 *H*)). Purity was 86% using *p*-toluenesulfonic acid as internal standard. The remainder was bound solvent (water or methanol).

7.2.2. Synthesis of p(MBA-2AMPBA)

$\text{N,N}'$ -methylene bisacrylamide (2.98 g, 19 mmol) and the boronated monomer M1 as the free amine (4.94 g, 19 mmol) were dissolved in 9.5 ml of 2/3 v/v methanol/water mixture. The reaction was left to proceed overnight at 45 °C under argon-atmosphere, during which the solution became to viscous to stir. 5.0 ml methanol/deionized water (2/3, v/v) was added and the polymerization proceeded overnight until the solution was very viscous again. Subsequently, 17 mol% excess (0.85 g, 3.3 mmol) of the boronated monomer dissolved in 2 ml deionized water was added to end-cap unreacted acrylates for two days. The polymer was purified using an ultrafiltration membrane ($M_w\text{CO}$ 1000 Da) with deionized water (pH ~ 5). After freeze-drying, p(MBA-2AMPBA) was collected as an off-white foam-like material. Yield: (4.30 g, 50%).

^1H NMR (p(MBA-2AMPBA), HCl salt, D_2O , 300 MHz):

δ 7.7–7.8 (1H, m, Ar*H*), δ = 7.4–7.5 (3H, m, Ar*H*), δ = 4.55 (2H, s, $\text{CONH}-\text{CH}_2-\text{NHCO}$), δ = 4.2–4.4 (2H, m, ArH- CH_2-NH), δ = 3.45 (4H, t, $\text{NHCO}-\text{CH}_2-\text{CH}_2-\text{N}$), δ = 3.25 (2H, t, $\text{NHCO}-\text{CH}_2-\text{CH}_2)_2-\text{N}-\text{CH}_2$), δ = 3.10 (2H, t, ArH- $\text{CH}_2-\text{NH}-\text{CH}_2$), δ = 2.75 (4H, t, $\text{N}-\text{CH}_2-\text{CH}_2-\text{CONH}$), δ = 1.75 (4H, m, $\text{N}-\text{CH}_2-\text{CH}_2-\text{CH}_2-\text{CH}_2-\text{NH}$)

7.2.3. Synthesis of the non-boronated control p(MBA-Bz)

The parent p(MBA-DAB) was synthesized by the Michael addition polymerization of N-BOC-1,4-diaminobutane (4.37 g, 22.5 mmol) to methylene bisacrylamide (MBA) (3.5 g, 22.5 mmol) in methanol/water (11.6 ml, 1/1, v/v). The reaction mixture was homogeneous after 10 min at 45 °C and the polymerization was left to proceed for 7 days at 45 °C in the dark under nitrogen atmosphere, until the solution had become viscous. Subsequently, 12 mol% excess (0.52 g, 2.68 mmol) of N-BOC-1,4-diaminobutane in 3.6 ml methanol/deionized water (1/1, v/v) was added to end-cap unreacted acrylates for another 3 days. The polymer solution was then purified using an ultrafiltration membrane ($M_w\text{CO}$ 3000 Da). After freeze-drying, p(MBA-BOC-DAB) was collected as a white foam-like material. The isolated yield was 46% (3.65 g) and the structural composition was confirmed with ^1H NMR (D_2O , 300 MHz).

^1H NMR (D_2O , 300 MHz): δ = 4.4 (2H, s, $\text{CONH}-\text{CH}_2-\text{NHCO}$), δ = 3.3 (4H, t, $\text{CONH}-\text{CH}_2-\text{CH}_2-\text{N}$), δ = 3.1 (2H, t, $\text{CONH}-\text{CH}_2-\text{CH}_2)_2-\text{N}-\text{CH}_2-$), δ = 2.6 (4H, t,

N-CH₂-CH₂-CONH), $\delta = 1.6$ (2H, t, N-CH₂-CH₂-CH₂-CH₂-NH), $\delta = 1.4$ (2H, t, N-CH₂-CH₂-CH₂-CH₂-NHCO), $\delta = 1.2$ (9H, s, NHCO-O-C(CH₃)₃)

For the deprotection of the parent polymer, 3.65 g of p(MBA-BOC-DAB) was dissolved in methanol (100 ml) and perfused with HCl (g) for 1 h after which ¹H NMR showed that deprotection was complete. The solvent was evaporated and the residue dried *in vacuo* for 2 days. The HCl-salt of the deprotected polymer p(MBA-DAB) was obtained as a white powder and stored in the freezer after drying.

Polymer p(MBA-Bn) was synthesized by post-modification of the deprotected parent polymer using benzaldehyde. To this purpose, 0.85 g (3.5 mmol of the repeating unit) of the HCl salt of the deprotected parent polymer was dissolved in methanol (20 ml) and an excess of 1.1 equivalents of triethylamine (0.40 g, 4.0 mmol) was added to deprotonate the (primary) amines of the polymer. Excess of benzaldehyde (0.88 g, 8.25 mmol) was added to the polymer solution. The reaction mixture was stirred at ambient temperature under nitrogen atmosphere. The reaction was allowed to proceed for two days, during which the reaction mixture turned turbid and a yellow darkening was observed, which indicated the formation of the Schiff base. Reduction of the Schiff bases occurred through the portion-wise addition of excess of NaBH₄ (0.38 g, 10 mmol) to the solution, and the reaction mixture became a clear solution again. The solvent was removed by rotary evaporation under reduced pressure, and subsequently deionized water was added to the polymer mixtures, resulting in a suspension. The pH was adjusted to approximately 5 with aqueous HCl (4 M) until the turbid suspension became a clear solution and some remaining insoluble material was removed by vacuum filtration. The filtrates were then purified using an ultrafiltration membrane (M_wCO 1000 Da) with deionized water (pH ~ 5). The product p(MBA-Bn) was isolated after freeze-drying as a white solid material (0.60 g, 52% yield).

¹H NMR (p(MBA-Bn), HCl salt, D₂O 300 MHz):

$\delta = 7.4\text{--}7.8$ (5H, m, ArH), $\delta = 4.55$ (2H, s, CONH-CH₂-NHCO), $\delta = 4.2$ (2H, s, ArH-CH₂-NH); $\delta = 3.4$ (4H, t, NHCO-CH₂-CH₂-N), $\delta = 3.15$ (2H, t, NHCO-CH₂-CH₂)₂-N-CH₂), $\delta = 3.08$ (2H, t, ArH-CH₂-NH-CH₂), $\delta = 2.75$ (4H, t, N-CH₂-CH₂-CONH), $\delta = 1.75$ (4H, m, N-CH₂-CH₂-CH₂-CH₂-NH)

7.2.4. Acid-base titration of the polymers and the monomer M1

For the polymer p(MBA-2AMPBA), the non-boronated control polymer p(MBA-Bn), and the boronic acid monomer M1 in their HCl-salt form, known amounts (corresponding to *ca.* 0.50 mMol amino nitrogen atoms) were dissolved in 10 ml of 150 mM NaCl (aq) that was degassed and subsequently saturated with N₂ (g) prior to use. All solutions were adjusted to pH < 3 and then titrated with 0.1M NaOH by using an automatic titrator (Metrohm 702 SM Titrino). The pK_a values were determined from the titration curves.

7.2.5. Gel preparation

Solutions with different concentrations of poly(vinyl alcohol) ($M_w = 27, 47, 72, 125$ and 195 kDa) were prepared by dissolving the PVA in deionized water at $80\text{ }^\circ\text{C}$ to obtain stock solutions of 10% w/v that were diluted (10%, 7.5%, 5%, 2.5% w/v). Stock solutions of p(MBA-2AMPBA) (10%, 7.5%, 5%, 2.5% w/v) were also prepared by dissolving the polymer in deionized water followed by dilution. The pH of each polymer stock solutions was measured and if necessary adjusted with a few drops of monovalent strong acid (1M HCl (aq)) or base (1 M NaOH (aq)).

Hydrogels were prepared by mixing 0.5 ml of PVA solution with 0.5 ml of PAA solution. Mixing of the solutions occurred in closed vials by 5 s vigorously vortexing. The resultant gels were allowed to equilibrate for at least 48 h at room temperature prior to the measurements.

7.2.6. Characterization of the gels by oscillatory rheology

Rheology experiments were performed on a US 200 Rheometer (Anton Paar). Parallel plates with 25 mm diameter, between which the gels were squeezed with a gap of 1 mm (gel thickness) was used in all experiments. The gels were subjected to oscillating rotational deformations with angular frequencies (ω) from 0.1 to 500 Hz (frequency sweeps) at a strain (γ) of 2%. For each gel a strain sweep from 0.01 to 100% at an angular frequency of 10 Hz was taken afterwards, to determine the linear viscoelastic region, as the frequency sweep should be run in this range. To check the reproducibility samples were prepared in duplo and each sample was measured 2–4 times. Measurements were performed at $25\text{ }^\circ\text{C}$ and for a number of samples also at $37\text{ }^\circ\text{C}$ after temperature equilibration, in order to evaluate the effects of the temperature. Before each new frequency sweep, oscillatory time sweeps at 2% strain and low angular frequency (1 Hz) conditions were performed until the gel was stabilized (constant value of the storage and loss modulus in time). To minimize evaporation of water from the gel, a thin layer of silicon oil was applied on top. From each frequency sweep a crossover frequency (ω_c) was determined at the angular frequency where $G' = G''$. From this crossover frequency the characteristic relaxation time (τ) could be calculated, with the formula:

$$\tau = 2\pi/\omega_c.$$

Another characteristic value that was obtained from the frequency sweep is the plateau value of the storage modulus (G'_{max}) at high frequencies.

7.2.7. Thermo-reversibility of the gels

Gel was prepared by mixing of a solution of p(MBA-2AMPBA) (5% w/v) and PVA (195 kDa, 7.5% w/v) 48 h prior to the oscillatory rheology experiments. A strain sweep at 25 °C (10 Hz) showed a constant gel strength of *ca.* 2100 Pa and frequency sweeps at 25 °C and 37 °C showed relaxation times of 0.59 s and 0.32 s and G'_{\max} of 3550 Pa and 3400 Pa, respectively. Next, the gel was continuously measured during alternating 30 min intervals at 25 °C and 37 °C at 2% strain and 10 Hz.

7.2.8. Swelling and degradation of the gels

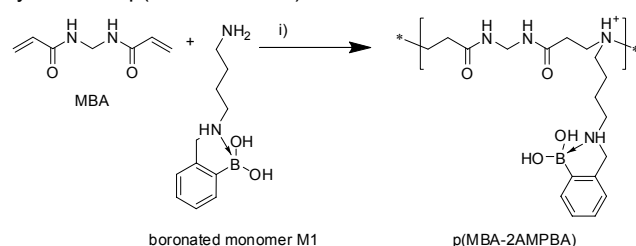
For swelling and degradation tests, gels were prepared by mixing of a solution of p(MBA-2AMPBA) (5 %w/v) and PVA (195 kDa, 7.5 % w/v) at pH ~ 5. The resultant gels were allowed to equilibrate for at least 48 h at room temperature before the gels were transferred into empty vials of known weight and the initial weight of the gels were determined ($t = 0$). Aqueous glucose solutions (10 ml) of four different concentrations (0 %, 2.5 %, 5 %, and 10 % w/v) were put on top of the gels. The gels were stored at ambient temperature, and after decantation of the supernatant the remaining gels were weighed. This procedure was repeated at regular time intervals in which fresh solutions were added to the gels after each weighing. The swelling ratio is defined as the weight of the swollen gel (W_t) after time t (1 h 15 min, 4 h and 7 h 45 min, respectively) divided by the initial weight of the gel at $t = 0$ (W_0).

7.3. Results

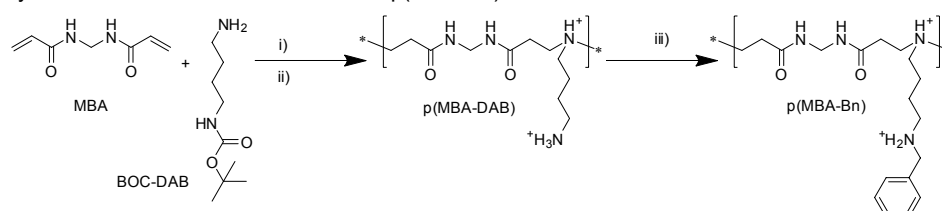
7.3.1. Boronic acid polymer synthesis

The polymer p(MBA-2AMPBA) with the aminomethyl group in the *ortho*-position with respect to the boronic acid was synthesized by Michael addition polymerization of the boronic acid containing monomer M1 with MBA. The non-boronated control polymer p(MBA-Bn) was synthesized by *post*-modification of the parent polymer p(MBA-DAB) with pending aminobutyl side chains, originating from Michael addition polymerization of methylene bisacrylamide (MBA) with N-BOC-1,4-diaminobutane followed by deprotection of the amines. The pending free amines were functionalized by reduction of the Schiff base formed with benzaldehyde. A synthetic overview is given in Scheme 7.2.

Synthesis of p(MBA-2AMPBA)



Synthesis of the non-boronated control p(MBA-Bn)

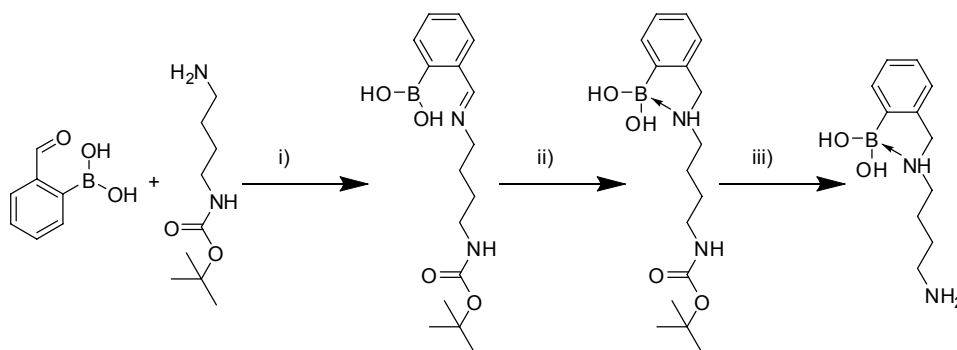


Scheme 7.2. Synthesis of boronic acid containing poly(amido amine)s by direct polymerization of the boronated monomer or by *post*-modification of p(MBA-DAB). i) Michael addition polymerization in water/methanol at 45 °C under nitrogen atmosphere in the dark. ii) Deprotection with HCl (g) in methanol. iii) Schiff base formation with benzaldehyde in methanol followed by reduction with NaBH₄.

The direct polymerization of the boronated monomer M1 with a bisacrylamide is most straightforward and avoids multiple synthesis steps. To this purpose a boronic acid containing monomer was synthesized by reductive amination of 2-formylphenyl boronic acid (2-FPBA) and N-BOC-1,4-diaminobutane (BOC-DAB), followed by deprotection of the BOC-protected monomer, as illustrated in Scheme 7.3.

Formation of the Schiff base was confirmed by ¹H NMR as no aldehyde peaks were observed in the spectrum of the reaction mixture after reacting overnight, indicating a complete conversion of the reactants. Formation of Schiff base was

accompanied by a color change from yellowish to dark orange that was already visible after several minutes. The reaction mixture turned colorless again after reduction. The BOC-protected form of the monomer was also characterized by ^1H NMR and found to be pure. The compound was highly soluble in methanol and DCM, but insoluble in water. Removal of the BOC-protecting group via HCl (g) was complete within one hour according to ^1H NMR as the characteristic *tert*-butyl signal (singlet) at 1.40 ppm had completely disappeared. The HCl -salt of the monomer was soluble in methanol and water. Additional extraction from a basic solution with DCM was performed to obtain the monomer as free base and the deprotonated primary amine was soluble in water, methanol, and DCM. The purity was determined at 86% via ^1H NMR using *p*-toluenesulfonate as internal standard and the remainder was bound solvent (mono- and di methoxy boronate ester and/or a bound molecule of water).



Scheme 7.3. Synthesis of boronic acid monomer M1. i) Schiff base formation with 2-FPBA and BOC-DAB in methanol at RT. ii) Reduction with NaBH_4 in methanol. iii) Deprotection with HCl -gas in methanol, thereby yielding the HCl -salt, that was converted to the free amine with NaOH (aq) and isolated from DCM.

This monomer was used in Michael addition polymerization with MBA to obtain p(MBA-2AMPBA) in a mixture of 1/1 v/v methanol/water. This direct polymerization proceeded very rapidly, within a few hours the viscosity of the polymer solution had dramatically increased, indicating the formation of high M_w polymers. The polymer was obtained after freeze drying with a yield of 50% and was highly soluble in water and methanol, resulting in viscous solutions at concentrations of 10% (w/v) in water. Since the polymerization was terminated by adding excess of M1 the ^1H NMR spectrum of p(MBA-2AMPBA) did not show any sign of unreacted acrylates, see Figure 7.1. The characteristic peak of $\text{Ar-CH}_2\text{-NH-}$, present as a triplet at 4.0–4.2 ppm, was found to shift *ca.* 0.1–0.2 ppm depending on the degree of protonation. In theory, the presence of the secondary amine in the boronic acid monomer could also participate in the polymerization, resulting in a branched structure. Since no additional peaks of branched structures are visible in the ^1H NMR spectrum

of p(MBA-2AMPBA), it can be concluded that the primary amine of the boronated monomer was the only nucleophile (Michael donor) in the Michael-type polymerization. The formation of a dative B–N bond reduces the nucleophilicity of the secondary amine and in combination with the steric hindrance of the phenylboronic acid group, reaction with MBA is prevented. GPC analysis of this polymer was unsuccessful. Alternatively, M_w was estimated by ^1H NMR, by comparing the proton integration of the methylene bisacrylamide peak ($\text{CONH-CH}_2\text{-NHCO}$) with the proton integration of the aminobutyl side chain ($-\text{N-CH}_2\text{-CH}_2\text{-CH}_2\text{-CH}_2\text{-NH-}$), yielding the stoichiometric ratio of the MBA units versus the butylamine units. As the polymer is end-capped with the butylamine-containing M1 monomer, from the stoichiometric unbalance in the polymer M_w can be calculated by the equation $n = 1/x$, with n being the number of repeating units and x the excess of amine units over bisacrylate units. From this the number of repeating units n was estimated to be *ca.* 11.8, corresponding with a M_w of *ca.* 4860 g/mol.

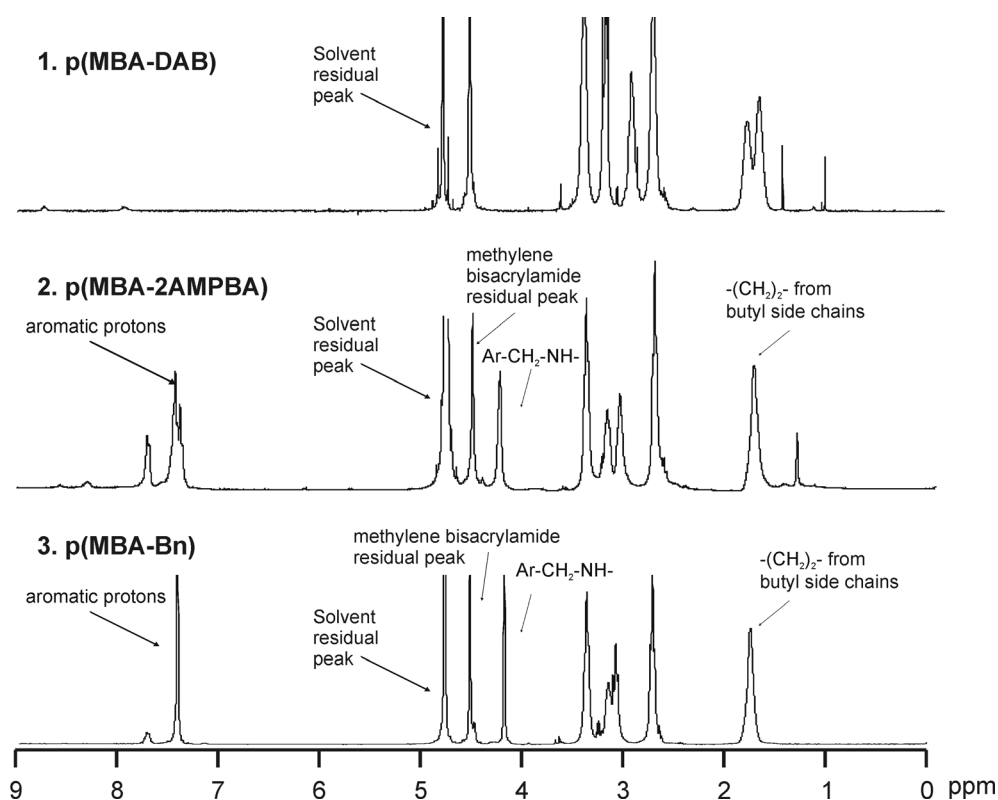


Figure 7.1. ^1H NMR spectra of the parent p(MBA-DAB) (line 1), p(MBA-2AMPBA) (line 2) and the non-boronated control p(MBA-Bn) (line 3).

For the reference polymer prepared by post-modification, p(MBA-BOC-DAB) was synthesized first by the Michael addition of BOC-DAB to MBA and termination of the polymerization reaction by addition of excess of BOC-DAB resulted in a polymer that did not contain any acrylate end-groups, as was confirmed by ^1H NMR. By reaction of HCl (g) with the BOC-protected amines, the removal of the BOC-protecting groups was completed after reaction according to ^1H NMR. The M_w was estimated to be 3600 g/mol from proton integration of the methylene protons from MBA compared to the methylene protons of the butyl side chains. The reductive amination of the pending aminobutyl side chains with the benzaldehyde was monitored by ^1H NMR, and complete conversion of the primary amines to imines (Schiff base) was observed after two days. The polymer formed a white suspension that redissolved after the reduction with NaBH_4 . The polymer was isolated in good yield after dialysis and freeze-drying (Table 7.1). A complete functionalization of the pending aminobutyl amines was confirmed by proton integration of the ^1H NMR spectra (Figure 7.1). The polymers p(MBA-2AMPBA) and p(MBA-Bn) in their HCl-salt form (ultrafiltrated at pH \sim 5) were well soluble in water and methanol.

The number of repeating units n was estimated to be *ca.* 9–10, corresponding with a M_w of *ca.* 3760 g/mol for p(MBA-Bn), which is slightly lower compared to the M_w of *ca.* 4860 g/mol for p(MBA-2AMPBA), see Table 7.1.

Table 7.1. Synthetic yield and M_w of the polymers.

Polymer	Yield (%)	# repeating units ^a	M_w repeating unit ^b	Average M_w (g/mol)
p(MBA-2AMPBA)	50	11.8	412.72	4860
p(MBA-Bn)	52	9.3	404.17	3760

^a Determined with ^1H NMR by proton integration.

^b Polymer was isolated as HCl-salt after ultrafiltration

7.3.2. Acid-base titration of the polymers

The boronic acid functionalized poly(amido amine)s were subjected to acid-base titration in order to determine the pK_a -values of the amines and boronic acid moieties in the polymer. For comparison, also the monomer M1 was included in the measurements and the results are shown in Figure 7.2.

For the boronic acid monomer M1 two distinct plateaus can be observed, corresponding with two pK_a values. The first pK_a at 5.1 is matching the proton dissociation constant of the nitrogen atom that is involved in the formation of the dative B–N bond [28]. The second pK_a observed at 10.3 is matching to the pK_a of the primary amine [11].

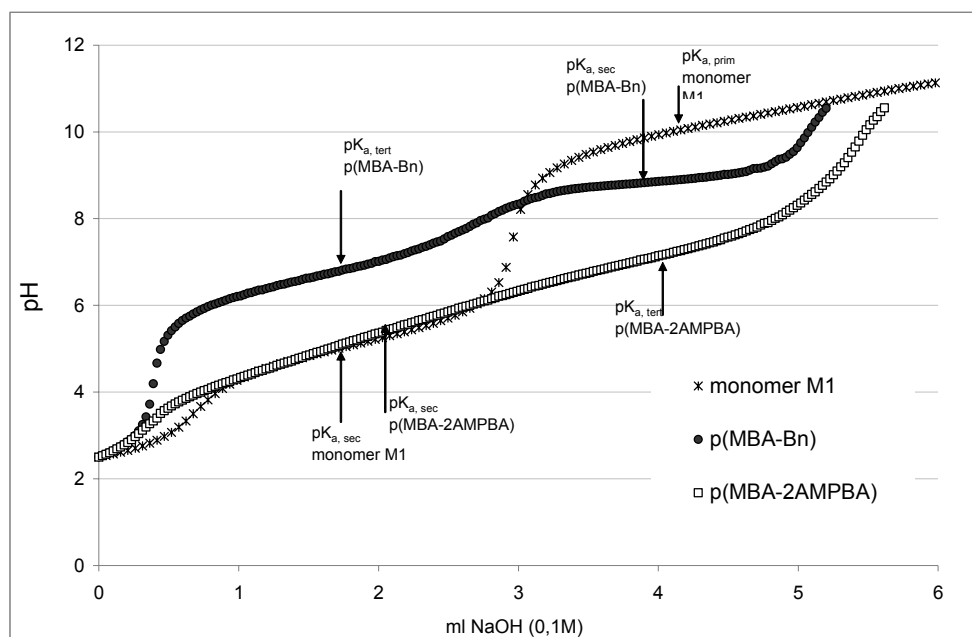


Figure 7.2. pH profile upon addition of 0.1 M NaOH to 10 ml solution of monomer M1 (0.25 mMol) in 150 mM NaCl, and solutions of polymer p(MBA-2AMPBA), and the non-boronated control p(MBA-Bn) dissolved in 150 mM NaCl (aq) (0.25 mMol polymer repeating unit).

Both polymers are derivatives of p(MBA-DAB) and therefore have an identical polymer backbone comprising tertiary amino groups in the main chain. Differences in pH profile are due to the different functional groups introduced at the aminobutyl side chains. The titration curve of the non-boronated polymer p(MBA-Bn) shows two distinct plateaus. The pK_a of ca. 6.7 can be attributed to the proton dissociation of the tertiary amines in the backbone, and this value is in accordance with the value earlier found for similar SS-PAAAs [8]. The second pK_a value at ca. 8.8 is originating from the secondary amines of the pendant aminomethylbenzyl moiety.

The polymer p(MBA-2AMPBA) with the *ortho*-aminomethylphenylboronic acid moieties yielded a titration curve with one long plateau. Taking into account that a B–N interaction is possible between pH 5 and 7, the plateau can be regarded as two overlapping parts; the first pK_a can be calculated for the secondary amine participating in the dative B–N bond. This value is 5.1 found for the boronic acid monomer M1. The second part corresponds with the tertiary amines in the polymer backbone with a pK_a value of ca. 6.7. Table 7.2 gives an overview of the pK_a values and the pH at which the polymers start to precipitate.

Table 7.2. pK_a values of the different amines of the PAAs.

Sample	pK _{a, prim}	pK _{a, sec}	pK _{a, tert}	pH* ^a
monomer M1	10.3	5.1	-	-
p(MBA-Bn)	-	8.8	6.7	8.6
p(MBA-2AMPBA)	-	5.1	6.7	7.9

^a The pH at which the polymers start to precipitate at the concentration used during the titration.

7.3.3. Gel formation with boronated PAAs and poly(vinyl alcohol)

Several boronated polymers have demonstrated the capacity of hydrogel formation with different polyols, and predominantly with PVA [24-25, 29]. Therefore, PVA was selected as the ideal candidate as the complexing partner for the boronated PAA polymers as PVA is non-toxic and widely used in the biomedical field due to its biocompatibility [30]. To this purpose p(MBA-2AMPBA) was dissolved in milliQ water to a final concentration at 5% w/v of pH 5. Solutions were mixed 1:1 with 5% w/v 125 kDa PVA yielding a rigid and transparent gel, see Figure 7.3. Notably, the gelation was instantaneous, and the gelation time could not be determined by vial tilting. The dynamic restructuring property of this hydrogel is due to the fast reversible formation of boronate ester crosslinks, which results in self-healing properties of the hydrogel. To demonstrate this self-healing property, the gel was ruptured gel by stirring the homogeneous gel with a spatula. Upon stirring, the gel behaved like a brittle solid, showing high frequency rheological behavior, and was fractured. After 3 hours of standing, the fragmented gel has completely restructured to the original homogenous gel.



Figure 7.3. Self-healing properties of a rigid gel of 5% w/v of p(MBA-2AMPBA) and 1:1 v/v 5% w/v 125 kDa PVA. The time between the left picture and the right picture was three hours. On the left (**A**) a gel is observed that has been milled into pieces. On the right (**B**), after three hours, the same gel has completely restructured.

The very interesting instantaneous gel formation and the self-healing behavior was only observed for p(MBA-2AMPBA), whereas no gel was formed with the non-boronated analog p(MBA-Bn). This points out that gelation is due to the presence of boronic acid moieties in the side chains of the PAA that form reversible covalent boronate esters with the diol moieties of PVA.

7.3.4. Effect of PVA molecular weight and PVA concentration on gel strength

The potential of boronated PAA for crosslinking of PVA was further explored. To this purpose 5% w/v solution of p(MBA-2AMPBA) were mixed 1:1 with different molecular weight 5% w/v solutions of PVA solutions and the transparent gels that were obtained immediately after mixing were subjected to oscillatory rheology measurements. G'_{\max} was determined as the plateau value for the storage modulus at high angular frequencies, while the crossover frequency ω_c , at which $G' = G''$, was used to calculate the relaxation time (τ) according to $\tau = 2\pi/\omega_c$. The results for G'_{\max} and the relaxation time of the different gels are depicted in Figure 7.4.

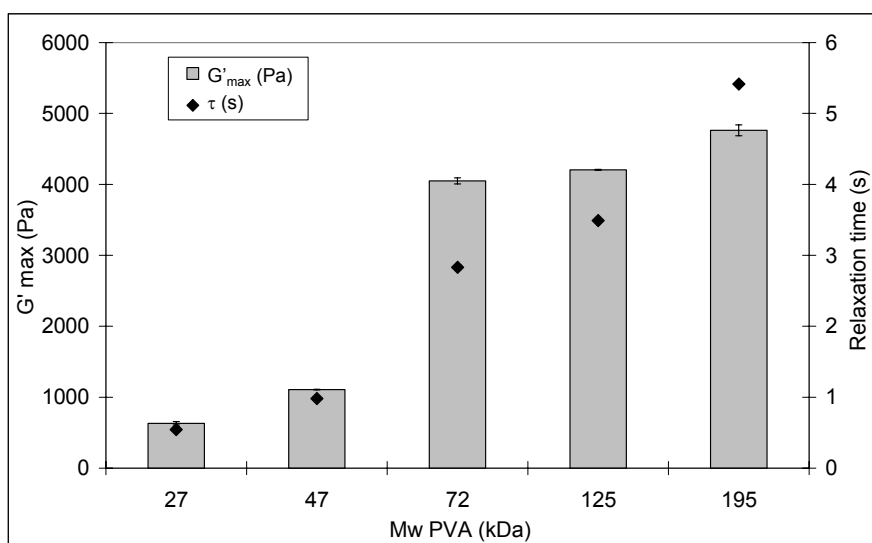


Figure 7.4. Gel strength as a function of M_w of poly(vinyl alcohol) (PVA) of gels from 5% w/v p(MBA-2AMPBA) and 5% w/v PVA. The plateau gel strength G'_{\max} is shown in bars and the relaxation time is shown in diamonds.

It can be observed from Figure 7.4 that the gel strength G'_{\max} (shown in bars) increases with the M_w of PVA used. Notably, p(MBA-2AMPBA) already forms weak gels with 27 kDa PVA and 47 kDa PVA, despite the low PAA and PVA concentrations selected, while stronger gels with G'_{\max} of 4-5 kPa were formed with PVA with M_w of 72 kDa and higher. For these higher M_w PVAs the gel strength only mildly increases from 4050 to 4760 Pa upon increasing the M_w of PVA from 72 kDa to 195 kDa, but the relaxation time τ (shown in diamonds) gradually increases from 3 to 5.4 s.

As G'_{\max} reflects the gel strength at high frequency it can be viewed as a measure for the crosslink density, hence with increasing M_w PVA the crosslink density is leveling off. As the relaxation time reflects the average crosslink lifetime, increasing the M_w of the PVA significantly increases the rigidity or shape-stability of the gel, due to more polymer entanglement. As a result, the viscosity of the gel increases with the chain length of the PVA polymers and the boronate esters in the gel become less mobile. Since the boronate ester formation is a dynamic equilibrium, it is increasingly difficult for the hydrolyzed boronate esters to diffuse apart in a highly viscous medium, explaining the longer relaxation times. A similar relation between the gel strength and the molecular weight polymers was reported for gels of boronated poly(N-vinyl-2-pyrrolidone) [24] and acrylamide polymers [29].

Next, the influence of the PVA concentration in the gels was investigated. Higher PVA concentrations generally yield stronger gels, as was demonstrated by higher maximum storage moduli G'_{\max} found for gels of boronated poly(N-vinyl-2-pyrrolidone) with PVA [24], whereas no significant effect of the PVA concentration on the relaxation times was found [29, 31]. Upon mixing of a 7.5% w/v solution of p(MBA-2AMPBA) with equal volumes of PVA (125 kDa) solution varying in PVA concentrations from 2.5 to 5.0, 7.5 and 10% w/v gels were instantaneously formed. The characteristic values for G'_{\max} and τ of gels prepared by the 1:1 v/v mixing of PVA and PAA solutions are shown in Figure 7.5.

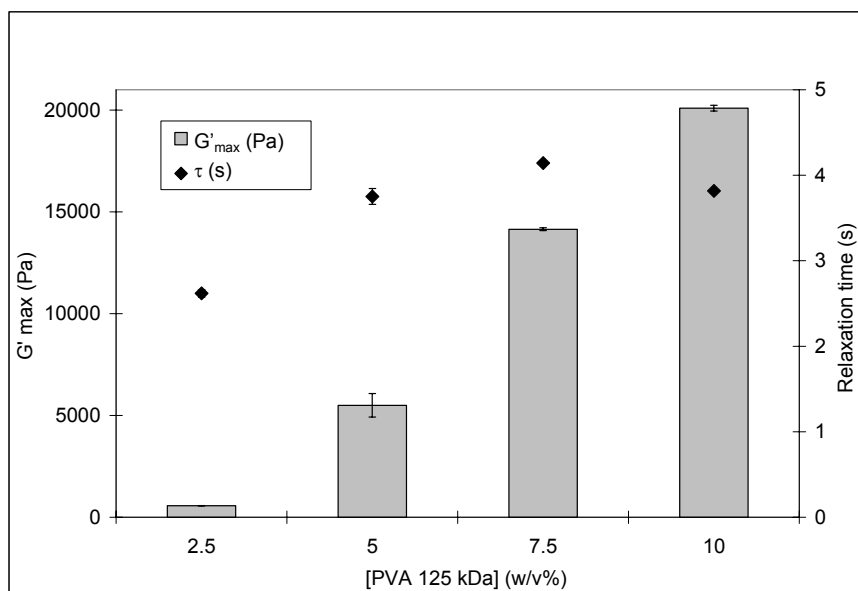


Figure 7.5. Gel strength as a function of the concentration of poly(vinyl alcohol) (PVA). Gels were prepared with 7.5% w/v p(MBA-2AMPBA) and 125 kDa PVA and the plateau gel strength G'_{\max} is shown in bars and the relaxation time τ is shown in diamonds.

Using 7.5% w/v p(MBA-2AMPBA), it proved to be possible to form gels upon mixing with a solution of 125 kDa PVA already with PVA concentration of only 2.5% w/v. These gels with extreme low PVA content demonstrate the efficiency of boronated PAAs for PVA crosslinking. In comparison to other systems [24, 29], the boronated PAA p(MBA-2AMPBA) has a very high density of phenylboronic acid moieties, as it is present on every repeating unit, and this enables the formation of cooperative boronate esters with PVA diols of different polymer chains even at low PVA concentration. Moreover, it was found that the plateau storage modulus increased dramatically at higher PVA concentrations to > 20 kPa for gels prepared from 7.5% w/v p(MBA-2AMPBA) and 10% w/v 125 kDa PVA.

As mentioned earlier the relaxation time can be viewed as a measurement for the average crosslink lifetime, primarily determined by entanglement of the PVA chains, an increase in PVA concentration only minimally increases the relaxation time, which is in accordance with previous results obtained with PVA hydrogels reported in the literature [29, 31]. Most importantly, with the boronated PAAs produce very strong hydrogels can be prepared with PVA, depending on the M_w and the concentration of PVA selected. This opens many possibilities for the development of glucose-responsive drug delivery devices, but also for preparation of strong gels for load-bearing applications, such as described by Konno *et al.* that used boronated phospholipids gels as temporal cell containers [32].

7.3.5. Effect pH on crosslinking of PVA

The pK_a of the boronic acid and amino groups in the polymer not only governs the charge distribution and solubility of the polymer, it also determines the stability of the boronate esters that are formed after mixing of the polymer with PVA. The presence of protonated amines can charge-stabilize the boronate esters formed with the 1,3 diols of PVA and the unprotonated proximal amines can donate their free electron pair to a sp^2 hybridized boronic ester forming a dative B–N bond. As a result boronate ester bond formation and hence gel strength is strongly depending on the pH. To investigate the role of pH, p(MBA-2AMPBA) was dissolved at 5% w/v and the pH was adjusted to 4, 5, 6, and 7 respectively. At 5% w/v concentration the polymer p(MBA-2AMPBA) was soluble at all pH values, while at higher concentration solubility problems arose at pH values > 6. The 5% w/v p(MBA-2AMPBA) solutions were mixed with 5% w/v of PVA (47 kDa). PVA of 47 kDa was selected, since for higher M_w PVA solubility problems (gel collapse and phase separation) were observed at pH values > 6. The resulting transparent and homogenous hydrogels were subjected to frequency sweeps at a strain of 2% at 25 and 37 °C and the results are shown in Figure 7.6.

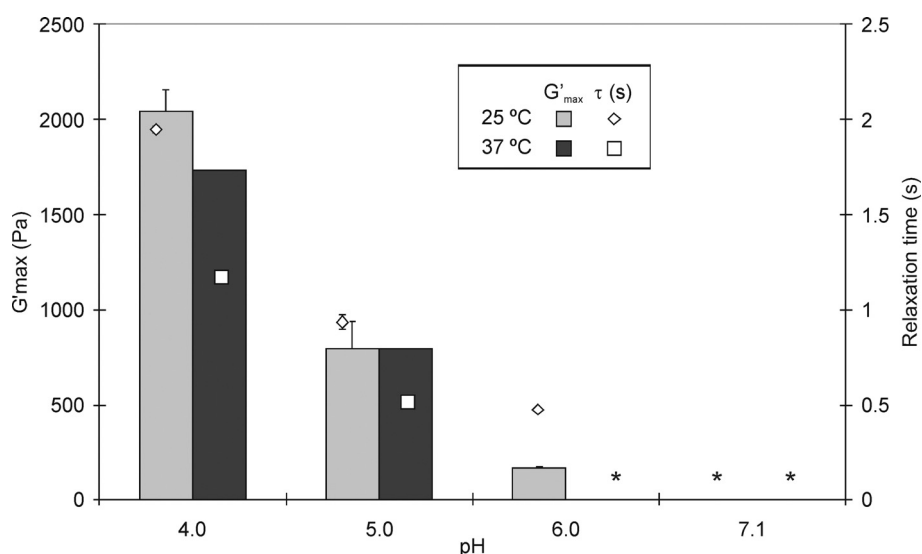


Figure 7.6. Gel strength as a function of the concentration of pH and temperature. Gels were prepared with 5% w/v p(MBA-2AMPBA) and 5% w/v 47 kDa PVA and the plateau gel strength G'_{max} is shown in bars and the relaxation time is shown in symbols, measured at 25 °C (light grey, diamonds) and 37 °C (dark grey, squares). The symbol * means that no G'_{max} and τ were observed as no gel was formed at higher pH.

It was observed that upon increasing the pH, the gel strength decreased. At pH \sim 7 demixing occurred as a white lump was formed in a clear, colorless, low-viscosity solution. The same trend was observed at both measured temperatures (25 and 37 °C). At 37 °C the maximum storage modulus did not change significantly as compared to 25 °C at pH 4 and 5, while a significant decrease in relaxation time was noticed at elevated temperatures. This weaker complexation at elevated temperatures can be explained by the dynamic covalent nature of the boronic crosslinks. The boronic acid/diol complex formation is exothermic and upon increasing the temperature the equilibrium is shifted to the dissociated state to gain entropy.

7.3.6. Thermo-responsive behavior

Strong gels could be prepared from 5% w/v p(MBA-2AMPBA) (pH 5.0) and 7.5% w/v PVA (195 kDa), as a strain sweep at 25 °C (10 Hz) showed a constant gel strength of *ca.* 2100 Pa. The reversible properties of these gels are also demonstrated by their immediate thermo-responsive behavior, when the gel was continuously measured during alternating 30 minute intervals at 25 °C and 37 °C (2% strain, 10 Hz) and the results are shown in Figure 7.7.

From the frequency sweeps at 25 °C and 37 °C relaxation times of 0.59 s and 0.32 s were derived and G'_{max} was 3550 Pa and 3400 Pa, respectively. The response in gel strength upon temperature change was nearly instantaneous and completely reversible, and the gel strength kept constant in time alternating between 4.1 kPa at

25 °C and 3.9 kPa at 37 °C. The values of the stability test at 10 Hz were slightly higher than derived from the frequency sweeps, which was attributed to additional mixing during the initial frequency sweep measurements. The rapid response to temperature changes demonstrates that these gels could be applied as bioactuators due to their immediate response to temperature changes, which could be regarded as “on-off switching” behavior.

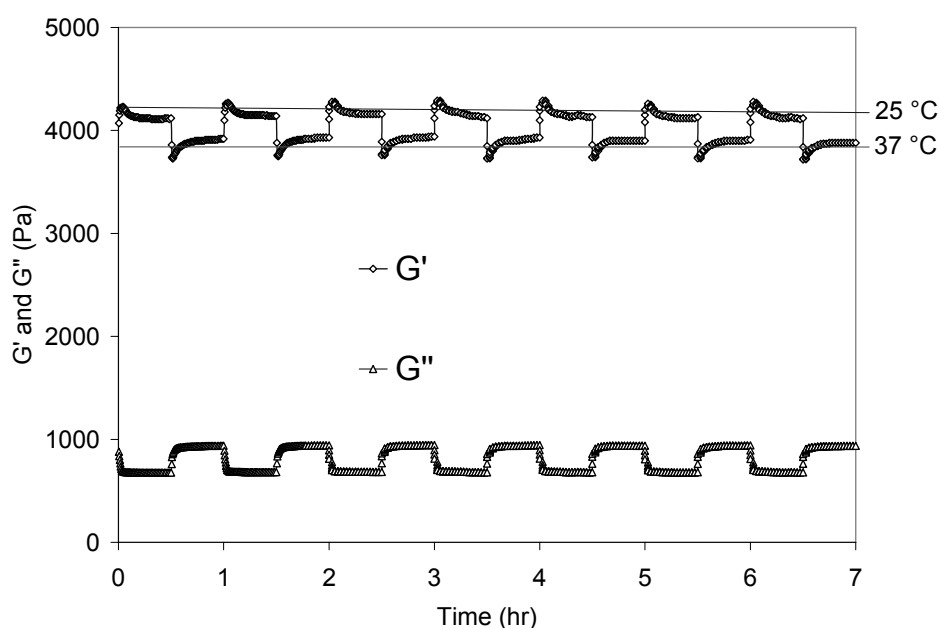


Figure 7.7. G' and G'' for a gel of p(MBA-2AMPBA) (5% w/v) and PVA (195 kDa, 7.5% w/v) as at 30 minute intervals at 25 and 37 °C. Lines are shown for clarity.

7.3.7. Glucose responsive gel degradation

Boronic acids have received considerable attention in glucose sensing [19, 25, 33-35]. Boronic acid containing hydrogels have been developed as glucose-responsive gels that either swell [36] or completely degrade upon the addition of glucose [24, 32]. Such glucose-responsive hydrogels have been suggested for glucose triggered insulin release in order to develop improved therapies for diabetic patients [24]. To test the potential of boronated PAAs for glucose-responsive drug delivery systems, gels were prepared from 5% w/v of p(MBA-2AMPBA) mixed 1:1 v/v with 7.5% w/v 195 kDa PVA at pH ~ 5, as described in section 3.6. Swelling and degradation studies were performed in the presence of various concentrations of glucose (0, 2.5, 5.0 and 10 % w/v). The swelling ratio was determined as the weight at time t (W_t) divided by the initial weight at $t = 0$ (W_0). The swelling ratio as a function of time results in a different degradation profile for the different glucose solutions that are displayed in Figure 7.8.

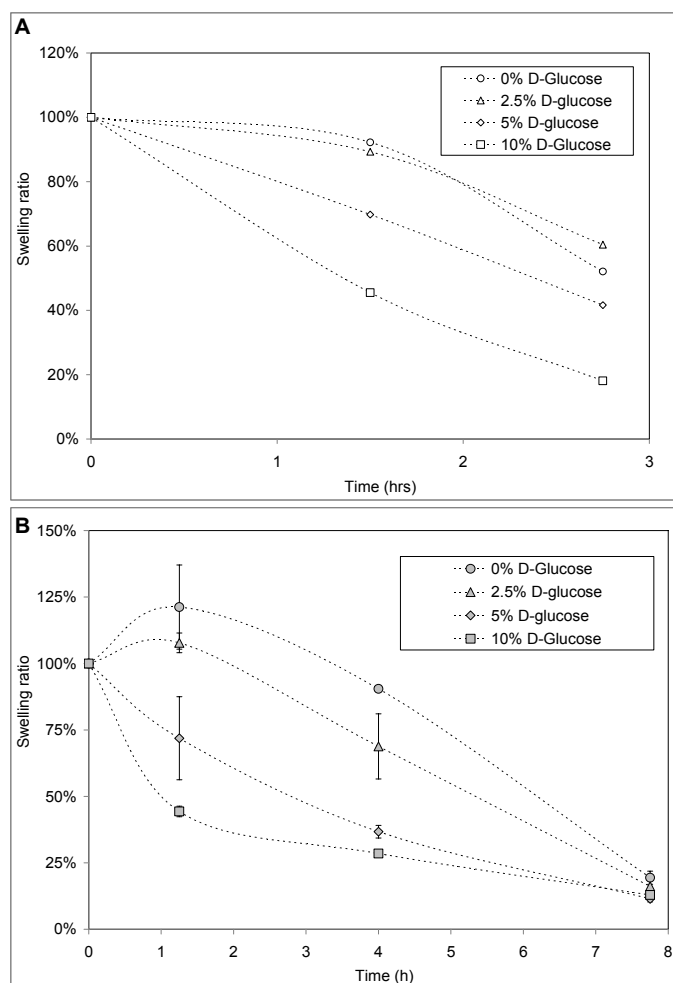


Figure 7.8. Degradation profile of a gel prepared with 5% w/v of p(MBA-2AMPBA) mixed 1:1 v/v with 7.5% w/v 195 kDa poly(vinyl alcohol) at pH-5. The effect of different pH 5 (A) or pH-neutral (B) aqueous D-glucose solutions on the swelling and degradation of the gels is shown for 0% (circles), 2.5% (triangles), 5% (diamonds), and 10% (squares) glucose. Lines are added for clarity.

At pH 5 (Figure 7.8A), it can be observed that the gel degradation proceeds fast and within 3 hours the gel is degraded to 52% of its initial mass. The addition of glucose results in a significant faster degradation. For example at the highest glucose concentration of 10% w/v the gel is degraded to 18% of its initial mass within 3 hours. After 3 hours the remainder of the gel appeared more rigid and it took approximately 15–20 hours to completely degrade the remainder of the gel (data not shown). In pH neutral environment the gels show a different behavior (Figure 7.8B). First, it can be observed that the PAA gel initially swelled to about 120% in the absence of glucose. This can be explained by the gradual deprotonation of the PAA backbone in the gel reducing the charge stabilization between the boronate esters and the cationic amines.

As a result the negatively charged boronate esters with PVA diols will start to repel each other, causing the gel to swell. Furthermore, it can be observed that after 4 hours the gel was still intact for *ca.* 90%. This significant increase in stability as compared to degradation in pH 5 medium can be explained by the fact that the hydrolysis of the boronate esters is slower as more amines are deprotonated upon exposure to the pH neutral medium. In addition, the deprotonated PAA backbone is more hydrophobic and thus the hydrolysis of the boronate ester crosslinks proceeds slower. Only after 7 hours the gel was largely degraded as the swelling ratio was reduced to *ca.* 19%. Regarding the glucose-responsive degradation, already in the presence of 2.5% w/v glucose the swelling was significantly reduced. For the high sugar concentrations of 5% and 10% w/v glucose an immediate decrease in swelling ratio was observed, indicating a rapid degradation due to the presence of glucose. The decreased swelling ratio with increasing glucose concentration is indicative for increased gel degradation due to the presence of glucose; hence these gels clearly demonstrate glucose-responsive behavior that is more dominant in pH neutral media where degradation times are longer.

7.4. Discussion

It was hypothesized that the p(MBA-2AMPBA) in which the boronic acid has an *ortho*-aminomethyl group in the *ortho*-position could form strong gels at lower (physiological relevant) pH values, as the possibility of an *intra*-molecular B–N interaction lowers the pK_a of the amine and facilitates boronate ester formation. Moreover, the presence of protonated amines in the PAA backbone can electrostatically stabilize the anionic boronate esters formed with the 1,3 diols of PVA. At pH 4–5 below the pK_a of the boronic acid, the formed gel was strongest, while at $pH \geq 6$ above the pK_a of the boronic acid, the resulting gel was very weak or not formed at all. Based upon these results it is likely that the formation of a B–N dative bond at pH values > 5 is strongly reducing the capability of the 2AMPBA group to form a boronic ester with PVA, thereby preventing crosslinking. After protonation, the proximal amines provide anchimeric assistance to facilitate reversible boronic/boronate ester bond formation. With respect to the crosslinking mechanism, several authors assume that complexation with PVA is strongest at $pH > pK_a$ [19, 33, 37–38]. Following this assumption, at $pH < pK_a$ the complexation between the boronic acid and PVA and thus crosslinking of the hydrogel would be weaker. However, our findings were opposite, as the strongest gels with the highest relaxation times were formed at $pH \sim 4$, which is significantly below the pK_a (5.1) of 2AMPBA as found by acid-base titration. At $pH < pK_a$ the dominant boronic acid species is the neutral (trigonal) form with the secondary amine in the *ortho*-position protonated (i.e. no B–N interaction).

This is also confirmed by the swelling and degradation experiments of p(MBA-2AMPBA) gels with PVA. For the p(MBA-2AMPBA) gels that were degraded in pH 5 medium, the B–N interaction benefits from additional charge stabilization in the cationic microenvironment of the PAA backbone. This mechanism of charge stabilization might be preferred over the formation of a dative *intra*-molecular B–N bond, whereas at pH 7 the deprotonation of the amines results in a more hydrophobic environment where the formation of a covalent B–N bond is preferred. As a result in pH neutral medium the transesterification process is slower and thus gel degradation proceeds slower. Consequently, these gels could be prepared at low pH and applied at physiological pH. For example, these PAA hydrogels could be applied as vaginal gels, due to the shifting pH of 4–7 in the vaginal lumen [39]. Alternatively, boronated PAAs based hydrogels may find an application in oral drug delivery, where gels are stable in the acidic environment of the stomach but are rapidly degrading at neutral pH in the small intestines.

7.5. Conclusions

A poly(amido amino) (PAA) with *ortho*-aminomethylphenylboronic acid moieties (2AMPBA) was successfully developed. The resulting water-soluble polymer p(MBA-2AMPBA) had a very high boronic acid density, as it was present as a pendant group on all repeating units of the polymer. The 2AMPBA moieties are capable of diol-complexation, resulting in formation of cyclic boronic/boronate esters. The presence of adjacent *ortho*-amino group in 2AMPBA shifts the optimal pH for diol complexation to more physiologically relevant pH. As a result the polymer p(MBA-2AMPBA) was able to instantaneously form dynamically restructuring hydrogels with poly(vinyl alcohol) (PVA). It proved to be possible to form gels with 7.5% w/v of p(MBA-2AMPBA) after 1:1 v/v mixing with PVA solutions with concentrations as low as 2.5% w/v, demonstrating the high efficiency of this crosslinking system. The gels formed with these boronated PAAs and PVA have self-healing properties as the crosslinks are highly dynamical due to reversible boronic ester formation with the 1,3-diols of (PVA). The gel strength could be tuned by selecting PVA with different molecular weights or by using higher concentrations of PVA and/or PAA. For example, an increase of PVA concentration from 2.5% to 10.0% w/v was found to dramatically increase the plateau gel strength (G'_{\max}) up to 20 kPa, while there was little effect on the relaxation time. The gel strength is temperature dependant and the temperature response was fast and completely reversible. Strongest gels were formed at low pH of 4–5, where the cationic environment provided by the PAA backbone could stabilize the anionic boronate esters. The boronated PAA-PVA gels showed glucose-responsive behavior as was

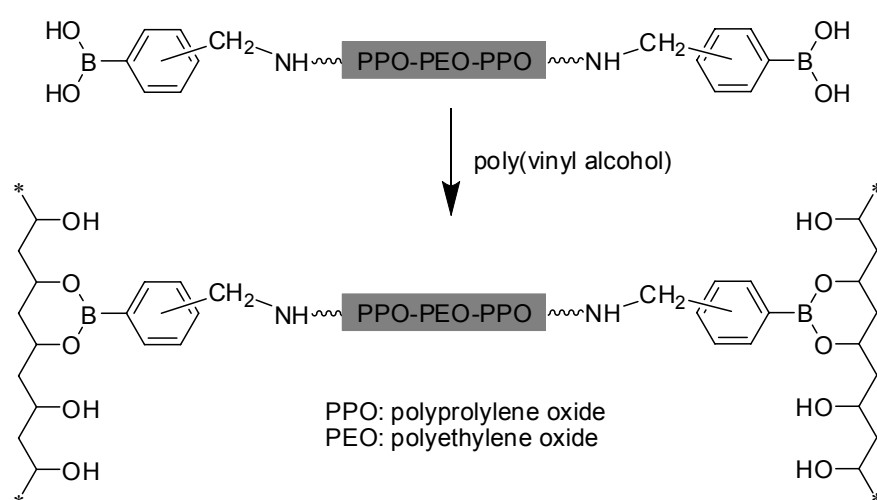
demonstrated by the increased gel degradation rate upon exposure to higher concentrations of glucose.

7.6. References

- [1] P. Ferruti, M.A. Marchisio, R. Duncan, Poly(amido-amine)s: Biomedical applications, *Macromol. Rapid Comm.*, 23 (2002) 332-355.
- [2] J. Franchini, P. Ferruti, Perspectives on: Recent advances in poly(amidoamine)s chemistry, *J. Bioact. Compat. Pol.*, 19 (2004) 221-236.
- [3] E. Emilietri, E. Ranucci, P. Ferruti, New poly(amidoamine)s containing disulfide linkages in their main chain, *J. Polym. Sci. Pol. Chem.*, 43 (2005) 1404-1416.
- [4] C. Lin, J.F.J. Engbersen, Effect of chemical functionalities in poly(amido amine)s for non-viral gene transfection, *J. Control. Release*, 132 (2008) 267-272.
- [5] M.A. Mateos-Timoneda, M.C. Lok, W.E. Hennink, J. Feijen, J.F.J. Engbersen, Poly(amido amine)s as gene delivery vectors: Effects of quaternary nicotinamide moieties in the side chains, *Chemmedchem*, 3 (2008) 478-486.
- [6] C. Lin, Z.Y. Zhong, M.C. Lok, X.L. Jiang, W.E. Hennink, J. Feijen, J.F.J. Engbersen, Linear poly(amido amine)s with secondary and tertiary amino groups and variable amounts of disulfide linkages: Synthesis and in vitro gene transfer properties, *J. Control. Release*, 116 (2006) 130-137.
- [7] C. Lin, C.J. Blaauboer, M.M. Timoneda, M.C. Lok, M. van Steenberg, W.E. Hennink, Z.Y. Zhong, J. Feijen, J.F.J. Engbersen, Bioreducible poly(amido amine)s with oligoamine side chains: Synthesis, characterization, and structural effects on gene delivery, *J. Control. Release*, 126 (2008) 166-174.
- [8] M. Piest, C. Lin, M.A. Mateos-Timoneda, M.C. Lok, W.E. Hennink, J. Feijen, J.F.J. Engbersen, Novel poly(amido amine)s with bioreducible disulfide linkages in their diamino-units: Structure effects and in vitro gene transfer properties, *J. Control. Release*, 130 (2008) 38-45.
- [9] C. Lin, J.F.J. Engbersen, The role of the disulfide group in disulfide-based polymeric gene carriers, *Expert Opin. Drug Del.*, 6 (2009) 421-439.
- [10] S.C.W. Richardson, N.G. Patrick, N. Lavignac, P. Ferruti, R. Duncan, Intracellular fate of bioresponsive poly(amidoamine)s in vitro and in vivo, *J. Control. Release*, 142 (2010) 78-88.
- [11] M. Piest, J.F.J. Engbersen, Effects of charge density and hydrophobicity of poly(amido amine)s for non-viral gene delivery, *J. Control. Release*, 148 (2010) 83-90.
- [12] J. Franchini, E. Ranucci, P. Ferruti, Synthesis, physicochemical properties, and preliminary biological characterizations of a novel amphoteric agmatine-based poly(amidoamine) with RGD-like repeating units, *Biomacromolecules*, 7 (2006) 1215-1222.
- [13] P. Ferruti, E. Ranucci, S. Bianchi, L. Falciola, P.R. Mussini, M. Ross, Novel polyamidoamine-based hydrogel with an innovative molecular architecture as a Co²⁺-, Ni²⁺-, and Cu²⁺-sorbing material: Cyclic voltammetry and extended X-ray absorption fine structure studies, *J. Polym. Sci. Pol. Chem.*, 44 (2006) 2316-2327.
- [14] P. Ferruti, S. Bianchi, E. Ranucci, F. Chiellini, V. Caruso, Novel poly(amido-amine)-based hydrogels as scaffolds for tissue engineering, *Macromol. Biosci.*, 5 (2005) 613-622.
- [15] P. Ferruti, S. Bianchi, E. Ranucci, F. Chiellini, A.M. Piras, Novel agmatine-containing poly(amidoamine) hydrogels as scaffolds for tissue engineering, *Biomacromolecules*, 6 (2005) 2229-2235.
- [16] R. Annunziata, J. Franchini, E. Ranucci, P. Ferruti, Structural characterisation of poly(amidoamine) networks via high-resolution magic angle spinning NMR, *Magn. Reson. Chem.*, 45 (2007) 51-58.
- [17] L. Calucci, C. Forte, E. Ranucci, Water/polymer interactions in a poly(amidoamine) hydrogel studied by NMR spectroscopy, *Biomacromolecules*, 8 (2007) 2936-2942.
- [18] E. Jacchetti, E. Emilietri, S. Rodighiero, M. Indrieri, A. Gianfelice, C. Lenardi, A. Podesta, E. Ranucci, P. Ferruti, P. Milani, Biomimetic poly(amidoamine) hydrogels as synthetic materials for cell culture, *J. Nanobiotechnology*, 6 (2008) 14.
- [19] D.G. Hall, *Boronic Acids - Preparation and applications in organic synthesis and medicine*, John Wiley & Sons, 2005.
- [20] M. Piest, J.F.J. Engbersen, Role of boronic acid moieties in disulfide containing poly(amido amine)s for non-viral gene delivery, See chapter 3 of this thesis, (2010).
- [21] M. Piest, J.F.J. Engbersen, Boronic acid functionalized disulfide containing poly(amido amine) with improved polyplex stability for pDNA and siRNA delivery in vitro, See chapter 4 of this thesis, (2010).

- [22] M. Piest, J.F.J. Engbersen, A boronic acid functionalized poly(amido amine) for drug delivery and combined drug and gene delivery, See chapter 5 of this thesis, (2010).
- [23] G. Springsteen, B.H. Wang, A detailed examination of boronic acid-diol complexation, *Tetrahedron*, 58 (2002) 5291-5300.
- [24] S. Kitano, Y. Koyama, K. Kataoka, T. Okano, Y. Sakurai, A novel drug delivery system utilizing a glucose responsive polymer complex between poly (vinyl alcohol) and poly (N-vinyl-2-pyrrolidone) with a phenylboronic acid moiety, *J. Control. Release*, 19 (1992) 161-170.
- [25] I. Hisamitsu, K. Kataoka, T. Okano, Y. Sakurai, Glucose-responsive gel from phenylborate polymer and poly(vinyl alcohol): Prompt response at physiological pH through the interaction of borate with amine group in the gel, *Pharmaceut. Res.*, 14 (1997) 289-293.
- [26] S. Chaterji, I.K. Kwon, K. Park, Smart polymeric gels: Redefining the limits of biomedical devices, *Prog. Polym. Sci.*, 32 (2007) 1083-1122.
- [27] D. Roy, J.N. Cambre, B.S. Sumerlin, Future perspectives and recent advances in stimuli-responsive materials, *Prog. Polym. Sci.*, 35 (2010) 278-301.
- [28] S.L. Wiskur, J.J. Lavigne, H. Ait-Haddou, V. Lynch, Y.H. Chiu, J.W. Canary, E.V. Anslyn, pK(a) values and geometries of secondary and tertiary amines complexed to boronic acids - Implications for sensor design, *Org. Lett.*, 3 (2001) 1311-1314.
- [29] A.E. Ivanov, H. Larsson, I.Y. Galaev, B. Mattiasson, Synthesis of boronate-containing copolymers of N,N-dimethylacrylamide, their interaction with poly(vinyl alcohol) and rheological behaviour of the gels, *Polymer*, 45 (2004) 2495-2505.
- [30] E. Chiellini, A. Corti, S. D'Antone, R. Solaro, Biodegradation of poly (vinyl alcohol) based materials, *Prog. Pol. Sci.*, 28 (2003) 963-1014.
- [31] I.D. Robb, J. Smeulders, The rheological properties of weak gels of poly(vinyl alcohol) and sodium borate, *Polymer*, 38 (1997) 2165-2169.
- [32] T. Konno, K. Ishihara, Temporal and spatially controllable cell encapsulation using a water-soluble phospholipid polymer with phenylboronic acid moiety, *Biomaterials*, 28 (2007) 1770-1777.
- [33] T.D. James, Saccharide-selective boronic acid based photoinduced electron transfer (PET) fluorescent sensors, *Top. Curr. Chem.*, 277 (2007) 107-152.
- [34] A.E. Ivanov, K. Shiomori, Y. Kawano, I.Y. Galaev, B. Mattiasson, Effects of polyols, saccharides, and glycoproteins on thermoprecipitation of phenylboronate-containing copolymers, *Biomacromolecules*, 7 (2006) 1017-1024.
- [35] C. Cannizzo, S. Amigoni-Gerbier, C. Larpent, Boronic acid-functionalized nanoparticles: synthesis by microemulsion polymerization and application as a re-usable optical nanosensor for carbohydrates, *Polymer*, 46 (2005) 1269-1276.
- [36] T. Hoare, R. Pelton, Engineering glucose swelling responses in poly(N-isopropylacrylamide)-based microgels, *Macromolecules*, 40 (2007) 670-678.
- [37] J. Yan, G. Springsteen, S. Deeter, B.H. Wang, The relationship among pK(a), pH, and binding constants in the interactions between boronic acids and diols - it is not as simple as it appears, *Tetrahedron*, 60 (2004) 11205-11209.
- [38] J. Yan, H. Fang, B.H. Wang, Boronlectins and fluorescent boronlectins: An examination of the detailed chemistry issues important for the design, *Med. Res. Rev.*, 25 (2005) 490-520.
- [39] J.I. Jay, S. Shukair, K. Langheinrich, M.C. Hanson, G.C. Cianci, T.J. Johnson, M.R. Clark, T.J. Hope, P.F. Kiser, Modulation of viscoelasticity and HIV transport as a function of pH in a reversibly crosslinked hydrogel, *Adv. Funct. Mater.*, 19 (2009) 2969-2977.

Dynamically restructuring hydrogels from the reversible covalent crosslinking of poly(vinyl alcohol) by ortho- or para-aminomethylphenylboronic acid functionalized PPO-PEO-PPO spacers (Jeffamines®)



Abstract

Dynamically restructuring (“self-healing”) hydrogels were prepared by reversible formation of boronic-ester crosslinks between bis-boronic acid containing compounds and polyols, such as poly(vinyl alcohol) (PVA). To this purpose two different bis-(phenylboronic acid) functionalized crosslinkers with a PPO-PEO-PPO spacer Jeff-2AMPBA and Jeff-4AMPBA were synthesized via reductive coupling of 2-, and 4-formylphenylboronic acid to JeffamineED1900. Due to the different position of the secondary amino group with respect to the boronic acid moiety (ortho or para) the pK_a of the amino and boronic acid groups in the spacer endgroups differ significantly, thereby influencing the optimal pH for boronic ester formation. Using alizarin red S at varying pH (5.0, 6.5 and 7.4), highest binding with alizarin was found for the ortho-aminomethylphenylboronic acid at pH 6.5, while highest binding with alizarin was found for the para-aminomethylphenylboronic acid at pH 7.4. Fairly strong hydrogels could be formed by both Jeff-2AMPBA and Jeff-4AMPBA at low pH 4, but strongest gels were formed with the para boronic acid at pH 9. Apparently, the presence of an inter-molecular B–N interaction by Jeff-4AMPBA is favored over the presence of an intra-molecular B–N interaction by Jeff-2AMPBA for strong hydrogel formation with PVA at physiological pH.

This chapter is being prepared for publication as: M. Piest, X. Zhang, J. Trinidad, and J.F.J. Engbersen. *Dynamically restructuring hydrogels from the reversible covalent crosslinking of poly(vinyl alcohol) by ortho- or para-aminomethylphenylboronic acid functionalized PPO-PEO-PPO spacers (Jeffamines®)*

8.1. Introduction

Hydrogels are composed of hydrophilic polymer chains that are interconnected in a network that makes them water-insoluble. Hydrogels can contain large amounts of water (over 99% by weight) and possess also a degree of flexibility very similar to natural tissue, due to their significant water content. Hydrogels are attractive materials for many biomedical and pharmaceutical applications, as for example in drug delivery, tissue engineering, regenerative medicine. Therefore, a great variety of polymeric hydrogels have been developed for these purposes in the past decades. [1-4]. The most common way of network formation in hydrogels is either by covalent or by physical crosslinking of the polymer chains. However, depending on the application, hydrogels that are crosslinked by permanent covalent bonds can be too rigid and possess limited swelling behavior, whereas physically crosslinked hydrogels often are often not robust enough. An attractive alternative in the formation of a crosslinked network in hydrogels is by using reversible covalent bonds. In this way a relatively strong chemically crosslinked network with dynamic (bioresponsive) properties can be formed [5]. These types of hydrogels are not only more stable than physically crosslinked hydrogels, but these dynamically restructuring materials also have self-healing abilities [6-7]. The unique ability of self-reorganization could render such materials a longer lifetime [8].

From the biomedical application perspective, a particular interesting type of dynamic covalent bond formation is the reversible boronic ester formation of boronic acids with compounds that have a 1,2-diol or 1,3-diol moiety in their structure, as is found in several polyols, carbohydrates, glycoproteins, RNAs, *etc.* [9]. The reversible complexation between boronic acid and polyhydroxy compounds has been utilized in many different fields including saccharide sensing technology [10], affinity column chromatography [11, 12], and more importantly boronic acid chemistry is applied in the field of bioresponsive, self-healing materials [6, 11-13].

The formation of a hydrogel upon mixing a poly (vinyl alcohol) (PVA) solution with a sodium borate (borax) solution is already known for more than five decades [14]. The cross-link reaction is believed to be a so-called “di-diol” complexation, between two diol units of PVA and one borate ion [15-16]. These PVA-borax gels are only formed at pH above the pK_a of boric acid ($pK_a \sim 9$), and therefore these gels are not suitable for most biomedical applications that operate at relevant physiological pH. It has been shown that the efficiency of crosslinking of PVA can be improved by using polymers containing phenylboronic acid (PBA) functional groups, as cooperative binding of the PBA moieties to the 1,3-diols of PVA is entropically favored over borax crosslinking [7, 11-13]. Moreover, the phenyl substituent enhances the electron deficiency of the boron centre, thereby reducing the pK_a of the boronic acid ($pK_a = 8.8$), and facilitating boronic ester formation at a slightly reduced pH.

The pH sensitivity of reversible boronic ester formation that links the boronic acid with the 1,3-diols of PVA is a key parameter in gel formation, gel strength and eventual gel degradation, and therefore, it determines to a large extent the specific applicability of the gel. It has been reported that the presence of the aminomethyl group in the *ortho* position to the boronic acid center allows for a dative B-N interaction that lowers the basicity of the amine and acidity of the boronic acid, thereby facilitating the formation of boronic esters at reduced pH. To investigate the possibilities to tune the properties of PVA gels by making use of relatively simple pH-sensitive phenylboronic acid based crosslinkers, we have designed two novel crosslinkers in which a Jeffamine® ED1900 spacer is substituted at both terminal positions with *ortho*-aminomethylphenylboronic acid (2-AMPBA) or *para*-aminomethylphenylboronic acid (4-AMPBA) moieties, respectively. Jeffamine® ED1900 is a polyether diamine with two small blocks of amino-terminated poly(propylene oxide) and an intermediate longer block of poly(ethylene oxide) and was selected as a spacer since it has a high water-solubility and good biocompatibility. [19]

It is expected that the presence of the aminomethyl moiety in the *ortho* or *para* position with respect to the phenylboronic acid will display distinct differences in the boronic ester formation and thus on the crosslinking of PVA due to differences in the pK_a of the boronic acid groups involved in the ester formation [20]. The rheological properties of gels prepared with JeffamineED1900-bis-(2-aminomethylphenylboronic acid) (Jeff-2AMPBA) and JeffamineED1900-bis-(4-aminomethylphenylboronic acid) (Jeff-4AMPBA) with different molecular weight PVAs were systematically investigated, particularly focusing on the effects of pH and temperature.

8.2. Materials and methods

8.2.1 Materials

JeffamineED1900 (Jeff1900, Aldrich), sodium borohydride (NaBH_4 , Aldrich), 2-formylphenylboronic acid (Aldrich), 4-formylphenylboronic acid (Aldrich), benzaldehyde (Aldrich), D-glucose (Aldrich), poly(vinyl alcohol) (PVA, M_w 195kDa, 125 kDa, Aldrich, 72 kDa, Merck), phosphate buffered saline (PBS, Braun), 2-(*N*-morpholino) ethanesulfonic acid (MES, Aldrich), 4-(2-hydroxyethyl)-1-piperazineethanesulfonic acid (HEPES, Aldrich), acetic acid (Aldrich), 1,2-dihydroxy-9-10-antraquinone sulfonic acid (alizarin red S, Fluka), were purchased with highest purity available and used as received. The water used for binding studies was purified by a MilliQ filtration system.

8.2.2 Synthesis of diboronated JeffamineED1900 based crosslinkers

JeffamineED1900 was used as provided, without further purification. Excess of reagents were used to ensure complete functionalization of the α,ω -amines. The structure, degree of functionalization and composition of the Jeffamine crosslinkers were confirmed by ^1H NMR spectra recorded on a 300 MHz Varian Inova spectrometer.

JeffamineED1900-di-(2-aminomethylphenylboronic acid) (Jeff-2AMPBA) was synthesized by dissolving JeffamineED1900 (5.71 g, 3.0 mmol) and *ortho*-formylphenylboronic acid (1.26g, 8.2 mmol) in 20 ml methanol to yield a bright yellow solution. The reaction was left to proceed for 4 days at ambient temperature under nitrogen atmosphere, during which the solution turned dark yellow. ^1H NMR showed that imine formation was complete. Next, NaBH_4 (0.39 g, 10.1 mmol) was added portion-wise and evolution of hydrogen gas and a concomitant color change from yellow to colorless were observed. The reduction was left to proceed for 4 h at ambient temperature. Next, the methanol was removed by rotational evaporation yielding an off-white solid. Subsequently, the crude product was dissolved into MilliQ water and the pH was set to 7 with 1M HCl (aq). The solution was then purified by dialysis with a 1000 Da M_w CO membrane against MilliQ water. Jeff-2AMPBA was isolated after lyophilization as an off-white solid (2.40 g, 39% yield).

JeffamineED1900-di-4-aminomethylphenylboronic acid (Jeff-4AMPBA) was synthesized as described above by reacting JeffamineED1900 (5.78 g, 3.0 mmol) and 4-formylphenylboronic acid (1.36 g, 9.1 mmol), and Jeff-4AMPBA was isolated as an off-white solid after lyophilization (3.72 g, 60% yield).

JeffamineED1900-di-aminomethylbenzene (Jeff-Bn) was synthesized as a non-boronated control as described above by reaction of JeffamineED1900 (6.02 g, 3.0 mmol) and benzaldehyde (0.81 g, 7.6 mmol). Jeff-Bn was recovered after lyophilization as an off-white solid (2.6 g, 40 % yield).

8.2.3 Differential Scanning Calorimetry (DSC) measurements

Melting points and melting enthalpies of diboronated Jeff1900 crosslinkers were determined with a Pyris I differential scanning calorimeter (DSC), calibrated with indium and gallium. During each measurement, 5–10 mg of the Jeffamine sample was cooled to $-100\text{ }^\circ\text{C}$ and kept at this temperature for 2 min. Next, the sample was heated to $60\text{ }^\circ\text{C}$, annealed for 2 min, and subsequently cooled to $-100\text{ }^\circ\text{C}$. Finally, the sample was kept at $-100\text{ }^\circ\text{C}$ for 2 min and heated to $60\text{ }^\circ\text{C}$ again. Both the cooling and heating rate were $10\text{ }^\circ\text{C}/\text{min}$. Melting temperature (T_m) was determined from the corresponding temperature at maximum heat flow. Melting enthalpies (ΔH_m°) were determined by integration of the melting peaks. The data presented were selected from the second run of heating scanning.

In parallel, the melting range of each crosslinker was visually verified via a micro melting point apparatus (Olympus). The heating rate was set at 10 °C/min and the initial temperature was 25 °C.

8.2.4 Determination of pK_a values

The pH-profiles of the JeffamineED1900 based crosslinkers Jeff-2AMPBA, and Jeff-4AMPBA, and that of the reference compound Jeff-Bn were determined by potentiometric acid-base titration. For each compound, 0.25 mmol in protonable nitrogens (the α,ω -amino groups in Jeffamine, *ca.* 0.25 g) were dissolved in 10 ml of 150 mM NaCl aqueous solution saturated with nitrogen gas. Subsequently, all solutions were set to pH \sim 2 with 1 M HCl prior to titration with 0.1 M NaOH using an automatic titrator (Metrohm 702 SM Titrino). The pK_a values were determined from the plateau values of the titration curves.

8.2.5 Determination of the equilibrium constant of boronic ester formation with alizarin red S

Alizarin red S (ARS) was dissolved to a 9.0×10^{-5} M stock solution in MilliQ water. Stock solutions of 1.8×10^{-3} M Jeff-2AMPBA, and Jeff-4AMPBA were prepared in 0.1 M HEPES (pH 7.40), MES (pH 6.50), and acetate buffers (pH 5.00). The pH of each buffer solution was adjusted with 1M NaOH or HCl, and the ionic strength was set at 0.15 M with NaCl.

A series of 10 samples of each boronated Jeffamine-ARS complex at the three different pH values was prepared by adding 0.1 ml of the ARS stock solution to appropriate volumes of Jeff-2AMPBA or Jeff-4AMPBA (0–0.9 ml) and the total volume was supplemented to 1.1 ml with the corresponding buffer solution. All samples with a final concentration of 8.2×10^{-6} M of ARS were vortexed for 5 s. Next, 1.0 ml was transferred to a quartz cuvette and a fluorescence emission spectrum was recorded from 560 nm to 600 nm with the excitation wavelength set at 468 nm using a Cary Eclipse fluorescence spectrophotometer. Fluorescent binding measurements for each crosslinker with ARS were carried out in triplicate at maximal emission that was found to be buffer dependant, being 572 nm in acetate (0.1 M, pH 5.0), 585 nm in MES (0.1 M, pH 6.5) and 580 nm in HEPES (0.1 M, pH 7.4).

8.2.6 Determination of the gel strength by oscillatory rheology

Poly(vinyl alcohol) (PVA) with different M_w (72 kDa, 125 kDa, 195 kDa) was dissolved in MilliQ water at 80 °C for several hours to prepare 10% w/v stock solutions. Next, 10% w/v stock solutions of Jeff-2AMPBA and Jeff-4AMPBA were prepared in MilliQ water. Subsequently, these stock solutions were used to prepare solutions of pH 3.0, 4.0, 5.0, 6.0, 7.0, 8.0, and 9.0, respectively by addition of minimal amounts of 1 M HCl (aq) and/or 1 M NaOH (aq).

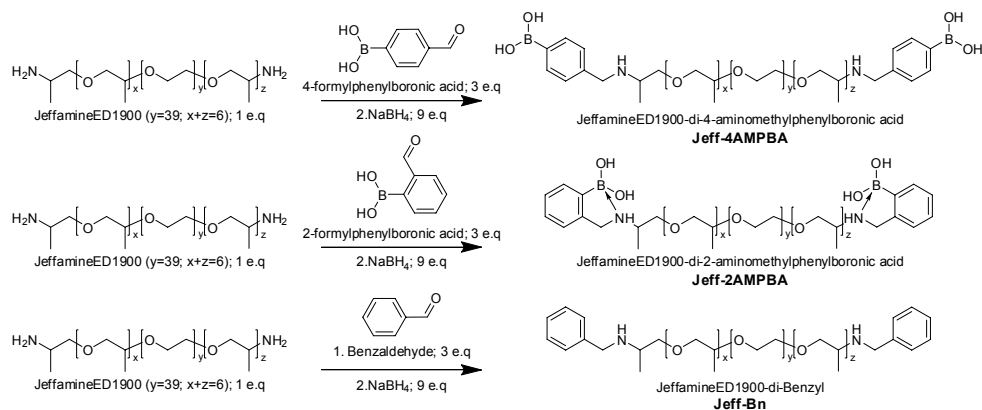
Gel samples were prepared *in duplo* by addition of 0.5 ml solution of 10% w/v of Jeff-2AMPBA or Jeff-4AMPBA with set pH to 0.5 ml of the desired PVA stock solution in a closable vial. Next, the samples were vortexed for 10 s to homogenize the sample and every gel sample was allowed to equilibrate for at least 24 hours at ambient temperature prior to oscillatory rheology measurements. All rheology experiments were performed using a Physica MCR 301 oscillatory rheometer (Anton Paar), programmed by Rheoplus software. The gap between the rotation discs (gel thickness) was fixed at 0.45 mm and a layer of silicon oil was added on top to prevent the evaporation during the measurement. For each type of gel, in addition to the duplicate samples, 2 to 4 measurements per sample were performed. Gel samples were subjected to rotational deformation under the frequency range from 100 Hz to 0.1 Hz at constant strain (γ) of 1%. A series of frequency sweeps were measured upon increasing the temperature from 25 to 60 °C for each specimen. From each measurement, the plateau value of the storage modulus (G') was determined as it reached a plateau at high angular frequency (typically 50 Hz). The crossover frequency (ω_c), being the angular frequency at which the G' equals to G'' (storage modulus = loss modulus), was used to calculate the relaxation time (τ) according to $\tau = 2\pi/\omega_c$.

8.3. Results and discussion

8.3.1 Synthesis of Jeffamine-based boronic acid crosslinkers

As arylboronic acids are typically not very water-soluble at gel-forming concentrations, the spacer should favorably contribute to the water-solubility of the boronic acid moieties. Furthermore, such a spacer should easily be available and allow for the quantitative functionalization with phenylboronic acid. As the spacer length is of major influence on the material properties, different spacers originating from different diamines were screened in exploratory experiments. Although shorter spacers may result in higher crosslink densities and more rigid hydrogels, longer spacer lengths result in more flexible/elastic materials that are often desired in biomedical applications. Preliminary experiments showed that short alkyl spacers (e.g. from 1,4-diaminobutane) resulted in poor solubility of the resulting crosslinkers; this was also observed for the relatively short JeffamineED600 and JeffamineED900 based crosslinkers. Therefore JeffamineED1900 was selected as a spacer with high water-solubility. Phenylboronic acid moieties were attached to the terminal aminogroups of JeffamineED1900 by reductive coupling of 2- and 4-formylphenylboronic acid, yielding the crosslinkers Jeff-2AMPBA and Jeff-4AMPBA, (Scheme 8.1). The resulting Jeff-2AMPBA spacer has a secondary amino group in the *ortho* position and the Jeff-4AMPBA has a secondary amino group in the *para* position of the boronic acid moiety. In addition, a non-boronated control

polymer Jeff-Bn was prepared via reductive amination of benzaldehyde to JeffamineED1900. Complete conversion of the amines was confirmed by ^1H NMR by comparing the proton integration of aryl protons in the low-field region to that of the protons of the JeffamineED1900 backbone. Yields after dialysis were in the range of *ca.* 40% and all the JeffamineED1900 derivatives exhibited good water-solubility.



Scheme 8.1. Synthesis of the JeffamineED1900 derivatives by reductive amination.

The JeffamineED1900 derivatives were further characterized by differential scanning calorimetry (DSC) to investigate the effect of the different end group functionalization on the crystallinity of the materials that is quantified by the melting temperature (T_m) and melting enthalpy (ΔH_m°). The results of these measurements are shown in Table 8.1.

Table 8.1. Melting points (T_m) and melting enthalpy (ΔH_m°) of Jeff1900 derivatives.

Crosslinker	T_m (°C)	Melting range (°C)	ΔH_m° (kJ/mol)
JeffamineED1900	38.5	40–42	199
Jeff-4AMPBA	33	33–35	167
Jeff-2AMPBA	32	32–34	155
Jeff-Benz	35	35–36	179

The melting points as obtained from the DSC measurements of the Jeffamine derivatives were approximately within the melting ranges observed by microscopy. However, the melting point of 38.5 °C for the parent compound JeffamineED1900 deviates from the value of 43 °C given by the manufacturer. The introduction of the different aryl functional groups was found to reduce the melting point by 3–6 °C and the melting enthalpy by 20–44 kJ/mol.

8.3.2 Determination of the pK_a values of the Jeffamine derivatives

Acid-base titration was performed to determine the pK_a of the amine and (if possible) boronic acid moieties in each JeffamineED1900 derivative. The titration curves are shown in Figure 8.1 and the functional groups contributing to each pH plateau are indicated by the arrows. The different transitions and corresponding pK_a values are listed in Table 8.2.

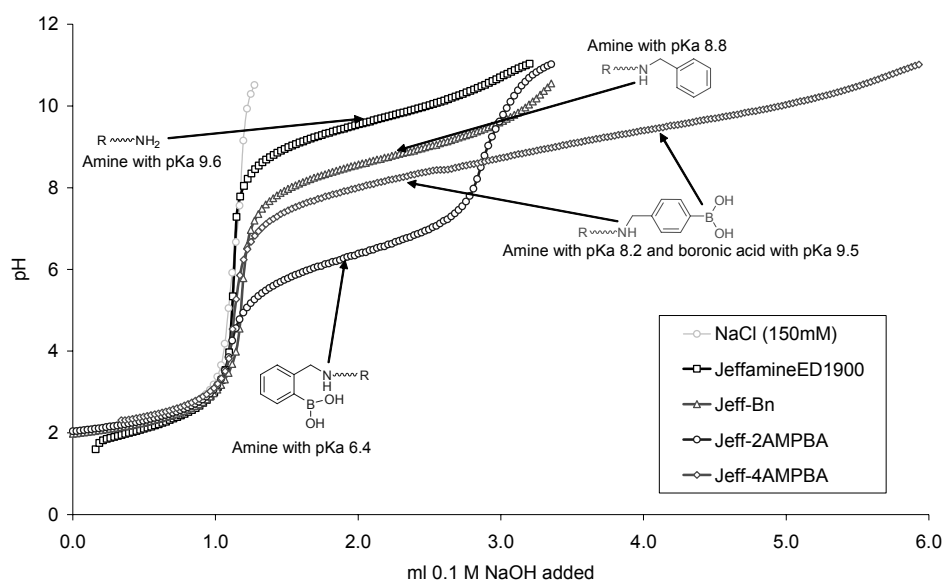


Figure 8.1. The pH profiles upon acid-base titration with 0.1 M NaOH of different JeffamineED1900 derivatives (ca. 12.5 mMol). Jeffamine ED1900 is shown in black squares; Jeff-Bn in green triangles; Jeff-2AMPBA in blue circles and Jeff-4AMPBA in red diamonds.

The unfunctionalized JeffamineED1900 exhibited a plateau in the pH titration curve in the range pH 9–10, yielding an estimated pK_a value for deprotonation of the terminal primary aminogroups of 9.6, which is close to the value of 9.7 reported earlier in the literature [21]. The presence of the benzyl moieties at the aminogroups in Jeff-Bn resulted in buffering at reduced pH 8–10 and the pK_a value of 8.8 was calculated for the deprotonation of the secondary amines in this compound.

Jeff-4AMPBA gave a titration curve that is similar to Jeff-Bn in the acidic and neutral pH range. It was observed that in the pH range 7.0–10.0 the amount OH⁻ consumed was approximately 0.48 mmol, which is twice as much as for Jeff-Bn in the same pH-range, indicating that not only the secondary amines but also the boronic acids contribute to the pH buffering effecting the titration. In this case the two plateaus are partially overlapping due to the fact that the pK_a values for deprotonation of the

secondary amine (pK_a ca. 8.2) and that for the hydroxyl addition to the phenylboronic acid moiety (pK_a ca. 9.5) are close to each other.

Jeff-2AMPBA was expected to have a reduced pK_a as the possibility of an *intra*-molecular B–N interaction was reported to reduce the pK_a of the (protonated) amine and to raise the pK_a of the boronic acid (*i.e.* OH^- addition) [20]. This was indeed observed in the titration curve; Jeff-2AMPBA showed buffering in the pH range 5 to 7 from which a pK_a value of ~ 6.4 can be calculated. A second plateau due to the hydroxyl addition to the boronic acid centre was not observed until titrated to pH 11, indicating that the pK_a of the boronic acid must be raised to a value above pH 11 due to the B–N interaction (Scheme 8.2).

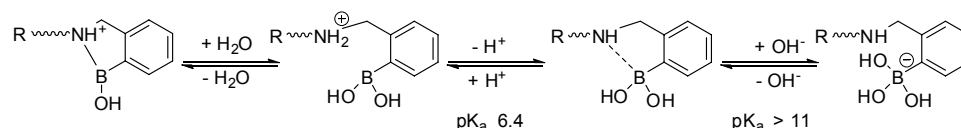
Table 8.2. Overview of the different transitions and corresponding pK_a values.

Jeffamine	$^+\text{H}_3\text{N}\text{---}\text{Jeff}\text{---}\text{NH}_3^+ \xrightleftharpoons[+\text{H}^+]{-\text{H}^+} \text{H}_2\text{N}\text{---}\text{Jeff}\text{---}\text{NH}_2$	$pK_a = 9.6$
Jeff-4AMPBA		$pK_a = 8.2$ $pK_a = 9.5$
Jeff-2AMPBA		$pK_a = 6.4$ $pK_a > 11$
Jeff-Bn		$pK_a = 8.8$

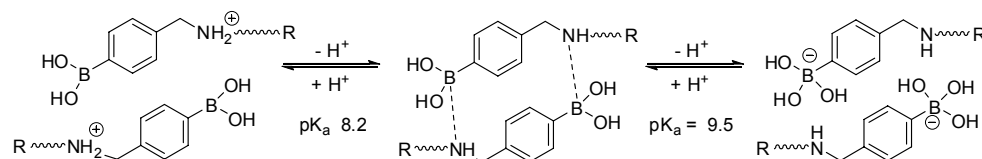
The pK_a of the secondary aminogroup in Jeff-4AMPBA (pK_a 8.2) is lower than the pK_a of the reference compound Jeff-Bn (pK_a 8.8) while the pK_a of the boronic acid group (pK_a 9.5) was higher than the value of 8.8 reported for PBA by Wang and coworkers [22]. As mutual inductive effects of both groups in Jeff-4AMPBA are expected to be only small and at least in opposite direction for the pK_a of the boronic acid group, we propose that the deviation in pK_a 's of both groups by approximately 0.7 units in Jeff-4AMPBA is due to the formation of *inter*-molecular B–N interactions. The comparison between the effect of a possible *intra*-molecular B–N interaction on the pK_a of Jeff-2AMPBA and the effect of a possible *inter*-molecular B–N interaction on the pK_a of Jeff-4AMPBA are depicted in Scheme 8.2.

B–N interaction

Jeff-2AMPBA



Jeff-4AMPBA



Scheme 8.2. Influence of the possibility of an *intra*-molecular B–N interaction in Jeff-2AMPBA and an *intra*- or *inter*-molecular B–N interaction in Jeff-4AMPBA on the pK_a values of the amines and boronic acid centers.

After deprotonation of the secondary amino groups of Jeff-4AMPBA the 4AMPBA functionality has become self-complementary in Lewis acid-base interaction and two functional 4AMPBA groups can participate in a double B–N interaction. Such interaction leads to a significantly increase of the pK_a of the boronic acid moiety.

8.3.3 Determination of the binding constants with alizarin red S

The binding affinity of boronic acids with various sugars has been successfully determined by Wang and coworkers in a competitive binding assay with alizarin red S (ARS) [23-24]. ARS is nonfluorescent by itself but forms with boronic acid a fluorescent boronic ester which allows easy determination of changes in equilibria of ARS in free and boronic ester form both in the presence or absence of competing agents for boronic ester formation.

To evaluate the effect of pH on the affinity of the two differently boronated Jeffamine linkers for boronic ester formation, the binding constants of ARS with Jeff-2AMPBA and Jeff-4AMPBA were determined in aqueous solutions of different pH. For the ester formation between phenylboronic acid moiety (PBA) and ARS, the relationship between the change of fluorescence intensity (ΔI_f) and the binding constant (K_{ARS}) is expressed in Equation 8.1. [23-24] The double reciprocal of Equation 8.1 yields the Benesi-Hildebrand equation (Equation 8.2). The binding constant of the ARS-boronic acid ester (K_{ARS}) is the quotient of the intercept and the slope in a plot of $1/[PBA]$ vs $1/\Delta I_f$.

$$\Delta I_f = \frac{\Delta k p_o \times K_{ARS} \times [PBA] \times [ARS]_0}{1 + K_{ARS} \times [PBA]} \quad \text{Equation 8.1.}$$

$$\frac{1}{\Delta I_f} = \left(\frac{1}{\Delta k p_o \times K_{ARS} \times [ARS]_0} \right) \times \left(\frac{1}{[PBA]} \right) + \left(\frac{1}{\Delta k p_o \times [ARS]_0} \right) \quad \text{Equation 8.2.}$$

ΔI_f = change in fluorescent intensity in %.

$\Delta k p_o$ is a constant derived from the intrinsic fluorescence and the laser power.

K_{ARS} = binding constant of alizarin red S (ARS) with a phenylboronic acid moiety (PBA)

In the measurement, the concentration of ARS in the samples was selected to be 8.2×10^{-6} M, which was within a linear response range of the reciprocal plot of the fluorescent intensity ($1/\Delta I_f$) versus the reciprocal of the concentration of boronic acid moieties ($1/[PBA]$). The binding constants K_{ARS} were calculated from Equation 2 and in Table 8.3 binding constants of ARS with Jeff-4AMPBA and Jeff-2AMPBA in buffer solutions of pH 5.0, 6.5 and 7.4 are given.

Table 8.3. K_{ARS} (M^{-1}) of Jeff-4AMPBA and Jeff-2AMPBA in different buffers.

Buffer	pH	K_{ARS} (M^{-1})	
		Jeff-4AMPBA	Jeff-2AMPBA
Acetate	5.0	3600 ± 100	18500 ± 240
MES	6.5	7200 ± 110	28400 ± 900
HEPES	7.4	7600 ± 130	11200 ± 700

It is shown that the binding strength of the boronated Jeffamine linkers with ARS is strongly dependent on the pH. For Jeff-4AMPBA K_{ARS} increases with pH, as the K_{ARS} is more than doubled upon increasing the pH from 5.0 to 7.4. Compared to the value of K_{ARS} of 1100–1500 M^{-1} for PBA as determined by Springsteen *et al.* [24], the K_{ARS} of Jeff-4AMPBA was significantly higher in all three buffers measured.

For example, at pH 7.4 the K_{ARS} of 7600 M^{-1} is more than 5 times that of PBA, which further supports the proposed *inter*-molecular B–N interaction that stabilizes the boronic-ARS ester.

Jeff-2AMPBA has a stronger binding affinity for ARS than Jeff-4AMPBA as is apparent in the higher K_{ARS} . The value found for Jeff-2AMPBA at pH 7.4 ($K_{ARS} = 11200 \pm 700 \text{ M}^{-1}$) is in agreement with the K_{ARS} ($8110 \pm 95 \text{ M}^{-1}$) for *ortho*-aminomethyl phenylboronic acid reported by Mulla *et al.* [25]. At slightly more acidic pH (6.5) an even higher K_{ARS} of $28400 \pm 900 \text{ M}^{-1}$ was acquired for Jeff-2AMPBA, which weakens upon further acidification, indicating that there is an optimal pH for boronic ester formation where the intramolecular B–N interaction maximally contributes to boronic ester stabilization.

A logical next step was to use a competitive binding assay with ARS to establish the binding affinity of the different boronic acid moieties in Jeff-2AMPBA and Jeff-4AMPBA with PVA and in PVA gels. It was observed that addition of low amounts of PVA to a solution of the fluorescent Jeffamine boronic acid-ARS esters did not result in a significant decrease of fluorescence, indicating a relatively weak binding of PVA at high dilution. Upon increasing the PVA concentration above a certain threshold the fluorescence disappeared and gelation occurred. This nonlinear behavior prevented the quantitative determinations of boronic ester formation constants.

8.3.4 Effect of pH on the gel properties

Boronic acid containing hydrogels typically demonstrate frequency-dependent viscoelastic behavior. Two frequency-dependent moduli are used to characterize the viscoelasticity of a dynamic network: the elastic modulus G' (storage modulus) and the viscous modulus G'' (loss modulus). These two moduli can be determined by oscillatory rheology within the linear viscoelastic region, where hydrogels display both viscous and elastic behavior. Boronic acid containing hydrogels exhibit viscous behavior at a long time scale (at low angular frequency), at which the network of hydrogel has sufficient time to reorganize and can flow accordingly ($G' < G''$). In contrast, these gels exhibit elastic behavior on a short time scale (at high angular frequency), at which the crosslinks of the network can not completely dissociate and the network is more rigid ($G' > G''$) [7,11-13, 26-27]. Moreover, at higher frequencies, the elastic modulus G' becomes frequency-independent and reaches a plateau. It is worth noting that pH and temperature can dramatically affect the viscoelastic behavior of the gel formed by PVA and di-boronic acid based crosslinkers, since the equilibrium of boronic/boronate ester formation and the resulting crosslink density of the network is strongly dependant on pH and temperature [27]. Two main parameters, as a function of angular frequency, were investigated to quantify the rheological behavior of viscoelastic hydrogels: the relaxation time (τ) reflecting the lifetime of the crosslinks

and the plateau value of the storage modulus G' obtained at high angular frequencies (G'_{\max}), reflecting the maximal strength attainable. The relaxation time τ can be determined by $\tau = 2\pi/\omega_c$, where ω_c is the crossover angular frequency at which G' equals to G'' , and τ could be viewed as the average lifetime of the crosslinks. Gels with longer relaxation times show more elastic behavior and have a higher shape-stability.

It was observed that gel formation occurs immediately upon mixing of the di-phenylboronic acid functionalized Jeffamine crosslinkers with PVA and the resulting hydrogels were transparent. The mixing of Jeff-4AMPBA and Jeff-2AMPBA crosslinkers with PVA yielded strong hydrogels, depending on the pH and molecular weight of the PVA used, see Figure 8.2. As expected, the Jeff-Bn crosslinker did not form hydrogels with PVA and moreover no increase in viscosity was observed over the full pH range from 3 to 9.

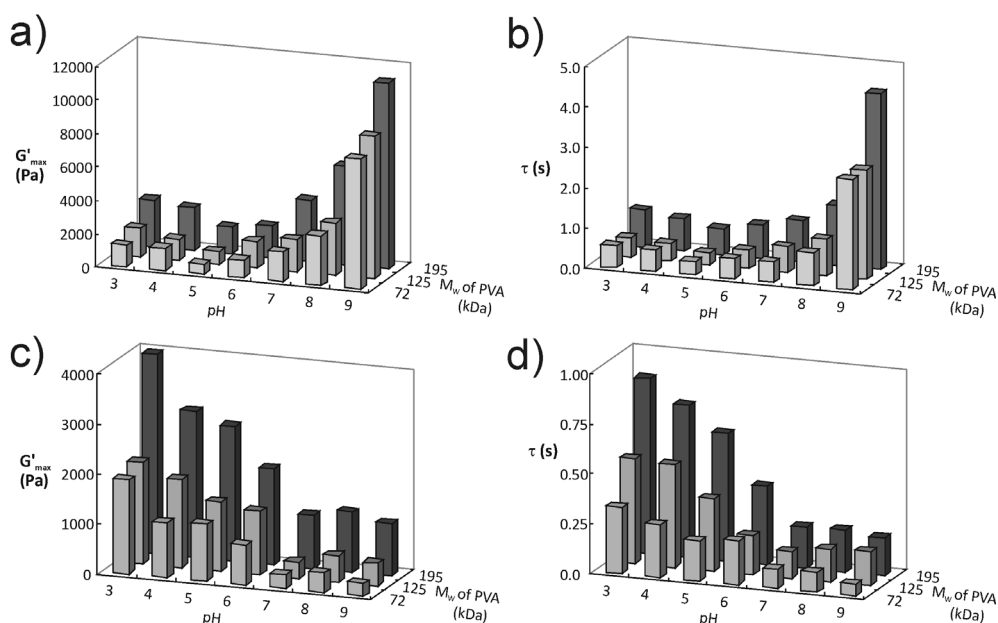


Figure 8.2. Plateau value of storage modulus G'_{\max} (a, c) and relaxation time τ (b, d) for hydrogels prepared by mixing of 10% w/v Jeff-4AMPBA (a, b) and Jeff-2AMPBA (c, d) crosslinkers and 10% w/v PVA with different M_w (72, 125, and 195 kDa) at pH ranging from 3–9 at 25 °C.

From the G'_{\max} values in Figure 8.2 it is clear that under all conditions stronger gels are formed with higher molecular weight PVA, which can be explained by an increase in polymer entanglement, thereby enhancing the gel strength. With increasing M_w of PVA an increase in viscosity was observed that is slowing the relaxation process and thus explains the longer relaxation times observed in Figure 8.2. Remarkably different behavior was observed for the pH dependency of the two types of Jeffamine-based hydrogels. For Jeff-4AMPBA the strongest gels were formed in basic

media (Figure 8.2a and b), whereas the Jeff-2AMPBA hydrogels showed increasing gel strength in acidic media (Figure 8.2c and d). For example, for Jeff-4AMPBA hydrogels with PVA 195 kDa, the gel strength G'_{\max} increases from 3000 (\pm 230) Pa at pH 3 to 11100 (\pm 180) Pa at pH 9, with a concomitant increase of the crosslinking lifetime τ from 0.93 (\pm 0.06) s to 4.38 (\pm 0.07) s. Surprisingly, a minimum in gel strength was observed at pH 5, where G' plateau was only 1600 \pm 20 Pa and τ was 0.65 \pm 0.04 s. For the hydrogels prepared with Jeff-2AMPBA, the strongest gels were formed at acidic pH. For example, mixing PVA 195 kDa with Jeff-2AMPBA at pH 3 immediately gave a strong hydrogel with $G'_{\max} = 4000$ (\pm 130) Pa, and $\tau = 0.87$ (\pm 0.02) s, which is stronger than the gel observed for Jeff-4AMPBA under the same conditions.

The properties of the gels are determined by the relative stability of the boronic esters and therefore the degree of crosslinking at different pH in the gel. The kinetics of boronic ester formation with diols follows a complicated balance of equilibria and has been the subject of much debate in literature [22, 29-31]. Formation of the boronic ester must proceed via the neutral trigonal boron, which is more predominantly present in neutral or acidic solution than in alkaline solution, where OH^- addition forms the tetrahedral boronate anion. Although sometimes advocated in the literature, it is not easy conceivable how the anionic tetrahedral boronate anion can be the reactive species for ester formation, since nucleophilic substitution of a hydroxide ion from the negative, electronically saturated boron center by a neutral alcohol is a highly unlikely process. However, once formed, the boronic ester is most stabilized in its anionic tetrahedral form (for the same reason of unlikely nucleophilic substitution by water or OH^-), where it is the predominant species in alkaline solution. An extra complication in the deconvolution of the effects of pH on the different parameters governing the stability and density of the boronic ester crosslinks in the hydrogels is the fact that the boronic acid group of Jeff-4AMPBA can form intermolecular complexes with the aminomethyl groups present, and the *ortho*-positioned aminomethyl group of Jeff-2AMPBA can form an intramolecular dative B-N ($\text{N} \rightarrow \text{B}$) interaction with the boronic acid group (Scheme 8.2).

Considering the observation that the gel strength of Jeff-2AMPBA is low at neutral and basic pH where a dative B-N interaction is present, and is strongly increased at acidic pH, where the formation of a dative B-N interaction is prevented by protonation of the nitrogen, it can be assumed that the B-N interaction is not favorable for boronate ester formation and/or stabilization. At more acidic pH the trigonal neutral boronic acid (possibly in equilibrium with its tetrahedral water adduct) can readily form a boronic ester with the surrounding 1,3-diol groups of PVA, explaining the observed increase in gel strength. The proximity of the protonated *ortho*-aminomethyl group can possibly contribute to stabilization of the boronate ester in its (anionic) tetrahedral form, formed by addition of a water molecule and expulsion of a proton.

For the Jeff-4AMPBA hydrogel system, the assumption of a prohibitive effect of a B-N interaction on boronic ester crosslinking can explain the minimum gel strength in the rather neutral pH regime, where both neutral free amine and neutral trigonal boronic acid can coexist in the gel to form intermolecular B-N interactions. It is noted that this explanation also requires that the pK_a values of the amine and boronic acid groups in the hydrogel are significantly lower than those given in Scheme 8.2 for purely aqueous solution. However, such a decrease of pK_a can generally be expected in the less aqueous microenvironment of the PVA hydrogels. The increasing gel strength and crosslink lifetime for the Jeff-4AMPBA hydrogels at more basic pH can then be attributed to the formation of more stable anionic tetrahedral boronate ester linkages, formed by hydroxide ion addition to the boron center of the esters.

8.3.5 Effect of temperature on the gel properties

Since the dynamically covalent crosslink formation in boronic acid-PVA based hydrogels is a thermodynamically controlled process, the gel properties are also strongly depending on the temperature. Therefore, the gel strength and relaxation time of both hydrogel systems based on 195 kDa PVA with Jeff-4AMPBA and Jeff-2AMPBA were investigated at 25, 40 and 60 °C in the pH range 3–9. The results are shown in Figure 8.3.

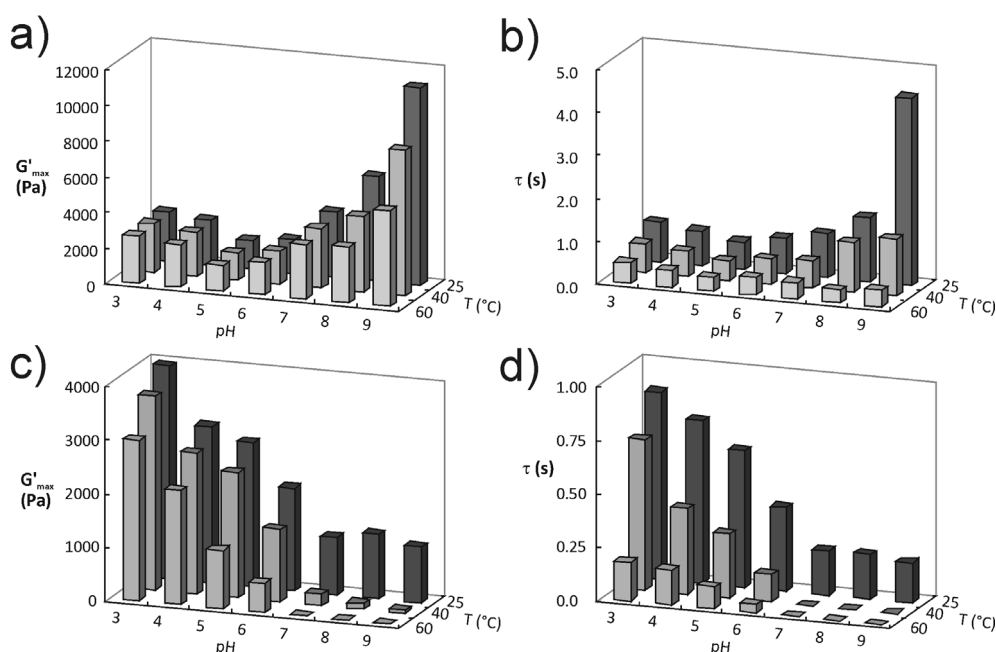


Figure 8.3. Maximum of storage modulus G'_{max} (a, c) and relaxation time τ (b, d) for hydrogels prepared by mixing of 10% w/v 195 kDa PVA and 10% w/v of Jeff-4AMPBA crosslinker (a, b) and 10% w/v of Jeff-2AMPBA crosslinker (c, d) at pH ranging from 3 to 9.

From Figure 8.3, it is clear that for both gel systems G'_{\max} and especially the relaxation time τ decreases dramatically when the temperature is increased from 25 °C to 60 °C, indicating that the crosslink density in the network is lower at higher temperature. The decrease of the relaxation time points to a faster kinetics of the equilibrium reactions of formation and dissociation of the boronate ester linkages in the gel. The decrease in gel strength, G'_{\max} , indicates that this equilibrium is shifted towards the dissociated state, which is in accordance with a dominating entropy gain obtained at increase of temperature.

8.4. Conclusions

Two different boronic acid functionalized crosslinkers for dynamically restructuring gel formation with polyols could be readily synthesized by reductive coupling of the appropriate boronic acid substituted benzaldehydes to the terminal amines of the water-soluble spacer JeffamineED1900. The resulting Jeffamine crosslinkers, possessing either *ortho*-aminomethylphenylboronic acid groups (Jeff-2AMPBA) or *para*-aminomethylphenylboronic acid groups (Jeff-4AMPBA) at the α,ω -positions have very different pH dependency for boronic acid esters formation with diols. This enabled the tuning of the pH-sensitive properties of the hydrogels prepared with polyvinylalcohol (PVA) and these crosslinkers. It was found that Jeff-2AMPBA formed strong hydrogels with PVA at pH 3 ($G'_{\max} = 4000$ Pa) but only weak hydrogels in neutral and basic solution. In contrast, Jeff-4AMPBA formed very strong hydrogels with PVA at pH 9 ($G'_{\max} = 11100$ Pa) whereas the gelation strength in neutral and acidic solution was much weaker. The pH dependent behavior of the hydrogels can be explained by the relative concentrations of reactive and inhibitory species in solution that determine the formation and stabilization of the boronic ester crosslinks in the gel. As the diboronated Jeff1900 based hydrogel systems can be employed at different pH-ranges, these novel gel systems may be exploited in future biomedical applications.

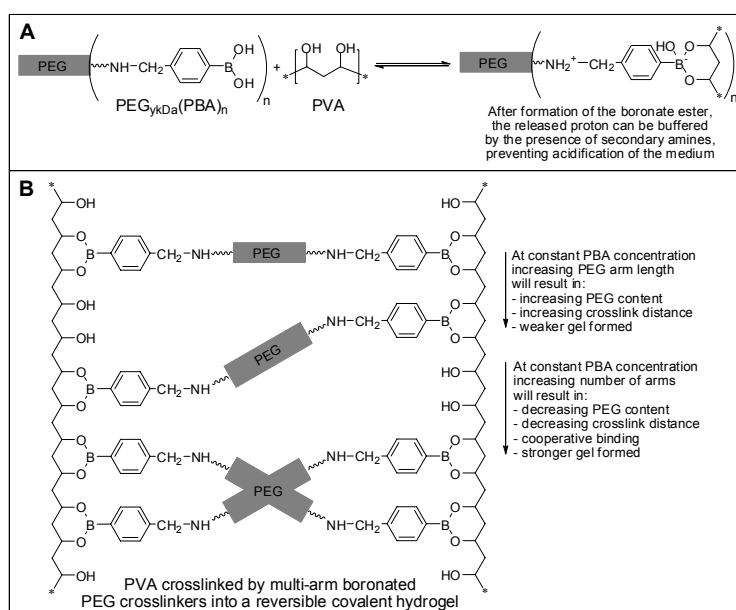
8.5 References

- [1] P. Gupta, K. Vermani, S. Garg, Hydrogels: from controlled release to pH-responsive drug delivery, *Drug Discov. Today*, 7 (2002) 569-579.
- [2] A.S. Hoffman, Hydrogels for biomedical applications, *Adv. Drug Deliv. Rev.*, 54 (2002) 3-12.
- [3] N.A. Peppas, P. Bures, W. Leobandung, H. Ichikawa, Hydrogels in pharmaceutical formulations, *Eur. J. Pharm. Biopharm.*, 50 (2000) 27-46.
- [4] N.A. Peppas, J.Z. Hilt, A. Khademhosseini, R. Langer, Hydrogels in biology and medicine: From molecular principles to bionanotechnology, *Adv. Mater.*, 18 (2006) 1345-1360.
- [5] G.H. Deng, C.M. Tang, F.Y. Li, H.F. Jiang, Y.M. Chen, Covalent cross-linked polymer gels with reversible sol-gel transition and self-healing properties, *Macromolecules*, 43 (2010) 1191-1194.
- [6] M.C. Roberts, M.C. Hanson, A.P. Massey, E.A. Karren, P.F. Kiser, Dynamically restructuring hydrogel networks formed with reversible covalent crosslinks, *Adv. Mater.*, 19 (2007) 2503-2507.

- [7] S.J. Rowan, S.J. Cantrill, G.R.L. Cousins, J.K.M. Sanders, J.F. Stoddart, Dynamic covalent chemistry, *Angew. Chem.-Int. Edit.*, 41 (2002) 898-952.
- [8] A. South, L. Lyon, Autonomic self-healing of hydrogel thin films, *Angew. Chem. Int. Ed.*, 49 (2010) 767-771.
- [9] D.G. Hall, *Boronic Acids - Preparation and applications in organic synthesis and medicine*, John Wiley & Sons, 2005.
- [10] T.D. James, Saccharide-selective boronic acid based photoinduced electron transfer (PET) fluorescent sensors, *Top. Curr. Chem.*, 277 (2007) 107-152.
- [11] A.E. Ivanov, H. Larsson, I.Y. Galaev, B. Mattiasson, Synthesis of boronate-containing copolymers of N,N-dimethylacrylamide, their interaction with poly(vinyl alcohol) and rheological behaviour of the gels, *Polymer*, 45 (2004) 2495-2505.
- [12] S. Kitano, K. Kataoka, Y. Koyama, T. Okano, Y. Sakurai, Glucose-responsive complex-formation between poly(vinyl alcohol) and poly(N-vinyl-2-pyrrolidone) with pendent phenylboronic acid moieties, *Makrom. Chem-Rapid Commun.*, 12 (1991) 227-233.
- [13] M.C. Roberts, A. Mahalingam, M.C. Hanson, P.F. Kiser, Chemorheology of phenylboronate-salicylhydroxamate cross-linked hydrogel networks with a sulfonated polymer backbone, *Macromolecules*, 41 (2008) 8832-8840.
- [14] H. Duell, H. Neukom, Über die Reaktion von Borsäure und Borax mit Polysacchariden und anderen hochmolekularen Polyoxy-verbindungen, *Makromol. Chem.*, 3 (1949) 13-30.
- [15] E. Pezron, L. Leibler, A. Ricard, F. Lafuma, R. Audebert, Complex-formation in polymer ion solutions 1. Polymer concentration effects, *Macromolecules*, 22 (1989) 1169-1174.
- [16] S.W. Sinton, Complexation chemistry of sodium-borate with poly(vinyl-alcohol) and small diols - a B-11 NMR-study, *Macromolecules*, 20 (1987) 2430-2441.
- [17] M. Piest, J.F.J. Engbersen, Role of boronic acid moieties in disulfide containing poly(amido amine)s for non-viral gene delivery, See chapter 3 of this thesis, (2010).
- [18] M. Piest, J. Trinidad, J.F.J. Engbersen, Bioresponsive, restructuring hydrogels based on boronic acid functionalized poly(amido amine)s for reversible covalent crosslinking of poly(vinyl alcohol), See chapter 7 of this thesis, (2010).
- [19] W. Agut, A. Brulet, D. Taton, S. Lecommandoux, Thermoresponsive micelles from jeffamine-b-poly(L-glutamic acid) double hydrophilic block copolymers, *Langmuir*, 23 (2007) 11526-11533.
- [20] S.L. Wiskur, J.J. Lavigne, H. Ait-Haddou, V. Lynch, Y.H. Chiu, J.W. Canary, E.V. Anslyn, pK(a) values and geometries of secondary and tertiary amines complexed to boronic acids - Implications for sensor design, *Org. Lett.*, 3 (2001) 1311-1314.
- [21] P. Abiman, G.G. Wildgoose, A. Crossley, J.H. Jones, R.G. Compton, Contrasting pK(a) of protonated bis(3-aminopropyl)-terminated polyethylene glycol "Jeffamine" and the associated thermodynamic parameters in solution and covalently attached to graphite surfaces, *Chem.-Eur. J.*, 13 (2007) 9663-9667.
- [22] J. Yan, G. Springsteen, S. Deeter, B.H. Wang, The relationship among pK(a), pH, and binding constants in the interactions between boronic acids and diols - it is not as simple as it appears, *Tetrahedron*, 60 (2004) 11205-11209.
- [23] G. Springsteen, B.H. Wang, Alizarin Red S. as a general optical reporter for studying the binding of boronic acids with carbohydrates, *Chem. Commun.*, (2001) 1608-1609.
- [24] G. Springsteen, B.H. Wang, A detailed examination of boronic acid-diol complexation, *Tetrahedron*, 58 (2002) 5291-5300.
- [25] H.R. Mulla, N.J. Agard, A. Basu, 3-methoxycarbonyl-5-nitrophenyl boronic acid: high affinity diol recognition at neutral pH, *Bioorg. Med. Chem. Lett.*, 14 (2004) 25-27.
- [26] M. Bishop, N. Shahid, J.Z. Yang, A.R. Barron, Determination of the mode and efficacy of the cross-linking of guar by borate using MAS B-11 NMR of borate cross-linked guar in combination with solution B-11 NMR of model systems, *Dalton T.*, (2004) 2621-2634.
- [27] R.G. Loughlin, M.M. Tunney, R.F. Donnelly, D.F. Murphy, M. Jenkins, P.A. McCarron, Modulation of gel formation and drug-release characteristics of lidocaine-loaded poly(vinyl alcohol)-tetraborate hydrogel systems using scavenger polyol sugars, *Eur. J. Pharm. Biopharm.*, 69 (2008) 1135-1146.
- [28] G. Wulff, Selective binding to polymers via covalent bonds - the construction of chiral cavities as specific receptor-sites, *Pure Appl. Chem.*, 54 (1982) 2093-2102.
- [29] S. Iwatsuki, S. Nakajima, M. Inamo, H.D. Takagi, K. Ishihara, Which is reactive in alkaline solution, boronate ion or boronic acid? Kinetic evidence for reactive trigonal boronic acid in an alkaline solution, *Inorg. Chem.*, 46 (2007) 354-356.
- [30] M. Rietjens, P.A. Steenbergen, Crosslinking mechanism of boric acid with diols revisited, *Eur. J. Inorg. Chem.*, (2005) 1162-1174.

[31] C. Miyamoto, K. Suzuki, S. Iwatsuki, M. Inamo, H.D. Takagi, K. Ishihara, Kinetic evidence for high reactivity of 3-nitrophenylboronic acid compared to its conjugate boronate ion in reactions with ethylene and propylene glycols, *Inorg. Chem.*, 47 (2008) 1417-1419.

Effects of arm length and number of arms of phenylboronic acid functionalized poly(ethylene glycols) on the viscoelastic properties of reversible covalent crosslinked poly(vinyl alcohol) hydrogels



Abstract

Dynamically restructuring or so-called “self-healing” hydrogels can be prepared by complexation of boronic acid containing materials with polyols, such as poly(vinyl alcohol). To this purpose a series of novel boronated PEG-crosslinkers have been synthesized by reductive amination of amine-functionalized PEGs with 4-formylphenylboronic acid. Different PEG architectures were selected and the effects of the PEG arm length and the number of arms on the rheological properties of the resulting hydrogels with PVA were investigated under physiological conditions (PBS, pH 7.4, 37 °C). The gel strength, as based on the plateau storage modulus determined by oscillatory rheological measurements, was found to decrease for the 2-arm crosslinker with increasing PEG arm length (increasing PEG M_w). Similarly, the gel strength was found to increase with increasing number of arms of the multiarm boronated PEG-linkers. With this novel linker system, transparent thermo-reversible gels with storage moduli up to 30 kPa were attainable in PBS (pH 7.4, 37 °C). The gel strength, shape stability, and visual appearance of hydrogels formed with this novel linker and PVA can be tuned by proper adjustment of molecular architecture, M_w and concentration of both the PEG-linker and the PVA.

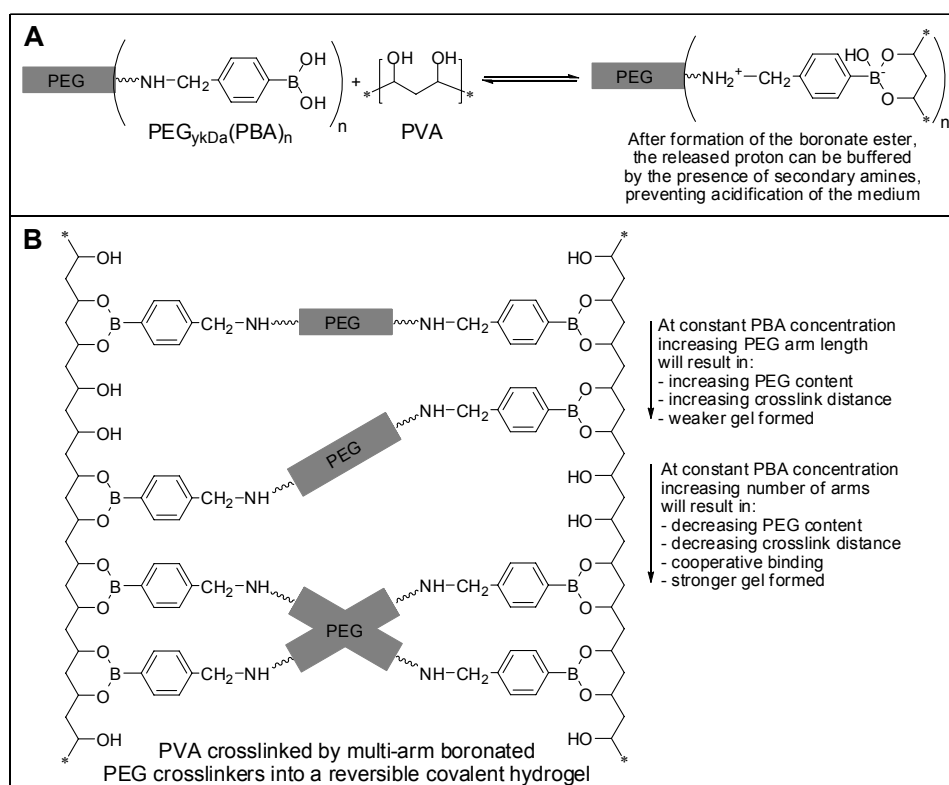
This chapter is being prepared for publication as: M. Piest, S.D. Hujaya, X. Zhang, and J.F.J. Engbersen. *Effects of arm length and number of arms of phenylboronic acid functionalized poly(ethylene glycols) on the viscoelastic properties of reversible covalent crosslinked poly(vinyl alcohol) hydrogels*

9.1. Introduction

Reversible covalent bond formation can be used to prepare dynamically restructuring, or so-called “self-healing”, materials with unique properties [1]. A typical example is the children’s toy from the 1950’s, called “Silly Putty”. This material owes its properties to the reversible boronic ester formation of boric acid with hydroxy-terminated poly(dimethylsiloxane) [2]. In the biomedical field reversible boronic or boronic ester formation has been employed to crosslink polyols such as poly(vinyl alcohol) (PVA) into a hydrogel [3-4]. Due to the pH- and temperature-sensitive boronic ester equilibrium, hydrogels can be prepared that are not only pH- and temperature-responsive, but also chemo-responsive as the boronic ester equilibrium is sensitive towards competing diols, as present in carbohydrates like glucose [5]. As a result, these type of boronic acid containing hydrogels could prove to be attractive materials for biomedical and pharmaceutical applications, including drug delivery, bioactuation, tissue engineering, regenerative medicine, *etc.* [6-8].

PVA is a neutral polymer with good properties for preparation of biomaterials, in the respect that PVA is biocompatible, as there are many examples of FDA approved PVA-based materials including hydrogels [9-10]. PVA can be crosslinked simply by borax (sodium borate), resulting in dynamically restructuring hydrogels at elevated pH [11-13]. However, the elevated pH > 9 needed for efficient boronic ester formation is not very suitable for most biomedical applications. The optimal pH for PVA crosslinking can be reduced by selecting phenylboronic acid (PBA) crosslinkers that also contain amine groups [14]. Several examples of PBA containing (co-)polymers for reversible crosslinking of PVA have been described [15-16], but many are complicated in their synthesis or application as they sometimes have limited water-solubility [17], or comprise poly(electrolytes) [18]. Ideally, a neutral and non-toxic biocompatible boronated complexing partner is desired. We have previously demonstrated that boronated Jeffamines can be used to efficiently crosslink PVA into self-healing hydrogels [19]. It was found that reductive amination of 2- and 4-formylphenylboronic acid to Jeffamine was an easy method to produce the diboronated crosslinkers Jeff-2AMPBA and Jeff-4AMPBA that could form intermediately strong hydrogels with PVA at low pH, whereas Jeff-4AMPBA could form strong gels at physiologically relevant pH 7.4. In this work these types of gel systems were further explored to improve gel strength for load-bearing applications (high G'_{\max}) or to increase gel degradation times. To this purpose PEG-diamines with different spacer length (M_w) or branched multi-arm PEG-amines were synthesized as starting materials for the development of 4AMPBA containing crosslinkers. These crosslinkers are abbreviated as $\text{PEG}_{y\text{kDa}}(\text{PBA})_n$, with y being the M_w and n the number of arms, and were screened on their ability to form gels with PVA under physiological mimicking conditions (in phosphate buffer saline, pH 7.4, 37 °C). The viscoelastic properties of the gels are

characterized by the plateau gel strength (G'_{\max}) and the relaxation times (τ). G'_{\max} is the maximum storage modulus, reflecting the gel strength upon deformation at high oscillatory frequency, and the relaxation time τ is a measure for the shape-stability of the gel, which should be long enough to ensure that the gel does not disintegrate if no force is applied, but also short enough to maintain the “self-healing” character of the hydrogel.



Scheme 1. A). Mechanism of boronic ester formation from a 4-aminophenylboronic acid functionalized PEG-arm with the 1,3-*cis*-diols of poly(vinyl alcohol) resulting in the formation of a boronate ester and water. The acidification due to boronate ester formation can be buffered by the secondary amines. **B).** The effect on the molecular architecture of the different crosslinkers on the gel strength. Increasing the PEG arm length can increase the crosslink distance and increasing the number of arms can result in cooperative binding.

It is known that mixing of PVA and PEG can result in the formation of hydrogels [20], depending on the concentration, the M_w , and the ratio of PVA and PEG in the system. This gel formation is due to phase-separation in microdomains, leading to the formation of an interpenetrating double network in which the crystalline PVA domains serve as physical crosslinks. These phase-separated gels are not transparent and have no “self-healing” character. However, we hypothesized that homogenous and

transparent hydrogels with “self-healing” abilities could be formed by using multi-arm PEG based crosslinkers enabling reversible boronic ester formation with PVA. Therefore, we have developed a series of novel boronic acid terminated PEG crosslinkers having different chain length and number of arms and have evaluated the rheological effect of these crosslinkers on PVA gels.

9.2. Materials and methods

9.2.1. Materials

4-Formylphenylboronic acid (4-FPBA, Aldrich), trioctylamine (TOA, Fluka), sodiumborohydride (NaBH_4 , Aldrich), poly(vinyl alcohol) (PVA, M_w 27, 47, 125, 195 kDa, Aldrich, 72 kDa, Merck), poly(ethylene glycol, α,ω -hydroxy terminated) (PEG-(OH)₂, M_w 3350, 5000, 10000 Da, Aldrich; 4ARM-PEG-10K (PEG-(OH)₄ M_w 10000 Da); 8ARM-PEG-10K and 8ARM-PEG-25K (PEG-(OH)₈ M_w 10000, and 25000 respectively) Da, JenKem Technology USA), methane sulfonyl chloride (Ms-Cl, Aldrich), were purchased in the highest purity available and used as received.

The degree of functionalization of all synthesized boronated PEG-linkers were determined by ¹H NMR (300 MHz, CD₃OD) spectra using a Varian Inova spectrometer.

9.2.2. Synthesis of multi-arm boronated PEG-crosslinkers

The conversion procedure of hydroxy-terminated PEGs to amine-terminated PEGs was adopted from [21]. The incorporation of aminomethylphenylboronic acid moieties by reductive amination of formylboronic acids to the amino end-groups of the multi-arm PEGs (Scheme 9.2) was performed as described previously by our group [22-23]. As the synthesis of the multi-arm boronated PEG crosslinkers was close to identical for all different PEG architectures, only the synthesis of PEG_{10kDa}(PBA)₈ will be given here as a typical example.

First, 20.7 g (2.0 mmol) of PEG_{10kDa}(OH)₈ with a hexaglycerine core (10 kDa, JenKem Technology USA) was dried by thrice azeotropic distillation from dry toluene (70 ml) under argon atmosphere. The residual dry PEG_{10kDa}(OH)₈ was dissolved in 10 ml freshly distilled dichloromethane, and 22 ml TOA was added dropwise under continuous stirring under argon atmosphere. Next, 4 ml of Ms-Cl was added dropwise at 0 °C using an ice bath. The yellow/brown solution was left to react for 2 days at ambient temperature. The PEG_{10kDa}(OMs)₈ was twice precipitated in diethylether and was isolated as white material (17.7 g, 81% yield). Next, the PEG_{10kDa}(OMs)₈ was dissolved in 70 ml aqueous ammonia for 4 days. The yellow solution was reduced to *ca.* 15 ml under rotational evaporation. The pH was adjusted to 13 with 4 M NaOH (aq) and the reaction product PEG_{10kDa}(NH₂)₈ was extracted thrice with 75 ml

dichloromethane. The combined organic phase was dried over Na_2SO_4 for 2 h and the solid was filtered-off. The clear yellow solution was evaporated by rotational evaporation to dryness and the residue was additionally dried *in vacuo* for 3 days, yielding 15.0 g of $\text{PEG}_{10\text{kDa}}(\text{NH}_2)_8$ as off-white powder (72% yield).

For the reductive amination, $\text{PEG}_{10\text{kDa}}(\text{NH}_2)_8$ (1.00 g; 0.04 mmol) and 4-formylphenylboronic acid (58 mg; 0.39 mmol) were dissolved in 5 ml methanol. The reaction was stirred at ambient temperature for 4 days under nitrogen-atmosphere during which the solution turned yellow. Next, NaBH_4 (36 mg; 0.96 mmol) was added portion-wise to the yellow solution. The reduction was allowed to proceed to completion for 2 h during which hydrogen gas evolution and a concomitant discoloring of the solution were observed. Next, the methanol was removed by rotational evaporation, and the residue was dissolved in milliQ water and purified by dialysis using 10 kDa M_w CO membrane. The retentate was then freeze-dried and $\text{PEG}_{10\text{kDa}}(\text{PBA})_8$ was obtained as white spongy material. Yield: 85%.

^1H NMR (CD_3OD): 7.4–7.1 ppm (*dd*, 32 H, Ar), 3.9 ppm (*s*, 16 H, Ar- CH_2 -NH-), 3.05–3.8 ppm (*m*, 890 H, -O- CH_2 - CH_2 -O-), 2.96 ppm (*t*, 16 H, -NH- CH_2 - CH_2 -O-).

9.2.3. Gel Preparation

To prepare gel samples, stock solutions of PVA with different M_w (27, 47, 72, 125, and 195 kDa) were prepared by dissolving the corresponding PVA in MilliQ water at 80 °C to a final concentration of 10% w/v.

Phosphate buffered saline (PBS, pH 7.4, 10 mM phosphate; 150 mM NaCl) was obtained from Braun and used as received. Stock solutions of all boronated materials were obtained by dissolving the corresponding boronated materials in PBS to obtain stock solutions of 10%, 20%, and 40% w/v. Gel samples were prepared by mixing 0.25 ml of the desired PVA solution with 0.25 ml of the desired boronated material in a closable small test tube and vortexed for 5 s. The tube was then sealed with Parafilm and the gel was allowed to equilibrate for at least 24 h at ambient temperature. For each type of gel sample, two identical gels were prepared as duplicates.

9.2.4 Oscillatory rheology

Oscillatory rheology experiments were performed on a Physica MCR 301 Rheometer (Anton Paar) equipped with a parallel plates sensor system. The gap (gel thickness) was varied between 0.3–0.6 mm in accordance to the specific gel system. Samples were prepared in duplo and each gel sample was measured 2–4 times. Gel samples were measured after temperature equilibrium was established. Water evaporation was prevented by applying a layer of silicon oil on top of the parallel plates.

For each sample a frequency sweep was measured in duplo at 25 and 37 °C, during which the gels were subjected to oscillating rotational deformations with frequencies (ω) from 100 to 0.05 Hz at the strain (γ) of 2%. The temperature was set to be constant at 25 or 37 °C. From each measurement, the crossover frequency ω_c was determined as the frequency where the loss modulus G'' was equal to the storage modulus G' (damping factor = 1). Relaxation time (τ) was calculated using the formula $\tau = 1/\omega_c$. Plateau value (G'_{\max}) was obtained as value of G' when it reaches a plateau at high frequency ($\omega = 20$ Hz).

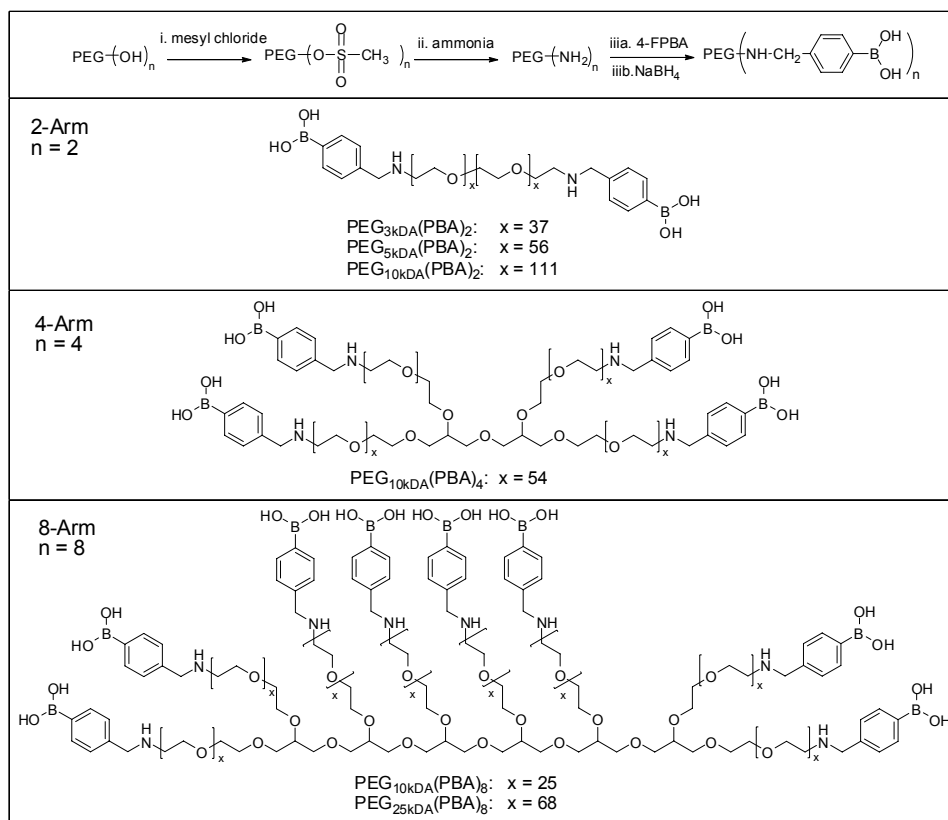
For temperature reversibility measurements, gels were subjected to oscillating rotational deformations at frequency of 20 Hz and strain of 2%. Temperatures were set to alternate between 25 °C and 37 °C, and kept constant during the time interval selected (typically 0.5 or 1.0 h). G'_{\max} was measured as function of time/temperature.

9.3. Results

9.3.1. Synthesis of multi-arm boronated PEG-linkers

The syntheses of the various PEG-linkers started with the functional group interconversion from PEG-hydroxyl starting materials to PEG-amine, according to a literature procedure [21], see Scheme 9.2.

Different from the procedure described in [21], the use of TEA as base in the mesylation step was substituted by TOA that proved to be better soluble in diethyl ether, thereby preventing coprecipitation with the PEG-mesylate. Ammonia removal was performed by rotational evaporating under reduced pressure to reduce work-up time. The reaction was monitored with ^1H NMR through the appearance of a triplet signal at δ 2.8 ppm, indicative of the methylene protons next to the amine functionalities. The benzyl conversion was calculated by comparing the integration of these protons with the proton integration value of the PEG backbone signal at δ 3.20–3.95 ppm and to that of the *alpha* hydrogens of the PEG chain. The benzyl conversion was found to be complete in all cases, yielding white powders with an average isolated yield of *ca.* 90%. Next, phenylboronic acid (PBA) moieties were introduced by reductive amination with 4-formylphenylboronic acid (4-FPBA), as described previously [22-23]. Schiff base formation was allowed to proceed for 4 days, ensuring the complete conversion of all amines after which the yellow solutions were reduced by NaBH_4 and turned colorless again. Dialysis was selected as purification method of choice as small molecular weight byproducts and unreacted excess of 4-FPBA could be easily removed from the high molecular weight product. After lyophilization, the complete conversion of amines was confirmed by ^1H NMR by integration of the aromatic protons of the PBA moieties.



Scheme 9.2. Synthetic pathway and overview of the structure of the various PEG-linkers. i) Multi-arm PEG-OH was converted into PEG-mesylate in dichloromethane. ii) The PEG-mesylate is reacted with ammonia (aq) to yield the corresponding PEG-amine. iiia) The Schiff base of the PEG-amine and 4-formylphenylboronic acid (4FPBA) was formed in methanol and iiib) reduced with NaBH₄. Structures of 2-arm, 4-arm and 8-arm PEG derivatives with general formula PEG_{ykDa}(PBA)_n, with y being the M_w and n the number of arms. The parameter x is defined as the number of ethylene oxide groups per PBA functionality.

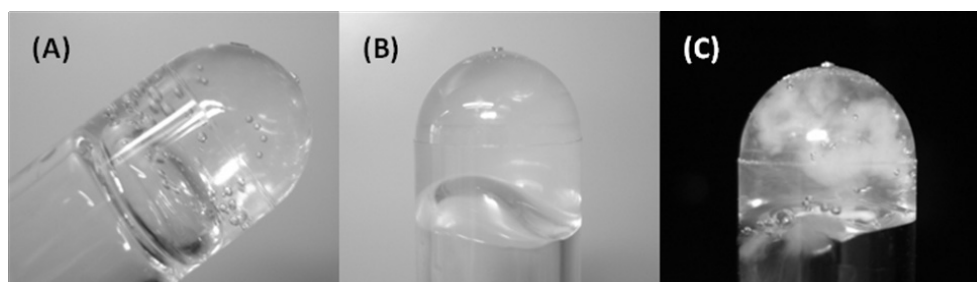


Figure 9.1. Examples of different visual appearances of the gels prepared: (A) type I transparent gel, (B) type II opaque gel, (C) type III turbid and cloudy gel.

9.3.2. Gel appearance and gel strength due to the molecular architecture

The different boronated PEG crosslinkers were tested on their ability to form dynamically restructuring hydrogels with PVA. To this purpose 10% w/v of the

different boronated PEG-derivatives were prepared and mixed 1:1 v/v with 10% w/v of 195 kDa PVA. Gels were classified as type I, indicating a transparent dynamically restructuring hydrogel; type II, indicating a turbid or opaque hydrogel with higher shape stability; and type III, including cloudy fragments of crystalline PVA, sometimes accompanied by phase separation or gel collapse. An overview is given in Figure 9.1.

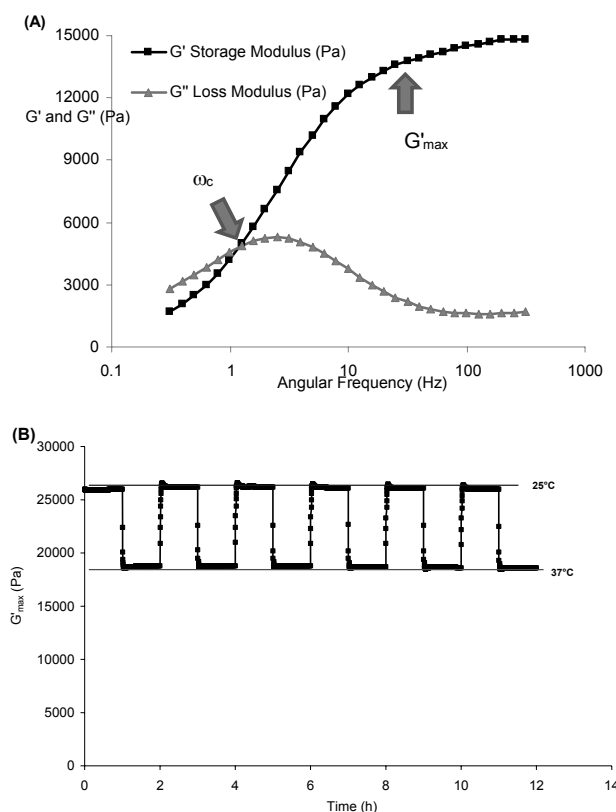


Figure 9.2. Typical frequency sweep (A) and temperature reversibility / time stability graph (B) for $\text{PEG}_{x\text{kDa}}(\text{PBA})_y$ and 195 kDa PVA (at 20 Hz). The gel sample was kept for 1 h at alternating temperature of 25 and 37 °C. Lines are added for clarity to stress that gel strength was constant during the measurement and response to temperature changes were immediately and completely reversible.

Besides the physical appearance, rheology measurements were performed consisting of frequency sweeps at 25 and 37 °C to determine the plateau storage modulus G'_{max} at 20 Hz and the relaxation time τ derived from the crossover frequency at which the storage modulus G' equals the loss modulus G'' . A typical example of a frequency sweep is depicted in Figure 9.2A, where the gel strength is plotted versus the angular frequency. The crossover frequency (ω_c) indicates the change from an elastic gel at high angular frequency to a viscous solution at low angular frequency, and the presence of a crossover frequency is indicative of the “self-healing” properties of a gel.

Additional strain sweeps were taken to confirm that these measurements were in the linear-viscoelastic region at the strain of 2% selected. To verify whether the gels were in equilibrium, additional time/temperature stability tests were performed, and a typical temperature reversibility graph can be seen in Figure 9.2B. From the temperature reversibility graph, it can be observed that the temperature response is fast and completely reversible. Ideally, G'_{\max} of a gel should not change in time, which is observed in Figure 9.2.

In the first series of experiments, crosslinkers with different M_w and number of arms were investigated for their property of gel formation with 195 kDa PVA. In these experiments relatively low concentrations of PEG and PVA of 10% w/v were selected to prevent demixing of the gels. The results are shown in Figure 9.3.

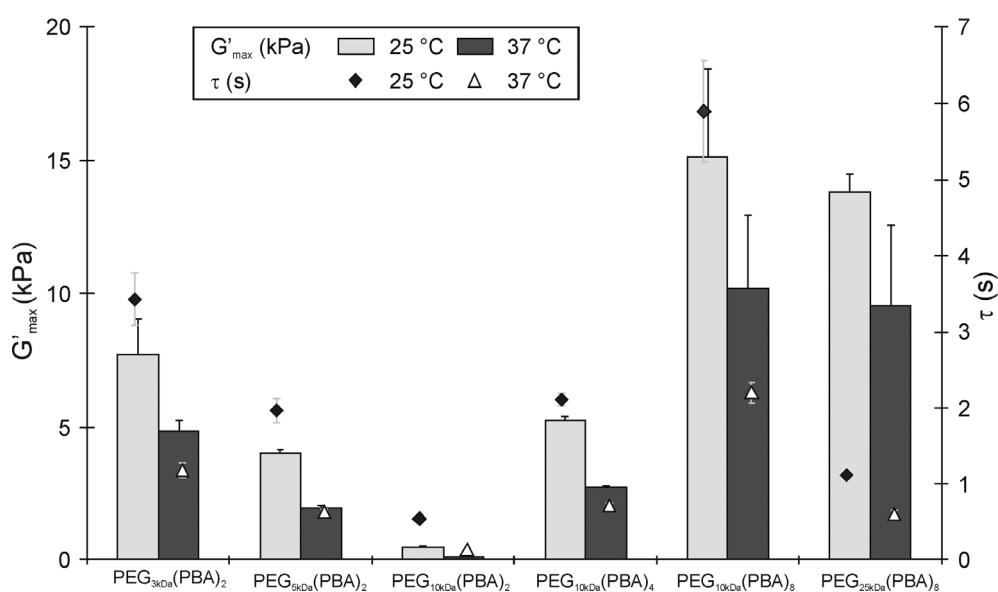


Figure 9.3. G'_{\max} (bars) and τ (symbols) of various gels prepared upon mixing of 10% w/v PEG_{kDa}(PBA)_n 1:1 v/v with 10% w/v of PVA 195kDa in PBS pH 7.4. Samples were measured at 25 °C (light bars and black diamonds) and at 37 °C (dark bars and white triangles).

Frequency sweeps of the gels prepared by mixing of equal volumes of the different boronated crosslinker solutions with 195 kDa PVA solutions at 25 and 37°C yielded the plateau gel strengths G'_{\max} (kPa) that are depicted in Figure 9.3 as light and dark bars, respectively. The crossover frequencies of these gels were also determined from these frequency sweeps and the relaxation times τ (s) are included in Figure 9.3, depicted as diamonds and triangles respectively. Depending on the molecular architecture of the crosslinkers, gels with strengths up to 15 kPa could be obtained. It can be observed that the 2-arm crosslinkers decrease in gel strength with increasing

arm length from 3 to 5 and 10 kDa. Also, the gel strength increases with increasing number of arms. As the PEG content is kept constant, the strongest gel was expected for the sample with the highest crosslink density due to boronate ester formation. This was expected for PEG_{25kDa}(PBA)₈ of which the arm length is shortest, as the ratio of repeating units of ethylene oxide per PBA functional group (x) is only 25 (Scheme 9.2). Therefore, this system has a significantly higher phenylboronic acid concentration [PBA], resulting in the highest crosslink density within this series. Remarkably, the highest gel strength of 15 kPa was observed for PEG_{10kDa}(PBA)₈. The gels prepared from PEG_{25kDa}(PBA)₈ and PVA of 195 kDa initially showed low gel content, with a small fraction of colorless liquid visibly separated from the bulk gel. Whereas for the other gels longer equilibration times typically resulted in more homogeneous gels, in this special case of PEG_{25kDa}(PBA)₈ the demixed state did not homogenize in time. One possible explanation is gel-collapse due to the high M_w architecture of the PEG backbone, as phase separation is strongly depending on both the concentration and the M_w of the PVA and PEG [20]. In conclusion, the hydrogel properties are dominated by the PBA concentration in the gel and phase separation was only observed for the PEG_{25kDa}(PBA)₈.

To elaborate on the effects of the hydrogel properties resulting from the molecular architecture of the crosslinkers, gels were prepared with identical crosslink density by keeping the PBA concentration constant. Two effects of the different molecular geometries of the crosslinker were assessed separately. First, the effect of the crosslink distance (the arm-length of the linker) was investigated by comparing samples with varying PEG chain length at constant PBA concentration. Second, the cooperative effect of the multi-arm PEG architecture was investigated by comparing samples with increasing number of arms at constant PBA concentration.

9.3.3. Effects of arm length on the hydrogel properties

The effect of the length of the arm was investigated with the gels prepared with 13.4% w/v PEG_{3kDa}(PBA)₂, 20% w/v of PEG_{5kDa}(PBA)₂, and 40% w/v of PEG_{10kDa}(PBA)₂ mixed 1:1 v/v with 10% w/v of PVA 195 kDa in PBS (pH 7.4). This corresponds to a PBA concentration of 0.04 M and a concentration of hydroxyl groups of PVA of 1.14 M in the resulting hydrogel, or on average 39 phenylboronic ester moieties per PVA chain. Upon increasing the M_w of the PEG derivatives from 3 kDa to 5 kDa and 10 kDa, the number of ethylene oxide units per PBA moiety increases from 37 to 56 to 111, respectively (Scheme 9.2). This means that not only the PEG content increases (from 13% to 40% w/v of the stock solutions), but also that the crosslinks are spaced further apart. Although the crosslink density was similar, it was observed that the increase in PEG content resulted in a different physical appearance of the gels. Gels prepared with 13.4% w/v PEG_{3kDa}(PBA)₂ were of type I (transparent),

gels with 20% w/v of PEG_{5kDa}(PBA)₂ were of type II (opaque), and gels with 40% w/v of PEG_{10kDa}(PBA)₂ were of type III (turbid), see Figure 9.1. These gels were further characterized by oscillatory rheology and the resulting gel strengths and relaxation times are depicted in Figure 9.4.

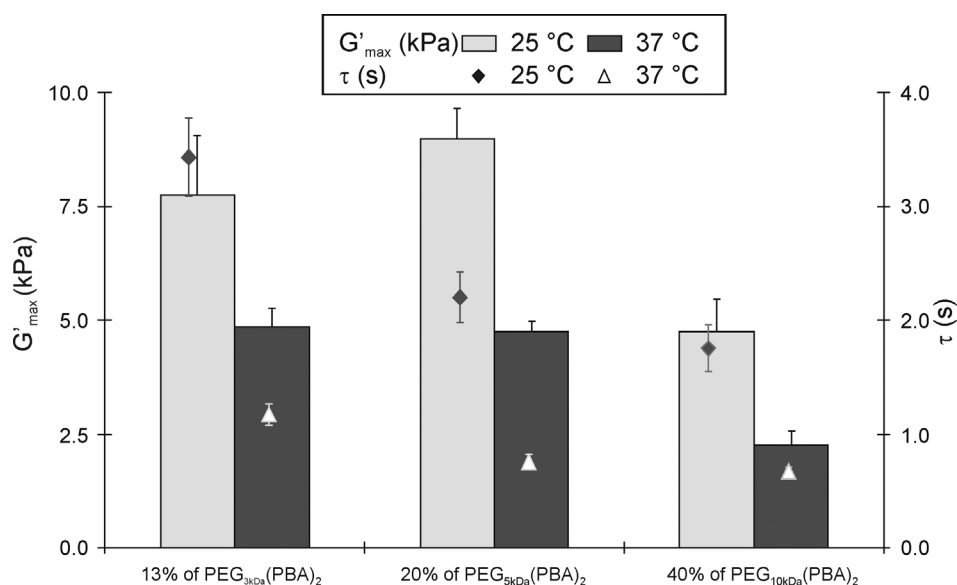


Figure 9.4. Effect of length of the arm on the gel properties of 13.4% w/v PEG_{3kDa}(PBA)₂, 20% w/v of PEG_{5kDa}(PBA)₂, and 40% w/v of PEG_{10kDa}(PBA)₂ mixed 1:1 v/v with 10% w/v of PVA 195 kDa in PBS (pH 7.4). G'_{max} was determined at 20 Hz (bars) and τ was determined from the cross-over frequency (symbols) at 25 °C (light grey, diamonds) and 37 °C (dark grey, triangles).

It was observed that for all three two-arm PEG derivatives fairly strong gels were obtained in the range of 5–10 kPa (Figure 9.4). Gels prepared from PEG_{3kDa}(PBA)₂ and PEG_{5kDa}(PBA)₂ were significantly stronger than gels prepared from PEG_{10kDa}(PBA)₂. From these results it appears that increasing the PEG content weakens the gel. Moreover, by increasing the crosslink distance by increasing the PEG arm length from 37 to 111 ethylene oxide units per PBA (PEG_{3kDa} and PEG_{10kDa}, respectively) the relaxation time is drastically reduced from 3.43 s to 1.75 s at 25 °C. From this it appears that shorter crosslink distances result in more rigid and stronger gels, accompanied by a higher shape-stability as demonstrated by the longest relaxation times observed for the PVA gel crosslinked by PEG_{3kDa}(PBA)₂. Moreover, the weakening of the gels upon increasing the temperature from 25 to 37 °C is most dramatic for the PEG_{10kDa}(PBA)₂ based gel, as G'_{max} is reduced from *ca.* 5.0 kPa to only 2.2 kPa. This is most likely resulting from the higher mobility of the PBA moieties at the end of the PEG chains, as these ends are further spaced apart for PEG_{10kDa} as compared to PEG_{3kDa} and PEG_{5kDa}.

9.3.4. Effect of the number of boronated PEG- arms on the gel properties

In order to study the cooperative effects of the multi-arm PEG derivatives, samples were prepared with 40% w/v of PEG_{10kDa}(PBA)₂, 20% w/v of PEG_{10kDa}(PBA)₄, and 10% w/v of PEG_{10kDa}(PBA)₂ mixed 1:1 v/v with 10% w/v of PVA. Again the concentration of phenylboronic acid [PBA] was constant while the PEG content was decreased upon increasing the number of arms. As the number of arms of the PEG derivatives increases from 2 to 4 and 8 arms, the number of ethylene oxide units per PBA moiety (x) decreases from 111 to 54 to 25, respectively (Scheme 9.2). Based upon the previous results regarding the 2-arm gels, it was expected that the 8-arm gels ($x = 25$) would result in strongest gels with highest relaxation times in this series. Moreover, it was expected that the cooperative binding, enabled by the multi-arm architecture, could also efficiently crosslink low M_w PVA into rigid hydrogels. Gels were formed using these multi-arm PEG crosslinkers and PVA of varying M_w and the resulting gel properties are shown in Figure 9.5.

From Figure 9.5 several trends can be observed. First, increasing the number of arms increases the gel strength, which was observed for each M_w of PVA selected. Second, the gel strength for both PEG_{10kDa}(PBA)₂ and PEG_{10kDa}(PBA)₄ based gels was increasing with the M_w of the PVA. In sharp contrast, the gel strength of gels prepared with PEG_{10kDa}(PBA)₈ seemed to be independent of the M_w of the PVA selected as G'_{max} at 25 °C was between 25.0 kPa for 47 kDa PVA and 15.1 kPa for 195 kDa PVA with standard deviations up to 6.3 kPa. Regarding the relaxation times, for the 2-arm and 4-arm it can be observed that τ gradually increases with the M_w of the PVA selected. A similar trend was observed for the 8-arm as τ increased from 1.93 s for 27 kDa PVA to 5.89 s for 195 kDa PVA. These very long relaxation times indicate that these gels are rigid and that the dynamic properties are reduced. It was observed that the rigid gels take longer time to homogenize.

In order to obtain an indication of the effect of non-ideal homogenization, the gel prepared from 10% w/v of PEG_{10kDa}(PBA)₈ mixed 1:1 v/v with 195 kDa PVA was subjected to a time-temperature reversibility test. The results given in Figure 9.6 show that the gel initial strength was 20–22 kPa, which is somewhat higher than the 15 kPa depicted in Figure 9.5 but still within the error margins of 3.2–6.3 kPa observed for the 8-arm gels (Figure 9.5). Remarkably, the gel strength further increased during the measurement up to 29 kPa. These data suggest that the diffusion for the 8-arm PEG crosslinker is limited and the mechanical mixing during the rheological measurement is increasingly homogenizing the sample, thereby significantly increasing G'_{max} . The reduced diffusion can be attributed to the high viscosity of the M_w PVA and PEG solutions used, and the instantaneous gel formation due to the cooperative binding of the multi-arm architecture. This behavior also explains the high standard deviations of up to 6.3 kPa found for these gels (Figure 9.5).

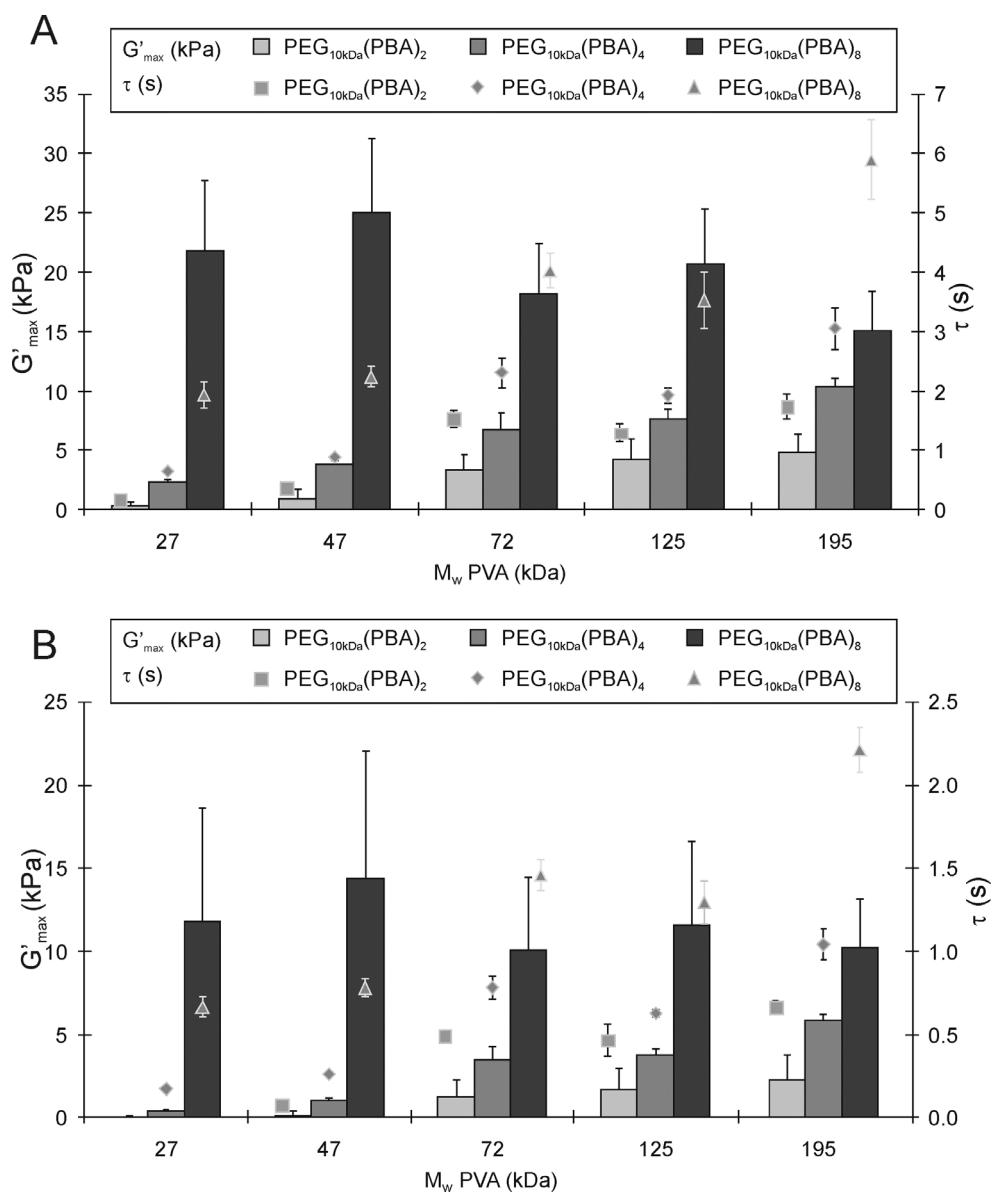


Figure 9.5. Effect of the number of the arm of the multi-arm boronated PEG-linkers on G'_{max} (bars) and τ (symbols) at 25 °C (A) and at 37 °C (B). Gels were prepared by mixing 10% w/v solutions of different M_w PVA 1:1 v/v with 40% w/v of PEG_{10kDa}(PBA)₂ (light grey, squares), 20% w/v of PEG_{10kDa}(PBA)₄ (dark grey, diamonds), and 10% w/v of PEG_{10kDa}(PBA)₈ (darkest grey, triangles) to keep [PBA] constant.

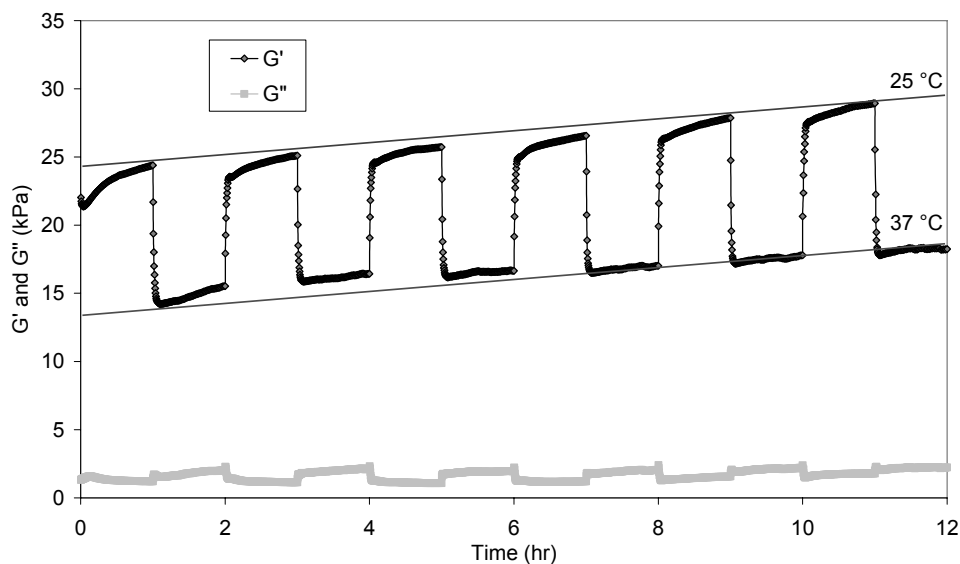


Figure 9.6. Time-temperature stability test for gels prepared with 10% w/v of PEG_{10kDa}(PBA)₈ mixed 1:1 v/v with 10% w/v of 195kDa PVA. The gel was allowed to equilibrate for 1 prior to the measurement. Next, samples were kept at 25 or 37 °C for 30 or 60 minute time intervals, lines are added for clarity.

9.4. Discussion

9.4.1. Gelation mechanism and hydrogel formation

Different PEG-based boronic acid crosslinkers with different architectures could be easily prepared in good yield. Upon mixing, these crosslinkers instantaneously form gels with PVA, of which the strength is strongly depending on the architecture of the crosslinker (Figure 9.3). The gels were typically transparent indicating that the components of the gel are homogeneously distributed in the gel. The formation of crosslinks in our hydrogel system is based on reversible boronic acid-diol ester formation giving gels self-healing and thermo-reversible properties. With higher M_w crosslinkers, stronger gels are formed, although for the highest M_w PEG crosslinkers (10 and 25 kDa, 8-arm) and for the 2-arm crosslinkers at higher concentration (40%) microphase separation was observed. Phase-separation of PVA and PEG in microdomains can result in the formation of a double penetrated network, resulting in the formation of a turbid gel [20]. In our system microphase separation results in weakening of the gels. Upon mixing of PVA and boronated PEG-linker solutions, boronic acid-diol complexation, and boronate ester formation, and accordingly gelation, takes place instantaneously, and this unique feature would allow for injectable hydrogels. However, a potential drawback is that after mixing of the two solutions a rapid increase in viscosity prevents the homogeneous distribution of the crosslinks

within the hydrogel. In time, most gels that started opaque turned transparent, indicating that there is a rearrangement in the crosslink distribution throughout the gel. This homogenization demonstrates that the gel has flow behavior, hence a “self-healing” character that is confirmed by the presence of a crossover frequency in oscillatory rheological measurements. The reversible nature of the complexation allows the crosslinks to break and reform to a state with lower energy, which is achieved upon a more homogeneous distribution. The gradual disappearance of crystalline PVA clusters that appear immediately after mixing also serves as a proof that the crosslink in the hydrogel is based on reversible boronate ester formation.

9.4.2. Effect of the arm length of the crosslinker

When gels were prepared with equal crosslink density, *i.e.* the concentration of PBA moieties [PBA] in the system is constant, it can be expected that increase of the arm length of the crosslinkers results in increase of the elasticity as reflected by G'_{\max} of the gels. Longer arm length allows for more polymer entanglement and hence stronger hydrogels. As [PBA] is constant, the concentration of PEG backbone also increases with increasing arm length (M_w), which was found to have a negative effect on the gel strength and the relaxation time (Figure 9.4). However, it was observed that the gels from 2-arm PEG with increasing arm length were increasingly opaque. From this it was concluded that although the PBA and PVA concentration are kept constant, upon increasing the concentration of PEG partial crystallization of the PVA is decreasing the G'_{\max} . This can be explained by the idea that the crystalline PVA chains are not available for boronic ester formation, hence the local crosslink density decreases as the phase separation increases. In conclusion, the rheological properties of the PVA based gels (G'_{\max} and τ) are not only depending on the crosslink density ([PBA]), but also negatively influenced by increasing PEG content.

9.4.3. Effect of the number of arms of the crosslinker

These multi-arm PEG-PVA gel systems can be viewed as PVA crosslinked by the PBA moieties of the multi-arm PEG crosslinkers, but also as multi-arm PEG crosslinked by the 1,3-diols of the PVA chains. In this respect, a 2-arm crosslinker is more prone to movement and repositioning upon the dissociation of a single boronic ester, whereas diffusion of the 4- and 8-arm crosslinkers requires that all but one of the boronic esters need to be hydrolyzed at the same time. In addition, it can be argued that the first formation of a PBA-PVA boronic ester crosslink will facilitate the formation of the next boronic ester by one of the other arms as the entropy loss is now less for the already immobilized PEG crosslinker. Even as the lifetime of a single crosslink is limited, the presence of other crosslinks prevents complete dissociation of the PVA and the PEG chains and as a result the diffusion of PBA moieties is limited for the

multi-arm system, which is resulting in gels with higher shape-stability and longer relaxation times.

Also for the PVA crosslinked by the multi-arm PEG crosslinkers at identical concentrations of PBA moieties the PEG content is decreased as the number of arms is increased. To verify whether there is a cooperative effect for the 4-arm PEG crosslinker, a comparison can be made with a 2-arm PEG crosslinker with similar number of ethylene oxide units per PBA moiety (x) under identical circumstances. The best comparison is between the gels prepared with 20% w/v of $\text{PEG}_{5\text{kDa}}(\text{PBA})_2$ with $x = 56$ (Figure 9.4) and 20% w/v of the $\text{PEG}_{10\text{kDa}}(\text{PBA})_4$ with $x = 54$ (Figure 9.5) mixed 1:1 v/v with 10% w/v of 195 kDa PVA. For both gels the concentration of PBA moieties, PVA, and PEG are close to identical, hence differences in gel properties are resulting from the cooperative binding of the PBA moieties to the PVA chains. For $\text{PEG}_{5\text{kDa}}(\text{PBA})_2$ G'_{max} is 9.0 ± 0.67 kPa, which is similar to the G'_{max} of 10.4 ± 2.70 kPa for $\text{PEG}_{10\text{kDa}}(\text{PBA})_4$, suggesting little beneficial effects for the cooperative binding due to the branched multi-arm architecture. Also the relaxation time of 2.2 ± 0.22 s for the linear crosslinker is almost similar to 1.8 ± 0.20 s for the 4-arm crosslinker, suggesting no significant change in diffusion or entanglement originating from the branched architecture.

However, for the 8-arm PEG it is apparent that the cooperative effect does play a major role. Already from Figure 9.3 it can be observed that mixing $\text{PEG}_{10\text{kDa}}(\text{PBA})_8$ or $\text{PEG}_{25\text{kDa}}(\text{PBA})_8$ with 195 kDa PVA, results in gels of approximately equal strength, as G'_{max} is 15.1 ± 3.2 kPa for the 10 kDa crosslinker and G'_{max} is 13.8 ± 0.7 kPa for the 25 kDa crosslinker, showing little dependency of the PBA concentration. As the number of ethylene oxide units per PBA functionality $x = 25$ for the 10 kDa crosslinker and $x = 68$ for the 25 kDa crosslinker, the concentration of PBA moieties of the 10 kDa crosslinker is approximately 2.7 times higher than that of the 25 kDa crosslinker. However, although this higher concentration of PBA moieties is not significantly affecting the G'_{max} , it is resulting in significant longer relaxation time for the 10 kDa crosslinker as $\tau = 5.9 \pm 0.67$ s, compared to $\tau = 1.1 \pm 0.01$ s for the 25 kDa crosslinker, indicating that the cooperative binding effect is stronger when the PBA moieties are residing closer together.

The real benefits of cooperative binding are observed for the lower M_w PVA, as the G'_{max} was independent of the M_w PVA for the 8-arm gels and not for the 2-arm and 4-arm gels. It could be argued that for the 8-arm gels the maximum achievable G'_{max} is already reached with the 27 kDa PVA and therefore no further increase of G'_{max} can be observed upon increase of the M_w of PVA (Figure 9.5). If it is taken into account that the 8-arm PEG based gels showed an increase in G' over time, attributed to the inhomogeneity of the gel, it can be assumed that the values of G'_{max} depicted in Figure 9.5 are underestimated compared to gels that would possess ideal mixing (at least

for gels with 195 kDa and 125 kDa PVA where increasing G' over time was observed). Importantly, as it was possible to produce strong gels with PVA of low M_w , and low M_w PVA solutions are significantly less viscous and easier to handle, injectable hydrogels for relevant biomedical applications become within reach with these systems.

9.5. Conclusions

Different 4-aminomethylphenylboronic acid functionalized PEG crosslinkers with different molecular architectures were synthesized to obtain hydrogels by reversible covalent crosslinking of PVA. It was found that the mixing of a solution of a boronated PEG crosslinker $\text{PEG}_{y\text{kDa}}(\text{PBA})_n$ with a solution of PVA results in the instantaneous formation of a transparent hydrogel. The gel strength, shape stability, and visual appearance of the hydrogels can be tuned by proper adjustment of the molecular architecture, M_w and concentration of both the $\text{PEG}_{y\text{kDa}}(\text{PBA})_n$ and the PVA, and it was possible to obtain strong gels with G'_{max} up to 30 kPa for the 8-arm PEG crosslinker.

It was hypothesized that upon increasing the arm length of the 2-arm PEG crosslinkers more entanglement would result in stronger gels. Opposite to the hypothesis, it was found that increasing the arm length decreases the strength of the gel. It was also hypothesized that multi-arm architectures would facilitate cooperative binding, resulting in stronger gels with high shape stability. It was found that upon increasing the number of arms of the PEG crosslinker system it is possible to increase the gel strength and shape stability, as G'_{max} was increased 3–4 times upon increasing the number of arms from 2 to 4, and 4–6 times as the number of arms is increased to 8. Most importantly, the cooperative boronic ester formation resulted in the fact that 8-arm boronated PEG derivatives were capable of crosslinking low M_w PVA into strong hydrogels. This finding implies that the preparation of strong hydrogels under physiological conditions is not only restricted to high M_w PVA systems, thereby paving the road for the development of new injectable biomaterials.

9.6. References

- [1] S.J. Rowan, S.J. Cantrill, G.R.L. Cousins, J.K.M. Sanders, J.F. Stoddart, Dynamic covalent chemistry, *Angew. Chem. - Int. Edit.*, 41 (2002) 898-952.
- [2] R.R. MacGregor, Treating dimethyl silicon polymer with boric acid in, Corning Glass Works, U.S.A., 1947.
- [3] S. Kitano, K. Kataoka, Y. Koyama, T. Okano, Y. Sakurai, Glucose-responsive complex-formation between poly(vinyl alcohol) and poly(N-vinyl-2-pyrrolidone) with pendent phenylboronic acid moieties, *Makrom. Chem-Rapid Commun.*, 12 (1991) 227-233.
- [4] A.E. Ivanov, K. Shiomori, Y. Kawano, I.Y. Galaev, B. Mattiasson, Effects of polyols, saccharides, and glycoproteins on thermoprecipitation of phenylboronate-containing copolymers, *Biomacromolecules*, 7 (2006) 1017-1024.
- [5] J. Yan, G. Springsteen, S. Deeter, B.H. Wang, The relationship among $\text{pK}(a)$, pH , and binding constants in the interactions between boronic acids and diols - it is not as simple as it appears, *Tetrahedron*, 60 (2004) 11205-11209.
- [6] W.Q. Yang, X.M. Gao, B.H. Wang, Boronic acid compounds as potential pharmaceutical agents, *Med. Res. Rev.*, 23 (2003) 346-368.

- [7] T. Konno, K. Ishihara, Temporal and spatially controllable cell encapsulation using a water-soluble phospholipid polymer with phenylboronic acid moiety, *Biomaterials*, 28 (2007) 1770-1777.
- [8] J.I. Jay, S. Shukair, K. Langheinrich, M.C. Hanson, G.C. Cianci, T.J. Johnson, M.R. Clark, T.J. Hope, P.F. Kiser, Modulation of viscoelasticity and HIV transport as a function of pH in a reversibly crosslinked hydrogel, *Adv. Funct. Mater.*, 19 (2009) 2969-2977.
- [9] E. Chiellini, A. Corti, S. D'Antone, R. Solaro, Biodegradation of poly (vinyl alcohol) based materials, *Prog. Pol. Sci.*, 28 (2003) 963-1014.
- [10] S.L. Bourke, M. Al-Khalili, T. Briggs, B.B. Michniak, J. Kohn, L.A. Poole-Warren, A photo-crosslinked poly(vinyl alcohol) hydrogel growth factor release vehicle for wound healing applications, *Aaps Pharmsci.*, 5 (2003) Artn 33.
- [11] I.D. Robb, J. Smeulders, The rheological properties of weak gels of poly(vinyl alcohol) and sodium borate, *Polymer*, 38 (1997) 2165-2169.
- [12] P.A. Sienkiewicz, D.C. Roberts, Chemical affinity systems .1. pH-dependence of boronic acid-diol affinity in aqueous-solution, *J. Inorg. Nucl. Chem.*, 42 (1980) 1559-1575.
- [13] S.W. Sinton, Complexation chemistry of sodium-borate with poly(vinyl-alcohol) and small diols - a B-11 NMR-study, *Macromolecules*, 20 (1987) 2430-2441.
- [14] I. Hisamitsu, K. Kataoka, T. Okano, Y. Sakurai, Glucose-responsive gel from phenylborate polymer and poly(vinyl alcohol): Prompt response at physiological pH through the interaction of borate with amine group in the gel, *Pharmaceut. Res.*, 14 (1997) 289-293.
- [15] A.E. Ivanov, H. Larsson, I.Y. Galaev, B. Mattiasson, Synthesis of boronate-containing copolymers of N,N-dimethylacrylamide, their interaction with poly(vinyl alcohol) and rheological behaviour of the gels, *Polymer*, 45 (2004) 2495-2505.
- [16] S. Kitano, Y. Koyama, K. Kataoka, T. Okano, Y. Sakurai, A novel drug delivery system utilizing a glucose responsive polymer complex between poly (vinyl alcohol) and poly (N-vinyl-2-pyrrolidone) with a phenylboronic acid moiety, *J. Control. Release*, 19 (1992) 161-170.
- [17] T. Hoare, R. Pelton, Engineering glucose swelling responses in poly(N-isopropylacrylamide)-based microgels, *Macromolecules*, 40 (2007) 670-678.
- [18] R.G. Loughlin, M.M. Tunney, R.F. Donnelly, D.F. Murphy, M. Jenkins, P.A. McCarron, Modulation of gel formation and drug-release characteristics of lidocaine-loaded poly(vinyl alcohol)-tetraborate hydrogel systems using scavenger polyol sugars, *Eur. J. Pharm. Biopharm.*, 69 (2008) 1135-1146.
- [19] M. Piest, X. Zhang, J. Trinidad, J.F.J. Engbersen, Dynamically restructuring hydrogels based on the reversible covalent crosslinking of poly(vinyl alcohol) by diboronated Jeffamines, See chapter 9 of this thesis, (2010).
- [20] I. Inamura, Liquid-liquid phase-separation and gelation in the poly(vinyl-alcohol) poly(ethylene glycol) water-system - dependence on molecular-weight of poly(ethylene glycol), *Polym. J.*, 18 (1986) 269-272.
- [21] D.L. Elbert, J.A. Hubbell, Conjugate addition reactions combined with free-radical cross-linking for the design of materials for tissue engineering, *Biomacromolecules*, 2 (2001) 430-441.
- [22] M. Piest, J.F.J. Engbersen, Role of boronic acid moieties in disulfide containing poly(amido amine)s for non-viral gene delivery, See chapter 3 of this thesis, (2010).
- [23] M. Piest, J. Trinidad, J.F.J. Engbersen, Bioresponsive, restructuring hydrogels based on boronic acid functionalized poly(amido amine)s for reversible covalent crosslinking of poly(vinyl alcohol), See chapter 7 of this thesis, (2010).

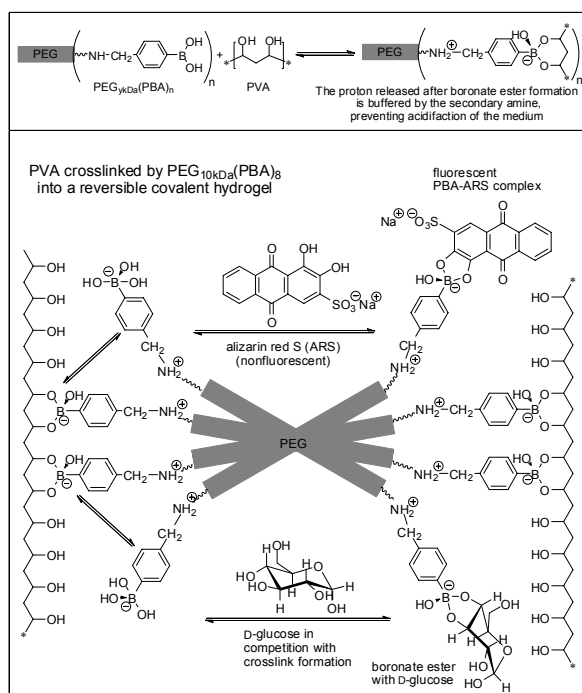
Appendix Chapter 9

Table 9.1. Visual appearances of gels.

Arm_Mw	Wt (%)	PVA (kDa)	G' _{max} at 25 °C	τ at 25 °C	G' _{max} at 37 °C	τ at 37 °C	Gel Type
2_3kDa	13.4	195	7740 ± 1320	3.43 ± 0.34	4843 ± 427	1.18 ± 0.09	I
2_5kDa	10	195	4005 ± 99	1.97 ± 0.16	1955 ± 93	0.63 ± 0.04	I
2_5kDa	20	195	8968 ± 666	2.20 ± 0.22	4760 ± 225	0.75 ± 0.07	II
2_10kDa	10	195	454 ± 58	0.54 ± 0.06	97 ± 18	0.14 ± 0.02	I
2_10kDa	40	27	259 ± 55	0.17 ± 0.02	16 ± 4	no gel	II
2_10kDa	40	47	921 ± 32	99 ± 3	0.36 ± 0.02	0.07 ± 0.00	II
2_10kDa	40	72	3268 ± 82	1.54 ± 0.14	1235 ± 44	0.50 ± 0.01	III
2_10kDa	40	125	4218 ± 429	1.30 ± 0.17	1625 ± 108	0.47 ± 0.10	III
2_10kDa	40	195	4755 ± 705	1.75 ± 0.20	2238 ± 331	0.67 ± 0.04	III
4_10kDa	10	16	5260 ± 124	2.12 ± 0.08	2713 ± 62	0.71 ± 0.02	I
4_10kDa	10	195	427 ± 68	0.35 ± 0.02	25 ± 5	0.08 ± 0.01	I
4_10kDa	20	16	4928 ± 271	1.07 ± 0.05	1513 ± 136	0.31 ± 0.01	I
4_10kDa	20	27	2305 ± 179	0.64 ± 0.04	352 ± 53	0.17 ± 0.01	I
4_10kDa	20	47	3845 ± 300	0.88 ± 0.05	986 ± 121	0.25 ± 0.01	I
4_10kDa	20	72	6840 ± 1375	2.31 ± 0.25	3420 ± 819	0.78 ± 0.07	I
4_10kDa	20	125	7650 ± 820	1.93 ± 0.13	3715 ± 337	0.63 ± 0.02	I
4_10kDa	20	195	10383 ± 734	3.06 ± 0.36	5855 ± 390	1.04 ± 0.09	I
8_10kDa	10	16	20025 ± 1253	1.64 ± 0.06	10425 ± 492	0.61 ± 0.02	I
8_10kDa	10	27	21875 ± 1389	1.94 ± 0.22	11775 ± 1021	0.67 ± 0.06	I
8_10kDa	10	47	25050 ± 1353	2.25 ± 0.17	14400 ± 1023	0.78 ± 0.05	I
8_10kDa	10	72	18250 ± 1050	4.03 ± 0.29	10095 ± 394	1.46 ± 0.09	II
8_10kDa	10	125	20775 ± 2895	3.53 ± 0.47	11608 ± 2451	1.29 ± 0.13	III
8_10kDa	10	195	15150 ± 3258	5.89 ± 0.67	10220 ± 2738	2.21 ± 0.14	I
8_25kDa	10	195	13800 ± 707	1.11 ± 0.01	9575 ± 3005	0.60 ± 0.05	I

All gells were prepared by mixing equal volume of 10% PVA solution and the multiarm PEG-linker solution at least 24 h of equilibration right before being subjected to rheology experiments.

Glucose-induced drug delivery from reversible covalent crosslinked poly(vinyl alcohol) by boronated multi-arm PEGs



Abstract

Dynamically restructuring hydrogels could be prepared by reversible covalent crosslinking of poly(vinyl alcohol) (PVA, 195 kDa) with multi-arm phenylboronic acid (PBA) functionalized poly(ethylene glycol) (PEG) crosslinkers, abbreviated as $\text{PEG}_{10\text{kDa}}(\text{PBA})_n$. Strong hydrogels were obtained by mixing of equal volumes of 10% w/v PVA and 10% w/v $\text{PEG}_{10\text{kDa}}(\text{PBA})_4$ or $\text{PEG}_{10\text{kDa}}(\text{PBA})_8$. It was found that the model drug compound alizarin red S (ARS) forms a fluorescent boronic ester when incorporated in the gel. The presence of ARS only mildly reduced the gel strength and prolonged the swelling and degradation of the hydrogel systems. The ARS release from the $\text{PEG}_{10\text{kDa}}(\text{PBA})_8$ based hydrogel was diffusion-controlled, whereas the ARS release from the $\text{PEG}_{10\text{kDa}}(\text{PBA})_4$ based hydrogel showed to be dependent on both diffusion and degradation. Moreover, the presence of D-glucose in solution increased the degradation of the hydrogel and fast release of ARS from the hydrogel systems was observed. These properties demonstrate that these hydrogels can be regarded as promising candidates for the development of D-glucose-responsive drug delivery systems.

10.1. Introduction

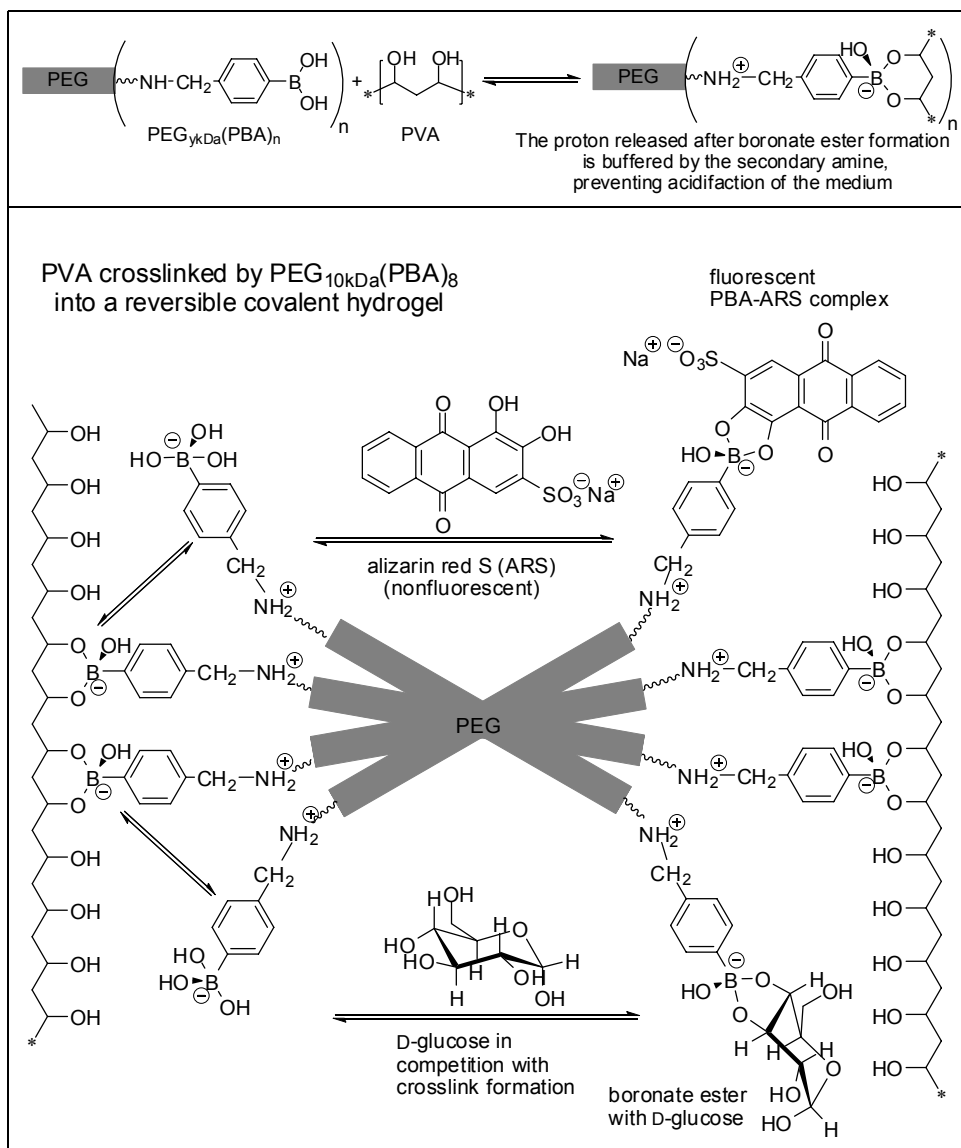
During the last decades, extensive investigations have been carried out to develop controlled drug delivery systems for advanced time-controlled and/or site-specific release of therapeutic agents. Among various polymeric systems designed as the depot for controlled drug delivery, hydrogel systems are considered as ideal candidates owing to their suitable chemical and physical properties such as hydrophilicity, biocompatibility, elasticity, high drug loading capacity. [1-2].

Boronic acid containing crosslinkers have been employed to form hydrogels through reversible boronic ester formation with polyols [3-6]. One of the most popular polyols used for the preparation of hydrogels using boronic acid based crosslinkers is poly (vinyl alcohol) (PVA), which is approved by the U.S. Food and Drug Administration (FDA) for pharmaceutical applications, due to its non-toxicity and biocompatibility [7]. Mixtures of PVA and poly(ethylene glycol) (PEG) can form a physically-crosslinked hydrogel after microphase-separation resulting in an interpenetrated network, and these turbid gels have high mechanical strength [8]. In addition, various boronic acid based crosslinkers for PVA have been developed resulting in dynamically covalently crosslinked hydrogels. These transparent boronic acid–PVA based gels are attractive candidates for drug delivery due to their peculiar “self-healing” property, arising from the rapid and reversible boronic ester formation [5]. Importantly, boronic acid–diol crosslinked hydrogels are susceptible to various external stimuli such as pH, temperature, ionic strength, and most interestingly they are responsive towards competing diols, including carbohydrates [9]. This carbohydrate-responsive behavior results from the fact that the vicinal 1,2- or 1,3-diols from carbohydrates, such as D-glucose, can compete with the 1,3-*cis*-diols from PVA for boronic ester formation, and transesterification will result in the dissociation of the crosslinks and weakening of the gel. For example, in 1991 Kataoka and coworkers have developed a hydrogel for the glucose-responsive delivery of insulin based on phenylboronic acid (PBA)-functionalized poly(*N*-vinyl-2-pyrrolidone) and PVA [9], followed by several other studies describing boronic acid containing polymeric crosslinkers that form glucose-responsive hydrogel systems with PVA [6, 10]. Mattiasson and coworkers demonstrated that a multi-boronated *N,N*-dimethylacrylamide copolymer was a more effective crosslinker of PVA than sodium borate [5]. Furthermore, their copolymer–PVA gel system exhibited a more elastic behavior (a longer relaxation time was observed) compared to borate–PVA gels. In their follow-up studies, it was found that this hydrogel was capable of formation of affinity complexes with mucin, and the reversible occlusion of mucosal lumen for controlled mucosal drug delivery was demonstrated [11]. More recently, Kiser and coworkers developed phenylboronic acid (PBA) and salicylhydroxamic acid (SHA) functionalized polymers that can spontaneously form a strong hydrogel upon mixing

[12-13]. These hydrogels performed well under physiological pH, due to reversible covalent ester formation between the PBA moieties and the SHA moieties. The potential of these PBA–SHA crosslinked hydrogels was further investigated for use as pH-sensitive vaginal drug-delivery system [14].

These examples demonstrate the potential of water-soluble boronic acid containing polymers to prepare hydrogels for controlled drug delivery. In our previous work, we aimed to develop a more simplified but effective boronated crosslinker system based on multi-arm polyethylene glycols (PEGs) to form reversible covalent hydrogels with PVA [15-16]. PEG is one of the most commonly used polymers in biomedical application as it is non-ionic, non-toxic, hydrophilic and biocompatible [1]. In addition, multi-arm PEG based hydrogels have been extensively studied as controlled drug delivery systems [17-21].

It was found that multi-arm boronated PEG-linkers synthesized via reductive amination of amine-functionalized PEGs with 4-formylphenylboronic acid could form strong hydrogels with PVA under physiological mimicking conditions (in PBS at 37 °C) [15-16]. Moreover upon increasing the number of arms, stronger gels with higher shape-stability could be formed, as was demonstrated by higher values for the plateau storage modulus G'_{\max} and relaxation time τ , and with this novel crosslinker system it was possible to obtain gels with G'_{\max} up to 30 kPa in PBS buffer pH 7.4 [16]. In this follow-up study, we were interested in the swelling and degradation behavior as well as the drug release kinetics, particularly in the presence of D-glucose. Alizarin red S (ARS) was selected as the model drug for the release study, as ARS is a non-toxic hydrophobic compound than can be considered as a model compound for drugs comprising a 1,2-catechol unit, like dopamine, L-dopa, and adrenaline. These catechols are relevant in various metabolic diseases including in Parkinson's and Alzheimer's disease. Moreover, ARS can form a fluorescent complex with boronic acids and this induced fluorescence upon boronic ester formation facilitates the detection of ARS released from the hydrogel by using fluorescence spectroscopy [22-23]. A conceptual overview is given in Scheme 10.1.



Scheme 10.1. Conceptual overview of PVA crosslinked by PEG_{10kDa}(PBA)₈ in presence of competing alizarin red S (ARS) and D-glucose that can weaken the gel as crosslink density is reduced.

10.2. Materials and methods

10.2.1. Materials

4-Formylphenylboronic acid (4-FPBA, Aldrich), sodium borohydride (NaBH_4 , Aldrich), poly(vinyl alcohol) (PVA, M_w 195 kDa, Aldrich), poly(ethylene glycol) (PEG-diamine 10000 Da, Aldrich; 4-arm 10000 Da; 8-arm 10000, 25000 Da, JenKem Technology USA), methanesulfonyl chloride (Ms-Cl , Aldrich), 4-(2-hydroxyethyl)-1-piperazineethanesulfonic acid (HEPES, Aldrich), alizarin red (1,2-dihydroxy-9-10-anthraquinonesulfonic acid, ARS, Fluka), D-glucose (Aldrich) were purchased in the highest purity available and used as received.

The degree of functionalization of all synthesized boronated PEG-linkers were determined by ^1H NMR (300 MHz, D_2O , CD_3OD , and CDCl_3) spectra (Varian Inova spectrometer).

10.2.2. Synthesis of multiarm boronated PEG-linkers

The alcohol-terminated PEGs were converted to amine terminated PEGs according to a literature procedure [20, 24]. The attachment of 4-aminomethylphenylboronic acid (4AMPBA) moieties by the reductive amination reaction of 4-formylphenylboronic acid with the terminal amino groups was described previously [25-26]. Also the synthesis of the multi-arm boronated PEG crosslinkers was reported earlier [16]. The synthetic procedure of $\text{PEG}_{10\text{kDa}}(\text{PBA})_8$ will be given here as a typical example.

Eight-arm PEG-amine $\text{PEG}_{10\text{kDa}}(\text{NH}_2)_8$ (1.00 g; 0.04 mmol) and 4-formylphenylboronic acid (58.2 mg; 0.39 mmol) were dissolved in 5 ml methanol. The reaction was left to proceed at ambient temperature for 4 days under nitrogen atmosphere. Subsequently, NaBH_4 (36.3 mg; 0.96 mmol) was added portion-wise to the yellow solution, and a discoloring was observed. This reduction was allowed to proceed to completion for 2 h, after which the methanol was removed by rotational evaporation. The residue was dissolved in milliQ water and purified by dialysis using 10 kDa $M_w\text{CO}$ membrane. The retentate was then lyophilized and $\text{PEG}_{10\text{kDa}}(\text{PBA})_8$ was obtained as white spongy material. Yield: 85%.

^1H NMR (CD_3OD): 7.4–7.1 ppm (*dd*, 32 H, Ar), 3.9 ppm (*s*, 16 H, Ar- CH_2 -NH-), 3.05–3.8 ppm (*m*, 890 H, -O- CH_2 - CH_2 -O-), 2.96 ppm (*t*, 16 H, -NH- CH_2 - CH_2 -O-).

10.2.3. Thermal analysis by differential scanning calorimetry

Melting points of boronated multi-arm PEG crosslinkers were analyzed with a Pyris 1 differential scanning calorimetry (DSC) equipment, calibrated with indium and gallium. During each measurement 5–10 mg of the polymeric crosslinker was cooled to -100 °C and kept at this temperature for 2 min. Next, the sample was heated to 60 °C, annealed for 2 min, and subsequently cooled to -100 °C. Finally, the sample was kept

at -100 °C for 2 min and heated to 60 °C again. Both the cooling and heating rate were 10 °C/min. The melting temperature (T_m) was determined from the corresponding temperature at the maximal heat flow and the melting enthalpies (ΔH_m°) were determined from the integration of the melting peak. The data presented were selected from the second heating scan.

10.2.4. Fluorescent binding study

ARS was used as received and a stock solution of 9.0×10^{-5} M ARS (Solution A) was prepared in MilliQ water. Stock solutions of PEG_{10kDa}(PBA)₂, PEG_{10kDa}(PBA)₄ and PEG_{10kDa}(PBA)₈ (with [PBA] = 3.6×10^{-3} M) were prepared in 0.1 M HEPES or PBS (Solutions B), respectively.

A series of samples were prepared from 0.1 ml of solution A and increasing volumes of solution B from 0–0.9 ml in a 1.5 ml Eppendorf tube. Next, the volume was adjusted to 1.0 ml with milliQ water and the mixture was vortexed for 5 s and allowed to equilibrate for at least 5 min. It was observed that equilibrium was achieved within 30 s and solutions were stable for several hours. The excitation wavelength was set to 468 nm and the range of emission wavelength was measured at 580 nm using a Cary Eclipse fluorescence spectrophotometer. Fluorescent binding measurements were carried out in triplicate.

10.2.5. Gel Preparation

To prepare gel samples, 195 kDa PVA was dissolved in MilliQ water at 80 °C to a final concentration of 10% w/v. Stock solutions of 10% w/v of PEG_{10kDa}(PBA)_n were prepared in phosphate buffer solution (PBS, 10 mM buffering agent, 150 mM NaCl). PBS was supplied by Braun and used as received.

Gel samples were prepared by mixing equal volumes (typical 500 μ l) of desired PVA solution with each PEG_{10kDa}(PBA)_n solution in a small test tube. Next, 100 μ l of PBS or ARS solution (100 mM in PBS) was added and the samples were vortexed for at least five seconds. The tube was then sealed with Parafilm and the gel was allowed to equilibrate for at least 24 h at ambient temperature. For each type of gel, two identical gel samples were prepared as duplicates.

10.2.6. Oscillatory rheology

Oscillatory rheology experiments were performed on a Physica MCR 301 Rheometer (Anton Paar) equipped with a parallel plates sensor system. The gap or gel thickness was varied between 0.3–0.6 mm in accordance to the specific gel system and each gel sample was measured 2–4 times after temperature equilibrium was established, either at 25 °C or 37 °C. Water evaporation was prevented by applying a layer of silicon oil on top of the parallel plates.

For each sample a frequency sweep was measured in duplo at 25 and 37 °C, during which the gels were subjected to oscillating rotational deformations with frequencies from 100 to 0.05 Hz at the strain (γ) of 2%. The temperature was set to be constant at 25 or 37 °C. From this measurement, crossover frequency (ω_c) was determined as the frequency where loss modulus (G'') equals storage modulus (G') (the damping factor = 1). Relaxation time (τ) was calculated using the formula $\tau = 1/\omega_c$. Plateau gel strength (G'_{\max}) was obtained at high frequency (typically $\omega_c = 20$ Hz).

10.2.7. Scanning electron microscopy (SEM)

Hydrogel samples were prepared on aluminum stubs by mixing 100 μ l 10% w/v of 195 kDa PVA with either 100 μ l 10% w/v of PEG_{10kDa}(PBA)₄ or 100 μ l 10% w/v of PEG_{10kDa}(PBA)₈ in the absence or the presence of ARS (1.8 mM, 20 μ l), respectively. The samples were equilibrated for 24 h and lyophilized to preserve the morphologies of the PEG–PVA based hydrogels. The surface of each sample was sputter-coated with Au (s). SEM imaging (10 KeV, spot size 5, working distance 12 mm) was performed with these samples using an EMRAM MCS-A1 scanning electron microscope (FEI Systems). Samples were examined at low magnifications followed by further assessment at higher magnifications to characterize the pores present at the surface.

10.2.8. Swelling, degradation and release of ARS from the gels

Gel samples were prepared as described in section 2.5. in a cuvette of 1 \times 1 \times 4 cm (1 \times w \times h) by mixing of 550 μ l stock solution of 10% w/v PEG_{10kDa}(PBA)_n and 550 μ l 10% w/v 195 kDa PVA solution in and the cuvettes were sealed with parafilm and vortexed for 5 s to homogenize. Similarly, gel samples with ARS incorporated were prepared by mixing of a dark red viscous solution of 550 μ l PVA and 100 μ l 1.0 \times 10⁻² M ARS with 550 μ l 10% w/v PEG_{10kDa}(PBA)_n. This was accompanied by a color change from dark red to yellow-orange. Each sample was allowed to equilibrate at 37 °C for minimally 24 h. For each type of gel sample, duplicate identical samples were prepared.

For the swelling and degradation studies of the gels under sink conditions and the corresponding one-dimensional ARS release from ARS loaded gels, cuvettes containing the hydrogels were stabilized in a frame and submerged in 500 ml PBS solution (pH 7.4, 0.01 M, IS = 0.15 M) at 37°C. The setup was covered with aluminum foil, and MilliQ water was added from time to time to compensate for the minimized evaporation, keeping the volume constant at 500 ml (Figure 10.1). A magnetic stirring bar was added in order to homogenize the surrounding PBS to maintain the sink conditions.

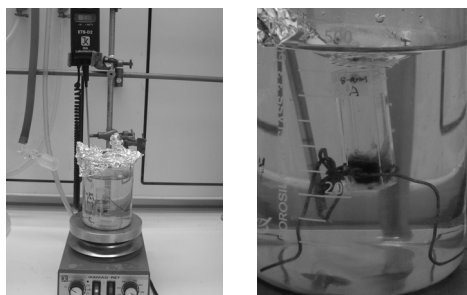


Figure 10.1. Experimental setup for swelling, degradation and ARS release of the hydrogel.

First data point ($t = 0$) was determined by the initial weight of hydrogel in the cuvette, defined as M_0 . After a certain time interval t (typically 0.5 h), the cuvette with the hydrogel was removed from the setup and adhering water was removed from the cuvette with tissue paper, and subsequently weighed to determine the remaining hydrogel weight (M_t). Relative mass was calculated by M_t / M_0 and this was used to reflect the swelling and/or degradation behavior of the hydrogel system. Simultaneous to each M_t determination, triplicate samples of 200 μl PBS of the surrounding PBS solution were collected in a 96 flat bottom well plate that was sealed and stored in the fridge for the determination of the cumulative ARS release until gel degradation was complete. The outmost wells of the well plate were filled with pure PBS in order to prevent evaporation of the samples. Extra 20 μl stock solutions of corresponding boronated multi-arm PEG crosslinkers (3.9 mmol PBA) were added to each sample in the 96-well plate to ensure complete ARS complexation. Cumulative ARS release was quantified via measurement of the fluorescent intensity by Tecan safire2 and software of Magellan, with excitation wavelength and emission wavelength set at 468 nm and 572 nm, respectively [22-23]. For each boronated multi-arm PEG based hydrogel, the degradation and ARS release experiments were carried out *in duplo*. In order to investigate the glucose-responsive swelling and degradation of the gels and the corresponding ARS release from the gels, ARS loaded gels were immersed in 500 ml of 1%, 5% and 10% w/v D-glucose solutions in PBS (pH 7.4, 0.01 M, IS = 0.15 M). By using the so-called power law (Equation 10.1), developed by Peppas and coworkers to describe drug release from polymeric systems [27], the results were used to analyze the effect of glucose on the of ARS release mechanism from the gels:

$$M_t/M_\infty = k t^n \quad \text{Equation 10.1}$$

Here, M_t and M_∞ are the cumulative amount of drug released at time t and infinite time $t = \infty$; and M_t/M_∞ is the mass fraction of drug released. k is a constant including structural and geometric characteristics for a particular system and k is in positive relation with the diffusivity of the drug in the hydrogel; whereas the release exponent n is indicative of the drug release mechanism.

10.3. Results and discussion

10.3.1. Design of the study

We have previously developed boronated multi-arm PEG compounds that can reversibly covalent crosslink PVA into strong and transparent gels with self-healing properties [15-16]. Next, we were interested in the application of these gels as reservoirs for glucose-responsive drug release. Alizarin red S (ARS) was selected as model for 1,2-catechol derived drug molecules, as it binds in the gel as a fluorescent boronate ester, allowing for easy and accurate detection by fluorescence microscopy. To this purpose we have determined the binding of ARS to the different multi-arm boronic acid crosslinkers, using a fluorescent binding assay as described by Wang and coworkers [22-23]. Since the binding of ARS with the boronic acid groups of the PEG crosslinker compete with crosslinking in the PVA gel, also the effect of ARS on the gel strength was investigated. Finally, the swelling and degradation behavior due to the presence of ARS and the effects of the presence of glucose on the ARS release from ARS loaded gels were studied.

The gels selected for these studies were prepared from PVA with M_{wt} 195 kDa, as it was found that the strongest gels with the slowest degradation rate were obtained with this PVA. Solutions of 10% w/v of PVA were mixed 1:1 v/v with 10% w/v of PEG_{10kDa}(PBA)_n and the only parameter varied was the number of arms (n) from 2 to 4 to 8. The relatively low concentrations of 10% w/v of PVA and PEG were selected to minimize phase separation of the PVA-PEG mixture. The swelling and degradation studies and drug release studies using these gels were performed under physiological mimicking conditions in PBS (pH 7.4) and at 37 °C.

10.3.2. Effect of the number of arms on the crystallinity of PEG_{10kDa}(PBA)_n

In this study, solutions of 10% w/v of 4-aminomethylphenylboronic acid functionalized PEG with a 2-, 4-, and 8-arm architecture were selected to prepare hydrogels with PVA. As the gel properties of physically crosslinked PVA-PEG based gels are determined to a large extent by the presence of crystalline PVA microdomains [8], it could be argued that increasing the number of arms would reduce the (micro)phase separation of the boronated PEG-PVA gels. In addition, high crystallinity of the PEG crosslinker could result in PEG cluster reducing the availability of PBA end-groups for diol complexation with PVA, thereby negatively affecting the gel strength. As known, the melting point and melting enthalpy are dependent on the crystallinity of a polymer and could serve as a measure for the crystallinity. Table 10.1 shows the melting point (T_m) and melting enthalpy (ΔH_m°) of PEG_{10kDa}(PBA)₂, PEG_{10kDa}(PBA)₄, and PEG_{10kDa}(PBA)₈. It was found that T_m was drastically reduced from 62 °C for PEG_{10kDa}(PBA)₂ to 32 °C for PEG_{10kDa}(PBA)₈.

From Table 10.1 it is obvious that both the melting point and the melting enthalpy decrease when the number of arms increases, indicating that the crystallinity decreases with increasing number of arms and increasing concentration of PBA moieties. Decreasing the crystallinity would decrease the tendency for (micro-)phase separation of the gels and therefore the branched architecture may contribute to a higher availability of PBA moieties for diol complexation.

Table 10.1. Melting points and melting enthalpies as function of number of arms

Sample	T _m (°C) ¹	ΔH _m ^o (kJ/mol) ¹
PEG _{10kDa} (PBA) ₂	62	1370
PEG _{10kDa} (PBA) ₄	50	1050
PEG _{10kDa} (PBA) ₈	32	640

¹ Determined by differential scanning calorimetry

10.3.3. Effect of the number of arms on the K_{ARS} of PEG_{10kDa}(PBA)_n

As it was intended to investigate the drug delivery properties of the gels under physiological mimicking conditions, it was desired to use phosphate buffered saline. However, Wang and coworkers claimed that the buffer can influence the equilibrium of boronic ester formation between PBA and ARS [23]. They found that the binding constant of PBA with ARS (K_{ARS}) decreased when the concentration of PBS buffer increased, indicating competitive binding of phosphate with the boronic acid groups. However, K_{ARS} appeared to be independent of the concentration of HEPES buffer. Therefore, K_{ARS} was determined both in HEPES and PBS for PEG_{10kDa}(PBA)₂, PEG_{10kDa}(PBA)₄, and PEG_{10kDa}(PBA)₈ using the fluorescent binding assay described by Wang and coworkers [22-23]. The results are included in Table 10.2. In case that the boronic acids moieties at the multi-arm crosslinkers form complexes with ARS independently, the K_{ARS} values found would be identical for all different crosslinkers. However, from Table 10.2, it can be observed that this holds only true for the 2-arm and 4-arm PEG crosslinkers in HEPES buffer with K_{ARS} of 7200 ± 20 M⁻¹ and 7420 ± 180 M⁻¹ for PEG_{10kDa}(PBA)₂ and PEG_{10kDa}(PBA)₄, respectively). The K_{ARS} found for these compounds is similar to the K_{ARS} previously found for the JeffamineED1900-di-4AMPBA crosslinker [15] (7600 ± 130 M⁻¹). However when the number of arms increases to 8, K_{ARS} is increased by a factor 2. This higher binding constant may be the result of hydrophobic clustering of the PBA groups ARS in micellar-like structures, leading to increased local concentrations of the reacting groups and consequently a shift of the equilibrium towards boronic ester formation. When comparing K_{ARS} in HEPES buffer with K_{ARS} in PBS, it is clear that for all three

species K_{ARS} in HEPES buffer solution is larger than K_{ARS} in PBS. The effect of competitive binding of phosphate ions of PBS is significant on the K_{ARS} all $PEG_{10kDa}(PBA)_n$ compounds, with the relatively largest decrease for K_{ARS} of $PEG_{10kDa}(PBA)_2$.

Although in HEPES buffer solution stronger ARS complexation was observed than in PBS, the use of PBS has been selected in further experiments, since PBS is a biocompatible buffer that is widely used in biomedical studies.

Table 10.2. K_{ARS} (M^{-1}) as function of number of arms

Sample	K_{ARS} (M^{-1}) HEPES ¹	K_{ARS} (M^{-1}) PBS ¹
$PEG_{10kDa}(PBA)_2$	7200 ± 20	4100 ± 75
$PEG_{10kDa}(PBA)_4$	7420 ± 180	6380 ± 100
$PEG_{10kDa}(PBA)_8$	14180 ± 360	11020 ± 400

¹ $pH = 7.4$, $0.01 M$, $IS = 0.015M$

10.3.4. Effect of ARS on the gel strength

The effects of the presence of ARS on the gel properties were investigated by oscillatory rheology measurements. To this purpose the gel strength (G'_{max}) and the relaxation time (τ) of hydrogels prepared from 10% w/v of 195 kDa PVA crosslinked by $PEG_{10kDa}(PBA)_2$, $PEG_{10kDa}(PBA)_4$, or $PEG_{10kDa}(PBA)_8$, respectively were determined in the presence or the absence of 1 mM ARS, see Figure 10.2.

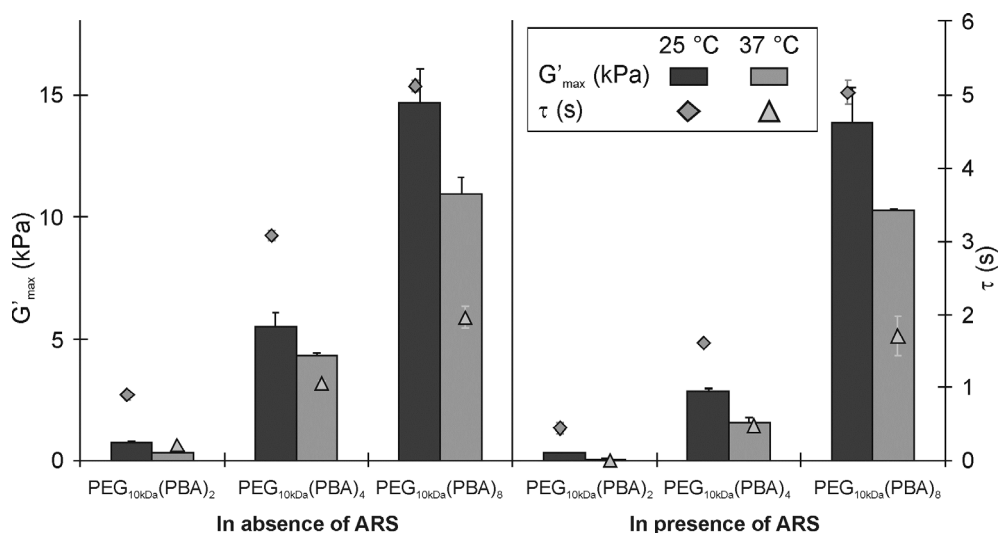


Figure 10.2. G'_{max} and τ of hydrogels from $PEG_{10kDa}(PBA)_y$ and 195kDa PVA in absence (left) of presence of ARS (right) at 25 °C (dark grey + diamonds) and at 37 °C (light grey + triangles), determined in PBS (0.01 M, pH7.4, IS = 0.15M).

From the results in Figure 10.2, it can be observed that for hydrogels prepared with $\text{PEG}_{10\text{kDa}}(\text{PBA})_n$ G'_{max} and τ increased with increasing number of arms (n). As boronic ester formation is kinetically controlled, an increase in temperature from 25 °C to 37 °C shifts the equilibrium of borate ester formation to the dissociated state. Therefore, at increased temperature a reduced G'_{max} for all hydrogels prepared from the multi-arms PEG crosslinkers is observed, no matter if ARS was present or not. Similarly, an increase in temperature from 25 °C to 37 °C significantly reduced the relaxation time τ of all hydrogel systems, even for the $\text{PEG}_{10\text{kDa}}(\text{PBA})_8$ based hydrogel (from 5.1 s to 2.0 s).

The presence of 1 mM ARS results in a decrease of the gel strength (G'_{max}), and was found to be most significant for the $\text{PEG}_{10\text{kDa}}(\text{PBA})_2$ based hydrogel. At 25 °C the gel strength decreased from 700 Pa to only 280 Pa, and at 37 °C no hydrogel was formed. Also for the $\text{PEG}_{10\text{kDa}}(\text{PBA})_4$ based hydrogel the decrease in G'_{max} at 37 °C from 4300 Pa to 1500 Pa was significant. However, the presence of ARS had little effect on the $\text{PEG}_{10\text{kDa}}(\text{PBA})_8$ based hydrogel, as G'_{max} only mildly reduced from 14700 and 10900 Pa in the absence of ARS to 13800 and 10300 Pa in the presence of ARS, at 25 and 37 °C respectively. This lower sensitivity can be explained by the cooperative binding of the multi-armed crosslinks as for the $\text{PEG}_{10\text{kDa}}(\text{PBA})_2$ based hydrogel the binding of one single PBA moiety to ARS immediately results in full breakage of a crosslink in the network. In contrast, after boronic ester formation with one PBA moiety from the $\text{PEG}_{10\text{kDa}}(\text{PBA})_4$ and $\text{PEG}_{10\text{kDa}}(\text{PBA})_8$ with ARS, the remaining 3 or 7 PBA moieties maintain the network between different PVA chains.

10.3.5. Effect of ARS on the morphology of freeze dried gels

It was found that mixtures of 10% w/v 195 kDa PVA with 10% w/v $\text{PEG}_{10\text{kDa}}(\text{PBA})_4$ or $\text{PEG}_{10\text{kDa}}(\text{PBA})_8$ in the presence of 1 mM ARS gave strong gels. Therefore, these gels were selected for further analysis by scanning electron microscopy (SEM). As ARS is a relatively hydrophobic compound, the incorporation of ARS into a PVA- $\text{PEG}_{10\text{kDa}}(\text{PBA})_n$ hydrogel could have a significant effect on the hydrogel properties, such as the hydrophobicity (wetting) and porosity. Gel samples with and without ARS (0.16 mM) were freeze-dried to keep their morphologies intact and gold-sputtered for SEM analysis and the results are given in Figure 10.3.

It can be observed that in the absence of ARS, the $\text{PEG}_{10\text{kDa}}(\text{PBA})_8$ -based freeze-dried hydrogels formed less porous structures than the $\text{PEG}_{10\text{kDa}}(\text{PBA})_4$ -based freeze-dried hydrogels, which had a more open / interconnected structure. In the presence of ARS the porosity of the freeze-dried hydrogel system of PVA crosslinked by both $\text{PEG}_{10\text{kDa}}(\text{PBA})_4$ and $\text{PEG}_{10\text{kDa}}(\text{PBA})_8$ was diminished. These observations suggest that the hydrophobic ARS creates a more hydrophobic and less porous surface, resulting in a different gel system.

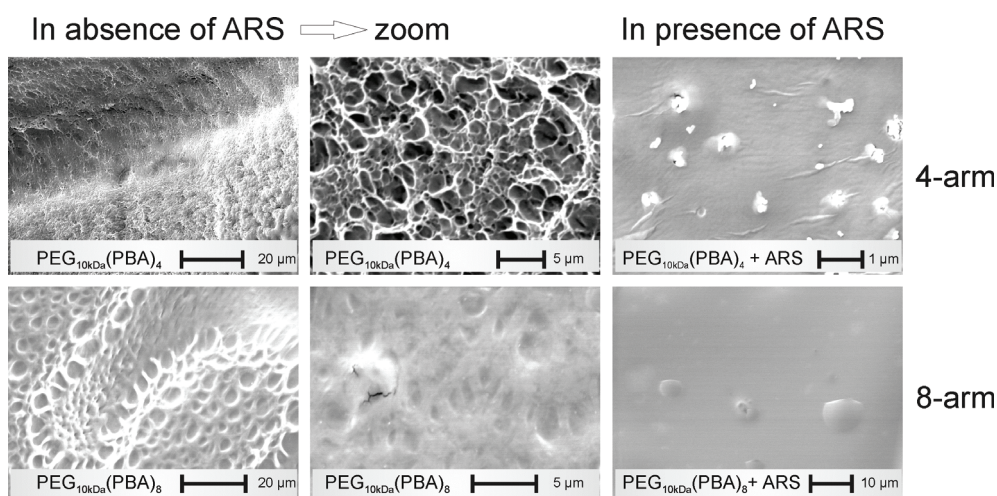


Figure 10.3. SEM pictures of freeze-dried hydrogel from 10% w/v PEG_{10kDa}(PBA)₄ (top row) and PEG_{10kDa}(PBA)₈ (bottom row) with 10% w/v of 195 kDa PVA. From left to right freeze-dried gels in absence of ARS (scale bar = 20 μm), which is followed by a close-up (scale bar = 5 μm) showing differences in pores size, and followed by the non-porous freeze-dried gels in the presence of ARS (0.16 mM) (scale bar = 1 and 10 μm respectively).

10.3.6. Effects of ARS on gel degradation

As the PEG_{10kDa}(PBA)₄ and PEG_{10kDa}(PBA)₈ upon mixing with PVA resulted in the instantaneous formation of strong gels, these gels were left standing for 24 hours to allow removal of air bubbles. It was observed that the PEG_{10kDa}(PBA)₄ based hydrogels were more homogenous than the PEG_{10kDa}(PBA)₈ based hydrogels, as some small bubbles were still visible in the PEG_{10kDa}(PBA)₈ based hydrogels. The PEG_{10kDa}(PBA)₈ based gel had a more orange/yellow color (Figure 10.4B), whereas the PEG_{10kDa}(PBA)₄ based gel had a deep red color (Figure 10.4A). This observation indicates that more of the ARS was complexed with PBA inside the PEG_{10kDa}(PBA)₈ based hydrogels than in the PEG_{10kDa}(PBA)₄ based gels, which is consistent with the 2-fold higher PBA concentration and the higher K_{ARS} of the PEG_{10kDa}(PBA)₈ system as compared to the PEG_{10kDa}(PBA)₄ system.

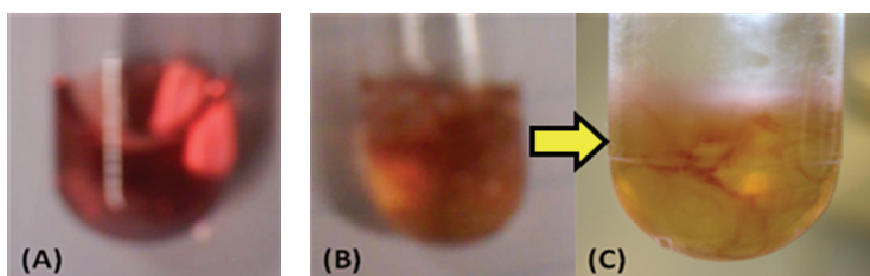


Figure 10.4. Visual appearances of gels prepared from (A) 10% w/v PVA 195 kDa mixed 1:1 v/v with 10% w/v of PEG_{10kDa}(PBA)₄ in PBS at pH 7.4 in presence of 1 mM ARS and (B) 10% w/v PVA 195 kDa mixed 1:1 v/v with 10% w/v of PEG_{10kDa}(PBA)₈ in PBS at pH 7.4 in presence of 1 mM ARS. (C) Gel of (B) at ca. 90% swelling ratio.

The degradation and ARS release of both PEG_{10kDa}(PBA)₄ based gels (Figure 10.5A) and PEG_{10kDa}(PBA)₈ based gels (Figure 10.5B) in the presence or the absence of ARS were measured. It was observed that during the gel degradation experiments, the color of the hydrogels changed to pale red, indicating hydrolysis of the PBA–ARS esters.

From Figure 10.5A, it can be observed that there was no mass increase for the 4-armed PEG_{10kDa}(PBA)₄ based gels during the first hours, which implies there was no swelling. The PEG_{10kDa}(PBA)₄ based gels degraded almost completely during a period of 12–15 hours in PBS in the absence of ARS, while in the presence of ARS the PEG_{10kDa}(PBA)₄ based gels were almost completely degraded after a longer 22 hour period. It appeared that the mass loss of the PEG_{10kDa}(PBA)₄ based gels decreased linearly during the first period, independent of the presence of ARS. Regarding the cumulative ARS release curve for the PEG_{10kDa}(PBA)₄ based gels, a fast ARS release was observed during the first 4 hours with a concomitant rapid mass loss. Next, the rate of ARS release was reduced while the degradation went on at a slower pace. A nearly complete cumulative ARS release of *ca.* 94% of the loaded ARS was observed after 12 hours and *ca.* 98% of the loaded ARS was released after 22 hours. It appears that the ARS release from PEG_{10kDa}(PBA)₄ based gels was approximately synchronous with the degradation.

However, for the 8-armed PEG_{10kDa}(PBA)₈ based gels (Figure 10.5B), still no complete degradation was observed after 400 hrs. For PEG_{10kDa}(PBA)₈ based gel in the absence of ARS it was observed that the gels were in a slightly swollen state during the first 5 hours (up to 105% of its initial mass). During the next 45 hours the relative mass of the hydrogel gradually degraded to *ca.* 60% of its initial mass, following a linear profile. Next, the degradation rate sharply decelerated and it took another 350 hours to degrade to *ca.* 20% of its initial mass.

The PEG_{10kDa}(PBA)₈ based gels in the presence of ARS remained significantly longer in a swollen state as the relative mass above 100% was maintained during the first 30 hours. Similar to the PEG_{10kDa}(PBA)₄ based gel, the degradation rate was reduced due to the presence of ARS within the PEG_{10kDa}(PBA)₈ based gel as it took 250 hours to degrade to 40% of its initial mass, whereas in absence of ARS the PEG_{10kDa}(PBA)₈ based gel took less than 100 hours to degrade to 40% and this remaining 40% degraded much slower, which was also observed in the absence of ARS. Regarding the ARS release, *ca.* 40% of the ARS was released during the first 50 hours in which the gel was predominantly in the swollen state. During the next linear degradation regime up to 300 hours, another *ca.* 30% of the ARS was released. After 300 hours a much slower degradation continued, during which the remaining ARS was slowly released up to *ca.* 97% after 480 hours. This behavior implies that the

initial ARS release in the PEG_{10kDa}(PBA)₈ based gels preceded the degradation, and only after release of the first 40% of ARS, the degradation of the hydrogel took off.

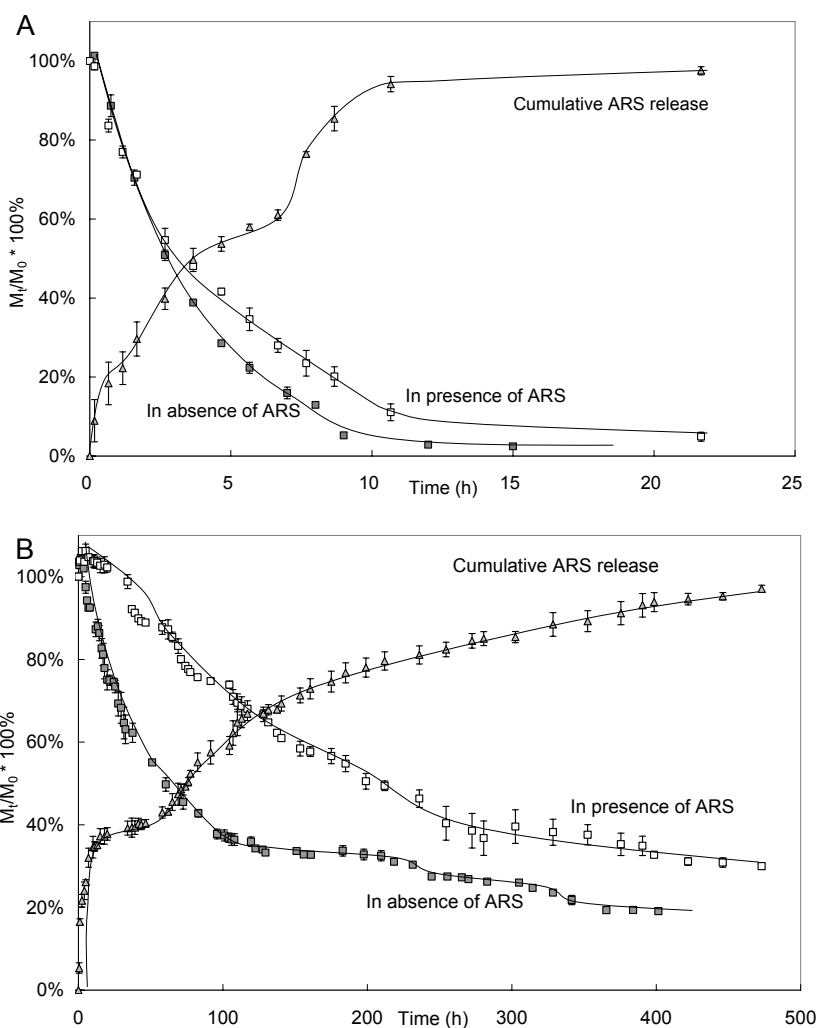


Figure 10.5. Relative mass and ARS release profile of hydrogel by 1:1 v/v mixing of 10% w/v PEG_{10kDa}(PBA)₄ (A), or 10% w/v PEG_{10kDa}(PBA)₈ (B) with 10% w/v 195 kDa PVA in PBS (pH = 7.4, 0.01 M, IS = 0.15 M) at 37 °C. M_t/M_0 in absence of ARS is depicted in grey squares, M_t/M_0 in presence of ARS in white squares and the cumulative drug release in grey triangles. Lines are added for clarity.

10.3.7. Glucose triggered drug release by using ARS as model drug

As competing diols from carbohydrates, e.g. D-glucose, can compete with PVA for boronic ester formation, the presence of D-glucose to PEG_{10kDa}(PBA)_n-PVA gels can result in transesterification and thereby weakening the gels as the crosslink density is reduced. Therefore, the glucose-induced gel weakening enables the glucose-responsive

release of the model drug ARS from these types of hydrogels, demonstrating the potential application of these gels for the treatment of diabetes. To demonstrate the glucose-responsive behavior of this gel system, hydrogels were prepared as described in section 2.5 and their degradation behavior was studied in PBS at 37 °C in the presence of increasing concentration of D-glucose (0%, 1%, 5% and 10% w/v).

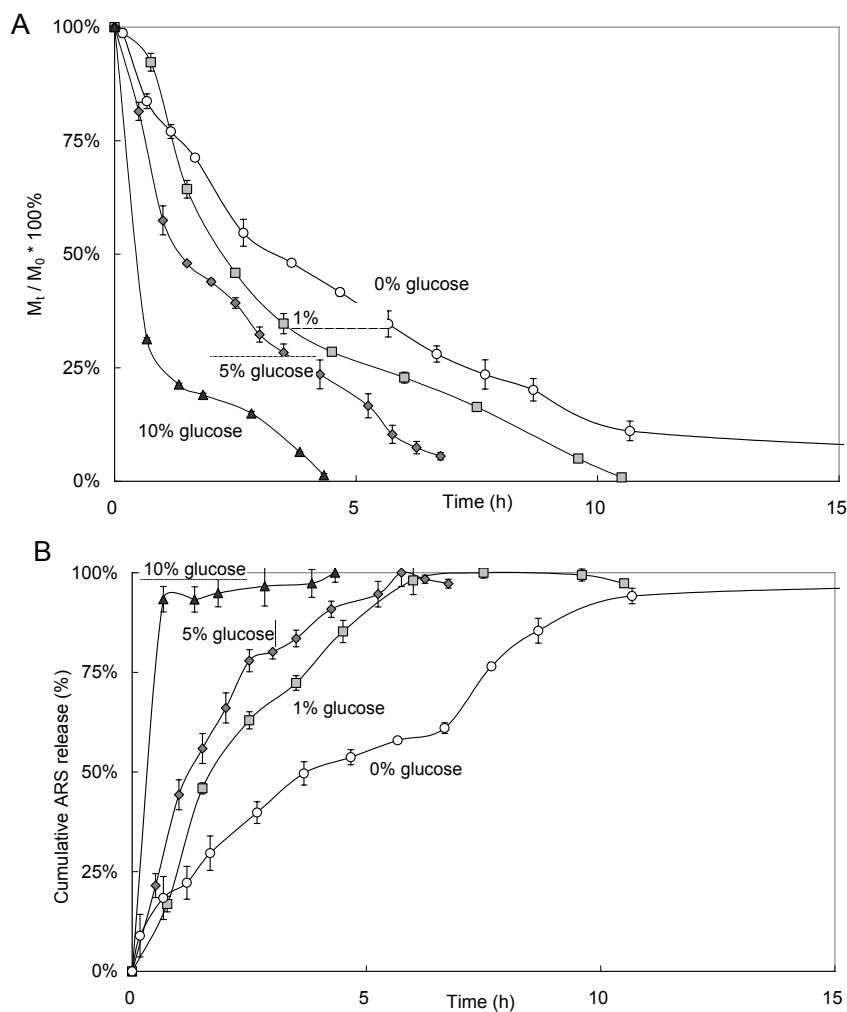


Figure 10.6. Relative mass (**A**) and cumulative ARS release (**B**) of hydrogels prepared by mixing of 10% w/v 195 kDa PVA with equal volume of 10% w/v PEG_{10kDa}(PVA)₄. Degradation and ARS release experiments were performed in PBS (pH = 7.4, 0.01 M, IS= 0.15 M) at 37 °C containing 0% (—○—), 1% (—□—), 5% (—◇—), 10% (—△—) w/v of D-glucose, respectively. Lines are added for clarity.

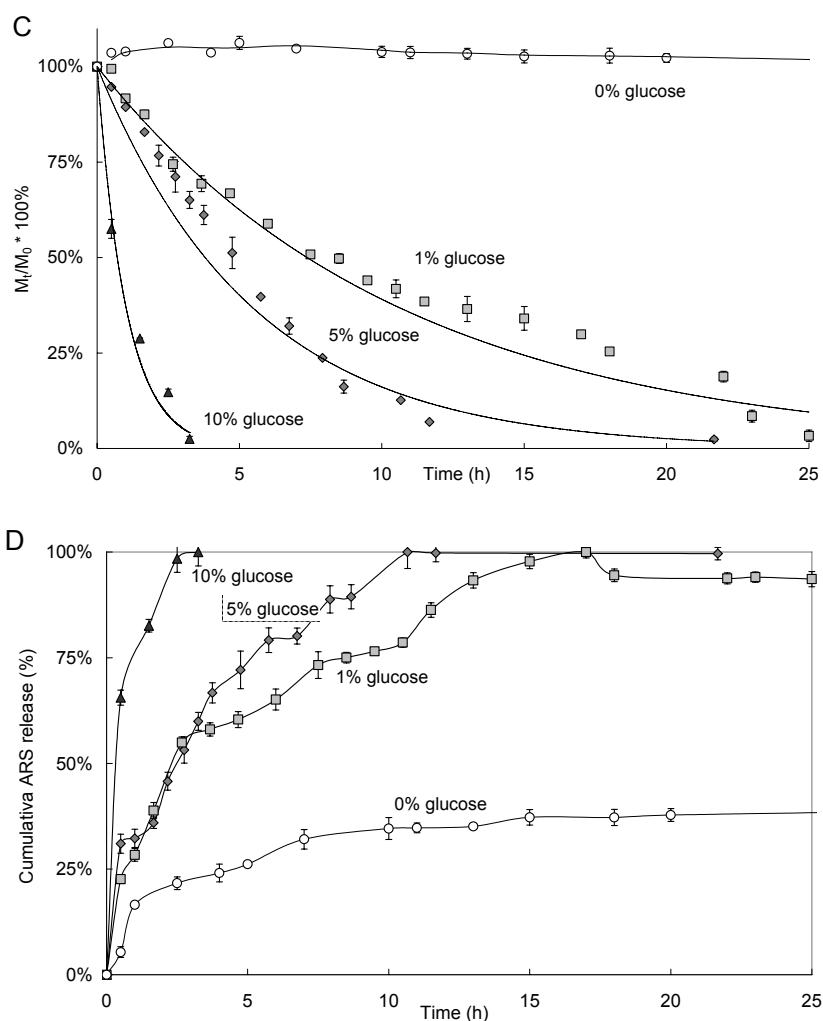


Figure 10.7. Relative mass (C) and cumulative ARS release (D) of hydrogels prepared by mixing of 10% w/v 195 kDa PVA with equal volume of 10% w/v PEG_{10kDa}(PVA)₈. Degradation and ARS release experiments were performed in PBS (pH = 7.4, 0.01 M, IS= 0.15 M) at 37 °C containing 0% (—○—), 1% (—□—), 5% (—◇—), 10% (—△—) w/v of D-glucose, respectively. Lines are added for clarity.

The relative mass and ARS release of the PEG_{10kDa}(PBA)₄ and of the PEG_{10kDa}(PBA)₈ based gels are depicted in Figure 10.7. It is evident that with increasing concentration of D-glucose both the degradation rate and ARS release rate are increased. In the presence of 10% w/v D-glucose, complete hydrogel degradation was observed well within 5 hours for the PEG_{10kDa}(PBA)₄ based gels, which was more than four times faster than in the absence of D-glucose (*ca.* 20 hours). More than 93%

of the ARS was released within the first hour, indicating a nearly instantaneous D-glucose-induced ARS release (burst release).

As mentioned before, it was found that the 8-armed PEG_{10kDa}(PBA)₈ based gels took much longer time to degrade in PBS at 37 °C than the 4-armed PEG_{10kDa}(PBA)₄ based gels. For example to achieve 70% of mass loss, the PEG_{10kDa}(PBA)₈ based gels took 500 hours (Figure 10.5B) whereas the PEG_{10kDa}(PBA)₄ based gels took only 7 hours (Figure 10.5A and Figure 10.7A). For the PEG_{10kDa}(PBA)₈ based gels in the presence of D-glucose no swelling was observed and the degradation started immediately. Remarkably, the degradation and ARS release rate of 8-arm PEG crosslinked hydrogel is increased 20-fold in the presence of 1% w/v D-glucose (25 hours for complete degradation, Figure 10.7C). At the highest concentration of 10% w/v D-glucose complete degradation was observed within 5 hours, indicating a 100-fold higher degradation rate. Moreover, the degradation of the PEG_{10kDa}(PBA)₈ based gels seemed to follow a more linear profile in the presence of D-glucose than in the absence of glucose.

10.4. Discussion

In the PBA functionalized multi-arm PEG crosslinkers with identical M_w of 10 kDa the number of repeating ethylene oxide units per PBA functionality reduces from 111 for PEG_{10kDa}(PBA)₂, to 54 for PEG_{10kDa}(PBA)₄, and 25 for PEG_{10kDa}(PBA)₈, respectively. Due to the branched architecture and the increased concentration of PBA moieties, less periodic arrangement of the PEG backbone is possible for the higher multi-arm crosslinkers, which is apparent in the decrease in crystallinity as shown by the reduced T_m and ΔH_m° observed upon increasing the number of arms (Table 10.1).

Due to the possibility of π - π stacking of the flat anthraquinone system of ARS with the flat boronic ester of PBA-ARS a local increase of the ARS concentration can be expected. As the number of arms increases, the PBA moieties at the end of these arms are residing increasingly closer to each other. PEG_{10kDa}(PBA)₈ has the lowest number of repeating hydrophilic ethylene oxide units per PBA functionality ($x = 25$), facilitating a more hydrophobic micro-environment for the hydrophobic ARS to complex with PBA moieties due to a locally increased PBA concentration. Moreover, after the first boronic ester formation of PBA with ARS the hydrophilicity of the local micro-environment is even more increase and more ARS molecules are attracted.

With respect to the ARS release from the gel, it is reasonable to assume that the degradation of the hydrogel is preceded by hydrolysis of the PBA-PVA boronic esters which serve as crosslinks in the network of the hydrogel. Penetration of water results in the solvation of both PEG and PVA chains, and further hydrolysis of boronic esters and degradation is accelerated due to the gain in entropy of the dissociated state. However, the presence of hydrophobic clusters from the PBA-ARS esters serves as barriers for

hydrolysis as it reduces the wetting around these PBA–ARS esters. An indication for the presence of such hydrophobic domains is also obtained from the SEM pictures which show a reduced porosity for the freeze-dried ARS containing hydrogels (Figure 10.3).

10.4.2. Mechanism of glucose-induced ARS release

It was observed that the presence of D-glucose accelerates the gel degradation and the release of ARS, due to the competition for boronic ester formation with PVA in the network. Since the boronic ester formation is reversible, free ARS is in equilibrium with complexed ARS when incorporated in the hydrogel. Ester bond formation of PBA with D-glucose instead of ARS results in a more hydrophilic local environment, which in its turn further promotes the hydrophilicity in the network, causing increased gel degradation.

It is observed that in the presence of 10% w/v D-glucose, the ARS release from the PEG_{10kDa}(PBA)₄ based gel was nearly instantaneous (Figure 10.7), thereby achieving a burst release. By comparing the results of the PEG_{10kDa}(PBA)₄ and the PEG_{10kDa}(PBA)₈ based hydrogel system it becomes evident that the ARS release mechanism from the PEG_{10kDa}(PBA)₄ based hydrogel system is more swelling/degradation-controlled whereas ARS release from the PEG_{10kDa}(PBA)₈ based gel is more diffusion-controlled. This is in agreement with the observation that degradation profile for the PEG_{10kDa}(PBA)₄ based gels is more synchronous with the ARS release than observed for the PEG_{10kDa}(PBA)₈ based gels.

These results indicate that the presence of D-glucose not only enhanced the degradation rate of the hydrogel but also increased the diffusivity of ARS in the gel. As a result, more unbound ARS was prone to diffuse from the gel into the surrounding media, explaining the somewhat faster initial release of ARS compared to the degradation of the gel. Hence, the potential of the PEG_{10kDa}(PBA)₄ and PEG_{10kDa}(PBA)₈ based gel as a D-glucose-triggered drug release system has successfully been demonstrated.

10.5. Conclusions

Phenylboronated 2-, 4-, and 8-arm PEG_{10kDa}(PBA)_n crosslinkers form dynamic restructuring hydrogels by reversible covalent crosslinking with poly(vinyl alcohol). The binding constant of the PBA moieties at the 8-armed PEG_{10kDa}(PBA)₈ with ARS is significantly higher than for those of the 2- and 4-armed crosslinkers, which is attributed to the formation of hydrophobic PBA–ARS clusters for the 8-armed compound.

It was found that the presence of ARS reduced the degradation rate of both PEG_{10kDa}(PBA)₄ and PEG_{10kDa}(PBA)₈ based gels. This is attributed to increased

hydrophobicity in the gel as the hydrophobic ARS can repel the penetration of water, resulting in a less porous network as observed by SEM. The presence of more hydrophobic ARS-PBA ester groups in the hydrogel significantly decreased the hydrolysis rate of the boronic ester crosslinks of PBA moieties with PVA. ARS loaded hydrogels based on PEG_{10kDa}(PBA)₈ demonstrated already in the presence of 1% w/v of glucose a 20 fold faster degradation. At a 10% w/v glucose complete degradation was observed within 5 hours.

The presence of D-glucose can enhance the diffusion of ARS as well as accelerate the degradation of both hydrogel systems, therefore, both PEG_{10kDa}(PBA)₄ and PEG_{10kDa}(PBA)₈ based hydrogels can be applied as D-glucose-triggered drug release system under physiological conditions.

10.6 Literature

- [1] A.S. Hoffman, Hydrogels for biomedical applications, *Adv. Drug Deliv. Rev.*, 54 (2002) 3-12.
- [2] N.A. Peppas, J.Z. Hilt, A. Khademhosseini, R. Langer, Hydrogels in biology and medicine: From molecular principles to bionanotechnology, *Adv. Mater.*, 18 (2006) 1345-1360.
- [3] D.G. Hall, *Boronic Acids - Preparation and applications in organic synthesis and medicine*, John Wiley & Sons, 2005.
- [4] W.Q. Yang, X.M. Gao, B.H. Wang, Boronic acid compounds as potential pharmaceutical agents, *Med. Res. Rev.*, 23 (2003) 346-368.
- [5] A.E. Ivanov, H. Larsson, I.Y. Galaev, B. Mattiasson, Synthesis of boronate-containing copolymers of N,N-dimethylacrylamide, their interaction with poly(vinyl alcohol) and rheological behaviour of the gels, *Polymer*, 45 (2004) 2495-2505.
- [6] S. Kitano, Y. Koyama, K. Kataoka, T. Okano, Y. Sakurai, A novel drug delivery system utilizing a glucose responsive polymer complex between poly (vinyl alcohol) and poly (N-vinyl-2-pyrrolidone) with a phenylboronic acid moiety, *J. Control. Release*, 19 (1992) 161-170.
- [7] E. Chiellini, A. Corti, S. D'Antone, R. Solaro, Biodegradation of poly (vinyl alcohol) based materials, *Prog. Pol. Sci.*, 28 (2003) 963-1014.
- [8] I. Inamura, Liquid-liquid phase-separation and gelation in the poly(vinyl-alcohol) poly(ethylene glycol) water-system - dependence on molecular-weight of poly(ethylene glycol), *Polym. J.*, 18 (1986) 269-272.
- [9] S. Kitano, K. Kataoka, Y. Koyama, T. Okano, Y. Sakurai, Glucose-responsive complex-formation between poly(vinyl alcohol) and poly(N-vinyl-2-pyrrolidone) with pendent phenylboronic acid moieties, *Makrom. Chem-Rapid Commun.*, 12 (1991) 227-233.
- [10] I. Hisamitsu, K. Kataoka, T. Okano, Y. Sakurai, Glucose-responsive gel from phenylborate polymer and poly(vinyl alcohol): Prompt response at physiological pH through the interaction of borate with amine group in the gel, *Pharmaceut. Res.*, 14 (1997) 289-293.
- [11] A.E. Ivanov, H.A. Panahi, M.V. Kuzimenkova, L. Nilsson, B. Bergenstahl, H.S. Waqif, M. Jahanshahi, I.Y. Galaev, B. Mattiasson, Affinity adhesion of carbohydrate particles and yeast cells to boronate-containing polymer brushes grafted onto siliceous supports, *Chem-Eur. J.*, 12 (2006) 7204-7214.
- [12] M.C. Roberts, M.C. Hanson, A.P. Massey, E.A. Karren, P.F. Kiser, Dynamically restructuring hydrogel networks formed with reversible covalent crosslinks, *Adv. Mater.*, 19 (2007) 2503-2507.
- [13] M.C. Roberts, A. Mahalingam, M.C. Hanson, P.F. Kiser, Chemorheology of phenylboronate-salicylhydroxamate cross-linked hydrogel networks with a sulfonated polymer backbone, *Macromolecules*, 41 (2008) 8832-8840.
- [14] J.I. Jay, S. Shukair, K. Langheinrich, M.C. Hanson, G.C. Cianci, T.J. Johnson, M.R. Clark, T.J. Hope, P.F. Kiser, Modulation of viscoelasticity and HIV transport as a function of pH in a reversibly crosslinked hydrogel, *Adv. Funct. Mater.*, 19 (2009) 2969-2977.
- [15] M. Piest, X. Zhang, J. Trinidad, J.F.J. Engbersen, Dynamically restructuring hydrogels based on the reversible covalent crosslinking of poly(vinyl alcohol) by diboronated Jeffamines, See chapter 9 of this thesis, (2010).

- [16] M. Piest, S.D. Hujaya, X. Zhang, J.F.J. Engbersen, Effects of arm length and number of arms of phenylboronic acid functionalized poly(ethylene glycols) on the viscoelastic properties of reversible covalent crosslinked poly(vinyl alcohol) hydrogels, See chapter 10 of this thesis, (2010).
- [17] C. Hiemstra, Z. Zhong, L. Li, P.J. Dijkstra, J. Feijen, In-Situ Formation of Biodegradable Hydrogels by Stereocomplexation of PEG-(PLLA)₈ and PEG-(PDLA)₈ Star Block Copolymers, 7 (2006) 2790-2795.
- [18] C. Hiemstra, Z. Zhong, S.R. Van Tomme, M.J. van Steenberg, J.J.L. Jacobs, W.D. Otter, W.E. Hennink, J. Feijen, In vitro and in vivo protein delivery from in situ forming poly(ethylene glycol)-poly(lactide) hydrogels, 119 (2007) 320-327.
- [19] S. Aryal, M. Prabakaran, S. Pilla, S.Q. Gong, Biodegradable and biocompatible multi-arm star amphiphilic block copolymer as a carrier for hydrophobic drug delivery, *Int. J. Biol. Macromol.*, 44 (2009) 346-352.
- [20] S.J. Buwalda, P.J. Dijkstra, L. Calucci, C. Forte, J. Feijen, Influence of Amide versus Ester Linkages on the Properties of Eight-Armed PEG-PLA Star Block Copolymer Hydrogels, 11 (2009) 224-232.
- [21] J.M. Jukes, L.J. van der Aa, C. Hiemstra, T. van Veen, P.J. Dijkstra, Z. Zhong, J. Feijen, C.A. van Blitterswijk, J. de Boer, A Newly Developed Chemically Crosslinked Dextran-Poly(Ethylene Glycol) Hydrogel for Cartilage Tissue Engineering, 16 (2010) 565-573.
- [22] G. Springsteen, B.H. Wang, Alizarin Red S. as a general optical reporter for studying the binding of boronic acids with carbohydrates, *Chem. Commun.*, (2001) 1608-1609.
- [23] G. Springsteen, B.H. Wang, A detailed examination of boronic acid-diol complexation, *Tetrahedron*, 58 (2002) 5291-5300.
- [24] D.L. Elbert, J.A. Hubbell, Conjugate addition reactions combined with free-radical cross-linking for the design of materials for tissue engineering, *Biomacromolecules*, 2 (2001) 430-441.
- [25] M. Piest, J.F.J. Engbersen, Role of boronic acid moieties in disulfide containing poly(amido amine)s for non-viral gene delivery, See chapter 3 of this thesis, (2010).
- [26] M. Piest, J. Trinidad, J.F.J. Engbersen, Bioresponsive, restructuring hydrogels based on boronic acid functionalized poly(amido amine)s for reversible covalent crosslinking of poly(vinyl alcohol), See chapter 7 of this thesis, (2010).
- [27] J. Siepmann, N.A. Peppas, Modeling of drug release from delivery systems based on hydroxypropyl methylcellulose (HPMC), *Adv. Drug Del. Rev.*, 48 (2001) 139-157.

Final Conclusions

In this chapter the final conclusions of this thesis are summarized according to the hypotheses of chapter 1, repeated below.

Hypotheses

1. Introduction of phenylboronic acids allows for additional binding of polyplexes of SS-PAAAs with the glycoproteins of the cell membrane (boronic ester formation), resulting in increased particle uptake and ultimately in higher transfection efficiencies. This hypothesis is addressed in Chapter 3.
2. Introduction of phenylboronic acids in SS-PAAAs containing hydroxybutyl side chains could result in polyplexes formed with nucleic acids with increasing stability due to crosslinking of the polymer chains in the polyplex upon boronic ester formation. This increased particle stability may prove especially beneficial for siRNA polyplexes, as the 3' ribose end group is also capable of additional boronic ester formation. These hypotheses are addressed in Chapter 4.
3. The presence of boronic acid moieties on the periphery of SS-PAA nanoparticles and polyplexes could allow for decoration of these particles with:
 - a. Saccharides for targeting specific cells in order to enhance transfection or gene silencing efficiency. This hypothesis is also addressed in Chapter 4.
 - b. Therapeutic diols (such as dopamine or L-dopa) for intracellular drug delivery and combined intracellular drug and gene delivery. This hypothesis is addressed in Chapter 5.
 - c. Polysaccharides such as dextran to reduce the zeta potential and provide stealth properties to the cationic polyplexes and may provide a possible alternative for PEGylation. This hypothesis is addressed in Chapter 6.
4. The presence of phenylboronic acids in PAAAs allows for crosslinking with polyvinylalcohol (PVA) resulting in a dynamically restructuring and bioresponsive hydrogel. This hypothesis is addressed in Chapter 7.
5. The presence of phenylboronic acids in PAAAs may allow for easy incorporation of polyplexes in other phenylboronic acid functionalized polymer based gels. In Chapter 8-10 work was expanded to other phenylboronic acid functionalized polymers with good water-solubility and biocompatibility to form hydrogels:
 - a. Jeffamine spacers (PPO-PEO-PPO) for PVA crosslinking. (Chapter 8)
 - b. Multi-arm PEG spacers for PVA crosslinking. (Chapter 9 and 10)

11.1 Final conclusions

- 1) Introducing phenylboronic acids in the side chains of SS-PAA for gene delivery showed distinct differences in their behavior as compared to the non-boronated control SS-PAA. Unfortunately, introduction of phenylboronic acids does not unambiguously result in higher transfection efficiencies. It did result in increased membrane interactions, as demonstrated by the higher hemolytic activity and altered polyplex behavior upon acidification. Especially polyplexes prepared with the ortho-aminomethylphenylboronic acid containing polymer p(DAB-2AMPBA) showed increased cytotoxicity towards the COS-7 cells. The specific boronic ester formation with glycoproteins on the cell membrane was not addressed in Chapter 3. However, the results presented in Chapter 4 demonstrated that addition of the strong binding D-sorbitol to polyplexes of p(ABOL-2AMPBA) improved the transfection efficiency, most likely by prevention of boronic ester formation with glycoproteins of the cell surface. Thus hypothesis 1 proved false, as it can be concluded that additional binding upon boronic ester formation with glycoproteins of the cell surface does not necessarily result in higher uptake or transfection efficiencies.
- 2) The results presented in Chapter 4 also showed that p(ABOL-2AMPBA) indeed was capable of forming nanoparticles and polyplexes with higher stability. Compared to the non-boronated p(ABOL) it seemed that the enhanced polyplex stability was more advantageous for siRNA delivery than for pDNA delivery.
- 3) During this research various attempts were made to decorate the boronic acid moieties on the periphery of p(ABOL-2AMPBA) nanoparticles and polyplexes:
 - a) Regarding the role of the saccharides for targeting specific cells, results were somewhat disappointing. After many transfection experiments no significant cell-specific improvement of the transfection efficiency was observed due to the presence of saccharides. However, results in Chapter 4 did show that the presence of saccharides improved the gene silencing using siRNA, also suggesting that the boronic acid moieties interacts with siRNA conform hypothesis 2.
 - b) The concept of decorating self-assembled nanoparticles and polyplexes with therapeutic diols such as dopamine or L-dopa was demonstrated using alizarin red S (ARS). ARS upon complexation with a boronic acid forms a fluorescent dye allowing for the visualization of the intracellular drug delivery and combined intracellular drug and gene delivery by FACS and confocal microscopy. Results presented in Chapter 5 show that ARS is efficiently incorporated in the nanoparticles and polyplexes after which it is efficiently taken up by the cells, without significantly reducing the transfection properties of the polyplexes.

- c) Results in Chapter 6 showed that the addition of the polysaccharide dextran did not significantly reduce the zeta potential. Surprisingly, the presence of dextran did improve the transfection efficiency of both p(ABOL-2AMPBA) and the control p(ABOL). Confocal microscopy experiments using FITC-labeled dextran showed that FITC-dextran was only endocytosed in presence of p(ABOL-2AMPBA), suggesting stable boronic ester formation.
- 4) The results in Chapter 7 showed that the presence of phenylboronic acids in PAAs allows for crosslinking of poly(vinyl alcohol) (PVA) in a dynamically restructuring and bioresponsive hydrogels.
- 5) Regarding boronic acid functionalized materials that form hydrogels with PVA:
 - a) Results in Chapter 8 show that medium strong gels were formed with boronated Jeffamine spacers (PPO-PEO-PPO).
 - b) Results in Chapter 9 show that stronger gels were formed with boronated multi-arm PEG spacers and their capacity for glucose-responsive drug delivery using ARS as a model drug compound was demonstrated in Chapter 10.

The concept of introducing phenylboronic acids into biomaterials offers many new possibilities in developing controlled drug delivery strategies. The examples studied in this thesis show that incorporation of phenylboronic acid moieties into a polymer system allows for reversible covalent chemistries setting the stage for new “intelligent” biomaterials with unique possibilities to tune the pH-, temperature-, and chemo-responsive properties. In addition, these boronic acid functionalized materials allow for new strategies to incorporate diol-containing therapeutics that can be released in a controlled manner in the presence of competing diols and/or polyols.

Appendix A. Unfinished work

Experiments are intended to increase our insights, and thus by definition experiments cannot fail. However, sometimes the experimental outcome is not to our liking. The reasons hereof may vary from experimental evidence that is inconclusive, differences that are not significant, or the outcome that does not fit within the story we would like to present. Of these categories the last is most interesting as these experiments often raise new questions and call for additional experiments. In this section three of these examples are presented.

A.1. Pyridinium boronic acid containing monomers

It was hypothesized that pyridinium boronic acids would have very high binding affinity towards vicinal diols at physiological relevant pH due to the increased electron deficiency of the boron centre attached to the pyridinium ring. Hence, many attempts were made to include a pyridinium boronic acid-containing compound within the series of SS-PAA tested. This monomer is depicted in Figure A.1.

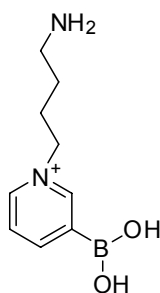
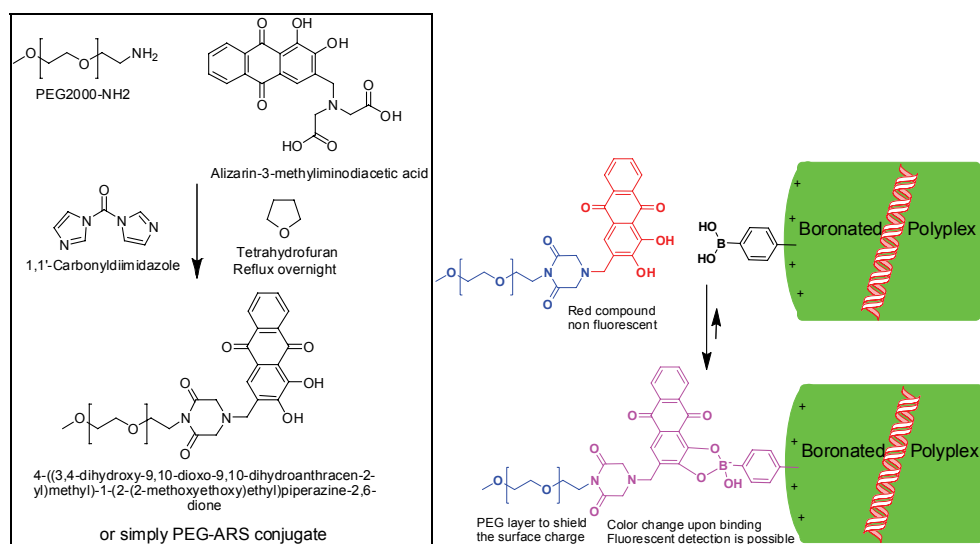


Figure A.1. Pyridinium boronic acid monomer suitable for Michael addition polymerization.

It was possible to synthesize this monomer, although the reaction was not complete according to ^1H NMR (not shown). Unfortunately, all attempts to isolate or further purify this monomer proved fruitless. A white powder turned into a purple to brown oil during filtration over a Büchner funnel. Upon extraction, the dissolved material changed in color from yellow to red, green, blue and purple depending on the solvent and pH selected, in all cases ultimately resulting in brown oils. These observations typically point towards oxidation, and some literature mentions the possibility of protolytic deboronation observed using similar compounds [1,2]. It can be argued that when these monomers have a poor chemical stability, also the resulting polymers are likely not very stable and further attempts to isolate this monomer were halted.

A.2. Post-PEGylation using salicylhydroxylamine PEG conjugates

Inspired by the work of Moffat and Stolowitz (see Chapter 2.3 and 2.3.3 of this thesis and [3,4]), it was hypothesized that a salicylhydroxylamine functionalized PEG (SHA-PEG) could form a bio-conjugate with a phenylboronic acid functionalized nanoparticles, such as presented in Chapter 3–6 of this thesis. This would enable an easy method for reversible *post*-PEGylation of polyplexes of boronic acid functionalized SS-PAA and pDNA or siRNA, thereby shielding the positive charges of these polyplexes that is desired for *in vivo* experiments. Various attempts were made to synthesize the SHA-PEG, but with limited success. This was due to high reactivity of the hydroxylamine group interfering in coupling reactions and the sensitivity of this group towards oxidation. Alternatively, an alizarin-PEG conjugate (ARS-PEG) was developed according to Scheme A.2.



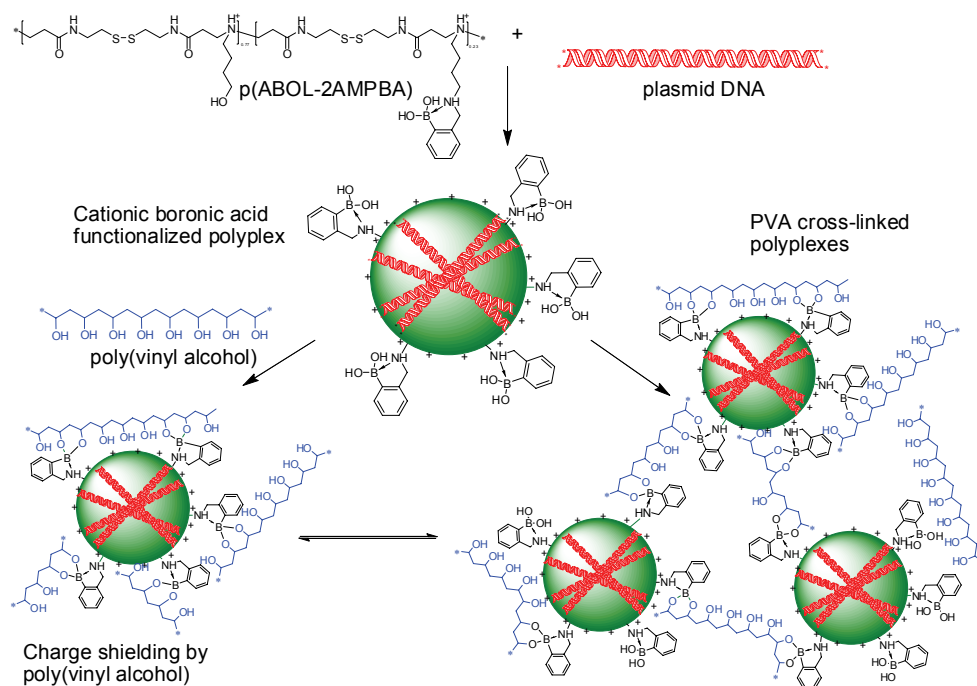
Scheme A.2. Synthesis of ARS-PEG conjugate and concept of *post*-PEGylation of boronated polyplexes.

As demonstrated in Chapter 5 of this thesis, polyplexes of phenylboronic acid containing SS-PAA could be easily functionalized with alizarin red S, forming a fluorescent complex. Similarly, it was anticipated that polyplexes of phenylboronic acid containing SS-PAA could be PEGylated after exposure to ARS-PEG, resulting in a fluorescent particle with reduced zeta potential. Preliminary results indeed showed a color change from the deep red ARS-PEG solution to a purple solution after addition to a colorless phenylboronic acid containing SS-PAA solution. Surprisingly, dynamic light scattering experiments showed a reduction in zeta-potential for both polyplexes of the boronated SS-PAA p(DAB-2AMPBA) and polyplexes of the non-boronated control SS-PAA p(DAB-Bz) with increasing ARS-PEG concentration.

These results might indicate that in addition to boronic ester formation hydrophobic driven association of the hydrophobic alizarin moiety can contribute to the reduction of the zeta potential that was observed. Unfortunately, there was no time left to conduct any additional experiments, such as fluorescence microscopy, transfection studies or confocal microscopy.

A.3. PVA coating of boronic acid containing polyplexes

It was hypothesized that reversible boronic ester formation between phenylboronic acid containing SS-PAAs/pDNA polyplexes and PVA could provide another alternative to PEGylation. Coating of these boronated polyplexes could reduce the zeta potential and possibly result in formation of nanogels or macrogels, see Scheme A.3.



Scheme A.3. Conceptual overview of boronated polyplexes formed by electrostatic interactions with pDNA, which can be coated with poly(vinyl alcohol) by ester formation of the *ortho*-aminomethylphenylboronic side group with the multiple 1,3- hydroxyl groups of the PVA. At higher concentration aggregation or gelation may occur.

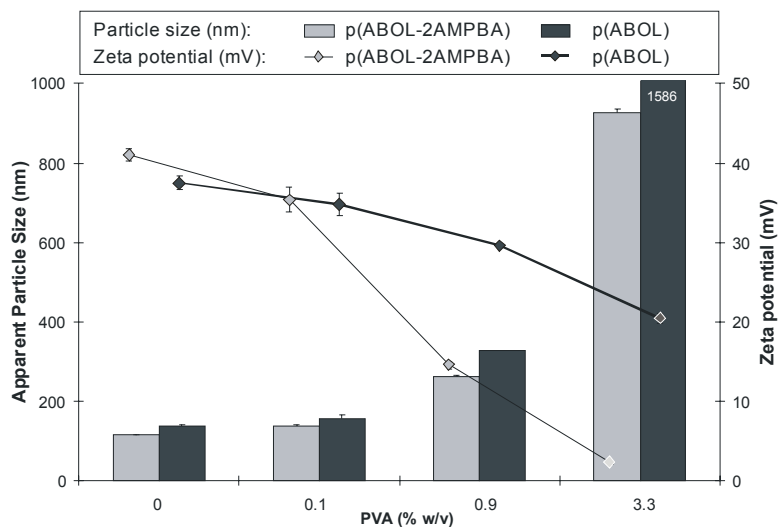


Figure A.2. Effect of poly(vinyl alcohol) (PVA) addition to polyplexes formed with p(ABOL-2AMPBA) (light grey) or p(ABOL) (dark grey) with DNA at a 48/1 polymer/DNA weight ratio. Particle size is shown in bars and zeta potentials are shown in diamonds. Lines are added for clarity. A significant viscosity increase was observed at higher PVA concentrations.

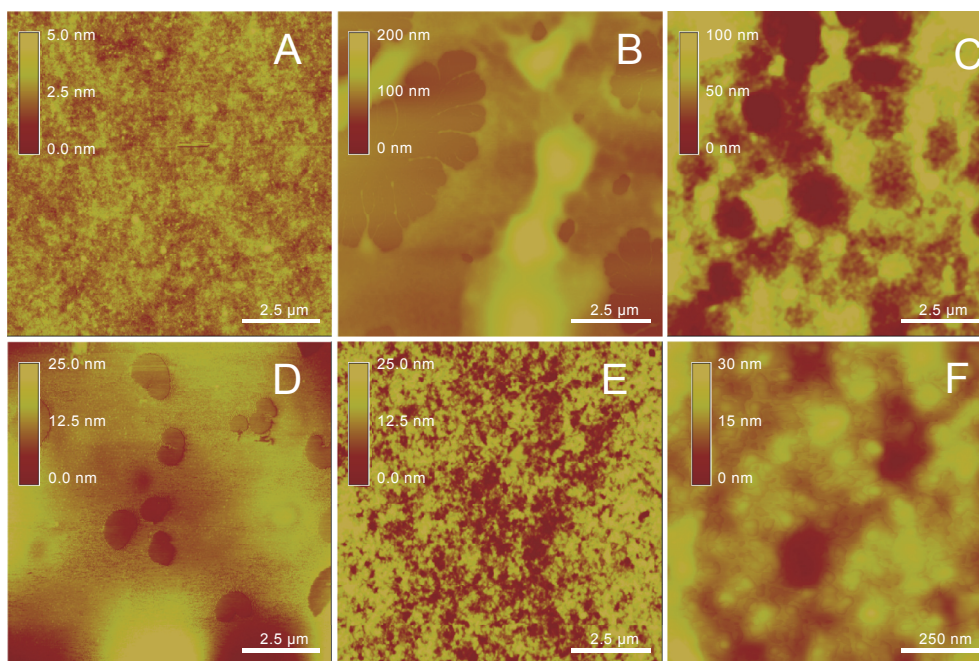


Figure A.3. Different polymer solutions were added to a freshly cleaved mica surface and dried to air before probing with AFM. **A)** PVA (47 kDa); **B)** p(ABOL); **C)** mixture of PVA and p(ABOL); **D)** p(ABOL-2AMPBA); **E)** mixture of p(ABOL-2AMPBA) and PVA; **F)** zooming in on the mixture of PVA and p(ABOL-2AMPBA).

However, it was found that the presence of PVA could significantly reduce the zeta potential at higher PVA concentrations where the medium was increasingly viscous (Figure A.2). Although the degree of zeta potential reduction was significantly higher for the boronic acid containing polyplexes, data was biased by the reduction of the electrophoretic mobility in the viscous high concentration PVA medium for which was not corrected. Several attempts were made to verify the data by atomic force microscopy experiments (Figure A.3). It was found that boronated PAAs in presence of PVA showed “nano-flat” surfaces with height differences less than 5 nm. Surprisingly, phase-contrast pictures showed more rigid regions with sizes matching to that of self-assembled nanoparticles and polyplexes (50-200 nm), suggesting that boronated PAAs are present in these gels as aggregates, perhaps even spherical particles. Preliminary transfection experiments (Figure A.4) showed that high concentrations of PVA were not toxic to the cells and as expected PVA was not capable of transfecting cells. Both the non-boronated p(ABOL) polyplexes and the boronated p(ABOL-2AMPBA) polyplexes were able to transfect the cells at PVA concentrations up to 0.9% w/w. At higher (almost gelling) concentrations of 3.3 % w/w transfection was inhibited, suggesting that polyplexes were immobilized.

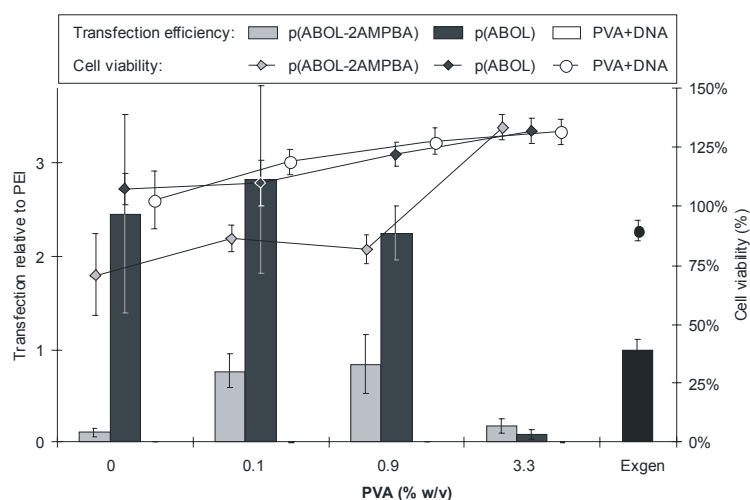


Figure A.4. Transfection (shown in bars) and cell viability (shown in lines) for polyplexes of p(ABOL-2AMPBA) (light grey) or p(ABOL) (dark grey) in presence of increasing concentration of PVA (47 kDa). PVA only (white) was selected as negative control and commercial PEI (Exgen at its optimal N/P ratio of 6) was used as positive control.

The AFM results suggest that it should be possible to immobilize polyplexes with therapeutic pDNA or siRNA intact in a PVA hydrogel. For example, boronated polyplexes may be stabilized in a boronated multi-arm PEG/PVA hydrogel that can be gradually released from the gel in a controlled manner.

A.4. References

- [1] T. Maki, K. Ishihara, H. Yamamoto, N-alkyl-4-boronopyridinium salts as thermally stable and reusable amide condensation catalysts, *Org. Lett.*, 7 (2005) 5043-5046.
- [2] T. Maki, K. Ishihara, H. Yamamoto, N-alkyl-4-boronopyridinium halides versus boric acid as catalysts for the esterification of α -hydroxycarboxylic acids, *Org. Lett.*, 7 (2005) 5047-5050.
- [3] S. Moffatt, S. Wiehle, R.J. Cristiano, Tumor-specific gene delivery mediated by a novel peptidepolyethylenimine-DNA polyplex targeting aminopeptidase N/CD13, *Hum. Gene Ther.*, 16 (2005) 57-67.
- [4] M.L. Stolowitz, C. Ahlem, K.A. Hughes, R.J. Kaiser, E.A. Kesicki, G.S. Li, K.P. Lund, S.M. Torkelson, J.P. Wiley, Phenylboronic acid-salicylhydroxamic acid biconjugates. 1. A novel boronic acid complex for protein immobilization, *Bioconjugate Chem.*, 12 (2001) 229-239.

Summary

Boronic acid chemistry is a relatively unknown part of organic chemistry that is not treated in most organic chemistry textbooks. Consequently, boronic acid functionalized materials are only rarely investigated in the field of biomedical applications. The goal of this thesis was to investigate the potential of boronic acid functionalized polymers and hydrogels in biomedical applications. **Chapter 1** describes the outline of the thesis and the hypotheses, starting from the concept of introducing phenylboronic acids in the side chains of disulfide containing poly(amido amine)s (SS-PAA) for gene delivery. **Chapter 2** provides an overview of the current status of boronic acid functionalized polymers, thereby especially focusing on biomedical applications.

In **Chapter 3**, the experimental work starts with the introduction of two different types of phenylboronic acids on the aminobutyl side chains of a disulfide-containing poly(amido amine) (SS-PAA). These materials were investigated in their effectiveness to function as gene delivery vectors *in vivo*, and to elucidate the effects of the presence of boronic acids functionalized side groups. A para-carboxyphenylboronic acid was selected, resulting in p(DAB-4CPBA) and an ortho-aminomethylphenylboronic acid was incorporated through copolymerization, resulting in p(DAB-2AMPBA). Both polymers contained 30% of phenylboronic acid side chains and 70% of residual aminobutyl side chains and were compared with a non-boronated benzoylated analogue p(DAB-Bz) of similar M_w . It was found that the presence of phenylboronic acid moieties improved polyplex formation with plasmid DNA as smaller and more monodisperse polyplexes were formed as compared to their non-boronated counterparts. The transfection efficiency of polyplexes of p(DAB-4CPBA) was approximately similar to that of p(DAB-Bz) and commercial PEI (Exgen), both in the absence and the presence of serum, indicating that p(DAB-4CPBA) and p(DAB-Bz) are potent gene delivery vectors. However, the polymers with phenylboronic acid functionalities showed increased cytotoxicity, which is stronger for the ortho-aminophenylboronic acid containing polyplexes of p(DAB-2AMPBA) than for the p(DAB-4CPBA) analog. The cytotoxic effect may be caused by increased membrane disruptive interaction as was indicated by the increased hemolytic activity observed for these polymers.

In **Chapter 4**, the effects of the presence of *ortho*-aminomethylphenylboronic acid moieties as side groups in disulfide containing poly(amido amines) for gene delivery were further investigated. To this purpose, the boronated polymer p(ABOL/2AMPBA) was developed, comprising 23% of *ortho*-aminophenylboronic acid side chains and 77% aminobutanol side chains. This polymer spontaneously forms self-assembled nanoparticles that are stabilized by reversible interactions of the Lewis-acidic boronic

acid groups with tertiary amine groups in the main chain and pending hydroxybutyl groups in the side chains of the polymer. Consequently, polyplexes with pDNA and siRNA of *ca.* 100 nm and 40 mV were formed with higher stability than p(ABOL), as no aggregation was observed after storage of 4 days at 37 °C. The nanoparticles release their nucleotide cargo completely in a reductive environment due to rapid cleavage of the disulfide bonds in the main chain of the polymer. DNA transfection efficiency of p(ABOL/2AMPBA) in different cell lines was approximately similar to commercial PEI, whereas p(ABOL) lacking the boronic acid moieties was *ca.* two times more effective than PEI. For siRNA transfection the use of p(ABOL) and p(ABOL/2AMPBA) as polymeric vectors resulted in knockdown efficiencies of luciferase expression in H1229-Fluc cells of *ca.* 28% and 35%, respectively. Most importantly, whereas addition of different monosaccharides to polyplexes of p(ABOL) have only marginal effects, the knockdown or efficiency of siRNA polyplexes of p(ABOL/2AMPBA) could be significantly enhanced (up to 67%) in the presence of these carbohydrates.

In **Chapter 5**, this copolymer p(ABOL/2AMPBA) containing the *ortho*-aminomethylphenylboronic acid moieties was further investigated as it spontaneously forms stable nanoparticles in HEPES buffer solution (pH 7.4). The presence of the *ortho*-aminomethylphenylboronic acid moieties in the nanoparticles allows for drug conjugation by dynamic covalent boronic ester formation with compounds containing vicinal diols (like dopamine and L-dopa) enabling new strategies for drug delivery. Moreover, with pDNA the copolymer readily forms nanosized polyplexes, which makes this copolymer excellently suitable for combined drug and gene delivery. In this study alizarin red S (ARS) was selected as a model drug, as ARS forms a fluorescent complex with boronic acids enabling the visualization of the uptake of boronic acid-ARS complexed nanoparticles. p(ABOL/2AMPBA) nanoparticles loaded with 12.5% ARS with respect to the PBA moieties, as well as ARS loaded polyplexes with pDNA were internalized up to 70–90% in COS-7 and H1299-Fluc cells, demonstrating efficient drug delivery and combined drug and gene delivery with this polymeric vector. The ARS-loaded polyplexes showed transfection efficiencies of 1.3–1.7 times that of PEI in COS-7 cells, while retaining almost full cell viability.

In **Chapter 6**, this copolymer p(ABOL/2AMPBA) was further investigated in its capacity for reversible boronic ester formation with vicinal diols, using the polycarbohydrate dextran. It was found that p(ABOL/2AMPBA) forms polyplexes with pDNA that were stable for at least up to 6 days at 37 °C in HEPES buffer. Dynamic light scattering showed that the presence of dextran did not significantly affect the size (100–140 nm) and the zeta potential (*ca.* 25 mV) of the polyplexes; however a clear indication of the shielding of the polyplexes by the presence of dextran

was obtained from AFM pictures showing that only in the presence of dextran the spreading of the disulfide containing polyplexes on a gold surface is prevented. The presence of dextran was found to improve the transfection efficiencies of p(ABOL/2AMPBA) in COS-7 cells and SH-SY5Y neuroblastoma cells. Confocal fluorescence microscopy studies showed that FITC-labeled dextran colocalized with polyplexes of p(ABOL/2AMPBA) and not with the non-boronated control polymer p(ABOL), suggesting that the dextran is bound to p(ABOL/2AMPBA) polyplexes through reversible boronic ester formation. Addition of dextran to siRNA- p(ABOL/2AMPBA) polyplexes also significantly improved the knockdown of luciferase expression in H1299-Fluc cells.

In **Chapter 7**, a water-soluble poly(amido amine) (PAA) with a high density of *ortho*-aminomethyl substituted phenylboronic acids was developed. Due to the possibility of a dative B–N interaction, the pK_a value of the *ortho*-aminomethylphenylboronic acid is significantly reduced and diol complexation is facilitated at lower pH. The boronated PAA readily formed dynamically restructuring strong hydrogels by reversible covalent crosslinking of poly(vinyl alcohol) (PVA) already at low concentrations of 5–10% w/v, with gel strengths G'_{max} up to 20 kPa, whereas the non-boronated control PAA did not form a gel. The gels were transparent, thermoresponsive and this response to temperature changes was instantaneous and completely reversible. These dynamically crosslinked hydrogels have self-healing capacities and degrade in a large excess of water within several hours, which make them suitable for controlled drug delivery applications. Addition of D-glucose solutions to these gels resulted in a significant increase of the degradation rate as a function of glucose concentration. The pH-, thermo-, and glucose-responsive behaviors of these types of gel systems render them ideal candidates for development of new glucose-responsive controlled drug delivery devices.

In **Chapter 8**, dynamically restructuring (“self-healing”) hydrogels were prepared by reversible formation of boronic-ester crosslinks between bis-boronic acid containing compounds and polyols, such as poly(vinyl alcohol) (PVA). To this purpose two different bis-(phenylboronic acid) functionalized crosslinkers with a PPO-PEO-PPO spacer Jeff-2AMPBA and Jeff-4AMPBA were synthesized via reductive coupling of 2-, and 4-formylphenylboronic acid to JeffamineED1900. Due to the different position of the secondary amino group with respect to the boronic acid moiety (*ortho* or *para*) the pK_a of the amino and boronic acid groups in the spacer endgroups differ significantly, thereby influencing the optimal pH for boronic ester formation. Using alizarin red S at varying pH (5.0, 6.5 and 7.4), highest binding with alizarin was found for the *ortho*-aminomethylphenylboronic acid at pH 6.5, while highest binding with alizarin was found for the *para*-aminomethylphenylboronic acid at pH 7.4. Both Jeff-2AMPBA and Jeff-4AMPBA could form fairly strong hydrogels with PVA

at low pH 4, but strongest gels were formed with the para-boronic acid at pH 9. Apparently, the presence of an inter-molecular B–N interaction by Jeff-4AMPBA is favored over the presence of an intra-molecular B–N interaction by Jeff-2AMPBA for strong hydrogel formation with PVA at physiological pH.

In **Chapter 9**, dynamically restructuring or so-called “self-healing” hydrogels were prepared by complexation of boronic acid containing PEG-crosslinkers with PVA. To this purpose a series of novel boronated PEG-crosslinkers have been synthesized by reductive amination of amine-functionalized PEGs with 4-formylphenylboronic acid. Different PEG architectures were selected and the effects of the PEG arm length and the number of arms on the rheological properties of the resulting hydrogels with PVA were investigated under physiological conditions (PBS, pH 7.4, 37 °C). The gel strength, as based on the plateau storage modulus determined by oscillatory rheological measurements, was found to decrease for the 2-arm crosslinker with increasing PEG arm length (increasing PEG M_w). Similarly, the gel strength was found to increase with increasing number of arms of the multiarm boronated PEG-linkers. With this novel linker system, transparent thermo-reversible gels with storage moduli up to 30 kPa were attainable in PBS (pH 7.4, 37 °C). The gel strength, shape stability, and visual appearance of hydrogels formed with this novel linker and PVA can be tuned by proper adjustment of molecular architecture, M_w and concentration of both the PEG-linker and the PVA.

Drug release from these systems was further investigated in **Chapter 10**, where dynamically restructuring hydrogels could be prepared by reversible covalent crosslinking of poly(vinyl alcohol) (PVA, 195 kDa) with multi-arm phenylboronic acid (PBA) functionalized poly(ethylene glycol) (PEG) crosslinkers, abbreviated as PEG_{10kDa}(PBA)_n. Strong hydrogels were obtained by mixing of equal volumes of 10% w/v PVA and 10% w/v PEG_{10kDa}(PBA)₄ or PEG_{10kDa}(PBA)₈. It was found that the model drug compound alizarin red S (ARS) forms a fluorescent boronic ester when incorporated in the gel. The presence of ARS only mildly reduced the gel strength and prolonged the swelling and degradation of the hydrogel systems. ARS release from the PEG_{10kDa}(PBA)₈ based hydrogel was diffusion-controlled, whereas ARS release from the PEG_{10kDa}(PBA)₄ based hydrogel showed to be dependent on both diffusion and degradation. Moreover, the presence of D-glucose in solution increased the degradation of the hydrogel and fast release of ARS from the hydrogel systems was observed. These properties demonstrate that these hydrogels can be regarded as promising candidates for the development of D-glucose-responsive drug delivery systems.

In **Chapter 11**, the postulated hypotheses of **Chapter 1** are answered and the final conclusions of this thesis are presented here. Appendix A gives a brief overview of unfinished work is presented resulting in recommendations for possibilities for additional research.

Samenvatting

Boorzuurchemie is een relatief onbekend onderdeel van de organische chemie dat nauwelijks wordt behandeld in de meeste organische chemie tekstboeken. Het gevolg is dat boorzuurhoudende materialen maar zelden worden bestudeerd als materialen voor biomedische toepassingen. De doelstelling van dit proefschrift was om te onderzoeken wat het potentieel is van boorzuurhoudende polymeren en hydrogelen voor biomedische toepassingen. In **Hoofdstuk 1** is een overzicht gegeven van de hypothesen, met als uitgangspunt het concept van de introductie van fenylboorzuren aan de zijketens van disulfide-houdende poly(amido amine)s voor afgifte van genetisch materiaal, waaronder DNA en siRNA. In **Hoofdstuk 2** wordt vervolgens een overzicht gegeven van de huidige stand der techniek betreffende boorzuurhoudende polymeren, met daarin de nadruk gelegd op de biomedische toepassing van deze materialen.

In **Hoofdstuk 3** begint het experimentele onderzoek met de introductie van twee verschillende fenylboorzuren aan aminobutyl zijketens van een disulfide-houdend poly(amido amine) (SS-PAA). Deze materialen zijn onderzocht op hun effectiviteit om genetisch materiaal af te geven aan cellen en daarbij de rol van de boorzuren op te helderen. Een para-carboxyfenylboorzuur werd geselecteerd, resulterend in het polymeer p(DAB-4CPBA) en een ortho-aminomethylfenylboorzuur was ingebouwd door middel van copolymerisatie, resulterend in het polymeer p(DAB-2AMPBA). Beide polymeren bevatten 30% fenylboorzuur zijketens en 70% van de oorspronkelijke aminobutyl zijketens en werden vergeleken met een boorzuurvrij gebenzoyleerd vergelijkbaar polymeer p(DAB-Bz) met een vergelijkbaar molecuul gewicht. Het bleek dat de aanwezigheid van fenylboorzuur groepen de formatie van polyelectroliet complexen (polyplexen) met DNA plasmides bevorderde zodat kleinere en beter gedefinieerde (monodisperse) nanodeeltjes werden gevormd dan ten opzichte van de polyplexen gevormd met het boorzuurvrije polymeer. De transfectie efficiëntie, d.w.z. de hoeveelheid van het DNA plasmide dat in de cellen tot expressie komt, van polyplexen met p(DAB-4CPBA) was nagenoeg identiek aan die van het boorzuurvrije polymeer p(DAB-Bz) en aan die van polyethyleenimine, wat de standaard is in het veld. Dit was zowel het geval in de aanwezigheid en afwezigheid van serum, wat betekent dat p(DAB-4CPBA) en p(DAB-Bz) potente transportmaterialen zijn van DNA plasmides. Echter, de polymeren met de fenylboorzuren lieten een verminderde levensvatbaarheid zien van de blootgestelde cellen. Vooral de polyplexen van p(DAB-2AMPBA) bleken erg giftig voor de cellen. Dit kan wellicht worden verklaard door de toegenomen interacties met het celmembraan, aangezien er voor de boorzuurhoudende polymeren ook een hogere hemolytische activiteit werd waargenomen.

In **Hoofdstuk 4** zijn de effecten van de introductie van fenylboorzuren in een disulfide-houdend poly(amido amine) (SS-PAA) op de afgifte van DNA en siRNA verder onderzocht. Hiertoe is het polymeer p(ABOL/2AMPBA) met 23% *ortho*-aminofenylboorzuur zijketens en 77% aminobutanol zijketens ontwikkeld. Dit polymeer bleek in staat om polyplexen te vormen met zowel plasmide DNA als siRNA van ongeveer 100 nm groot en met een positieve lading van ongeveer 40 mV. De aanwezigheid van het boorzuur kwam de stabiliteit van deze deeltjes ten goede, aangezien er geen aggregatie werd waargenomen gedurende 4 dagen bij 37 °C. Na reductie van de disulfide bindingen in de polymeer hoofdketens in een reductieve omgeving kon het DNA plasmide, respectievelijk het siRNA, volledig worden vrijgegeven. De transfectie efficiëntie van p(ABOL/2AMPBA) met DNA plasmide was ongeveer gelijk aan die van de standaard PEI, gemeten in verschillende cellijnen, terwijl transfectie efficiëntie van het boorzuurvrije p(ABOL) ongeveer 2 keer hoger was. Polyplexen van siRNA met zowel p(ABOL) als met p(ABOL/2AMPBA) resulteerden in een verlaging van de productie van het eiwit luciferase door inhibitie van de genexpressie in stabiel getransfecteerde H1229-Fluc cellen met respectievelijk 28% en 35%. Belangrijker was de observatie dat, waar de aanwezigheid van monosaccharides geen invloed hadden op de DNA transfectie, deze aanwezigheid van monosaccharides de genexpressie van luciferase met wel 67% konden verlagen wanneer het boorzuurhoudende polymeer p(ABOL/2AMPBA) werd gebruikt.

In **Hoofdstuk 5** is het copolymeer p(ABOL/2AMPBA) verder onderzocht, aangezien het spontaan nanodeeltjes vormt in HEPES buffer van pH 7.4. De aanwezigheid van de *ortho*-aminomethylfenylboorzuren in deze nanodeeltjes maakt het mogelijk om therapeutische moleculen met vicinale diolen (zoals L-dopa en dopamine) aan zich te binden door vorming van omkeerbare boorzuresters, wat kan leiden tot nieuwe strategieën voor medicijnafgifte. Daarbij vormt het copolymeer eenvoudig polyplexen met nucleïnezuren, waardoor dit copolymeer bij uitstek geschikt is voor gecombineerde medicijn en plasmide DNA afgifte. Alizarine rood sulfaat (ARS) is geselecteerd als model verbinding, aangezien het een fluorescent complex vormt met boorzuren, waardoor het mogelijk is om de opname door cellen van de met ARS beladen p(ABOL/2AMPBA) nanodeeltjes en polyplexen te volgen met confocale fluorescentie microscopie en FACS. p(ABOL/2AMPBA) nanodeeltjes konden worden beladen met 12.5% ARS ten opzichte van de aanwezige fenylboorzuurgroepen. Deze fluorescente deeltjes evenals de met ARS beladen polyplexen werden door 70–90% van de blootgestelde COS-7 en H1299-Fluc cellen opgenomen. Deze resultaten demonstreren het potentieel van p(ABOL/2AMPBA) als materiaal voor medicijnafgifte evenals voor gecombineerde medicijn en DNA afgifte. De met ARS beladen polyplexen resulteerden in een 1.3–1.7 keer hogere genexpressie dan polyplexen van

polyethyleenimine in COS-7 cellen, zonder dat er sprake was van giftigheid voor de cellen.

In **Hoofdstuk 6** is het copolymeer p(ABOL/2AMPBA) verder onderzocht in zijn capaciteit voor omkeerbare boorzurester vorming met vicinale diolen met behulp van dextran. Het bleek mogelijk om polyplexen met plasmide DNA te maken die gedurende 6 dagen stabiel waren in HEPES buffer van 37 °C. Lichtverstrooiingsmetingen (DLS) lieten zien dat de aanwezigheid van dextran nauwelijks invloed had op de deeltjesgrootte (100–140 nm) en de oppervlakte lading (ca. 25 mV) van de polyplexen. Echter, een duidelijke aanwijzing voor de afscherming van de polyplexen door de aanwezigheid van dextran kwam van “Atomic Force Microscopy” metingen die lieten zien dat de spreiding van de disulfidehoudende deeltjes op een goudoppervlak alleen in aanwezigheid van dextran kan worden voorkomen voor het boorzuurhoudende polymeer. De aanwezigheid van dextran leidde ook tot een verhoging van de transfectie efficiëntie van p(ABOL/2AMPBA) polyplexen met plasmide DNA in COS-7 cellen en SH-SY5Y neuroblastoma cellen. Confocale microscopie demonstreerde dat FITC-gelabelde dextran colocaliseerde met de polyplexen van p(ABOL/2AMPBA) en niet met het boorzuurvrije controle polymeer p(ABOL), wat suggereert dat het dextran is gebonden aan p(ABOL/2AMPBA) polyplexen door vorming van omkeerbare boorzuresters. De toevoeging van dextran aan p(ABOL/2AMPBA) polyplexen met siRNA resulteerde in een significante toename van de onderdrukking van de genexpressie van luciferase in stabiel getransfecteerde H1229-Fluc cellen.

In **Hoofdstuk 7** is een water-oplosbaar poly(amido amine) met een hoge dichtheid van *ortho*-aminomethylfenylboorzuur functionaliteiten ontwikkeld. Door de mogelijkheid van een coördinerende B–N interactie wordt de pK_a -waarde van het *ortho*-aminomethylfenylboorzuur aanzienlijk verlaagd waardoor de diol-complexering (vorming van boorzuresters) beter geschied bij lagere pH. Het boorzuurhoudende PAA vormt al bij lage concentraties van 5–10% w/v een dynamische omkeerbare sterke gel door de vorming van omkeerbare covalente boorzurester crosslinks met poly(vinyl alcohol) (PVA) met gel sterktes G'_{Max} tot wel 20 kPa, terwijl het boorzuurvrije controle PAA geen gel vormde. De gevormde gelen waren transparant en thermoresponsief en deze respons op een temperatuurverandering is instantaan en volledig omkeerbaar. Deze dynamische gelen hebben een zelfhelend gedrag, aangezien de crosslinks bestaan uit omkeerbare covalente boorzuresters, die kunnen worden gehydrolyseerd in aanwezigheid van een overmaat water binnen een tijdsbestek van enkele uren. Deze eigenschappen maken de gelen geschikt als gecontroleerde medicijnafgifte systemen. De toevoeging van D-glucose oplossingen aan deze gelen resulteert in een significant snellere degradatiesnelheid als functie van de opgelegde glucose concentratie. De pH-, thermo-, en glucoseresponsieve gedragingen van dit type

gelen maken het ideale kandidaten voor de ontwikkeling van nieuwe glucoseresponsieve medicijnafgifte apparaten.

In **Hoofdstuk 8** worden dynamische (zelfhelende) hydrogelen gemaakt door de omkeerbare vorming van boorzurester crosslinks tussen bisboorzuur gefunctionaliseerde crosslinkers en poly(vinyl alcohol) (PVA). De bisboorzuur gefunctionaliseerde crosslinkers Jeff-2AMPBA en Jeff-4AMPBA bevatten een PPO-PEO-PPO spacer en zijn gemaakt door de reductieve koppeling van 2-, en 4-formylfenylboorzuur aan JeffamineED1900. De pK_a -waarde van zowel de aminogroep als de boorzuregroep wordt beïnvloed door de verschillende positie van de secundaire aminogroep ten opzichte van de boorzuregroep (ortho of para) wat resulteert in een verschillende optimale pH voor vorming van boorzuresters. De bindingsconstante met ARS is bepaald bij verschillende pH (5.0, 6.5, en 7.4) en de hoogste bindingsconstante voor het ortho-aminomethylfenylboorzuur bij een pH van 6.5, terwijl de hoogste bindingsconstante voor het para-aminomethylfenylboorzuur werd gevonden bij een pH van 7.4. Met zowel Jeff-2AMPBA als Jeff-4AMPBA kon redelijk sterke gelen worden gevormd bij een lage pH van 4, maar de sterkste gelen werden gevormd met het paraboorzuur bij een pH van 9. Dit suggereert dat de mogelijkheid tot het vormen van een inter-moleculaire B–N interactie door Jeff-4AMPBA is te prefereren boven een de mogelijkheid tot het vormen van een intramoleculaire B–N interactie door Jeff-2AMPBA voor de vorming van een sterke hydrogel met PVA bij fysiologische pH.

In **Hoofdstuk 9** worden dynamische (zelfhelende) hydrogelen gemaakt door de omkeerbare vorming van boorzurester crosslinks tussen boorzuur gefunctionaliseerde crosslinkers op basis van poly(ethyleen glycol) (PEG) met poly(vinyl alcohol) (PVA). Hiertoe is een serie boorzurehoudende PEG crosslinkers gesynthetiseerd door de reductieve aminering van amino-gefunctionaliseerde PEG verbindingen met 4-formylfenylboorzuur. Verschillende PEG architecturen zijn geselecteerd en de effecten van de armlengte en het aantal armen van het PEG op de uiteindelijke rheologische eigenschappen van de gevormde hydrogelen met PVA zijn onderzocht onder fysiologische condities (PBS, pH 7.4, 37 °C). De gelsterkte, zoals gedefinieerd door de plateau opslag modulus, is bepaald door oscillerende rheologiemetingen en bleef af te nemen met een langere PEG arm lengte, d.w.z. met toegenomen M_w van het PEG. Op dezelfde wijze nam de gelsterkte ook toe door het verhogen van het aantal PEG-armen van de multi-arm boorzurehoudende PEG verbindingen. Met dit nieuwe crosslink system konden transparante en thermoresponsieve gelen worden gevormd met PVA met een gelsterkte tot wel 30 kPa in PBS (pH 7.4, 37 °C). De gelsterkte, vormvastheid en visuele kenmerken konden worden aangepast door de PEG samenstelling (het aantal armen) te veranderen evenals door de concentratie en het M_w van de PEG-crosslinker en het PVA te variëren.

De medicijnafgifte vanuit deze gellen was verder onderzocht in **Hoofdstuk 10**, waarin dynamisch herschikkende gellen konden worden bereid door de omkeerbare covalente verknoping van poly(vinyl alcohol) (PVA, 195 kDa) door multi-arm fenylboorzuurhoudende (PBA) poly(ethyleen glycol) (PEG) crosslinkers, afgekort als $\text{PEG}_{10\text{kDa}}(\text{PBA})_n$. Sterke hydrogelen konden worden gemaakt door het mengen van gelijke volumes van 10% w/v PVA en 10% w/v $\text{PEG}_{10\text{kDa}}(\text{PBA})_4$ of $\text{PEG}_{10\text{kDa}}(\text{PBA})_8$. Het bleek dat het model medicijn molecuul ARS een fluorescente boorzurester vormt wanneer deze wordt toegevoegd aan de gel. De aanwezigheid van ARS heeft een minimale invloed op de gelsterkte en verlengt de zwellings- en de degradatietijden van deze hydrogel systemen. De afgifte van ARS vanuit de $\text{PEG}_{10\text{kDa}}(\text{PBA})_8$ hydrogel was diffusie-gecontroleerd, terwijl de afgifte van ARS vanuit de $\text{PEG}_{10\text{kDa}}(\text{PBA})_4$ hydrogel afhankelijk was van zowel diffusie als degradatie. Nog belangrijker is het feit dat de aanwezigheid van D-glucose de degradatie van de hydrogel bevordert en leidt tot een versnelde afgifte van ARS uit de hydrogel. Deze gellen zijn daardoor geschikte kandidaten voor verdere ontwikkeling van glucoseresponsieve medicijnafgifte systemen.

In **Hoofdstuk 11** wordt er teruggekomen op de hypothesen zoals geformuleerd in **Hoofdstuk 1**, waarbij de eindconclusies van dit proefschrift worden gepresenteerd. In **Appendix A** wordt ook nog een kort overzicht gegeven van onafgemaakt werk, waarbij verschillende aanbevelingen worden gedaan voor eventueel vervolgonderzoek.

Curriculum Vitae

Martin Piest was born on July 24th, 1981 in Steenwijk, The Netherlands. In 1999 he obtained his Athenaeum diploma at 'Regionale Scholengemeenschap Steenwijk' and in the same year he started studying Chemical Engineering with a major in organic chemistry at the University of Twente, Enschede, The Netherlands. In 2004 he visited Wageningen University, The Netherlands, for a 4 month minor in molecular genetics and virology. In 2005 he did a 6-month internship at Clariant AG, Reinach, Switzerland, developing textile dyes. In April 2006 he became his Master of Science (Ingenieur) degree in the research group of prof. dr. Johan Engbersen under daily supervision of dr. Chao Lin with the research entitled 'Bioreducible poly(amidoamine)s for gene delivery'. He continued this work until he started his Ph.D. work in the same group on 'Novel boronated poly(amidoamine)s as multifunctional vectors for siRNA delivery. Since January 2011, he works as Formulation Scientist at InGell Labs BV in Groningen, The Netherlands, where he is responsible for load and release of proteins from injectable hydrogels.